Republic of Iraq
Ministry of Higher Education
and Scientific Research
University of Babylon
College of Engineering
Department of Mechanical Engineering

ASSESSMENT OF AIR AGE FOR PREDICTING OCCUPANT COMFORT BY ADOPTING COMBINED DISPLACEMENT VENTILATION AND COOLED CEILING SYSTEM IN IRAQ CLIMATE

A Thesis
Submitted to the College of Engineering, University of Babylon in Partial Fulfillment of the Requirements for the Ph.D degree in Engineering\ Mechanical Engineering\ Power

By
Ali Aedan Shbeeb Hemid

Supervised By

Prof.Dr. Ala'a Abbas Mahdi **Prof.Dr. Ahmed Kadhim Hussein**

2022 A.D. **1442 A.H.**

الآية القرآنية....

بسم الله الرحمن الرحيم

ألم تَرَ أنَّ الله أنزلَ من السَّماء ماءً فأخرجنا به ثمراتٍ مُخْتلفاً ألوانُها ومن الجبالِ جُدَدٌ بيضٌ وحمرٌ مختلفٌ ألوانُها وغرابيبُ سُودٌ ومن النَّاسِ والدَّوابِّ والأنعامِ مُختلفٌ ألوانُهُ كذلك إنَّما يَخشى الله من عبادهِ العلماءُ إنَّ الله عزيزٌ غفور

صدق الله العلي العظيم
فاطر آية (27-28).

Certification

We certify that this thesis entitled "**Assessment of air age for predicting occupant comfort by adopting combined displacement ventilation and cooled ceiling system in Iraq climate**" was prepared by "Ali Aedan Shbeeb" under our supervision at the University of Babylon as a partial fulfillment of the requirements for the degree of (Ph.D.) of science in Mechanical Engineering (Power Engineering).

Signature

Prof.Dr. Ala'a Abbas Mahdi

Department of Mechanical Engineering

College of Engineering

University of Babylon

Data: / / 2021

Signature

Prof.Dr. Ahmed Kadhim Hussein

Department of Mechanical Engineering

College of Engineering

University of Babylon

Data: / / 2021

Acknowledgments

First of all praise be to GOD for this uncountable blessing.

I would like to gratefully acknowledge my advisers, Prof. Dr. Ala'a Abbas Mahdi and Prof. Dr. Ahmed Kadhim Hussein, for your tireless guidance and support in my study. They have always give me valuable suggestions and encouragement throughout the completion of my academic study. Their knowledge and high level in research have helped me build up my research experience from where I will benefit in my whole life.

I give my sincere thanks to deanship of the faculty of engineering, chief of Mechanical Engineering Department Ass.prof. Dr. Samer Mohammed, and mechanical engineering laboratories staff in Babylon University for providing appropriate conditions throughout my study.

Finally, I am forever indebted to my wife for her understanding, trust, precious advice and encouragement.

Ali Aedan Shbeeb

Dedication

This work is dedicated to my family, and friends who have been an immense support and encouragement to me throughout my research.

Abstract

The Iraqi summer is characterized by high temperature during the daytime, especially in the middle and southern regions. High temperature caused to high energy consumption to cover people's need for air-conditions. This thesis studied a combined displacement ventilation with chilled ceiling system (DV/CC) in hot and dry climate. The Hilla city was taken as a region to study this system. It's located in the middle of Iraq at Longitude (44.42^{o}) and Latitude (32.46^{o}) and it's characterized by hot and dry climate in summer.

The insulated office room model was used in experimental work and numerical study. While the non-insulated office room and classroom were studied numerically only. The study investigated the portion of cooling load treated by chilled ceiling and the effect of air supply diffuser shape on the air age and thermal comfort parameters such as (Predicted Mean Vote (PMV), Predicted Percentage Dissatisfied (PPD) and Air Diffusion Performance Index (ADPI)). In addition to that, the required time to remove pollution (such as CO_2) from the equipped zoon in the room space was studied experimentally and numerically.

The overall aims of this work described in the thesis have been to study the performance of (DV/CC) system under (hot and dry climate). It's obtained a higher level of human comfort and indoor air quality by study the air age and thermal comfort parameters under varied conditions. The operating characteristics of displacement ventilation systems, used both with and without chilled ceiling. ANSYS AIRPAK.3.0.16 was used as (CFD) software in the numerical analyses.

The present study was divided into six cases, each case had four tests based on the cooling load treated by chilled ceiling as (0, 25, 50 and 80% with respect to the total cooling load). The first and two cases (case-I and II) were insulated

office room with rectangle and semi-circular air supply diffusers respectively. It studied experimentally and numerically with a total cooling load equal to (49.3W/m^2 of floor area). The third and fourth cases (case-III and IV) were non-insulated office room with cooling load equal to (106.6 W/m^2 of floor area) while the fifth and sixth cases (case-V and VI) were classroom with cooling load equal to (84.6W/m^2 of floor area).

To study the air age and thermal comfort parameters in each case the air supply velocity for cases (I, II, III and IV) was fixed at (0.25 m/s) while for cases (V and VI) it fixed at (0.3 m/s). The air supply temperature for each case depending on the cooling load treat by displacement ventilation. In addition to that, the study used the (CBE) tool (Center for the Built Environment) which was produced by building energy center to predict thermal comfort for each case.

The main results showed that the local air age increased by about (35 sec and 45 sec) as average for office and classroom respectively with increase (25%) of cooling load treat by the chilled ceiling. The semi-circle diffuser gave advantage to reduce air age by about (10%) in classroom and about (6%) in office room compared with rectangular diffuser. Its improve (PMV), (PPD) and (ADPI) by about (0.03, 0.5% and 2%) respectively as average, and gave better temperature distribution effectiveness by about (8%) in non-insulated office, and (2.5%) with classroom compared with the rectangular diffuser. The (DV/CC) system achieved thermal comfort conditions in insulated room, while in non-isolated room the thermal comfort was depending on the mean radiant temperature as main parameter.

Nomenclature

List of symbols	Description	Unit
A	surface area	m^2
C_p	specific heat of the air at constant pressure.	kJ/kg.K
$C_{1\varepsilon}$, $C_{2\varepsilon}$	coefficient in the specific dissipation rate	
DR	daily rang for outlet temperature.	^oC
D	equivalent diameter of panel (4 area/perimeter)	m
E_{ij}	the mean rate of deformation tenser	m
f	ratio of chilled ceiling area respect to the floor area	-
g	gravitational acceleration	m/s^2
h	convection heat transfer coefficient for inside air	$W/m^2.K$
K	color factor correct	
$k_{i,j,k}$	turbulent kinetic energy at cell (i,j,k)	m^2/s^2
M	metabolic heat generation	
P	Pressure	N/ m^2
V	air flow rate	l/s
q	cooling load for the heat conduction through the walls and transmitted solar radiation,	W
R	thermal resistance	$m^2.K/W$
s	source term for the rate of thermal energy production	J/kg
T	temperature	^oC
U	total heat transfer coefficient.	$W/m^2.K$
u,v,w	velocity component in x,y, and z-directions	m/s

Greek symbols

ρ	air density	kg/m^3
ε	turbulent energy dissipation rate.	J/kg.s
η	portion of cooling load treated by chilled ceiling	
Γ	diffusion coefficient (diffusivity)	m^2/s
α	thermal diffusivity	m^2/s
μ_t	turbulent viscosity	$N.s/m^2$
S	modulus of the mean rate-of-strain tensor	
ΔT	temperature difference	^oC
α	relaxation factor	
α_k, α_ε	coefficient in the specific dissipation rate	

Sub-Scripts

a	air	l	overhead light
av	average	o	outside
c	correct, convection	oe	occupants and equipment
rd	room design	p	person, plate
e	equivalent	r	radiation
ex	external	s	supply
f	floor	th	thermal
hf	head to foot level.	wr	water return
i	inside	ws	water supply
i,j,k	location of point in a cartesian grid	x	local

Abbreviations

ADPI	air distribution performance index
ASHRAE	American society for heating, refrigeration, and air conditioning
CC	chilled ceiling
CFD	computational fluid dynamics
CLF	cooling load factor.
CLTD	cooling load temperature difference, depend on type of wall.
CLTDc	correct cooling load temperature difference
DV	displacement ventilation
IAQ	indoor air quality
LM	corrector latitude and month
LMA	Local mean air
Pr	Prandtl number
RNG	re-normalization group
SC	shadow coefficient.
SHG	solar heat gain.

Table of contents

CHAPTER ONE

INTRODUCTION

Chapter One

Introduction

1. General Concept

The air quality in homes, offices, schools…etc, that people spend most of their time was one of the fundamental determinants of health. Hazardous materials emitted from buildings, such as burning fuel for cooking or heating, lead to health problems and may be fatal.

When people brought fire into their houses, an opening in the roof is required to allow smoke to escape and to supply air to keep the fire burning and control of combustion. This idea provided the first knowledge for the ventilation of a space, **[1].** The stone carvers in ancient Egyptians who work indoors had a higher rate of respiratory distress than their colleagues who work outdoor. They attributed that to large quantities of dust in a workspace. Thus, control of dust was the second recognized need for ventilation, **[2]**. In the middle ages, people notes that, air in a building could spread diseases among people in crowded rooms, **[3]**.

In today, the computers and other heat devices are frequently used in an office room's environment. These internal heat gains added to the heat gain from solar conditions which lead to a high heat load in enclosures. All these reasons led to the emergence of many challenges in the ventilation of offices, **[4]**. More than (90%) of many people times spend in an artificial climate, **[5].** Respiratory diseases have been noticed abnormally in many countries of the world, although the specific factors associated with health problems are unknown. Numerous studies had shown that these symptoms, most diseases, and complaints were due to the poor quality of indoor air, **[5]**.

The systems of ventilation deliver the condition air to the occupied spaces. Depending on types of the building, ventilation cold air may be supply of (100%) from outside air, or mixture of interior air and outside air, **[3]**.

Scientists and researchers used combined system between chilled ceilings and ventilation system as a design options in most commercial office project. The new design combines the energy efficiency of both two systems to improve ventilation performance, **[6]**. Ventilation system operators and designers should be aware of the human comfort requirements and air quality that important to realize acceptable indoor air conditions, **[7]**. This requires knowing the thermal balance between the human body and internal conditions, factors affecting thermal comfort and discomfort and the acceptable concentration of internal pollution that occupants can tolerate, and the nature of the physical activity, **[8]**.

1.1. Ventilation System

There are two main types of ventilation systems. The most common systems in practical applications, are mixing ventilation and displacement ventilation.

1.1.1 Mixing ventilation system (MV)

In this system the supply and indoor air were mixed well by the action of supplied buoyancy and jet momentum. The cooled air supplied from the upper zone. It's used for cooling and heating. The supplied air (cold or hot air) is used to decrease the concentration of pollutions inside the room. Fig.(1-1) shows the mixing ventilation system ,[3].

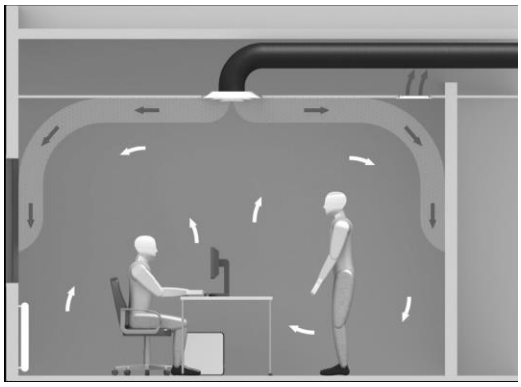

Fig.(1-1) Mixed ventilation system, **[9]**

1.1.2 Displacement Ventilation System (DV)

It can be define as a room ventilation caused by indoor air displacement, by supplying air at low velocity and level in a room at low temperature, **[10]** as shown in Fig.(1-2). The supplied air (outdoor air or a mixture of outdoor and indoor air) at low velocity and near the floor of a room with low cooling capacity (typically < 0.5 m/s, and (< 40 W per m^2) of floor area, **[11]**) which rises with height of the room due to effect of momentum and buoyancy forces. These phenomena are caused by the heating sources such as occupants and warm surfaces. Pollution concentration and temperature stratification then were developed due to cool air at a low level. The contaminated air moved up to the higher room level in a zone above the occupants,**[10]**. The main advantages for displacement ventilation system can be summarized as following, **[12]**:

- Heat and pollutants move into the upper zone and reduce contaminant concentration in the lower zone.
- Low turbulence intensities in the occupied zone leads to reduce risk of draught problems.
- Low supplied air velocities don't lead to draught problems (It is a local cooling that is not suitable for the human body due to the movement of air and the low air temperature in space, **[3]**).
- Give a good thermal efficiency when compared with mixing ventilation.

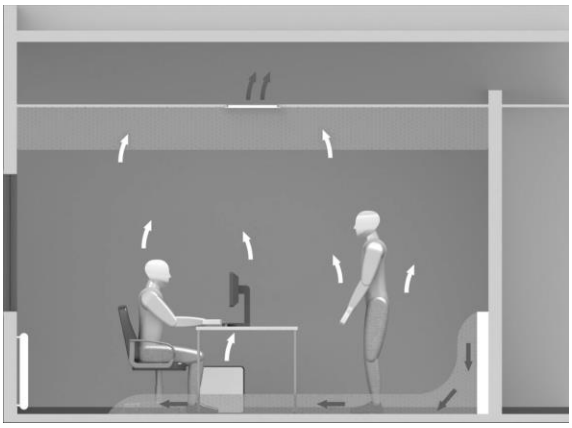

- Fig.(1-2) Principles of displacement ventilation, **[9]**.

1.2. Air supply devices

The most common problems related to displacement ventilation systems were draught problems due to severe cold and high velocity of supply air in the occupied zone. These problems due to the wrong choice of air diffuser type, **[13]**. Therefore it is necessary to choose a suitable diffuser for each case. The supplied air unit setup needs space in the wall or puts on the floor. Therefore, the position of the diffuser required joining with the architect. Diffusers fixed at the wall are most commonly used, **[14]**. There is more than one type of diffuser unit such as, **[15]**:

1- Rectangular diffuser, Fig.(1-3a): supply air in a one-way pattern directly into occupied zone. It's designed to install along sidewall. The low noise level make it suitable for office, schools, restaurants, and hotels.

2- Circular diffuser, Fig.(1-3b): It provides air at (360°) pattern, and supply large air flowrate into occupied space. It's a good choice to work in restaurants, airports, and lobbies.

3- Semicircular diffuser, Fig.(1-3c): It's designed to produce low horizontal air supply turbulence at (180°) pattern. Low noise realized makes it a good choice for used in office room, hotels, and schools or any application.

4- Corner diffuser, Fig.(1-3d): Its designed to supply air at low turbulence in (90°) pattern. It's joined on two walls or in (90°) corner. It suitable for office, schools, restaurants, and hotels, due to low noise level.

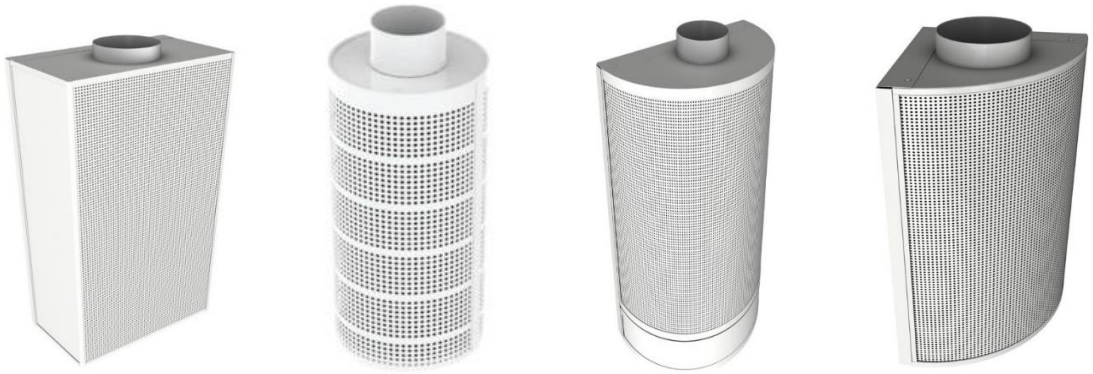

a- Rectangular diffuser b- Circular diffuser c- Semicircle diffuser d- Corner diffuser

Fig.(1-3) Different types of air supply terminals used in the displacement ventilation system**,[15]**

1.3 Chilled Ceiling System

A chilled ceiling is a type of radiation/convection system, it's designed to cool buildings, **[16]**. In this system, the air attaches chilled ceil, and becomes colder, and falls to the floor. After that it's replaced by hot air moving up from below zone, leading to a constant passive air movement called convection, due to that the room is cooled, **[17** and **18]**.

1.3.1 Advantages and disadvantages of chilled ceiling

Chilled ceilings technology has premium advantages compared with other air conditioning systems. For example, **[19, 20,** and **21]**:

1- More energy efficient (about 20%) and lower life costs, less noise, and less maintenance cost due to the lack moving parts.

2- Chilled ceilings use water flow at higher temperatures than fan coil units. And provide the best thermal comfort.

The disadvantages of a chilled ceiling system are very few:

1- It's not recommended to buildings with high ceilings, especially if the room is narrow. This for reasons related to unfavorable geometries that limit the view factor between active and passive surfaces, lower than a radiator system;
2- Structural limits that does not allow to install this type of system. For example inside historical environments or in presence of vaulted ceilings and frescoes.

1.3.2 Types of chilled ceiling

There are three types of a chilled ceiling as shows in Fig.(1-3):

- Radiant chilled ceilings (used in present work).
- Radiant and convective chilled raft.
- Convective chilled ceiling.

1.3.2.1 Radiant chilled ceilings

In this type, a matrix of pipes are located on the rear of metal ceiling tiles (Fig.1-4a). Chilled water flows through a coil, lead to decrease in ceiling surface temperature and provides space cooling by convection and radiation, **[20]**. Radiant cooling happened by absorbed directly of radiating heat from heat sources and hot surfaces in the room, due to the heat sources are visible to cooler surfaces, **[22]**. The advantages for radiant chilled ceiling can be summarized as, **[23, 24** and **25]**:

1- The useful cooling in the space is below the ceiling because the insulation is applied in most cases on the upper side of the chilled ceiling.
2- Reduce cooling energy by (15%) to (20%) due to direct absorption of heat radiated from heat sources.
3- The ventilation system is important as a separate fresh air source, (due to this reason, this type is used in this study).
4- This type of system providing good comfort levels, that's results due to low air velocity distribution in the occupied zone.

1.3.2.2 Radiant and convective chilled rafts

In this type (Fig.1-4b) the cooling water coil is placed at the back of the large flat panels that are installed under the roof. Its advantages summarized as, **[25** and **26]**:

1- Without any insulation on the back of the panel.
2- Heat transfer to the room by convection.
3- Cooled water flows through coil tubes, heat transfer by convective and radiant from the lower surface of raft.
4- Additional convective above the raft provides cold air also.
5- Friendly with architectural requirements due to the raft size and its shape can be easily varied.

1.3.2.3 Convective chilled ceiling

These systems usually include a set of fins connected to a chilled water pipe (Fig.1-4c). The advantages of this type are **[25]:**

1- There is a heat transfer from chilled water to the copper and then to the aluminum and cooling the fins.
2- Heat convection through the angled fins represented a greater proportion of cooling air more than radiation.
3- This system gives higher cooling levels than a typical radiant system, but less than a passive chilled beam.

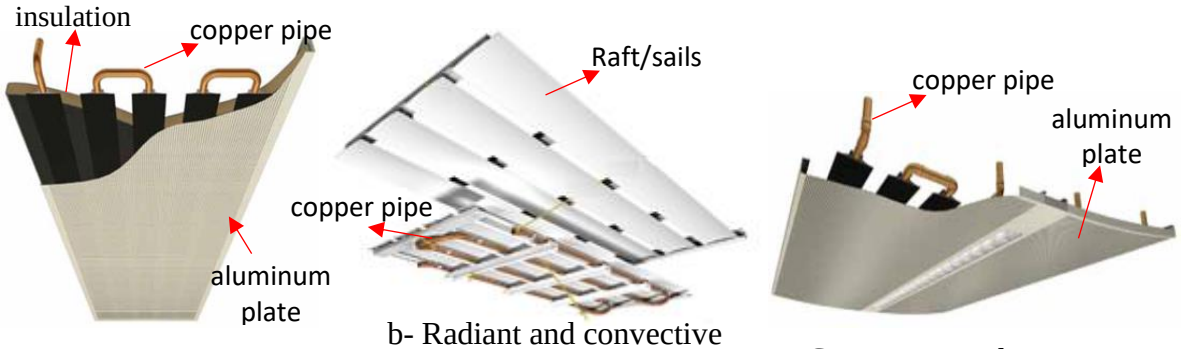

a-Radiant chilled ceiling panel

b- Radiant and convective chilled rafts/sails

c- Convective ceiling

Fig.(1-4) Shown the deference types of chilled ceiling, **[18].**

1.4 Age of Air

Air age was studied at the beginning of 1980, a new procedure has been introduced as "The ability of the ventilation process to replace the old air in a room with fresh air", **[26]**. The local mean air age was regarded as the average time for the air to move from a supply air terminal unit to any point in a ventilated space room, Fig.(1-5). Furthermore, room means air age was defined as the average time needed for the outdoor air to reach all local points in the space room, and it could be used to evaluate the overall ventilation performance in a room, **[27]**. In most time, the air being exhausted from the room before it's full of indoor contaminants. This is because the supply air does not mix perfectly with the room air. As a result, there will be different concentration rates in the occupied zone and to achieve the threshold limit value a larger supply air rate will be required, **[28 and 29].**

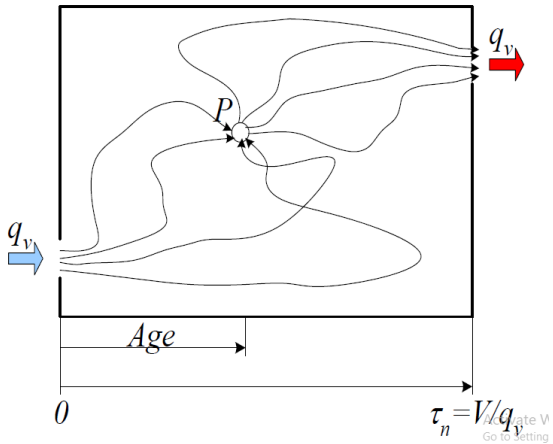

Fig.(1-5) Age of air in the room,**[29].**

1.4.1 The purpose of calculating air age

Knowing the age of air inside a closed room can provide us with many data, for example, **[30, 31** and **32]**:

1- Evaluating air quality in an indoor environment.

2- Referring to the effectiveness of replacing the air in the room by fresh air from the ventilation system.

3- Assessing air pollution control.

4- Evaluating the efficiency of the ventilation system.

1.4.2 Methods of measuring air age

To measure the local air age in a room, it is necessary to use a tracer gas. There are three following methods to measure the local air age, **[27]**:

1- **Pulse method**: at the starting time, short pulse of the tracer gas is emitted in the air inlet.
2- **Step-up method**: the tracer gas injected with air supply, at a constant rate throughout the test.
3- **Decay method:** A uniform concentration of tracer is achieved at the beginning of the test when the injection is stopped. It's modified to avoid problems of non-uniform air inlet. This method is used in the current experimental work (more details about this method in chapter three).

1.5 Combined Displacement Ventilation with Chilled Ceiling system

The combined displacement ventilation system with chilled ceiling shown in (Fig.1-6), represents a good design system. It combines between the energy efficiency of the displacement ventilation and energy saving of chilled ceiling. This leads to improve ventilation performance due to the thermally stratified displacement ventilation systems, **[33]**. For large sensible cooling loads, ventilation is provide by displacement ventilation and could be used with the chilled ceiling, **[34 and 35]**. This combined system is now used as design options for most commercial office project, **[36]**.

The cooling capacity absorbed by used displacement ventilation system only was limited to about (30–40W/m^2) of floor area. This is because limited of air supply temperature to avoid draught problems, **[37** and **38]**. To raise the cooling capacity

absorb, combine additional cooling systems used, such as a chilled beam or chilled ceiling, **[39]**.

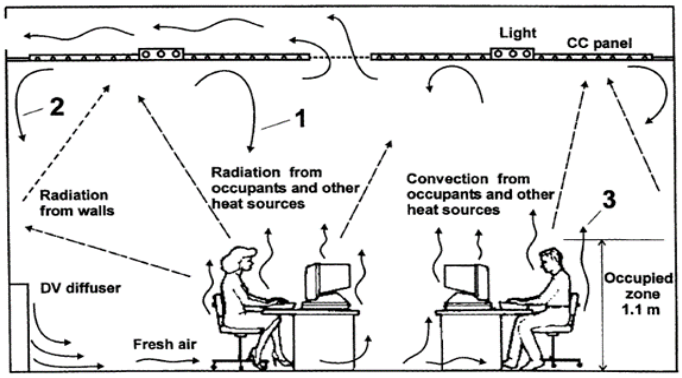

Fig.(1-6) Combined (DV/CC) system, (1) and (2)downward convection by CC, (3)thermal plume by heat source, **[40].**

1.5.1 Capital cost and energy

Fig.(1-7) shows three analyses for different ventilation systems, from the figure notes that the combined system (DV/CC) used less electrical energy than Variable Air Volume system (VAV). With a chilled ceiling, the total electrical energy consumption depends on the several factors, **[41]**:

1- Low consumption in fans electrical energy, due to lower volume of airflow rate.

2- Consumption of the electrical energy increases by using cooling tower and chilled ceiling pump. Then, the overall result showed that the high thermal capacity of water lead decrease in the total electrical energy consumption with the (DV/CC) system.

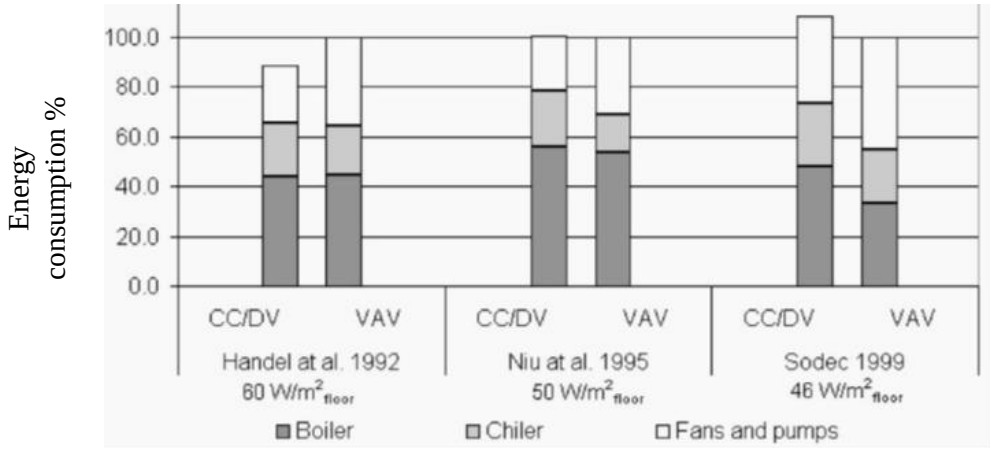

Fig.(1-7) Energy consumption comparison between VAV and DV/CC system, **[41].**

1.6 Indoor Air Quality (IAQ)

The phrase (sick building) is almost equivalent to the poor (indoor air quality) and a lot of professionals such as psychologists, medics and building designers, etc. tried to determine the reason for this phrase. They found that there is a relation between the quality of indoor air and productivity. The main factors associated with these buildings are the poor fresh air and ventilation system.

The indoor air quality problem is associated with many factors, **[3]**:

1 Poor in ventilation rate to reduce the energy consumption.

2 Increase in used of computers, photocopier printer and other equipment in office.

3 Increasing used of furnishing with high emission of pollutants.

4 Increase in used of air-conditioning.

5 Lack of maintenance.

1.7 Thermal Comfort

Providing an acceptable local climate is the main purpose of the ventilation system. ASHRAE Standard 55, **[42]** was defined thermal comfort as: "A state of mind expressing satisfaction with the thermal environment". (Fig.1-8) shows ASHRAE comfort chart for occupants.

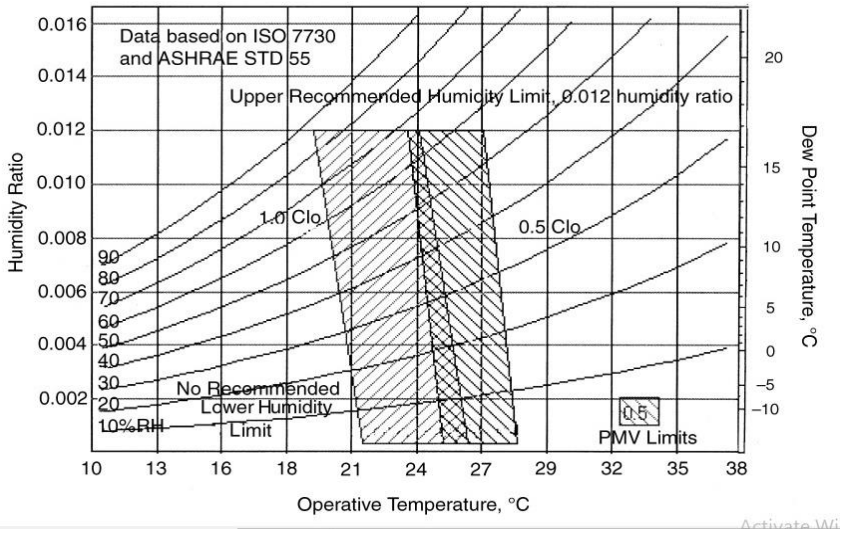

Fig.(1-8): ASHRAE comfort chart for occupants, **[42].**

1.7.1 Predicted Mean Vote (PMV)

Its index is used to predict thermal comfort and human conditions. (PMV) is related to the balance between the heat loss from human body and the rate of heat release required for optimal rest in a specific activity, **[43** and **44].**

The (PMV) value is classified into seven thermal sensation points scale (from -3 at cold indoor air to +3 at hot indoor air) as shows in Fig.(1-9), **[45]**. Depending on (ASHRAE standards) the best range of (PMV) for acceptable internal comfort is between (-0.5 to +0.5), **[46]**.

Fig.(1-9) PMV voting scale, **[45].**

1.7.2 Predicted Percentage Dissatisfied (PPD)

The (PPD) index was developed by **Fanger (1984), [43]**. The (PPD) predicted percentage of people thermally discomfort who feel too hot or too cold. (PPD) calculated from (PMV) as shown in Fig.(1-10). The recommended (PPD) limited for acceptable thermal environment for general comfort is (10%) with (- 0.5≤PMV≤ 0.5), **[42].**

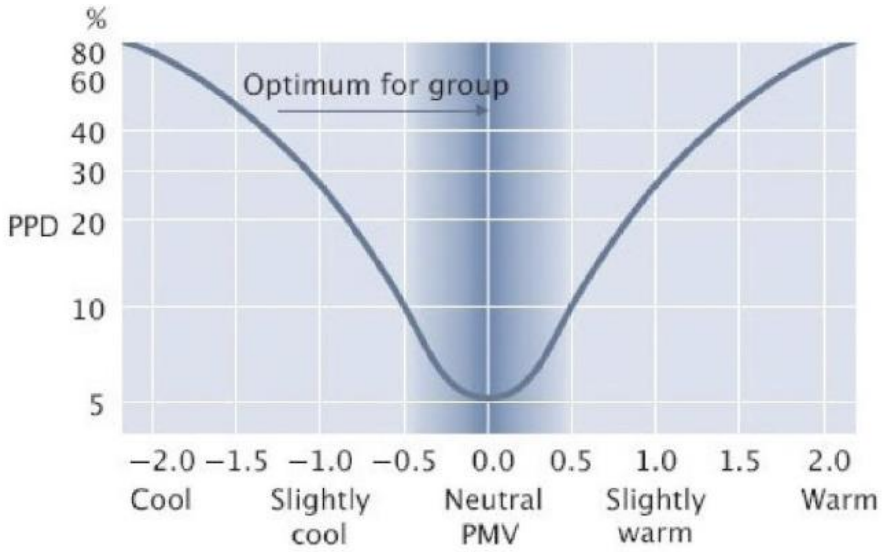

Fig.(1-10) Relation between (PPD) and (PMV), **[42].**

1.7.3 Air Diffusion Performance Index (ADPI)

(ADPI) used to satisfy the comfort level. It was defined as a ratio of the number of temperature points in the occupied zone that have effect draft temperature value (EDT) between (-1.7 and 1.1^{o}C) to the total number of temperature points in the same zone, **[8 and 41]**.

1.7.4 Temperature distribution effectiveness

The ventilation effectiveness at a local point for the temperature distribution describes the ventilation system able to satisfy thermal comfort level in a ventilated space. Its value must be greater than one,**[8]**. This is due to the exhausted air temperature is more than average indoor air temperature.

1.8 Objective of the Present Work

This thesis includes investigation the ventilation strategies by using displacement ventilation system in combination with chilled ceiling. The study is conducted in different indoor applications (office room and classroom). Assessing the age of air by adopting experimental and numerical investigation under Iraqi-Hilla climate (hot and dry climate). The displacement ventilation in combination with chilled ceiling

system not used yet in Iraqi building. Then this study will be a good starting point to assessing the performance of (DV/CC) system in a hot and dry climates.

The novelty of the present work is using displacement ventilation with chilled ceiling system under a range of operating conditions in a hot and dry climate to understand the indoor air age and analysis thermal comfort parameters such as (PMV, PPD and ADPI).

The main objectives of the present work are:

1. Building an experimental test rig including displacement ventilation system in combined with chilled ceiling system at different cases study.
2. Reaching the acceptable situation which gives the optimum human comfort, air distribution and indoor air quality.
3. Studying the variations age of air and thermal comfort parameters inside the room for combined (DV/CC) system at different cases studies under hot and dry climate).
4. Studying the effects of air diffuser types on air age and human thermal comfort.
5. Evaluating the effect of change portion of cooling load treated by chilled ceiling on the air age and human thermal comfort parameters.
6. Obtaining the performance of (DV/CC) system under hot and dry climate and obtain a higher level of human thermal comfort and IAQ (indoor air quality).

CHAPTER TWO

LITERATURE REVIEW

Chapter Two

Literature Reviews

This chapter is related with a review of literature concerned with chilled ceiling and displacement ventilation technology. Displacement ventilation system had been developed for office applications since 1980. The literature on DV system technology has grown gradually since then. The technology of chilled ceiling, although it preceded the development of displacement ventilation, has recently grown interest in the commercial applications and the research literature. The most literature was related with a study the benefits of a combined system in terms of thermal comfort and air quality. To analyze and predict detailed micro-climate conditions, two main approaches are commonly used, experimental measurement and computer simulation.

This review is subdivided into four main topics:

1- Theoretical and numerical simulations studies.
2- Experimental studies
3- Experimental and numerical studies.
4- Scope of the present work.

2-1 Theoretical and Numerical Simulation Studies

Ayoub et. al. (2006), [47] studied numerically the air and wall temperature variations with height in a test room (5×4×3m) by using combined displacement ventilation and chilled ceiling system to estimated wall plumes for non-isothermal surfaces. Three tested cases were studied at different cooling loads (40, 67, and100 W/m^2) and air supply flow rate (per unit area) of (22.5, 30 and 37.5 $m^3/h \cdot m^2$) respectively. Multilayer models were developed to represent thermal transport in enclosures conditioned. These models were validated by three dimensional simulations by using AIRPAK software. Also they developed to represent thermal transport in enclosures conditioned.

Wang and **Zhen (2006), [48]** presented a comparison between displacement and mixing ventilation systems with and without chilled ceiling in an office room (5.16×3.65×2.43m). Four cases were studied numerically at different location of air supply diffuser. FLUENT software with RNG-Kε turbulent model was used. They assumed that the room located in interior building and each wall side was adiabatic and the room without windows. The air supply velocity was (0.2m/s) at air change per hour equal to (8 1/h) and (60%) relative humidity for displacement ventilation system. They showed that the performance of displacement ventilation with chilled ceiling in ventilation efficiency, temperature field, thermal comfort, and contaminants concentration field were better than of the mixing ventilation with chilled ceiling. Combined chilled ceiling with displacement ventilation led to reduce the vertical temperature difference.

Hao et. al. (2007), [49] presented theoretical studies about combined system of chilled ceiling with displacement ventilation and desiccant dehumidification to design a space conditioning under a hot and humid climate. Indoor air quality, energy saving and thermal comfort, of the combined system were estimated by using a mathematical model in office building at total cooling load (60 W/m^2) of floor area under China-Beijing climate. The cooling load treated by displacement ventilation and chilled ceiling as (20 W/m^2) and (40 W/m^2) respectively. The indoor air design temperature and relative humidity were assumed as (25°C), and (50%) respectively. The air supply temperature and air flow rate were (20°C) and (60 m^3/h per person) respectively to treat (20 W/m^2) of cooling load. The chilled ceiling temperature was about (19°C) to treat 40 W/m^2 of cooling load. They found that the combined system led to decrease the total energy consumption by (8.2%) and improved indoor air quality (IAQ) and thermal comfort. Desiccant dehumidification succeeded to prevent condensation on the chilled ceiling system.

Karadag (2009), [50] investigated numerically the relations between convective and radiative coefficients at the chilled ceiling with isolated floor surface for different tested rooms (3×3×3m), (4×3×4m) and (6×3×4m) and different chilled ceiling surface emissivity's (0.7, 0.8 and 0.9) respectively. The temperatures of chilled ceiling surface was changed from (0 to 25°C). FLUENT software was used for numerical solutions. The results found that the coefficients ratio for radiative to convective heat transfer (h_{cr}/h_{cc}) between (0.7-2.3) based on the temperature difference. A heat transfer coefficient correlation was suggested for ceiling convective as follows:

$$h_{cc}=2.6(T_i-T_{cc})^{0.27} \quad \text{….. (2-1)}$$

Mateus and **Carrilho (2015), [51]** investigated numerically the effects of the chilled ceiling with displacement ventilation system on airflow and air temperatures distribution based on datasets collect from the twelve cases of three previous experimental studies, **([6], [52]** and **[53]**). The air supply temperature was varied between (18-22ºC) and chilled ceiling surface temperature was varied as (16-27ºC). The model was focused on thermal plumes as drivers of air flow and heat exchange for room air. The study presented a simplified three node model depended on the predicted vertical temperature profiles and the mixed layer location in the rooms with DV/CC system. The suggested model was validated by using twelve case studies from three independent experimental works. The study presented two design charts for DV/ CC system which can help designers in the early design phases. The two charts related with DV/CC system were designed at high and low heat gains scenario to specify optimal operation zone.

Itani et. al. (2015), [54] studied theoretically the performance of displacement ventilation with novel evaporative cooled ceiling under Beirut climate by using MATLAP software to solve the model equations. The case study was an office room (8.2m^2 floor area at 2.8m height). The model was simulated at (22°C) supply air temperature with (0.14 m^3/s) supply air flow rate to remove constant cooling load at (40 W/m^2) for different relative humidity at (10%, 50% and 90%). The novel evaporative cooled ceiling led to improve the cooling capacity for displacement ventilation system more than (40 W/m^2) without additional energy consumption. The total cooling load removed by using novel evaporative cooled ceiling reached to 68.9 W/m^2 with (10%) relative humidity and (47.46 W/m^2) with (90%) relative humidity. The results indicated that the system gave a better performance by (21.44 W/m^2) at lower relative air humidity (10%) compared with maximum relative air humidity (90%).

Teodosiua et. al. (2016), [55] investigated numerically the condensation and thermal comfort on the cooled ceiling surface for buildings by different systems of ventilation (displacement and mixing ventilation) with cooling ceilings in office room (6.2×3.1×2.5m) including four persons as shown in Fig.(2-1). Six cases were simulated as three cases with displacement ventilation system and three cases with mixing ventilation system due to different locations of air supply diffuser and exhausted grill at constant air supply temperature (35ºC) and fixed moisture content equal to (10.5 g/kg). The chilled ceiling surface temperature varied between (17-14ºC). ANSYS FLUENT.15.0.0 was used as CFD software with used Shear Stress Transport (SST) as turbulent model to simulate the cases addition to specific code used to condensation modeling. The results showed that the ventilation system by supplied untreated air, the thermal comfort in the office was not achieved by using radiant chilled ceiling systems only without treated supply air.

Muslmani et. al. (2016), [56] investigated theoretically the performance of a liquid desiccant dehumidification membrane cycle (LDMC) instead of the chilled ceiling. In this system the membrane used to remove sensible and latent load from indoor space. The case study was an office room in Beirut city of dimensions (5 × 5 × 3 m). Solar energy parabolic collector used as energy source to cover the heat required by the liquid desiccant. Displacement air supply temperature was varied between (17°C - 23°C) at air flow rat varied between (0.08-0.26 Kg/s) respectively. The temperature for the liquid desiccant entered to the dehumidifier was varied between (12 - 20ºC). The results showed that the (LDMC) prevented condensation on the ceiling and decreased energy consumption by about 49% compared with the conventional DV/CC system.

Yang et. al. (2017), [57] presented numerically a study for air flow and temperature fields in an office room ventilated by combined system (DV/CC). Office room

modeled without window (4.22×4.22×2.5m) was studied with seven cases depend on location of chilled walls shown in Fig.(2-2). The latter in each case had the same surface temperature and the area (17.8m^2). The cooling load in office room was fixed at (631W) by two persons, two overhead light, two computers and (19 W/m^2) as heat gain from side walls by assuming the floor and ceil was adiabatic. Both the air supply temperature and velocity were considered fixed at (18^{o}C) and (0.138m/s) respectively. AIRPAK3.0 software was used to develop room model by using indoor zero equation as turbulence model. They showed that the position of radiant cooling surface at ceil was better thermal comfort due to the values of (PMV) were around (-0.4 to zero) while for other cases the (PMV) values were more than zero at different levels in tested room.

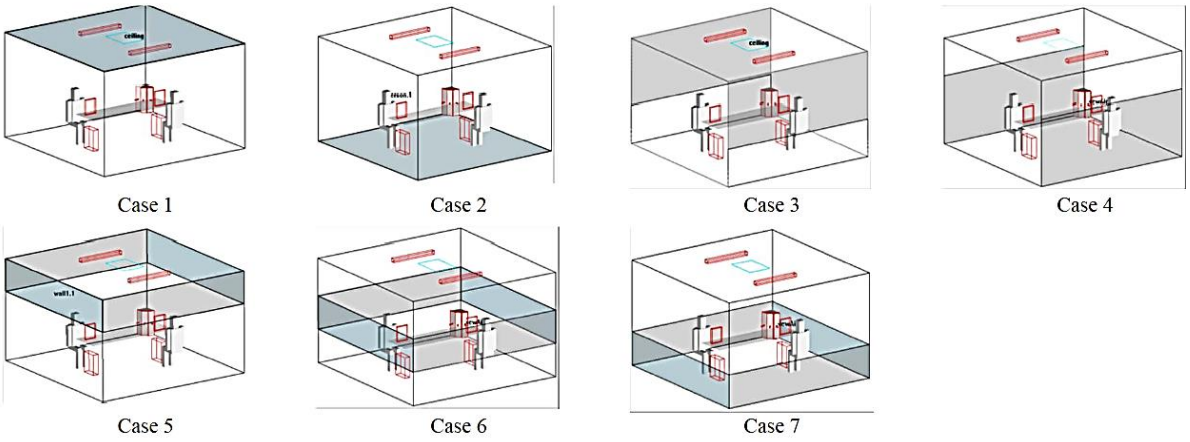

Fig.(2-2) Location of cooled ceiling for seven cases studied by Yang et. al., [57]

Hormigos et. al. (2018), [58] studied numerically the effect of furniture distribution on the local mean air age and decay indoor Co_2 concentration with time. Case study used two strategy of furniture arrangements in isothermal tested room at dimensions of (4×3×2.5m). The first strategy as a bedroom with a single bed while the second strategy as a bedroom with bed, shelving, chair and table. The study focused on local mean air age (LMA) parameters. ANSYS FlUENT (ANSYS 2013) with zero equation model used as CFD software. The ventilation flow was (5l/s), and the inlet

air conditions depended on data at the months of January and February for the first strategy, while the months of February and March for the second one. They found that the space geometry and the arrangement method for furniture had a large effect on the ventilation efficiency.

Shan and **Rim (2018), [59]** investigated numerically the performance of air conditioning and ventilation of combined passive chilled beam (PCB) with displacement and mixing ventilation systems. The study used two types of internal heat source arrangement in test room (6 ×4×3m) simulated by used ANSYS software (SSN k-ώ turbulent model). The air supply temperature was varied from (17^{o}C) to (20^{o}C) supplied by two diffusers. (PCB) output cooling was (100, 150 and 200 W) per each beam for mixing ventilation system and (100, 125, 150, 175, 200, 225 and 250W) with displacement ventilation system. They found that when the cooling output for (PCB) increases from (33% to 53%of total cooling load). Air exchange effectiveness decreases from (1.6 to 1.2), and led to decrease in vertical temperature difference from (4 to 1.5^{o}C) in breathing zone. At high cooling load absorbed by (PCB) (>50% of total load) could disperse thermal layers of displacement ventilation and increased draft rate in occupied zone.

Tian et. al. (2019), [60] studied numerically the variation of temperature, humidity and condensation phenomena on chilled ceiling in the room with DV/CC system. The tested room dimensions (4.5×4×2.5m) under Shanghai (China) climate with total cooling load (1280W).The air supply at (20^{o}C) and (0.3m/s). The design room temperature and relative humidity were (25^{o}C) and (45%) respectively and the chilled surface temperature was 20^{o}C. Before running the air ventilation system, the indoor temperature and the relative humidity were (28^{o}C) and (65%) respectively. A two steps approach was suggested to solve condensation problem. The study

discussed the displacement ventilation operation time before running chilled ceiling. ANSYS software was used to simulate tested room (standard k-ε turbulent model). They found that the dew condensation on chilled ceiling could be alleviated by running the displacement ventilation system for about 300s before running chilled ceiling. This time period led to reduce the dew point temperature for air near the chilled ceiling by about (2^{o}C).

Guo et. al. (2020), [61] studied numerically the comparison between novel operating strategy and conventional one to discuss the humidity ratio and problem of condensation near chilled ceiling. The suggested strategy depended on operated chilled ceiling after the dew point temperature for air near the chilled ceiling reduce by (2^{o}C) less than chilled ceiling surface temperature. The tested office room dimensions was (4.5×4.5×2.5m) with one widows as shown in Fig.(2-3), located in Shanghai (China) under summer periods. The heat gain was (790W) by two occupants, two computers, one lamp addition to heat gain from window and exterior wall. The chilled ceiling surface temperature fixed at (20^{o}C). Four cases were studied at different air supply humidity ratio varied between (6.5-8 g/kg) at constant supply air temperature (19^{o}C) and air flow rate varied between (0.05-0.01m^{3}/s) for each cases. ANSYS FLUENT software was used in numerical analyses by used RNG k-epsilon as turbulent model. The results found that the time needed to reduce air dew point temperature near the chilled ceiling before operating chilled ceiling was eliminated to (57.6%) (From 283 to 180s) by increasing the air supply flow rate from (0.05 to 0.1m^{3}/s). The results showed that after (12h) operation, the temperature of dew point near chilled ceiling was a safety rage and condensation problem was prevented.

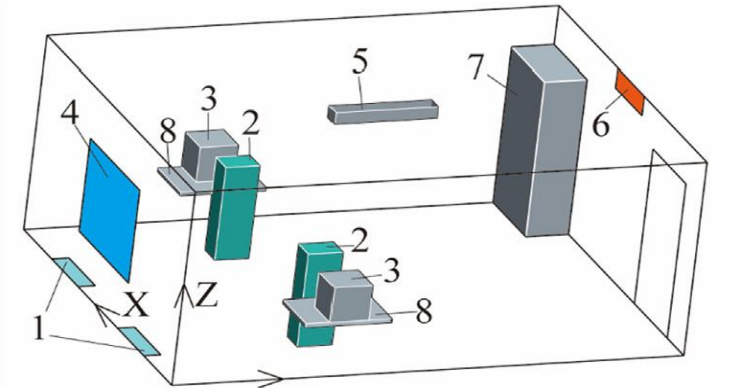

Fig.(2-3) Studied model, [61] . (1-Air inlet. 2-Human. 3-Computer. 4- Window. 5-Lamp. 6-Air outlet. 7-Cabinet 8- table).

Amini et. al. (2020), [62] presented a new method to control and treat the condensation problem in the CRCP (Ceiling Radiant Cooling Panels). This method depended on a dehumidification coil integrated with (CRCP) to remove latent heat and regulated the water condensation on ceiling. The condensation coils located over of the chilled ceiling and the condensed vapor removed from the room by drain pipe. ANSYS FLUENT software was used in numerical analyses (low-Re k-ε turbulence model used to simulated turbulent flow). The tested room dimensions was (3×3×3m). The temperature of walls and chilled ceiling were varied between (28-36^{o}C) and (12-20^{o}C) respectively. Two cases were studied, first case with four external walls while second one assumed that the south wall as an external wall with window, while other walls as internal walls (adiabatic surface) at outdoor temperature equal to 42^{o}C. They found that the proposed system led to saving energy by (30%) for first case and (15%) for second case compared with the conventional system. The new method led to decrease the humidity ratio in the tested room by removed latent heat.

2.2 Experimental Studies

Fonseca et. al. (2010), [63] studied experimentally the radiant ceiling system under cooling and heating mode with their environment (walls, fenestration and internal loads). Temperature of the supply water, distribution of thermal load and water mass flow rate were studied to show their effect. Forty six test were performed to observe

the influence of these parameters. Two tested office room was studied, big and small with dimensions (1.8×6×2.6m) and (1.3×6×2.6m) respectively made from wood in Brussels (Belgium). The supply water temperature and mass flow rate varied between (15.47-35.91^{o}C) and (0.06798-0.1998 Kg/s) respectively. The results specified that the surface temperature for room walls had a major impact on thermal comfort and the heat transfer coefficient of radiant ceiling was high by 10% with heating mode compared with using cooling mode.

Chakroun et. al. (2011), [64] investigated experimentally the saving energy by using exhausted air from ventilated room and mixed it with new supply fresh air under chilled ceiling with displacement ventilation (DV/CC) system in Kuwait climate. The tested room had dimensions of (4.59×4.95×3.8m). It included one door and two windows, the north and west walls were internal partitions. The chilled ceiling fixed at (2.8m) height and covered (80%) of ceiling surface. Supply air temperature and mass flow rate were (20^{o}C) and (0.2 Kg/s) respectively and the chilled ceiling temperature was fixed at (16^{o}C). Three cases were studied depend on ratio of fresh air mixed (60, 80 and 100%) at constant cooling load (52 W/m^2 of floor area). They found that the mixing fraction up to (60%) led to reduce energy consumption by (37%) compared with total fresh air.

Chicote et. al. (2012) [65], studied the heat transfer coefficients and cooling capacity for the cooled radiant ceiling. Experimental tests were made in a climate tested room at dimensions (3.6×3.6×3m). Walls are made from (30mm) thick sandwich type with polystyrene insulation included between two layers of steel sheet. Eighteen cases were tested at different total cooling load. The surface temperature of chilled ceiling and total cooling load varied between (15.6-21.2^{o}C) and (22.9-57.3 W/m^2 of floor area). They found that the operative temperature for cooled ceiling was not unique

reference to predict the output cooling of cooled radiant ceiling. Both convective and radiant phenomena separately was needed. The study provided approximate average values of (4.2 W/m^2K) and (5.4 W/m^2K) for convective and radiant heat transfer coefficients respectively.

Ho (2013), [22] studied experimentally thermal comfort in Hong Kong Aircraft company offices (China) (hot and humid climate) by using chilled ceiling system instead of fan coil unit (FCU) for total area equipped was (4,600 m^2). The capacity of radiant chilled ceiling system was estimated as (143 kW). The chilled ceiling made from aluminum plate with copper pipes. He found that using chilled ceiling most occupants found the temperature was evenly distributed, no uncomfortable draft and very low background noise level, in addition the chilled ceiling system was saving (40%) of total power energy and the routine maintenance was saving by (90%) compared with conventional (FCU). The relative humidity was kept below (60%). The maintenance of chilled ceiling system was simple and worker saving. It run automatically within the set parameters (pressures, temperatures, relative humidity, time schedules and carbon dioxide level).

Liu et. al. (2014), [66] investigated experimentally the STCC-DV (solar thermoelectric cooled ceiling combined with displacement ventilation system). The system modules were utilized as source and sinks for heating and cooling mode without needed to hydronic pipe. The floor area for tested room was (2.53 m^2) (2.3×1.1 m) at height (2.7 m), the total cooling load was (100 W/m^2) in Beijing (China). The displacement ventilation covered (20%) of total cooling load at air supply flow rate was (6 $m^3/h.m^2$) of floor area. The (STCC) was made of (1.8×0.6m) aluminum plate and thermoelectric (TE) modules as cold side fixed directly on the aluminum plate. Ten (TE) modules were used in (STCC) system, and distributed in

series panel as five (TE) modules in each raw. The results showed that the ambient temperature, operating voltage and indoor temperature were very affected on (STCC) performance. The (STCC) led to increase the total heat flux of system higher than (60 W/m^2) in cooling mode at operating voltage was (5V), while in heating mode the heat flux was higher than (110 W/m^2) at voltage (4V). The coefficient of performance (COP) reached to (0.9 and 1.9) for cooling and heating mode respectively.

Kim and **Leibundguta (2014), [67]** studied experimentally the performance of an airbox convector unit for dehumidification and cooling to reduce condensation risk on the surface of chilled ceil combined with displacement ventilation in humid and hot climates. The airbox unit led to cold and dehumidified indoor room air. The dehumidified air supply from the airbox at temperature below (17^oC) and dew point temperature was (18^oC). The temperature of water left the airbox to the chilled ceiling pipes was between (19-21^oC). The advantage of Airbox unit was to avoid condensation by dehumidifying indoor air and increasing supplied water temperature of chilled panel. The study assumed that the building was located in Singapore. The tested room volume was (42.772 m^3 at 14.77 m^2 floor area). Supply air flow rate was (1ACH) as a natural ventilation with open windows. The suggested system generated additional cooling capacity without needed for supplementary cooling sources. They found that the suggested system gave a cooling load about (25%) more than conventional ceiling panel system due to increase heat transfer by convection between room air and chilled ceiling. Their system was saved about (14-18%) of supply air cooling load.

Itani et. al. (2015), [68] studied the energy saving of combined displacement ventilation, and evaporative cooled ceiling (ECC) by using Maisotsenko cycle (M.cycle) under hot and humid climate in a tested room dimension (2×3×2.8m) with total cooling load (300W). The schematic of companied system is shown in Fig.(2-4).

The desiccant machine model consisted of two sections rotary wheel in one section, the hot dry air used to regenerate the desiccant (with temperature between 40-80^{o}C) and exhausted outside room, and in the two sections the air was dehumidified before cooled (between 24-34^{o}C). The air supply by displacement diffuser was (21^{o}C) at flow rate (0.118 m^3/s). The efficiency of (DV/ECC) system was predicted to improve by dehumidified the supplied air by using solid desiccant dehumidification system regenerated by used (parabolic solar concentrator thermal source). The suggested system gained (28.1%) saving in operating cost and electrical power consumption during the cooling season.

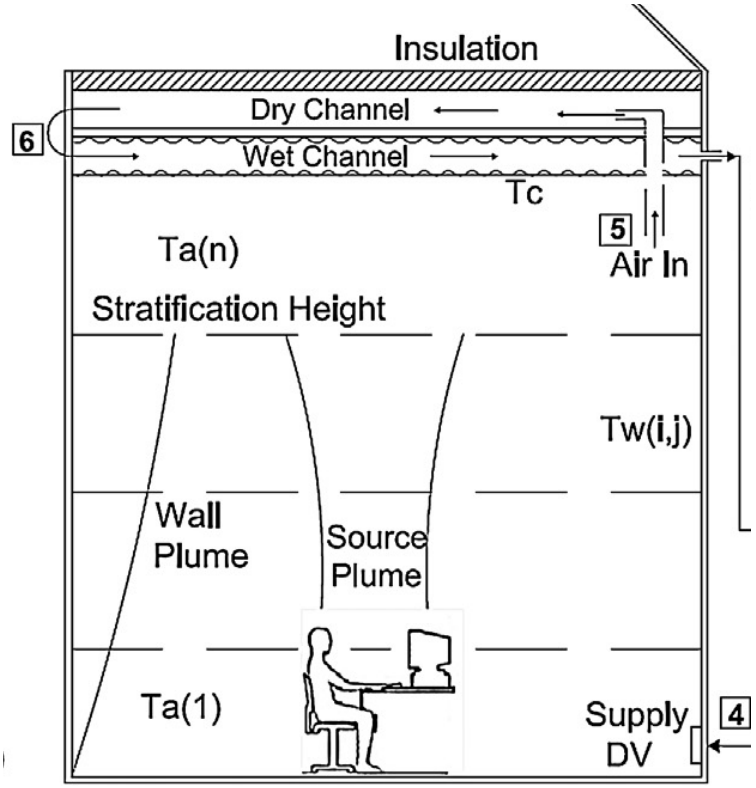

Fig.(2-4) Case study by **Itani et. al. [68]**

Yuan et. al. (2015), [69] developed experimentally a simplified correlation which connected between heat flux and temperature difference to calculate limited values of heat transfer coefficients at tested room floor area of (15.12m^2) located at Tongji University. The inside chilled ceil height was (2.4m) and covered (49%) of ceil area. The tested room walls were made from stainless steel with window at the south wall.

All walls temperature were controlled by using water pipe, only south wall was insulated while other walls simulated as exposed to the outside weather at temperature between (10-40^{o}C). Three cases were studied depending on three different of panel's structure with surface temperature varied between (14-20^{o}C). Total heat transfer coefficient was fluctuating from (6.5 to 9.7 W/m^{2}K) and average value was (8.5 W/m^{2}K). The total heat transfer coefficients were slightly fluctuating when the internal heat sources at uniform distribution and there was no strong solar radiation. The suggested correlation are given by:

$$q_{total}=7.24(T_a-T_b)^{1.09} \quad \text{..... (2-2)}$$

$$h_{total}=7.24(T_a-T_b)^{0.09} \quad \text{..... (2-3)}$$

Krajcik et. al. (2016), [70] studied experimentally the effects of displacement ventilation with cooled ceiling and floor on indoor climate by investigating six cases with different air flowrate and air supply temperature. The latter varied between (16 to 24^{o}C) and air change rate varied from (4.5 1/h) to (1.5 1/h) respectively. Experimental measurements were performed in a tested room at dimensions of (4.2 ×4×2.4 m) with total cooling load (981W), the cooling load treated by displacement ventilation varied between (9.8-80.3%) of total cooling load. Mean air age and pollutant removal were studied to describe the ventilation effectiveness. Profiles of operative and air temperature were measured with thermal manikin temperature to evaluate thermal environment. They found that the cooled floor caused high vertical temperature differences between foot and head for occupants (between 4.7-5.8^{o}C). These results caused thermal discomfort, that's gave preference to chilled ceilings compared with chilled floors for using with displacement ventilation system.

Cholewa et. al. (2017), [71] presented an experimental study to investigate heat transfer coefficients under cooled and heated radiant ceiling depending on heat and cold emit to the room located in laboratory. The environmental chamber was

(1.56×1.56×2.21m), the radiant ceiling covered (100%) of ceil area. The total cooling load for hot radiant ceiling was varied between (6.63-47.3 W/m^2 of floor area), and for cooled radiant ceiling was varied between (7.35-16.5 W/m^2 of floor area). The chamber walls and floor were insulated and pained by black color. The temperature of radiant ceiling varied from (25^{o}C to 65^{o}C) for heating and (7.5^{o}C to 15^{o}C) for cooling. They found that the decrease value of radiant surface emissivity from (0.9 to 0.1) led to decrease the radiant heat flux density and increased convective heat flux density for analyzed cases.

Karmanna et. al. (2018), [19] investigated experimentally the effect of ceiling fan with chilled ceiling on the cooling capacity. The tested room at dimensions of (4.27×4.27×3.0 m) located in laboratory with total cooling load equal to (1079 W). Ceiling fan was installed between the chilled ceilings (downward or upward blowing direction) with small fans located above chilled ceiling which blowing horizontally with ceiling level. The tested room walls were adiabatic and without windows. The chilled ceiling covered (73.5%) of ceil area. Twenty six cases were studied depending on the direction and amount of fan air. They found that the ceiling fan led to increase cooling capacity by up to (12%) when air fan was downward and up to (22%) when air fan was upward. The fan ceiling with chilled ceiling helped to expand the zone of thermal comfort by about (1.4^{o}C) and (2.9^{o}C) with fan blowing upward and downward respectively.

Seblany et. al. (2018), [72] presented a method to study humidity control where part of cool dry air adjacent to the liquid desiccant membrane cooled ceiling (LDMC) with displacement ventilation system. Desiccant solution flowed over ceiling membrane to remove the moisture and heat from tested room air near the membrane. In their system, portion of exhausted air was took and mixed with the stream of displacement ventilation air supply. The experiment was mainly consisted of a

chamber dimensions (1×1×1m) equipped with supply and grill of (25×25 cm), supply mass flow rate equal to (0.08 Kg/s) at air change per hour (ACH=0.4 1/h) and exhaust grill (50×15 cm). (LDMC) system making drop in humidity by about of (8.72%) in occupied zone after (12min) and (24%) was achieved in energy saving compared with conventional cooling system.

Wu et. al. (2020), [73] presented an experimental study about the effect of chilled ceiling on indoor air distribution combined with mixing ventilation system with changed the internal and external sensible cooling load. The vertical distribution of air velocity, air temperature and carbon dioxide concentration were evaluated by the vertical air temperature difference, contaminant removal effectiveness and turbulence intensity. Tested room dimensions were (3.7× 2.8×2.6 m) as shown in Fig.(2-5). The chilled ceiling covered (76%) of ceil surface. The temperature of chilled ceiling surface varied from (17 to 26^{o}C), the supply air temperature and air velocity varied from (16 to 22°C) and (0.12-0.39 m/s) respectively supplied by air diffuser located in the ceil center. Thermal manikin, ceiling lights and computers were used as heat sources in an office room, the total cooling load varied between (41-69.5 W/m^2 of floor area). They showed that the surface temperature of chilled ceiling had a slight effect on the indoor air distribution in a room with mixing ventilation system.

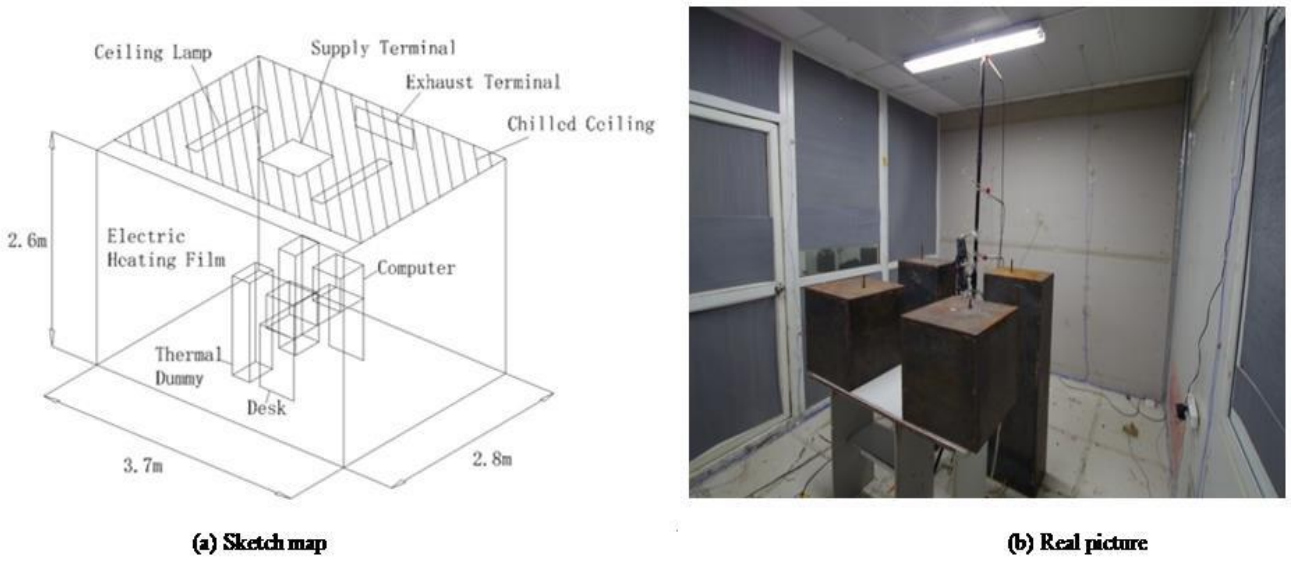

Fig.(2-5) Tested room studied by **Wu et. al., [73]**

Li and **Chen (2020), [74]** studied experimentally the capillary mat cooling with displacement ventilation system at different air flow rate. The tested room dimension were equal to (6×5×3.5 m). Three walls had stable conditions while ceiling and floor were isolated. The heat transfer coefficients for door and window (2.91 and 6.4 $W/m^2.K$) respectively. The capillary mat pipe diameter between (3 to 5 mm). The tests made in July and August under Chongqing (China) climate. The supply water temperature varied between (16-20^oC) and supply air temperature between (23-26^oC) with air velocity (0.27m/s). Nine cases were studied at different cooling load (between 55.2-74.3 W/m^2). They found that the dropped in supply water temperature from (20°C to 16°C) led to increase total heat flux by chilled ceiling from (10%) to (30%) and the temperature of supply water and air flow rate supply had a large influence on thermal environment in indoor zone.

2.3 Experiment and Numerical Studies

Bahman et. al. (2009), [75] investigated the air quality and energy saving for chilled ceiling with displacement ventilation (DV/CC) system and compared it with conventional systems under Kuwait climate in an office room space at dimension (4.59×4.96×3.80 m). The room had one door and two class windows. The supply diffuser located on the north wall. The chilled ceiling covered (80%) of ceil surface consisted of aluminum plate and copper pipes. Two experimental cases were considered with and without internal heat source at different total cooling load of (73.85 and 47 W/m^2) respectively. The air supply temperature for two cases was (23.5ºC) at velocity (0.25 m/s) and chilled ceiling surface fixed at (16ºC). (DV/CC) system was compared with a conventional one at (100%) and (30%) fresh supply air ratios. The software used in numerical was TRNSYS-2004. The experimental works done during August. Experimental and numerical results at the same thermal comfort level and (IAQ) showed that the energy consumption for (DV/CC) of (100%) fresh air system was less than (50%) of the conventional system energy consumption.

Taki et. al. (2011), [76] studied experimentally and numerically the performance of a suggested chilled ceiling technique combined with displacement ventilation. This technique depended on the fixed of honeycomb slat system on the bottom side of the chilled ceiling. Room dimensions was (5.4×3×2.8 m) located in Loughborough University (United Kingdom). The walls of the tested room was adiabatic with total cooling load varied as (15, 25, 35, 50 and 60 W/m^2). The air supply temperature was (19ºC) at flow rate (50l/s, ACH=4 1/h) and the chilled ceiling surface temperature varied as (12, 14, 16, 18 and 21ºC). Dimensions of the slats were (200 height, 100 wide and 2mm thick), it's fixed every (20mm) along the chilled ceiling. In this study, (Sabre-One) code was used in numerical analyses as CFD code. The results found that the natural convection suppressed by more than (80%) at slat depth to width ratio of (10).

Hui and **Leung (2012), [77]** investigated the system performance for chilled ceiling (thermal comfort and energy performance) in offices of an aircraft engineering company located in Lantau Island (Hong Kong) with area about (850 m^2) with nearly (60) staff as offices occupants. The parameters of thermal comfort were measured through one week in October (2011). The chilled ceiling surface temperature was varied between (21-22^{o}C). The clothing value and metabolic rate were assumed as (0.61 and 1.1) respectively. The indices of thermal comfort included operative temperature, predicted percentage of dissatisfied (PPD) and predicted mean vote (PMV) were calculated numerically. A software (VisualDOE 4.1) was used for numerical analyses. They found that the thermal comfort acceptable in most of the time by computing (PMV) and (PPD) varied between (0 to -0.7) and (5% to 15.3%) respectively. They concluded that the system was able to saving energy about (19.8%).

Rees and **Haves (2013), [6]** studied experimentally and numerically the temperature distribution and air flow of chilled ceiling with displacement ventilation in the room (5.43×3.08×2.78m) located in Hong Kong with isolated walls. Internal heat sources were simulated by using cuboid boxes with light bulbs at different watts. Twelve testes was made with different cooling load (small and large loads varied between 6 to 72 W/m^2 by floor area respectively). In the small load used single heat source located on the table in the tested room center, while in the large load used four heat sources on the tables seated symmetrically inside tested room. The air supply temperature, supply water temperature and air change per hour varied between (16.4-20^{o}C), (14-20^{o}C) and (1.5-5 1/h) respectively. CFX-FLOW3D software [CFDS (1996a) code] used in numerical analysis. They found that the thermal characteristics with and without chilled ceiling remained without change in a lower zone of room (between 0.15–1 m), while at height between (1.2-2.6m), the temperature profiles became very similar, with a small positive gradient in

temperature due to natural convection at ceiling caused enhanced mixing and reduced temperature gradients.

Kim (2016) [78], studied energy efficiency, thermal comfort and developed passive chilled beam performance. Dimension of test room was (5.46×5.18×2.74 m) located in Bowen Laboratory (Purdue University–U.S.A). The temperature of water supply was varied from (15^{o}C to 18^{o}C) at mass flow rate varied between (0.05-0.15 Kg/s). The temperature of supply air varied between (20 to 60^{o}C) at cooling and heating mode respectively with constant air flow rate at (600CFM). The experimental results collected between August to September 2016.The cooling capacity was depended on convective and radiative heat fluxes where the opposite side of the indoor space was perfectly insulated. The soft was used in numerical analyses was the TRNSYS by using a standard (k-ε) as turbulent model. They found that the passive chilled beam saved energy about (21%) compared with variable air volume (VAV) system. Based on the experimental results, the models predict total cooling capacity and chilled surface temperature of passive chilled beams were developed as follows:

$$Q_{cap}=Q_{rad}+Q_{con}=h_{rad}(T_{pan,m}-AUST)+h_{con}(T_{pan,m}-T_{ind}) \quad \text{….. (2-4)}$$

Ning et. al. (2016), [79] studied energy saving, chilled ceiling performance and air temperature distribution for cooling radiant ceiling which included thin air layer. Three optimized types of cooling radiant ceiling have been proposed to improve cooling capacity depending on the touching method between copper pipe and aluminum plate. The isolated tested room located in Zhuhai (China) at dimensions of (2.4×1.8×1.9m). The temperature of chilled water was (12^{o}C) at flow rate (0.107 m^3/h) and cooling load capacity was about (85.9 W/m^2). The thickness of thin air layer between aluminum plate and coper pipe was (1mm). FLUENT 6.3 used as CFD software to analyses numerical study. They deduced that the cooling radiant ceiling

with thin air layer had uniform temperature distribution and cooling capacity was increased by about (43-46%).

Yuan et.al (2016), [80] studied cooling ceiling radiant panel system to develop basic characteristic curve, and provided a simple process to calculate the system cooling capacity. The climate chamber dimensions (4.2×3.6×2.6 m) with window in the north wall located in a lager laboratory room. The experiment case included (12) tests, where in it design temperature varied from (24°C to 30°C). The temperature of supply water was varied between (14°C to 20°C) flowed in capillary tubes was fixed at (0.11 m/s). FLUENT software used to simulated test room by selected laminar model. They suggested the following correlation for the total cooling capacity:

$$q_{total} = 7.21(T_a - T_s)^{1.09} + 24\left[(T_s - T_{w,\sup}) - (T_s - T_{w,\sup})/3\right] \quad \ldots\ldots (2\text{-}5)$$

Shbeeb and **Mahdi (2016) [81]** made comparison among the four turbulence models (standard k-Ɛ, RNG k-Ɛ, realizable k-Ɛ, and SST k-ω) at different cases and different cooling load to find suitable model used with displacement ventilation system in Iraqi climate. Three cases were studied, two cases as isolated (3×1.75×3 m height) and non-isolated office room (4×3.5×3.75 m) with window at north wall while the third case as non-isolated classroom (7×4×3 m) with three windows at north wall. The supply air temperature and velocity for each case were calculated depending on internal and external heat gain. The air supply temperature and flow rate for three cases were (18, 20 and 18°C) and (20, 50 and 218L/s) respectively. GAMBIT (2.2.30) and (FLUENT 6.3.26) software used to build, meshed and numerically analyses for three cases. The results found that the (RNG.k-Ɛ) turbulent model was more accurate than other turbulent models for the predicted the air temperature distribution near heat sources, while for predicting air velocity distribution, the four turbulence models gave similarity for different cases.

Al-Tuarihi and **Mahdi (2017), [82]** made a comparison among three types of air supply diffuser with displacement ventilation in Iraqi climate. Three cases were studied depend on the shape of diffuser used in the tested room as (three way rectangular diffuser, semicircle diffuser and corner diffuser). The tested room dimensions were (4×3×3.2 m) with one window in south side located in Karbala (Iraq). The supply air temperature and flow rate for three cases were (20^{o}C and 122l/s) respectively. The experiments were done from May to July. ANSYS software used in numerical analyses with (RNG-kε) turbulent model. They found that the three way rectangular diffuser gave maximum value of air diffusion performance index (ADPI) and temperature effectiveness (ε_t) as (66% and 1.82) respectively. While, the corner diffuser gave minimum value of ADPI and (ε_t) as (35% and 1.7) respectively.

AbdulGhafor et. al. [83], (2019) studied experimentally and numerically the effect of air supply temperature and chilled ceiling surface temperature on the cooling capacity in an office room at dimension (4×3×3 m) under Baghdad (Iraq) climate. Eight cases were studied depending on different air supply temperature (18, 20, 22 and 24^{o}C) and chilled ceiling surface temperature at (16 and 20^{o}C). The office cooling load and air supply velocity were fix at (1600 W) and 0.75 m/s respectively. The chilled ceiling covered (54%) of ceiling area. ANSYS software used in numerical analyses. The results found that the cooling covered by displacement ventilation decreased by about (22.7 and 22.54%) when air supply temperature increased by about (33.3%) at chilled ceiling surface temperature equal to (16 and 20^{o}C) respectively. The cooling load covered by chilled ceiling increased by about (14 and 15.28%) at chilled ceiling surface temperature equal to (16 and 20^{o}C) respectively.

Recently **Jin et. al. (2020), [84]** investigated the dynamic change of chilled ceiling surface temperature by regulating the supply water flow rate to avoid condensation problem with other parameters as (water supply temperature, total heat dissipation and surface ceil temperature) were fixed. The tested room dimensions for the experiments were (5×3×2.4m), exterior south wall with a glass window of (3×1.4m). The water supply flow rate during experiments were supplied at three values (0, 0.12 and 0.24 m^3/h) with constant water supply temperature, total heat dissipation and surface ceil temperature as (16ºC, 240W and 26ºC) respectivelly. (FLUENT.2017) used as software in numerical study. The results explained that the smaller flow rate for water supply led to higher the ceiling surface temperature. The case at maximum water flow rate (0.24 m^3/s) had low risk of condensation due to decrease the difference temperature between chilled ceiling surface and indoor air.

2-4 Summary of Literature Review

Researches that have been reviewed previously are summarized in the following Tables (2-1, 2-2 and 2-3), as shown below. It was divided into the numerical studies, experimental studies and both experimental and numerical studies.

Table (2-1) Summary of numerical studies

Reference	Year	Place of study	Software	Main focus	Main findings
Ayoub. et. al. [47]	2006	Beirut (Lebanon)	Airpak	Variations of will temperature with height	Multilayer models were developed to represented thermal transport in enclosures conditioned.
Wang and Zhen [48]	2006	Xi'an (China)	ANSYS FLUENT	Made comparison between mixing and displacement ventilation with chilled ceiling	Combined chilled ceiling with displacement ventilation led to reduce the vertical temperature difference
Hao. et. al [49]	2007	Changsha (China)	-	Dehumidification and thermal comfort	Desiccant dehumidification succeeded to prevented condensation on the CC system
Karadag [50].	2009	Harran (Turkey)	ANSYS FLUENT	Relation between convective and radiative heat transfer coefficient	The ratio between radiative and convective coefficient (h_r/h_c) was ranged as (0.7-2.3)
Mateus and Grac. [51]	2015	Lisboa, (Portugal)	-	effects of (CC) in a room air flow and air temperature.	presented a set of (DV/CC) design charts that could assist system designers
Itani. et. al. [54]	2015	Beirut (Lebanon)	-	Saving energy consumption	The proposed system gained (28%) saving in operating cost and electrical power consumption during the cooling season.
Teodosiua. et. al. [55]	2016	Bucharest (Romania)	ANSYS FLUENT	thermal comfort and condensation risk	Ventilation system by suppled untreated air, thermal comfort in the office could not be properly assured only by radiant cooling ceiling systems.
Muslmani. et. al. [56]	2016	Beirut (Lebanon)	-	Prevent condensation on the ceiling.	The energy consumption was reduced by (49%), and prevented condensation problem.
Yang. et. al [57]	2017	Nanjing (China)	Airpak	position of radiant cooling surface	The position of radiant cooling surface at upper zone of the room was better thermal comfort.
Hormigos. et. al. [58]	2018	Madrid (Spain)	ANSYS FLUENT	influence of the presence of furniture to the local mean air age	Ventilation efficiency was affected by the furniture and it arrangement in a room.

Shan and Rim Et. al [59]	2018	Penn State University (USA)	ANSYS FLUENT	Thermal and ventilation performance	High cooling load absorbed by chilled ceiling (>50% of the total cooling) could disperses thermal stratification of displacement ventilation and increase draft rate in the occupied zone.
Tian. et. al. [60]	2019	Shanghai (China)	ANSYS FLUENT	condensation problem on chilled ceiling	Dew condensation on chilled ceiling can be alleviated by running the system for 300s before running ceiling.
Guo. et al [61]	2020	Shanghai (China)	ANSYS FLUENT	Condensation problem on chilled ceiling	after 12h operation, the condensation problem was prevented by operating chilled ceiling after air room temperature reached to 2^{o}C less than dew point
Amini. et. al. [62]	2020	Tehran (Iran)	ANSYS FLUENT	Condensation problem on chilled ceiling	Dehumidification coil up the chilled ceiling was succeeded to decrease the condensation on cooling panels.

Table (2-2) Summary of experimental studies

Reference		**Place of study**	**Main focus**	**Findings**
Fonseca. et. al. [63]	2010	Brussels (Belgium) .	mass flowrate and temperature of water supply to chilled ceiling.	The influence of surfaces temperature inside the room, especially the façade, was considerable.
Chakroun et. al. [64]	2011	Kuwait	Energy saving	Air mixing fraction up to (60%) led to reduce energy consumption (37%) compared with (100%) fresh air.
Chicote et. al [65]	2012	Valladolid (Spain)	Heat transfer coefficient and cooling capacity for radiant chilled ceiling.	The cooling output of the radiant cooling ceiling can neither be studied nor predicted based on the operating temperature such as the unique reference temperature and its corresponding parameter.
Ho [22]	2013	Hong Kong airport (China)	Thermal comfort in company offices by used chilled cieling	Most occupants found the temperature was quietly distributed, no uncomfortable draft and very low background noise level. The relative humidity is kept below 60%
Liu et. al [66]	2014	Beijing (China)	developing a solar thermoelectric cooled ceiling (STCC) system	The total heat flux and (COP) of the panels were strongly influenced by the ambient temperature, indoor temperature and operating voltage.

Kim and Leibundguta. [67]	2014	Zurich (Switzerland	cooling and dehumidification performance	Air cooling and dehumidification in the Airbox is a good process to provided cooling air and reduced the risk of condensation.
Itani. et. al. [68]	2015	Beirut (Lebanon)	Saving energy consumption	The proposed system gained 28.1% saving in operating cost and electrical power consumption during the cooling season.
Yuan. et. al [69]	2015	Tongji university (China)	develop a simplified correlation between the heat flux density and temperature difference	The destiny of heat flux can be measured independently in the different radiant plate structures.
Krajcik. et. al. [70]	2016	-	Ventilation effectiveness, air temperature and velocity distribution.	Thermal discomfort by high vertical temperature differences gave chilled ceiling the advantage over chilled floors for used with displacement ventilation.
Cholewa et. al [71]	2017	Lublin (Poland)	Coefficient of heat transfer	The value of heat transfer coefficient were being greater than the actual size, especially for the heated radiant ceiling.
Karmanna et. al. [19]	2018	California University (USA)	effect of ceiling fan with chilled ceiling to the cooling capacity.	The ceiling fan led to increase cooling capacity up (22%) when blowing upward.
Seblany. et. al. [72]	2018	Beirut (Lebanon)	humidity control	The relative humidity dropped in occupied zone by an average of (8.72%) within (12min) and energy saving of (24%) was achieved.
Wu et. al. [73]	2020	Dalian (China)	performance of chilled ceiling with mixing ventilation	The chilled ceiling had a slight effect on the indoor air distribution in a room with mixing ventilation system.
Li and Chen. [74]	2020	Chongqing (China)	Performance of capillary mat cooling with displacement ventilation	dropped in supply water temperature from (20°C to 16°C) led to increase total heat flux from 10% to 30%

Table (2-3) Summary of experimental and numerical studies

Reference	Year	Place of study	software	Main focus	Findings
Bahman et. al [75]	2009	Kuwait	TRNSYS	Air quality and energy savings in comparison with conventional systems	The DV/CC was not more efficient than a 30% fresh air, but it provided a better indoor air quality.
Taki et. al. [76]	2011	Loughborough (United Kingdom)	SABRE-ONE CODE	Performance of a new chilled ceiling technique	The ratio of slat depth to width of 10 for chilled ceiling raised the natural convection by more than 80%
Hui and Leung. [77]	2012	Hong Kong (China)	VisualDOE 4.1	Energy performance for chilled ceiling	Chilled ceiling led to improved energy consumption by (19.8%)

Rees and Haves. [6]	2013	Loughborough (United Kingdom)	NODAL model	temperature and air flow distribution in a room	Natural convection at the ceiling that caused enhanced mixing and reduced temperature gradients.
Kim [78]	2016	Zurich (Switzerland)	TRNSYS	Development of passive chilled beam performance prediction models.	Models that can predict the total cooling capacity and temperature of the chilled surfaces of passive chilled beams were developed.
Ning et. al. [79]	2016	Hunan (China)	ANSYS FLUENT	Energy saving and temperature distribution.	Add a thin air layer for cooling radiant ceiling panel led to a uniform surface temperature distribution and increased cooling capacity by (43- 46%).
Yuan et.al [80]	2016	Tongji University China	ANSYS FLUENT	coefficient for heat transfer and cooling capacity	provide a simple process to calculated cooling capacity
Shbeeb and Mahdi [81]	2016	Hilla (Iraq)	GAMBIT AND FLUENT	comparison among the four turbulence models in displacement ventilation system	RNG.k-Ɛ turbulent model was more accurate than other three turbulent models
Al Tuarihi and Mahdi [82]	2017	Karbala (Iraq)	ANSYS FLUENT	comparison between three types of supply diffuser in displacement ventilation system	Found that the three way rectangular diffuser is more suitable from two others type
Abdul Ghafor et.al [83]	2019	Baghdad (Iraq)	ANSYS FLUENT	effect of air supply temperature and chilled ceiling surface temperature on the room cooling capacity	Cooling covered by displacement ventilation decreased by about (22.7 and 22.54%) when air supply temperature increased by about (33.3%) at chilled ceiling surface temperature equal to (16 and 20^{o}C) respectively.
Jin. et. al [84]	2020	Tianjin University (China)	ANSYS FLUENT	Effect of supply water flow to condensation problem.	The flow rate regulation is not effective to prevent condensation
Present work	2021	Hilla (Iraq)	ANSYS AIRPAK	Study air age and thermal comfort parameters by compared two type of supply diffuser with used (DV/CC) system	The local air age increased with increase cooling load treat by the chilled ceiling. CO_2 concentration increase with height but this phenomena was fading with increase portion of cooling load treat by chilled ceiling. The semi-circle diffuser gave advantages in reducing air age and CO_2 concentration

2.5 Scope of the Present Work

The previous experimental and numerical studies had proved that the displacement ventilation system with chilled ceiling system gave a good indoor air quality and saving energy. However, the works deal with this problems are still limited. The combined (DV/CC) system under hot and dry climate, especially in the Middle East, not widely used. In addition to that, the combined ventilation system was not used in Iraqi buildings yet. Then, it's a good starting point for study the performance of this system in Hilla (Iraq) (hot and dry climate). Most of previous studies dealt with displacement ventilation and chilled ceiling system did not focused directly on the age of air and its effect on the thermal comfort. Therefore, this field needs to more investigation to study the effects of chilled ceiling on air age and thermal comfort parameters. Therefore, in this study the mean local air age is to be calculated through measurements and numerical simulation.

The present study will focus on:

- Effect portion of cooling load treated by chilled ceiling (η) by using (DV/CC) system in a hot and dry climate of (Hilla) on the age of air and human comfort.
- Examining effect of supply diffuser type on the age of air and human comfort.
- Examining the possibility of using the (DV/CC) system under Hilla climate (hot and dry) experimentally and numerically.

2.6 Originality Points of the Present Work

The present work investigates and predicts air age, airflow motion, air temperature distribution, CO_2 concentration, and indoor air quality parameters (PMV, PPD, and ADPI) in indoor rooms under a hot and dry climate by used combined displacement ventilation and chilled ceiling system. The data will be collecting by using experimental work and compare results with numerical data

obtained by adopting appropriate turbulence model in computational fluid dynamics (CFD). The originality of the present work can be summarized as:

1- There are limited studies that addressed combined displacement ventilation with chilled ceiling system to achieve the capacities demanded in many enclosed spaces applications under hot and dry climate (such as Hilla city (Iraq) climate).

2- The present study describes the concept of local mean air age by using combined displacement ventilation with a chilled ceiling system. The local mean age of air is to be calculated through measurements and numerical simulation. The use of this age provides a simple practical method for examining the air flow pattern in a closed indoor environment.

3- The study shows the effect of the shape of supply diffuser on thermal comfort parameters in displacement ventilation with a chilled ceiling system.

CHPTER THREE

EXPERIMENTAL WORK

Chapter Three

Experimental Work

Experimental measurements for displacement ventilation combined with chilled ceiling system (DV/CC) provide the most practical and dependable information for indoor air age, temperature distribution and other parameters at defined experimental points as (Temperature distribution effectiveness (ε_t), temperature different between head and foot (ΔT_{hf}) for persons and air exchange efficiency (η_a)).

This work conducted a set of full scale insulated office room to study the age of air and thermal comfort parameters with two types of supply diffusers (one way rectangle diffuser and semi-circle diffuser) to understand the thermal performance of chilled ceiling and displacement ventilation system under a variety of operating conditions in Hilla city (Iraq) climate. Hilla city located at Longitude (44.42^o) and Latitude (32.46^o). This city is characterized by its hot and dry climate in summer.

This was done by calculating the total cooling load and estimating the actual magnitude of the supply air flow rate, and supply air temperature needed for best ventilation. Set up and install chilled ceiling obtained to study the effect of it on air age and air temperature distribution around persons due to heat sources. All the experimental tests was made in July as primary tests and the measurement obtained in August and September

3.1 The Tested Room Setup

3.1.1 The tested room equipment

The experiments in this study consist mainly of a test room with a full-scale of chilled ceiling and displacement ventilation system to obtain data under steady state condition over a varied range of operating conditions. The method in which the variables vary is described in Section (3.2).

A set of a full scale office room at dimensions of (3×2.5×2.5 m) were conducted to study the local mean air age and temperature transport by adopting the (DV/CC) system. The insulated office room located in the laboratory building of Mechanical Engineering Department in Babylon university as shown in Figs.(3-1) and (3-2). The tested room delivered and setup by all the necessary equipment for (DV/CC) system.

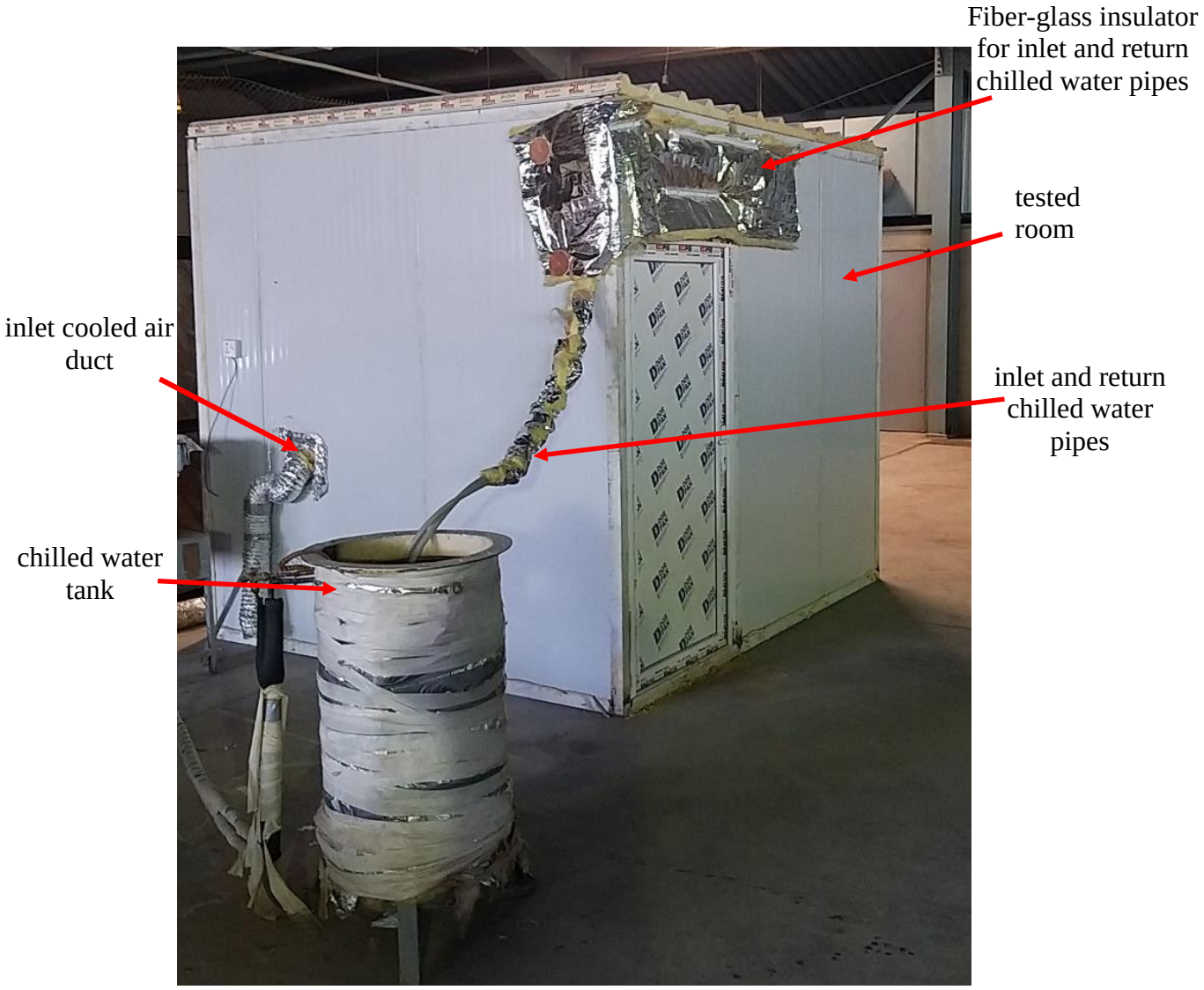

Fig.(3-1) Photograph of the experimental tested room from outside

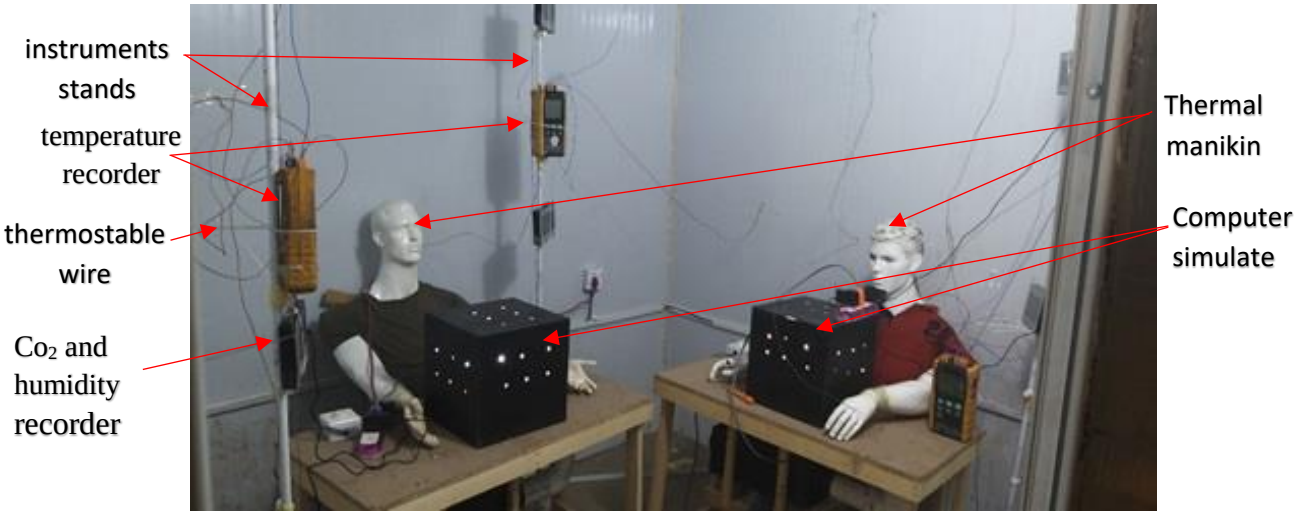

a-indoor the testing chamber

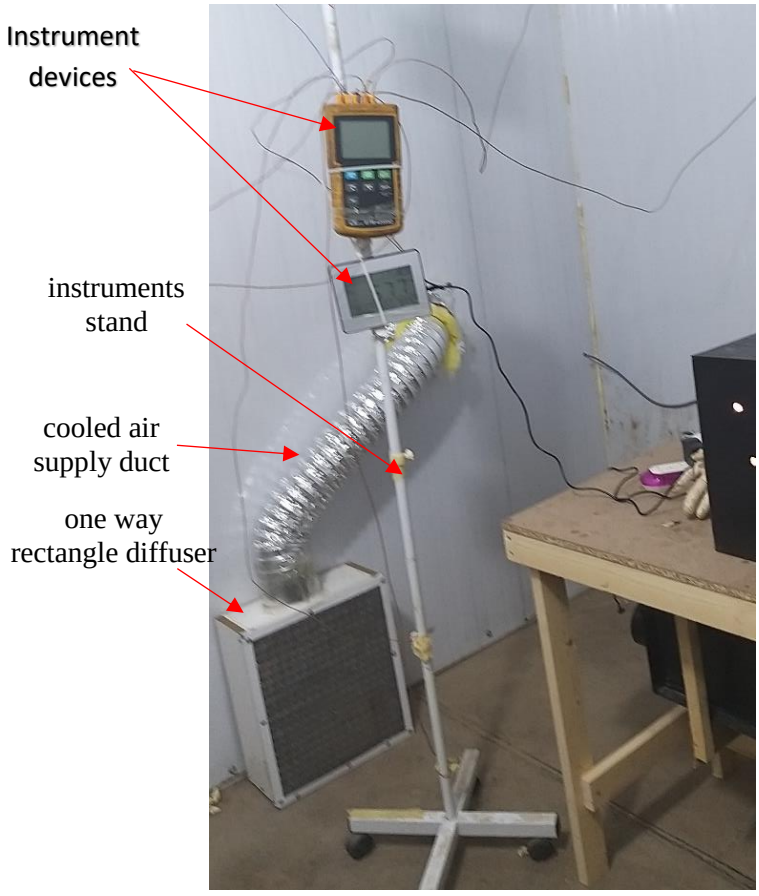

b-location of air supply diffuser at the north wall

Fig. (3-2) Photographs of the experimental tested room from inside

3-1-2 Room Configuration

Figs.(3-3) and (3-4) show the schematic diagram of the tested room model at dimension of (3×2.5×2.5 m). Tested office room has no windows, the walls and ceiling were made from insulated material (Sandwich panel with thermal conductivity of (K=0.14 W/m.K, **[85]**)). The displacement ventilation system was formed by a one way rectangle and semi-circular diffuser on the center line of the shorter north wall of the test room while the exhaust grille at the center of tested room ceil. Two persons, two computers and one overhead lamp are placed as heat sources equal to (370 W) (49.33 W/m^2 of floor area). Chilled ceiling puts at height (2.5m) from floor and represented (80%) of ceil area.

Table (3-1) gives a description of the configuration and location of the different objects in tested office room.

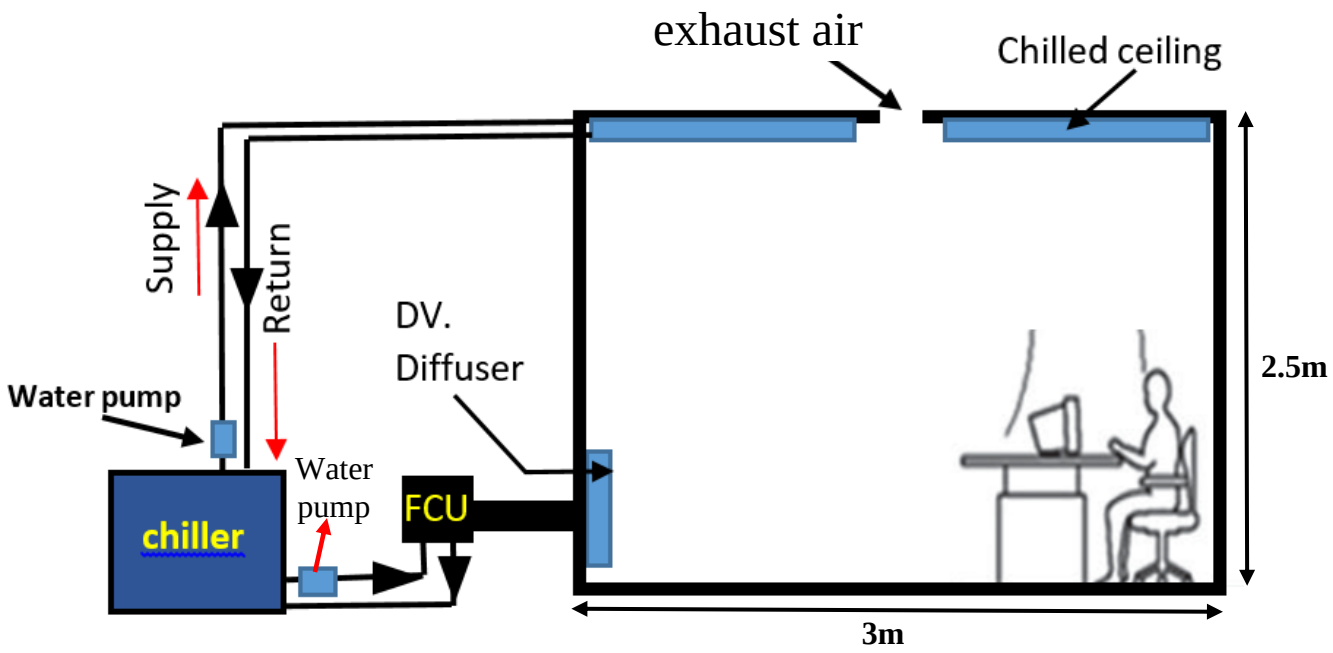

Fig.(3-3) Schematic diagram of the combined (DV/CC) system cycle.

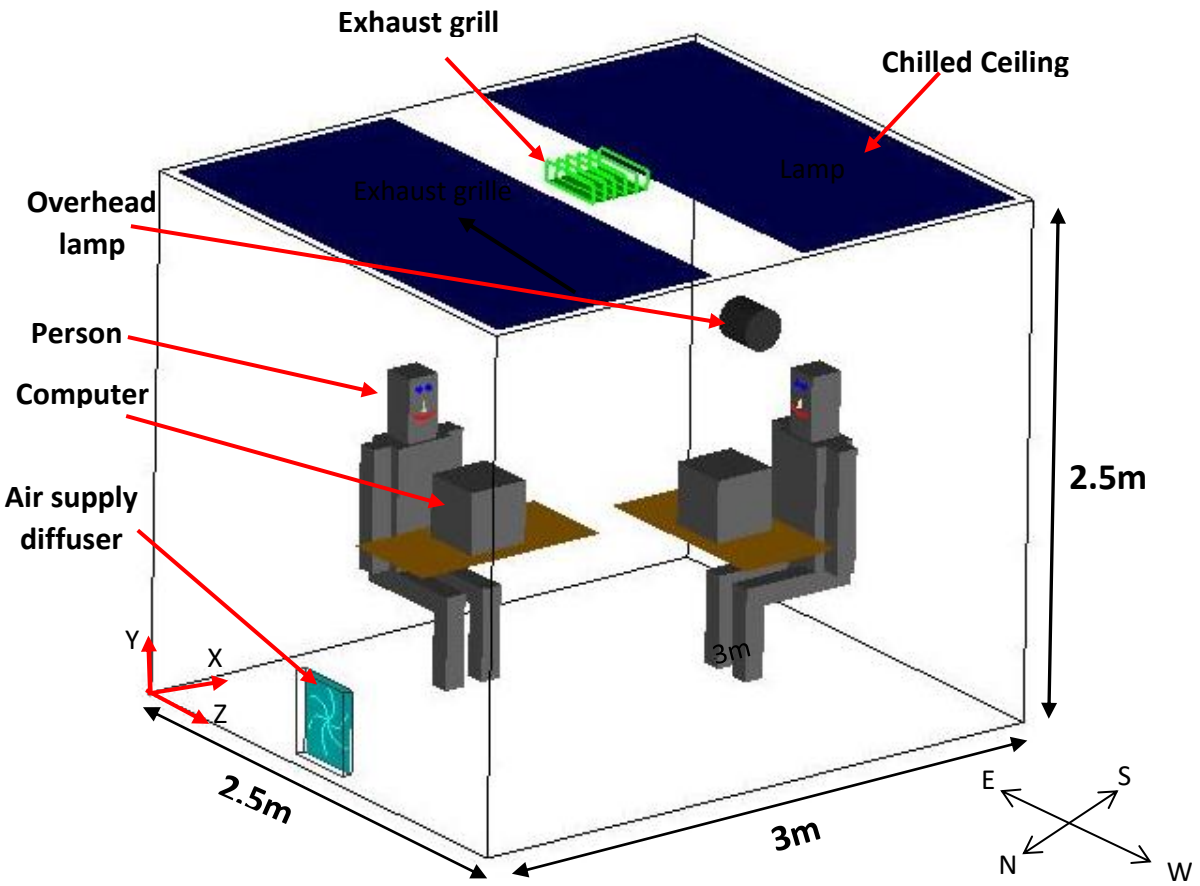

Fig.(3-4) Schematic diagram of the tested room components

Human body properties represented by using a seated manikin at breathing height level which is (1.1 m), **[42]** as shown in Fig.(3-5). The electric lamp was put inside of thermal manikin to generate heat about (75 W), **[86** and **87]**. The computers were simulated by using two wooden boxes had several holes with electric lamp to generate heat about (60 W) for each one, **[88]** as shown in Fig.(3-6).

Table(3-1) Test room configuration

Item	Location (m)			Size (m)			Heat (W)
	X	Y	Z	Δx	Δy	Δz	
Room	0	0	0	3	2.5	2.5	-
Rectangular diffuser	0.05	0.05	1.1	0.1	0.42	0.35	-
Sime-circular diffuser	0.05	0.05	1.1	Diameter 21 cm at height 42cm			-
Exhaust grille	1.35	2.5	1.1	0.3	0	0.35	-
Person1	1.25	0	0.25	0.4	1.15	0.125	75
Person2	2.75	0	1.25	0.125	1.15	0.4	75
Computer 1	1.1	0.7	0.6	0.3	0.3	0.3	60, **[88]**
Computer 2	2.1	0.7	1.1	0.3	0.3	0.3	60
Lamp	1.5	2.2	2.3	0.2	0.2	0.2	100, **[89]**
Table1	0.75	0.7	0.5	1	0.05	0.5	0
Table2	2	0.7	0.75	0.5	0.05	1	0
					Total cooling load		370W 49.33W/m^2 of floor area

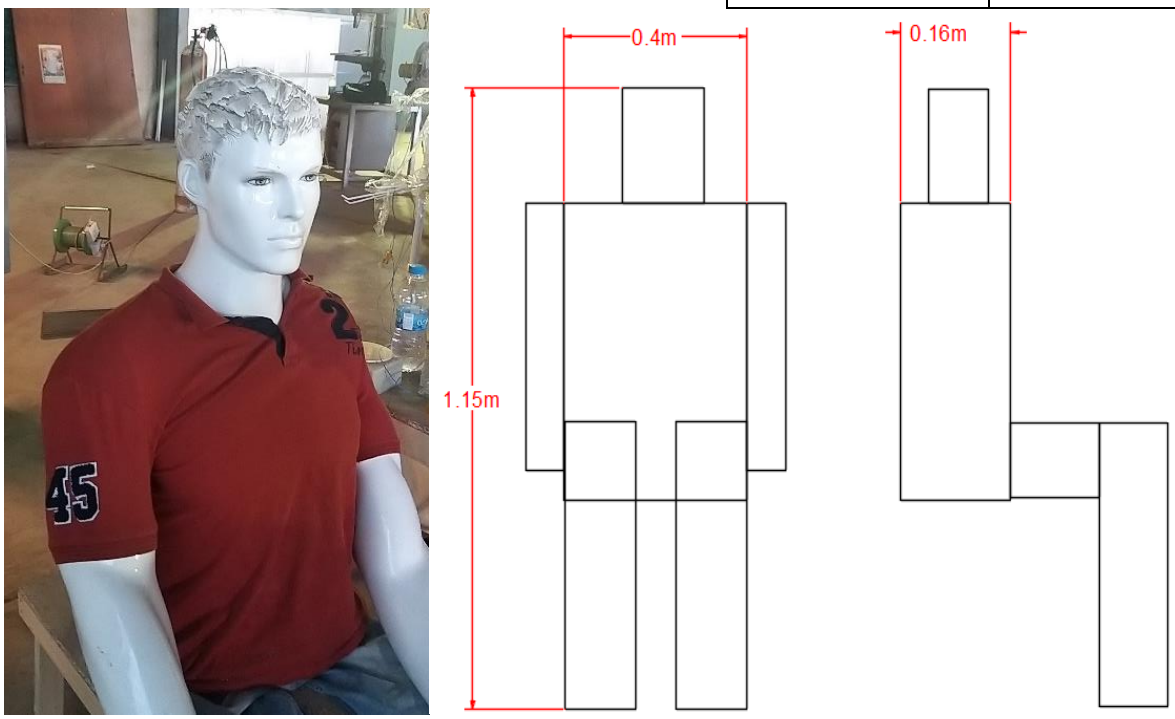

a- photograph b- front view c- side view

Fig.(3.5) Thermal manikin with its dimensions

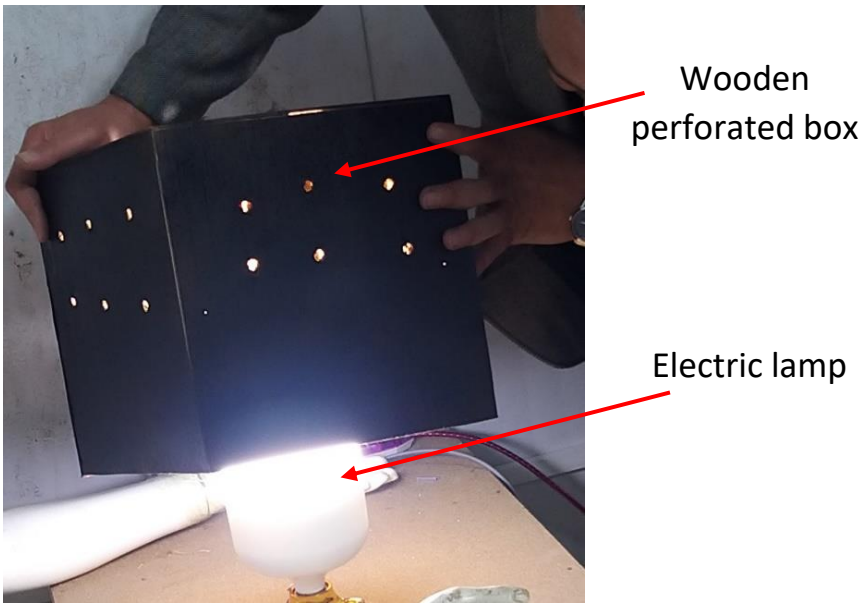

Fig.(3-6) Computer simulation with lamp to generate heat

3.1.3 Chiller unit

The cooled fresh air delivered by air fan coil unit which directly to treat the ventilation load. The chilled ceiling used chilled water to cover the load treated by it. The chilled water delivered from the water tank (evaporator unit) at volume ($0.2m^3$) connected to the chiller unit, (Fig.(3-7)).

Table (3-2) shows the chiller unit model used in this work. Chilled water moved inside plastic pipe at diameter (3/4in) to the chilled ceiling by used water pump as describe in section (3.2.2.2).

Table(3-2) Chiller unit model

Model	MT64-4VI
Capacity	4Ton
Manufacture	Danfoss Co./ France
Refrigeration	R22

a-condenser unit

b- chilled water tank (evaporator unit)

Fig.(3-7) Chiller unit

3.2 Experimental Conditions

An experimental study, the test rig as shown in Fig.(3-1) was designed and used in this work. The construction consists of the following steps in general:

1- Design and setup the environmental test room configured for heat sources and the air temperature, CO_2 and relative humidity sensors (The measurement devices will be described in section (3.5)). The work will focus experimentally on the insulated office room model.
2- Install and setup chilled ceiling (Radiant chilled ceilings type). It fixed at (80%) of ceil area at (2.5 m) height**.**
3- Install and setup displacement ventilation devices (one way rectangle diffuser and semi-circle diffuser as two types of air supply diffusers) combined with chilled ceiling system.
4- The mass flow rate and temperature for the cold water supplied are manually adjusted by used water valve (the range of cold water temperature described in sections (3.2.2 and 3.3)).
5- Human body properties are represented by using thermal seated manikin as shown in Fig.(3-5).
6- Decay method will be used to measure the local age of air as describe in section (3.3.2).

3.2.1 Supply air system for displacement ventilation

There are some steps to find ventilation flow rate, and supply air temperature for displacement ventilation applications. This will explained as follows:

Design guideline for the displacement ventilation systems, which consists of some steps as described by **Chen, and Glicksman, [90]**:

1- Determining the total cooling load as heat gain by the persons, equipment and overhead light.
2- Determining the ventilation flow rate (V_{DV}).

3- Determining supply air temperature (T_s).

4- Choice the suitable dimensions of air supply diffusers based on air supply velocity and flow-rate.

To design and operate of displacement ventilation system, the method developed by (**Chen**), **[90]** and by (**Skistad**), **[91]** were adopted as a most commonly references used as shown in sections (3.2.1.1 and 3.2.1.2).

ASHRAE Standard 55- 2010, **[42]** showed that the high difference between indoor air temperature and the air supply temperature caused local thermal discomfort due to draft. Then the difference between design indoor air temperature and air supply temperature should not exceed (5.5-6^{o}C), **[14]**.

3.2.1.1 Supply air flow rate

The supply air flow rate equals (100%) fresh air. The supply flow rate (V_{DV}) can be calculate by assuming the temperature difference between head and foot for persons (ΔT_{hf}) equal to (2^{o}C) and air density equal to (1.2 Kg/m^3). The flow rate calculating by, **[91]**:

$$V_{DV} = \frac{0.295q_{oe} + 0.132q_{l} + 0.185q_{ex}}{\rho C_p \Delta T_{hf}} \quad \text{….. (3-1)}$$

3.2.1.2 Supply Air Temperature

The supply air temperature for displacement ventilation can be calculated by using the following equation, **[91]**.

$$T_s = T_{rd} - \Delta T_{hf} - \frac{A_f CL_{DV}}{0.584(V_{DV})^2 + 1.2A_f V_{DV}} \quad \text{….. (3-2)}$$

Where:

$$CL_{DV} = q_{oe} + q_{l} + q_{ex} \quad \text{….. (3-3)}$$

$$CL_{DV} = \rho V_{DV} C_p (T_e - T_s) \quad \text{….. (3-4)}$$

The indoor air conditions for office room were designed as dry bulb temperature (T_{rd}) of (25°C due to ASHRAE.2011), **[92]**. The supply air temperature varied depended on the portion of cooling load covered by displacement ventilation (CL_{DV}) at constant air flow rate. For displacement ventilation the temperature difference between head and foot for person (ΔT_{hf}) equal to (2°C) (seated person) and (3°C) (standing person) due to (ASHRAE standard 55), **[42]**. The calculated values of air flow rate and air supply temperature for displacement ventilation which are computed by Eqs.(3-1) and (3-2) respectively are shown in Table(3-3). The computation procedures shown in (Appendix-A.1).

Table(3-3) Computed values of supply air temperature and flow rate for two experimental cases.

η (%)	**CL_{DV} (W)**	**V_{DV} (m^3/s)**	**T_s (°C)**
0	370	0.035	20
25	277.5	0.035	21.5
50	185	0.035	23
80	74	0.035	24

3.2.1.3 Air supply diffuser

In displacement ventilation, there are some steps must be satisfy such as thermal comfort, quiet operation and low velocity. Also the air is supplied at a low-velocity (between (0.2- 0.35m/s) as specified by **Awbi, [8] and Chen and Glicksman, [90]**). In this work the supply air velocity was assumed in this range as (0.25m/s) due to the small tested room volume.

Al-Tuarihi, [82] compared three types of air supply diffuser under Iraqi climate and found that the rectangle and circler diffusers gave acceptable performance. Then, in this work, two types of supply diffuser are used:

1- One way rectangle diffuser.

2- Semi-circle diffuser.

The area of diffuser can be calculated by assuming the air velocity is (0.25 m/s) at constant air flow rate (35L/s (74.1 cfm)) (this is the maximum flow rate needed at maximum load treated by displacement ventilation at (η=0) as shown in section 3.2.1.1). Then the effective area of supply air diffuser (A_s) is (0.14 m^2).

The diffuser was manufactured according to the specifications of the (PRICE.Co) specialized in the manufacture of the displacement air supply diffusers. The diffusers were made from wooden frame in the form of a rectangle and a semicircle face. The diffusers face made from aluminum plate at dimensions (37cm width and 42cm height) with (320) holes on its surface at diameter of (15 mm) as shown in Fig.(3-8). The aluminum plate with holes covered by metal mesh with small holes to ensure uniform air distribution over the effective air supply area. After that the aluminum plate with metal mesh fixed on the wooden frame to satisfy the shape of rectangle and semi-circle diffusers as shown in Figs.(3.9) and (3.10) respectively. All the side vents were closed to ensure that the cold air does not escape from it. The inlet air duct located at the top side of the wooden frame.

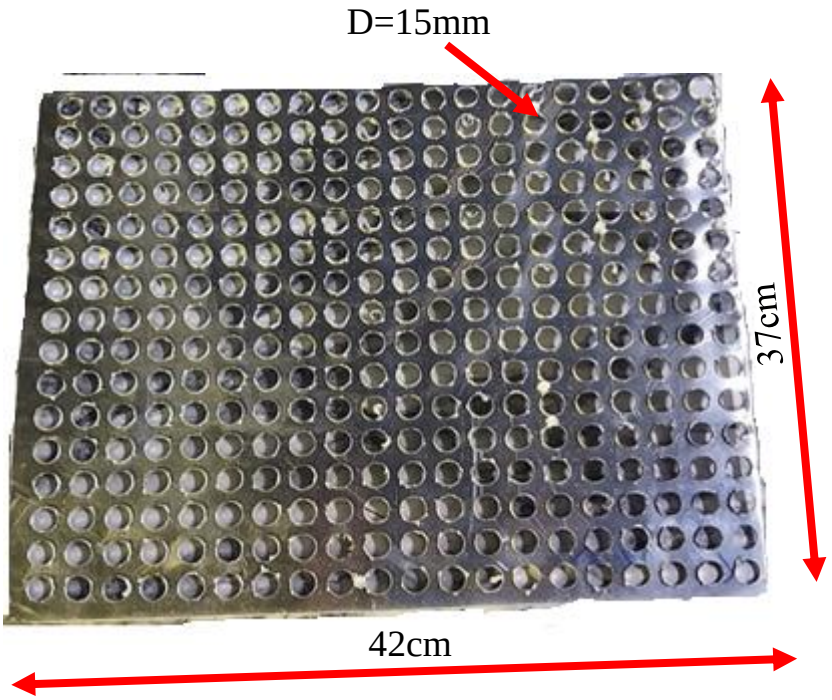

Fig.(3-8) Aluminum plate with holes used as affective area of air supply

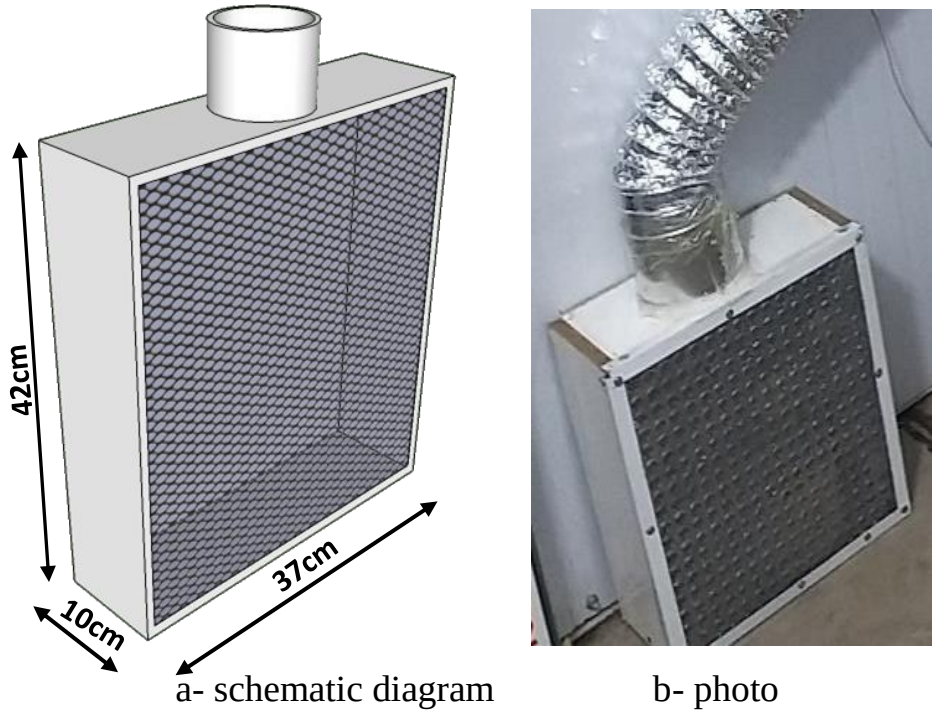

a- schematic diagram b- photo

Fig.(3-9) One way rectangle supply air diffuser

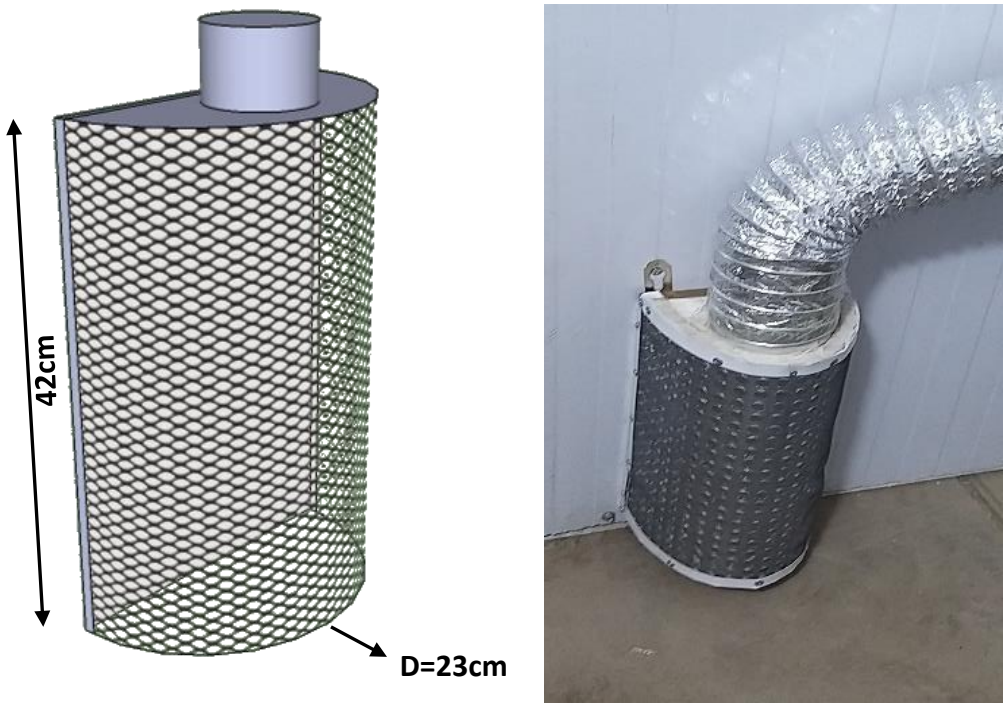

a- schematic diagram b- photo

Fig.(3-10) Semi-circle supply air diffuser

3.2.2 Chilled ceiling design

The radiant chilled ceiling used in this work due to its advantages with ventilation system as shown in section (1.3.2.1). A chilled ceiling surface provides space cooling by both radiation and convection **[93]**.

The cooling load removed by chilled ceiling (CL_{CC}) (convection and radiation heat transfer) can be calculated by measuring the water mass flow rate supplied and return water temperatures as given by, **[87]**:

$$CL_{cc} = \dot{m}_{ws} C_{P,w} (T_{w,r} - T_{w,s}) \quad \text{..... (3-5)}$$

The surface temperature of a chilled ceiling is an important factor affecting on problems of condensation, and regulation flow of supply chilled water is related to the fluctuation of surface temperature. Then, two methods used to avoid condensation problem, its:

1- The temperature of chilled ceiling surface (T_{CC}) should be at least (1°C) higher than the dew point temperature of indoor air to avoid condensation on chilled ceiling surface.
2- Running the displacement ventilation system for about 300s before running chilled ceiling as proving by **Tian et. al. (2019).**

By using psychrometric chart, the dew point temperature of indoor air for office room at (25°C) dry bulb temperature and (50%) relative humidity is (14°C) as shown in Fig.(3-11). Then the chilled ceiling surface temperature must be large than (15°C).

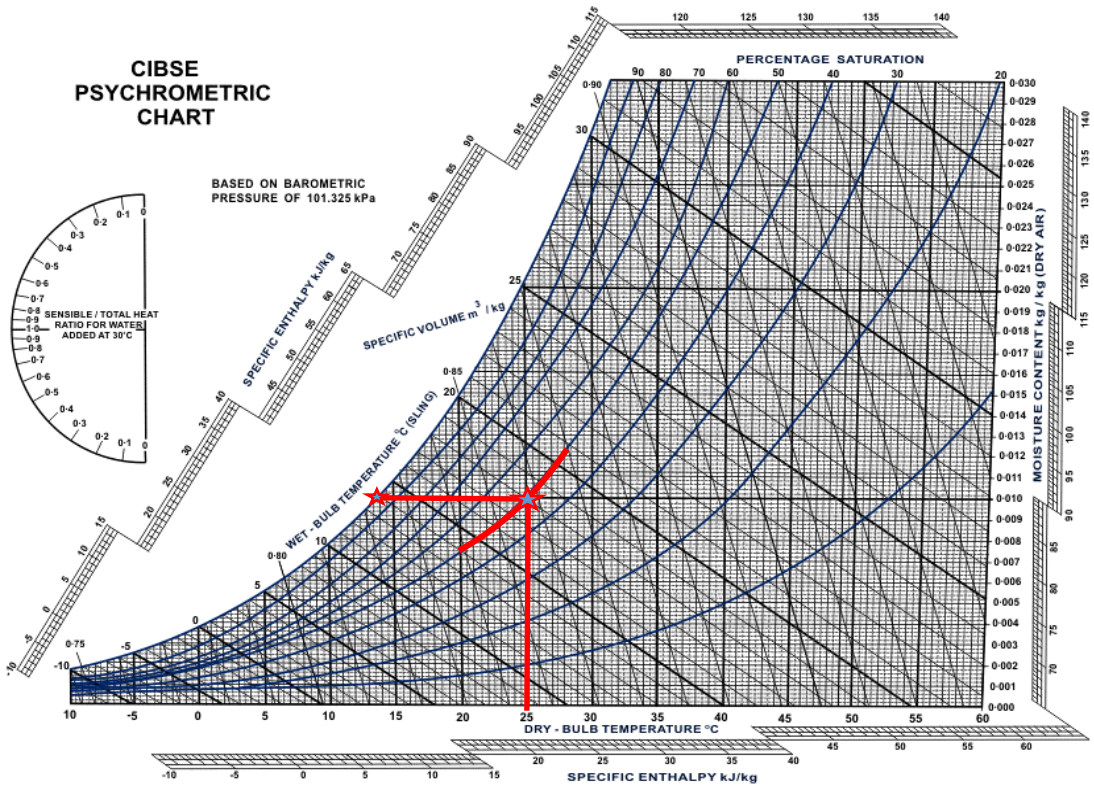

Fig.(3-11) Psychometric chart, **[92]**

The (η) which represents the ratio of the cooling load treated by chilled ceiling (CL_{CC}) to the total office cooling load given by, **[86** and **87]**:

$$\eta = \frac{CL_{cc}}{CL_{DV} + CL_{cc}} \quad \text{….. (3-6)}$$

The (η) values in experimental tests varied as (0, 25, 50 and 80%). In fact, η =0 means that a full displacement ventilation system is used.

3.2.2.1 Chilled ceiling plates

According to ASHRAE standard, **[93]**, the chilled ceiling consists of copper coil secured to the aluminum metal plate. Aluminum plate and copper pipe have high thermal conductivity are ((237 W/m.°C) for (AL) and (390 W/m.°C) for (Cu), **[93]**), addition to that the cooper is resistance to corrosion and ease to installation, then these materials is a good choice for used with a chilled water. The diameter of copper pipe is (1/2 in). The chilled ceiling plates cover about (80%) of the ceil area. There are four plates fixed at ceiling. The dimensions of each plate are (1.25 m (length) × 1.2 m (width) and 1 mm (thickness)). The back of each plate is covered by aluminum sheet and insulation made of glass wool (K= 0.04 W/m.°C) to prevent the heat loss and reduce the noise produces during the water passing through pipes according to ASHRAE standards, **[93]**.

3.2.2.2 Piping system

The piping system are divided into two types, the first type is supply and return water pipe as a main header to supply and return chilled water from the intake source to the chilled ceiling. These pipes made from plastic material at diameter and length at (3/4 in) and (20 m) respectively for supply and return pipes. The pipes covered by insulator to minimize the heat loss. The main header pipe is supply the child water for each chilled ceiling plate as alone to avoid irregular in plates temperature, and as the same method for collect and return main pipe as show in Fig.(3-12). The second type is the copper pipe at diameter (½ in) and (15m) length for each plate which used as thermal pipe in chilled ceiling plate. Fig.(3-13) shows the dimensions and specification of chilled ceiling plate with copper pipe.

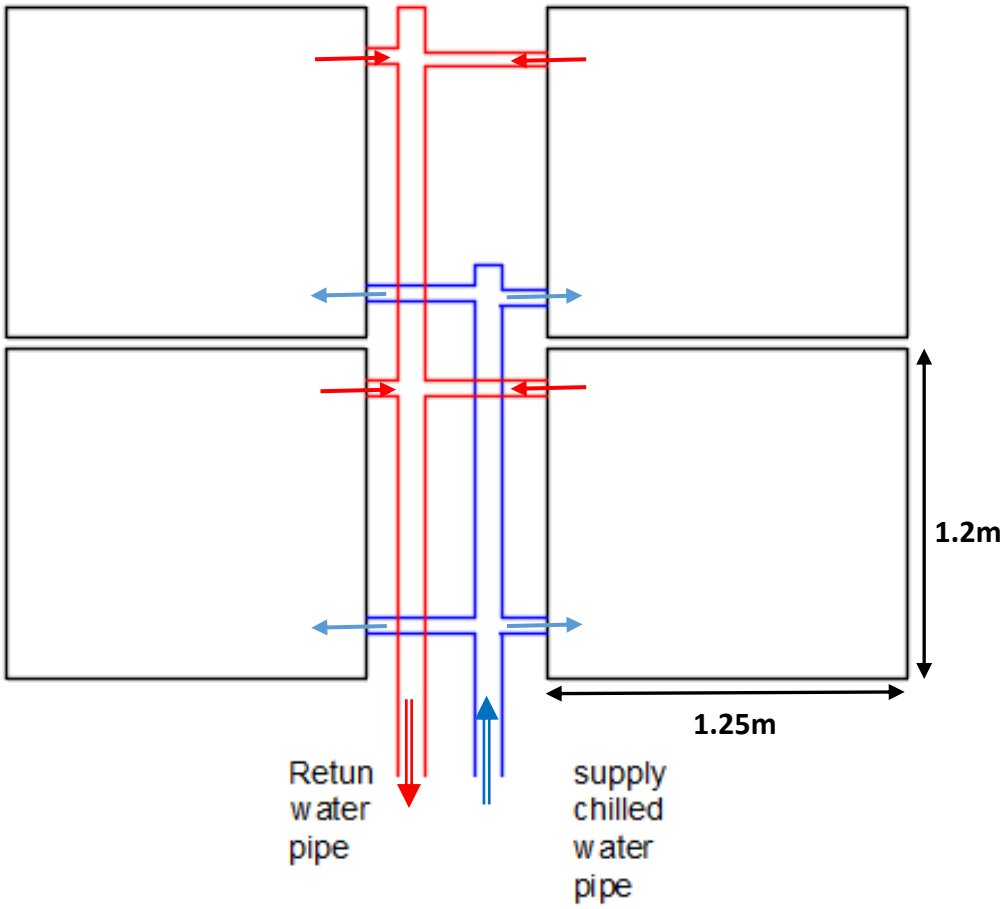

Fig.(3-12) diagram sketch for main piping system

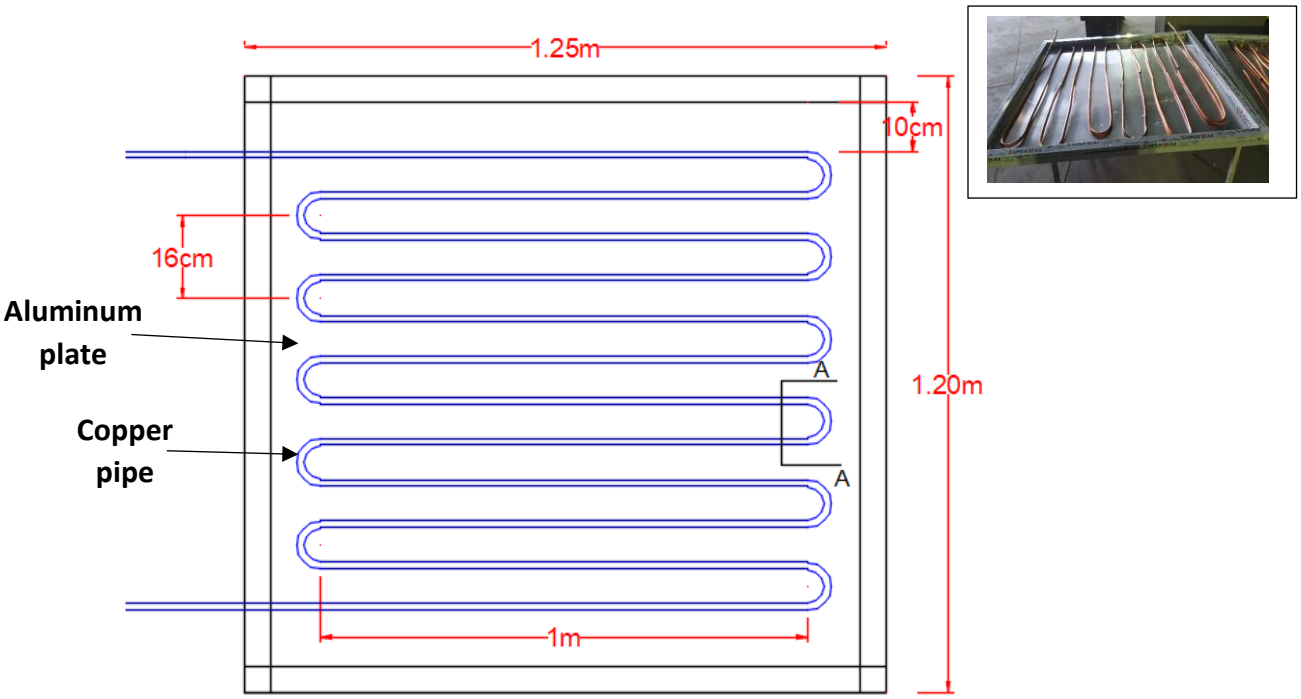

a-copper pipe matrex

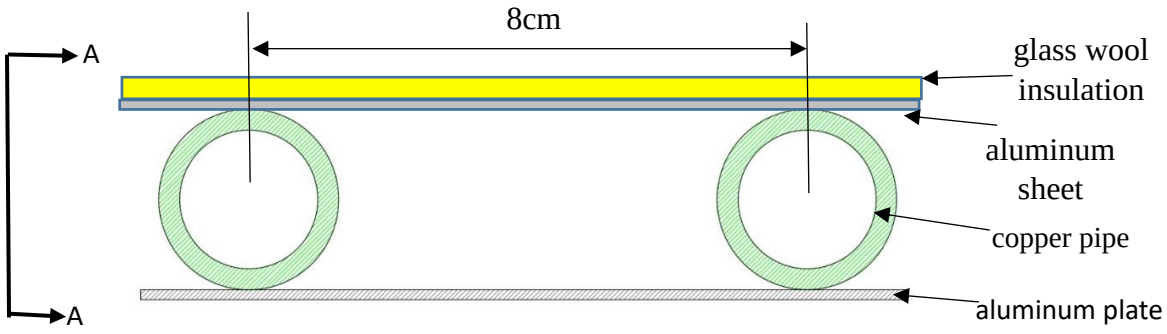

b-section of coper pipe arrengment

Fig.(3-13) Dimensions and specification of chilled ceiling plate with copper pipe

3.2.3 The water pump and piping size

The application of the chilled ceiling needs a pump to delivered chilled water from the chilled water tank to a pipe network of heat exchangers.

Copper pipes are used in most chilled water ceiling application due to its good resistance to corrosion and ease to installation, **[93]**. The diameters of pipes are depend on two main factors, its velocity of water flow and friction loss, **[94]**.

To estimate the friction pressure loss in copper pipes, the chart presented by ASHRAE 2009 are used, **[95]**. This chart is suitable for water temperature of (15.5°C) and can used up to (93.3°C).

The water mass flow rate can be estimated by using Eq.(3-8) depending on maximum cooling load removed by chilled ceiling in this study, which equals (296W) (80% of total cooling load) and assuming the difference between supply and return water temperature is (0.5°C). Therefore, from Eq.(3-8) the maximum value of water mass flow rate is (0.14 kg/s) divided on four chilled ceiling units. Then by using the charts in Figs.(3-14) and (3-15) the value of pressure drop in copper pipes and main plastic pipes were shown in Table (3-3).

Table (3-3) Pressure drop in copper pipes and plastic pipes

pipe and fitting	**Length (m)**	**Diameter (mm)**	**mass flow rate (Kg/s)**	**pressure loses (N/m^2)**
Copper pipe	60 m	12.5	0.035	6000
Copper elbow	44 elbow	-	0.035	431200
Plastic pipe	20 m	19.05	0.14	5200
Plastic elbow	8 elbow	-	0.14	78400
			Total	520800

From computed total pressure loss in pipes and mass flow rate, the minimum power requirement for the pump needed in this study can be calculated by used, **[96]**:

$$P_{water} = \frac{\text{water flow rate} \times \text{Pressure loses}}{\text{pump efficiency}} \qquad \ldots\ldots (3\text{-}10)$$

By assuming the efficiency of water pump is (80%), then the pump power is (98W).

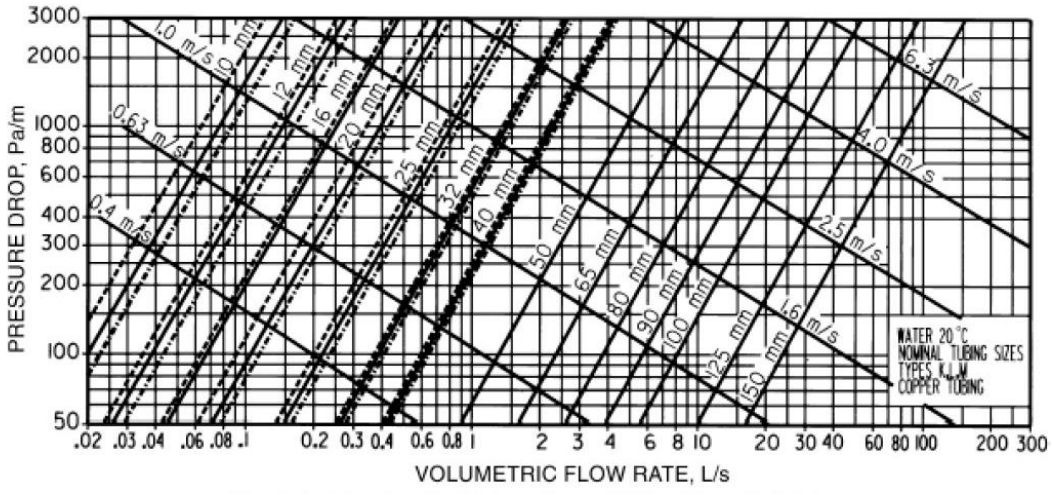

Fig.(3-14) Fraction loss for water in copper tube **[95]**.

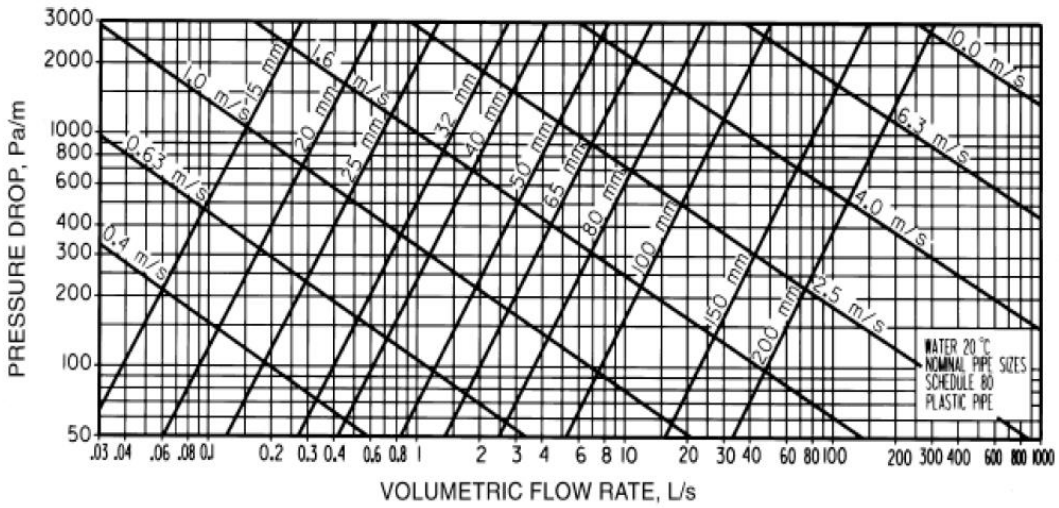

Fig.(3-15) Faction loss for water in plastic pipe **[95].**

3.3 Description of Cases Study

The experiments aim to investigate the displacement ventilation combine with chilled ceiling system at different operating conditions in a steady state and reported sets data of air age, carbon dioxide concentration and air temperature distribution. The operating conditions of the (DV/CC) system in the tested office room listed as follows:

1- The flow rate of air at diffuser is fixed at (35L/s (74.1cfm)).
2- The flow rate of chilled water supply to the chilled ceiling are (0.144, 0.288 and 0.5 m^3/h) depending on (CL_{cc}) values (25, 50 and 80%) respectively at constant water temperature difference.
3- The supply air velocity of displacement diffusers is fixed at (0.25 m/s) (for all the tests).
4- The supply temperatures of the chilled water and air are varied depending on the ratio of the cooling load removed by chilled ceiling (η).

3.3.1 Cases study

Two main cases were done with the (DV/CC) system and divided into eight tests as follow:

3.3.1.1 Case-I (used one way rectangle diffuser)

This case has four tests, one of these tests related with the displacement ventilation system operating alone, while other three tests with (DV/CC) system at different ratio of the cooling load removed by chilled ceiling (η) (as 25%, 50% and 80%). Supply air temperature and air supply flow rate for each tests can be calculated as shown in Appendix-A.1 at constant air flow rate (35 L/s) and design room temperature is (25°C). Table(3-4) shows the operating conditions for each tests in case-I , where (T_s, RH_s, $T_{w,s}$, $T_{w,r}$, V_{ws} and T_{cc}) are measured at experimental day for each test.

Table(3-4) Operating conditions for Case-I(Rectangular diffuser)

Test	η (%)	CL_{DV} (W)	CL_{CC} (W)	ACH (1/h)	T_s (°C)	RH_s (%)	$T_{w,s}$ (°C)	$T_{w,r}$ (°C)	V_{ws} (m^3/h)	T_{cc} (°C)
Test-1	0	370	0	6.7	20	72	-	-	0	-
Test-2	25	277.5	92.5	6.7	21.5	64	19.7	20.25	0.144	22.5
Test-3	50	185	185	6.7	23	57	18.4	18.93	0.288	21.2
Test-4	80	74	296	6.7	24	57	17	17.56	0.5	19.4

3.3.1.2 Case-II (used semi-circle diffuser)

This case has the same procedure for (case-I) but with semi-circle air supply diffuser. Table(3-5) shows the operating conditions for each tests in case-II , where (T_s, RH_s, $T_{w,s}$, $T_{w,r}$, V_{ws} and T_{cc}) are measured at experimental day for each test.

Table(3-5) Operating conditions for Case-II (Semi-circle diffuser)

Test	η (%)	CL_{DV} (W)	CL_{CC} (W)	ACH (1/h)	T_s (°C)	RH_s (%)	$T_{w,s}$ (°C)	$T_{w,r}$ (°C)	V_{ws} (m^3/h)	T_{cc} (°C)
Test-5	0	370	0	6.7	20	70	-	-	0	-
Test-6	25	277.5	92.5	6.7	21.5	66	19.2	19.8	0.144	22.3
Test-7	50	185	185	6.7	23	57	18.4	19.1	0.288	21.4
Test-8	80	74	296	6.7	24	54	16.8	17.27	0.5	19.5

3.3.2 Local air age measuring

In this, work the mean local age of air is measured to know the ability of the ventilation system to replace the old air in a room by new fresh air. Knowing the age of air provide us with much data as air quality, the effectiveness of replacing air

and assessing air pollution control, **[31** and **32]**. The minimum value of air age means better air quality.

The (CO_2) is used as a tracer gas to measure the mean local air age in the tested room by using the decay method. Most researchers used this method to record air age as **Meiss, [32]** and **Hormigos, [58].**

The decay method technique (as explained in ISO16000-8 standard, **[97]**) was depending on injecting (CO_2) into the tested room and record the time needed to change in (CO_2) concentration which record by (CO_2) recorder devices. The recorder devices put at different locations in the tested room (as shown in section (3.5.2)). The main advantages of this technique are, **[58]**:

1- It is an acceptable method in a single zone.
2- It is easy to record the initial concentration of tracer gas in the tested room.
3- This method is used when air change per hour (ACH) is below (10 h^{-1}).

3.3.3 Measuring CO_2 removing with time

ASHRAE standard, **[86]** suggested that the Co_2 concentration above (650ppm) is dangerous to human health. In this work, the effect portion of cooling load treated by the chilled ceiling (η) in removing CO_2 from the occupied zone is studied. The Co_2 is injected inside the tested room until it reaches (1000 PPm) as the initial value concentration. After that, the CO_2 concentration will be recorded by CO_2 recorder devices to estimate the time required to reach the normal concentration which is recorded outside the room at each value of (η).

3.3.4 Initial conditions and assumptions

The Initial conditions and assumptions for the two cases are summarized as follows:

1- The test room was built and installed as office room (3×2.5×2.5 m) which has no windows, the walls and ceil are insulated.

2- The chilled water flow rate in main pipes are varied from (0.04 to 0.14L/s) while the flow rate through each sub-circuit of the chilled water system varied from (0.01 to 0.035 L/s) at (η) varied from (25% to 80%) respectively.
3- Ambient temperature and relative humidity depending on the experimental test day under Hilla (Iraq) climate as shown in Table(3-6).

Table(3-6) CO_2 concentration, relative humidity and ambient temperature in tested days

Case	Test	Experimental day	T_{amb} (°C)	RH (%)	CO_2 concentration (ppm)
Case-I	Test-1	10/8/2020	41.5	32	488
	Test-2	12/8/2020	41	31	486
	Test-3	17/8/2020	42.5	29	484
	Test-4	19/8/2020	42	31	486
Case-II	Test-5	24/8/2020	39	34	484
	Test-6	26/8/2020	40	34	488
	Test-7	2/9/2020	38	33	486
	Test-8	7/9/2020	38	34	487

3.4 Measurement Devices Arrangement

Three vertical instruments stand are placed in the test room. Each stand has five levels at (0.1, 0.4, 1.1, 1.8, and 2.4m) as shown in Fig.(3-16). These heights represent the location of breathing levels (at 1.1 and 1.8m for set and stand person, **[42]**), while others represented air properties near floor and child ceiling. The three stands carried thermocouples, temperature recorder devices, CO_2 and humidity measurement devices to cover the environment in the occupied zone.

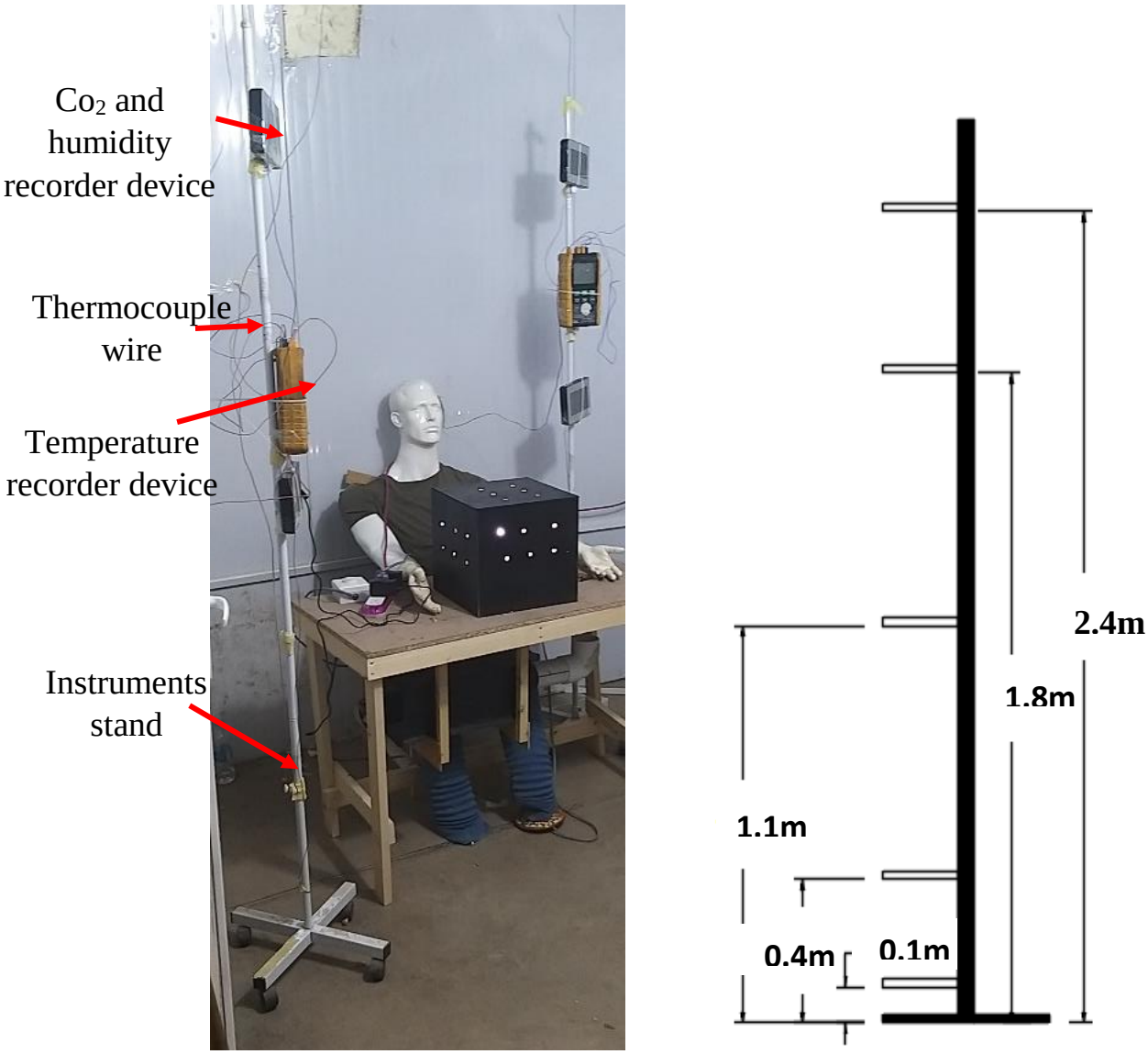

a- photograph of instruments stand b- schematic diagram of instrument stand

Fig.(3-16) Distribution of the measurement devices on instruments stand

The instruments stands inside the tested room were distributed at three locations as shown in Fig.(3-17). The first stand (stand-1) is located near the supply diffuser, while another stands (stand-2 and stand-3) near the thermal manikins. This method of distribution of instruments stand gives acceptable data to understand the air properties and pollutants concentration behavior in the occupied zone and near a person, **[6, 37]**.

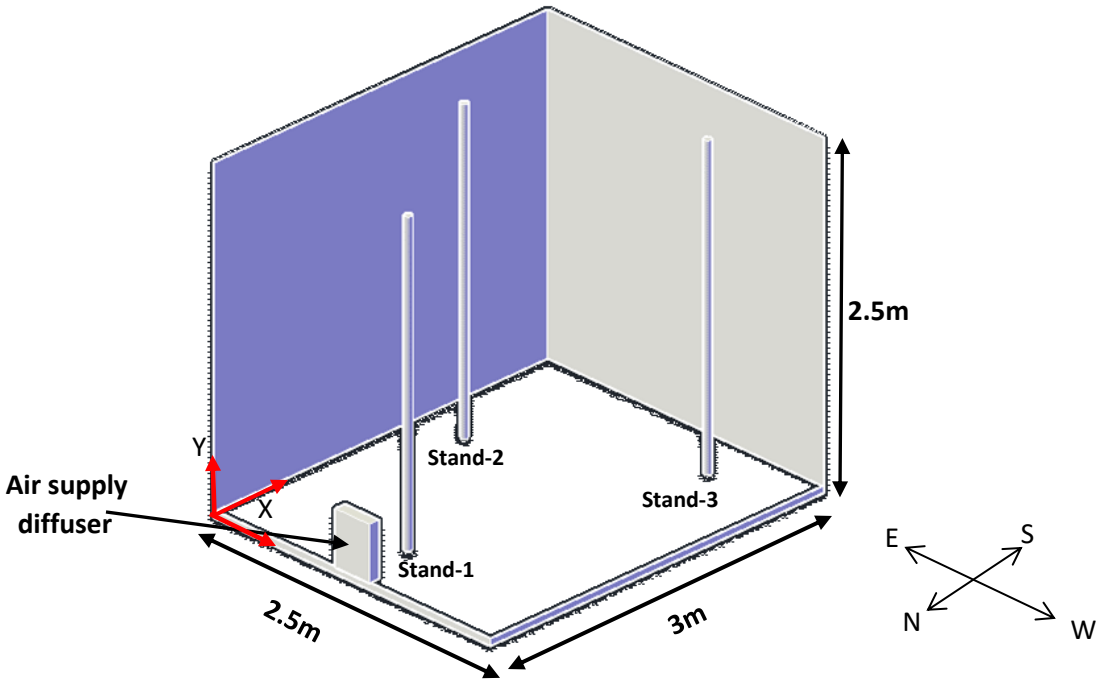

a- Isometric diagram of tested room with three instrument stands

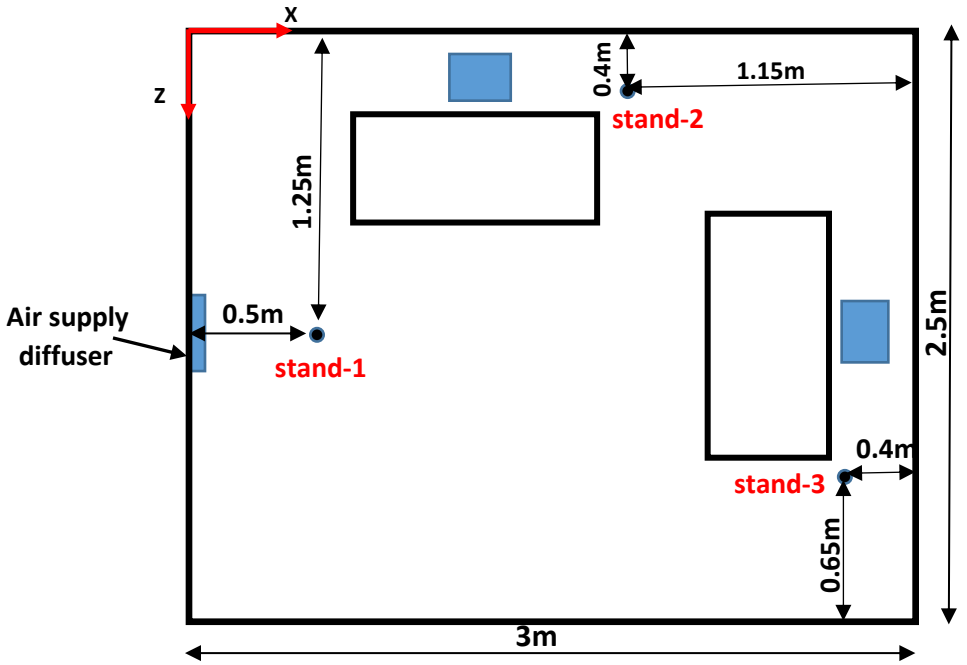

b-top view of tested room

Fig.(3-17) Locations of the three instrument stands inside tested room.

3.5 Measurement Devices

The measuring devices were divided into three main systems:

1- Air, walls, and chilled ceiling surface temperature measurement system.
2- CO_2 concentration and relative humidity measurement system.
3- Water flow rate and air supply velocity measurement system.

3.5.1 Air, walls, and chilled ceiling surface temperature measuring system

This system is based on a set of thermocouples (K-type) are fixed in the tested room. There are thirty-four thermocouples (K-Type) (Nickel_Chromium/ Nickel_Alumel) which are connected to three data temperature recorder devices (BTM4208 SD) as shown in Fig.(3-18), each supporting twelve channels. The measured temperatures are stored in a (RAM) and then it read by a computer. The properties of the temperature recorder device are summarized in Table(3-7).

Table(3.7) Properties of temperature recorder device

Type K thermometer range	-100 to 1300 ℃.
sampling time range	1 to 3600 seconds
Resolution	0.1ºC/1ºC
Accuracy	0.4%

During experiment tests the thermocouple sensors distributed as follow:

1- Fifteen sensors are placed on sidewalls and floor (three thermocouples fixed at each wall as shown in Fig.(3-19)). The temperature of each sidewall and floor were estimated as the average temperature of the three thermocouples temperature record. Four sensors are placed on the chilled ceiling surface and one sensor is fixed at the exhausted grill to measure the exit air temperature. The temperature of the chilled ceiling was estimated as the average temperature of the four thermocouples temperature record.

2- Fifteen sensors are fixed on a three vertical instruments stand as shown in Fig.(3-20) to allowed vertical temperature distribution in the tested room (each stand has five thermocouple sensors at different height (0.1, 0.4, 1.1, 1.8 and 2.4m) as shown in Fig.(3-18)).

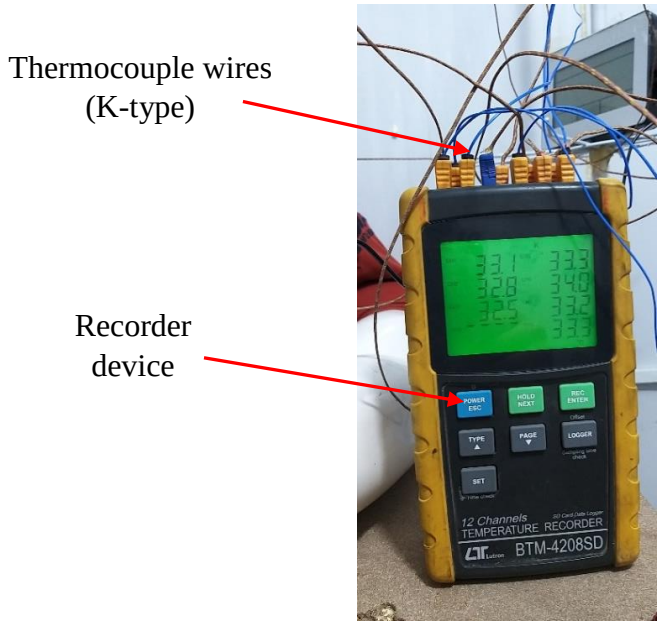

Fig.(3-18) Temperature recorder device (BTM4208 SD)

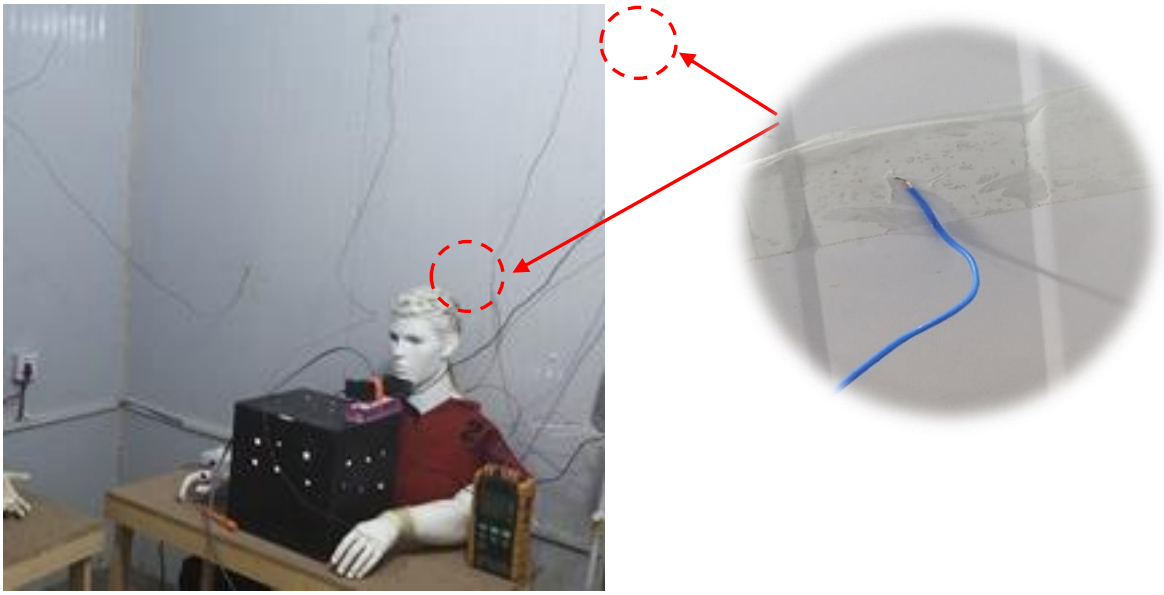

Fig.(3-19) Fixed thermocouple wire on the tested room wall

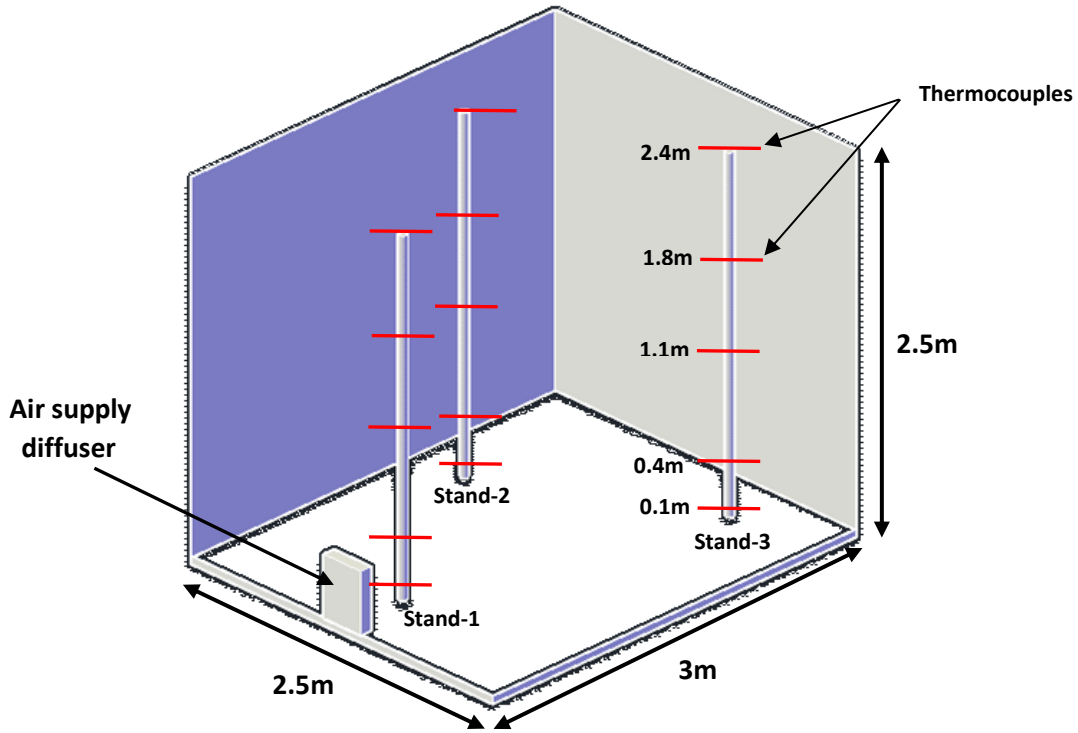

Fig.(3-20) Thermocouple sensors location on the three instrument stands

3.5.2 CO_2 concentration and humidity measuring system.

This system is based on a set of (CO_2 and humidity recorder devices) as shown in Fig.(3-21). The properties of these devices are summarized in Table (3-8). Special software was attached with the device through which all recorder data can be

download by USP cable to the computer. These data are arranged in a form of a table in (Excel). The device provides the ability to specify the interval time period between each reading. The certificate of compliance is shown in Appendix (B.3).

The devices were fixed at six points in different locations of test room at represented breathing levels for the sitting (1.1m) and standing person (1.8m). These points are divided as (0.5, 1.1, 1.25m), (0.5, 1.8, 1.25m), (1.85, 1.1, 0.4m), (1.85, 1.8, 0.4m), (2.1, 1.1, 1.85m) and (2.1, 1.8, 1.85m) as shown in Fig,(3-22).

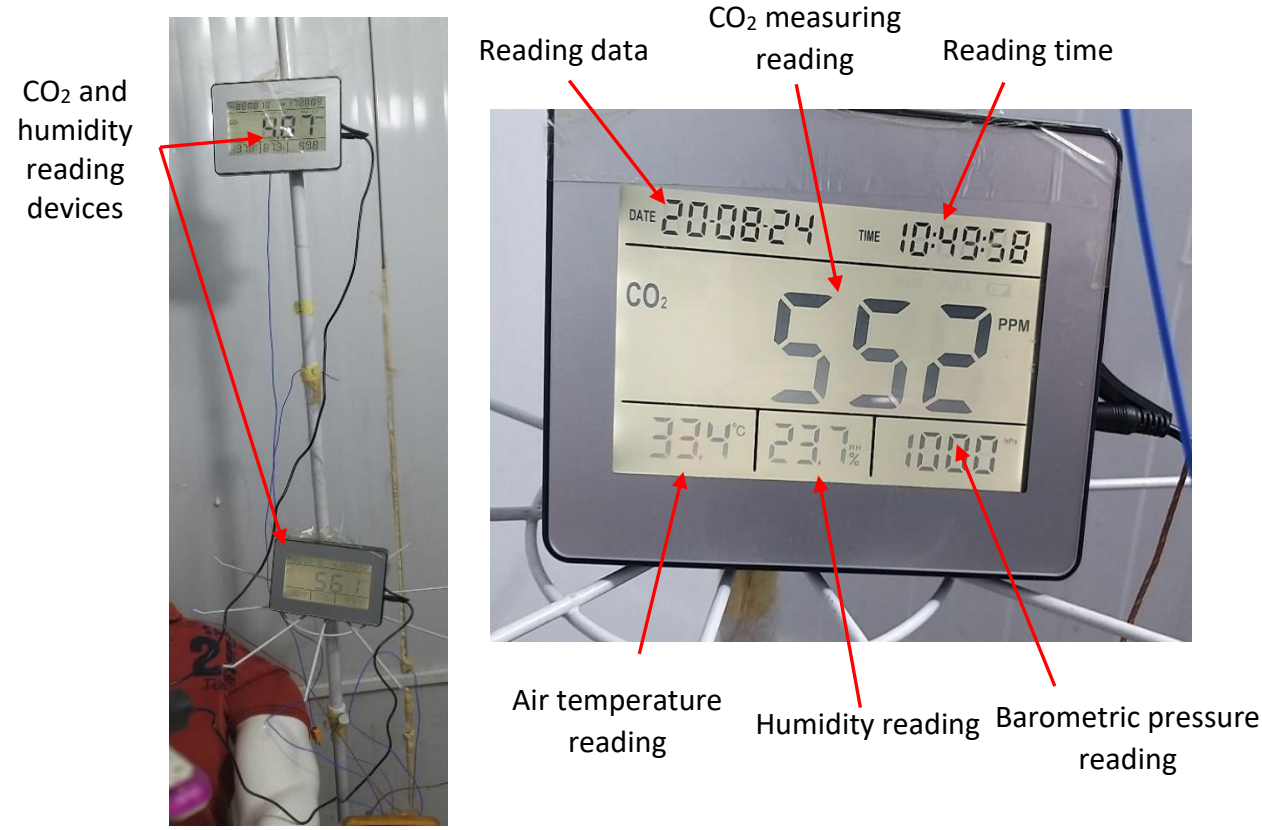

a- fixed the device on the stand b- recorder device

Fig.(3-21). CO_2 and humidity recorder devices

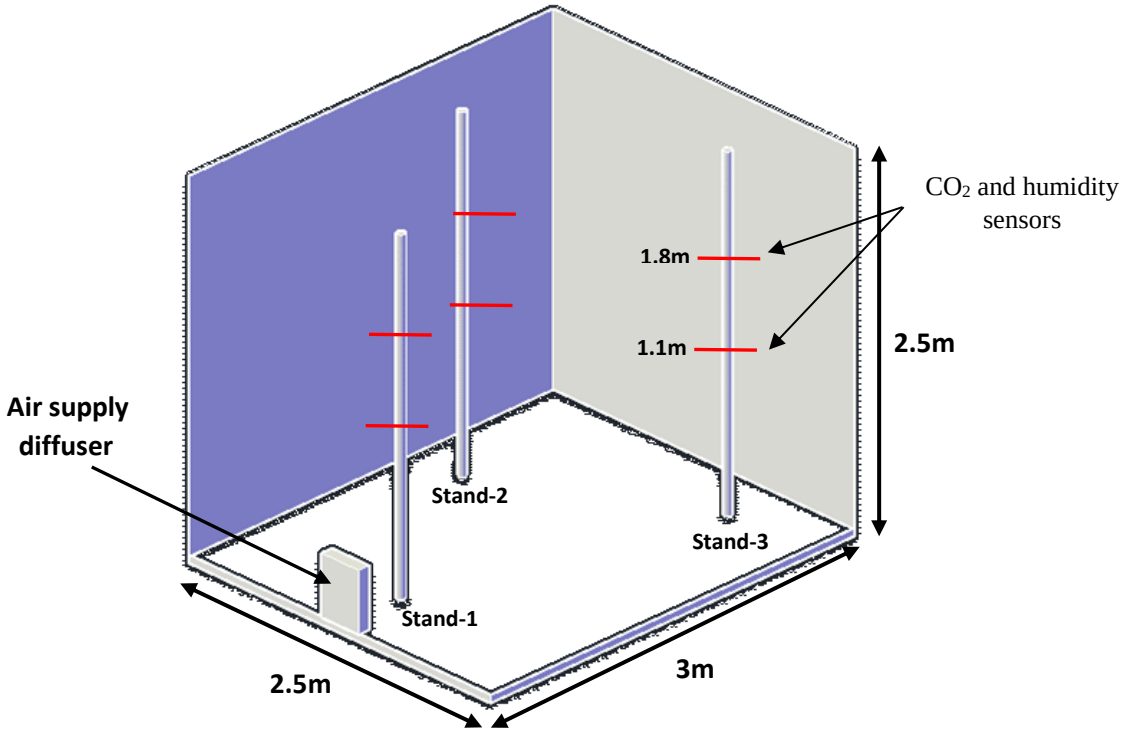

Fig.(3-22) CO_2 and humidity sensors location on the three instrument stands

Table.(3.8) Properties of CO_2 and humidity recorder devices

Carbon Dioxide reading	Range	0-9999 (ppm)
	Accuracy	±5 (ppm)
	response time	10 sec
Humidity reading	Range	0- 99.9%
	Accuracy	±2%

3.5.3 Water flow rate and air supply velocity measurement system

3.5.3.1 Flowmeter device

Flowmeter is used to measure the water flow rate supplied to the chilled ceiling. Flowmeter was positioned after the water pump as series with main plastic pipe. A control water valve is used to adjust the required water flow rate for each value of (η). Platon flowmeter device was used as shown in Fig.(3-23). The device range is between (0-10L/min) and accuracy is (±1.25%). This device is chosen due to the

maximum value of water flow rate in the main plastic pipe at (0.14L/s (8.4L/min)). Appendix (B.2) shows the calibration details of the flowmeter device.

Fig.(3-23) Water flowmeter device

3.5.3.2 Thermos-anemometer device

Air supply temperature and velocity were measured by (thermos-anemometer 8901) device by placing the device's fan in front of the air supply diffuser as shown in Fig.(3-24). This device has the ability to measure temperature, velocity and volume of air. The accuracy and resolution for air velocity were (±2%) and (0.01m/s) respectively with response time is (1s). The accuracy and resolution for air temperature are (±0.6°C) and 0.1 (ºF/ºC.). The device has a fan connect with it. The air velocity and temperature are reading after placing the fan in the stream of air (in the X-direction) near of diffuser and wait until the reading is stable.

Fig.(3-24) Thermos-anemometer device

3.6 Measurement Procedures

Measurement Procedures can be summarized as follows:

1- Decay method will be used to measure the local mean age of air at the study state. The air entering the room is marked with a gas (the tracer gas used in this work is CO_2), and the concentration of the tracer gas is recorded at the location of interest. The time needed to record the concentration is the air age. This method assumed that the tracer gas behaviors the same as the air.

2- Temperature distribution with height was measured at the steady-state condition at (15) points distribution and different locations in the occupied zone.

3- The relative humidity is measured at the steady-state condition at six points in the occupied zone.

4- The concentration of carbon dioxide measured every (100 sec.), starting from (1000 ppm) at the moment that (DV/CC) system reached to the steady state to observe the unique time to reach the natural concentration supply by air diffuser (ambient concentration).

Finally, the thermal comfort parameters as temperature effectiveness, air temperature distribution, (ADPI), (PMV) and (PPD) can be studied after collected the required experimental results.

CHAPTER FOUR

MATHEMATICAL MODELLING
AND
NUMERICAL ANALYSIS

Chapter Four
Mathematical Modelling and Numerical Analysis

The numerical method of calculating air age and thermal comfort parameters in a room has the advantages that the geometry of the room and its boundary conditions can be easily varied and that the details information is generated for the whole fields for temperature and velocity. The aims of making numerical analysis of the study cases in this work are:-

- To study air age and thermal comfort parameters in the experiments study cases in further details.
- To generate more sets of data for other rooms' geometries.

The numerical simulation aims to solve the mathematical equations related to a study cases that depend on fundamentals conservation laws (continuity, momentum and energy equations).

Six cases are studied numerically as shown in Table(4-1).

Table (4-1) description of numerical study cases

Cases	No. of tests	Case study	Discerption
Case-I	Tests 1-4	Experimental and Numerical study	Insulated office room with rectangular diffuser at different value of (η)
Case-II	Tests 5-8	Experimental and Numerical study	Insulated office room with semi-circle diffuser at different value of (η)
Case- III	Tests 9-12	Numerical study	Non-insulated office room with rectangular diffuser at different value of (η)
Case- IV	Tests 13-16	Numerical study	Non-insulated office room with semi-circle diffuser at different value of (η)
Case- V	Tests 17-20	Numerical study	Non-insulated classroom with rectangular diffuser at different value of (η)
Case- VI	Tests 21-24	Numerical study	Non-insulated classroom with semi-circle diffuser at different value of (η)

4-1 CFD Models

4.1.1 CFD software

The commercial (CFD) software used in this study is (AIRPAK.3.0.16). This software is easy, quick and accurate to use as a design tool. It simplifies the applications related to the airflow art by modeling technology to design and analysis ventilation systems which are required for deliver, thermal comfort, indoor air quality (IAQ), pollution and air conditioning, health and safety solutions, [**99]**.

Many researchers that studied the (DV/CC) system field had used (AIRPAK) software in numerical analysis such as **Gao [44], Ayoub [47], Yang [55], and Liang [100]** to predict air velocity and temperature distribution in the displacement ventilation process.

4.1.2 Governing equations

The Reynolds Averaged Navier_Stokes equations which govern the continuity, momentum and energy equations at constant density, steady, incompressible and three dimensional flow in a cartesian coordinate can be presented as follows, **[101]**:

1- Conservation of mass (continuity equation):

$$\frac{\partial}{\partial x}(u)+\frac{\partial}{\partial y}(v)+\frac{\partial}{\partial z}(w)=0 \qquad \ldots. (4\text{-}1)$$

2- Conservation of momentum:

X.direction (U.momentum):

$$\frac{\partial}{\partial x}(\rho uu)+\frac{\partial}{\partial y}(\rho uv)+\frac{\partial}{\partial z}(\rho uw)=-\frac{\partial p}{\partial x}+\frac{\partial}{\partial x}(\mu\frac{\partial u}{\partial x})+\frac{\partial}{\partial y}(\mu\frac{\partial u}{\partial y})+\frac{\partial u}{\partial z}(\mu\frac{\partial u}{\partial z})$$

$$+\frac{\partial}{\partial x}(-\rho\overline{u'u'})+\frac{\partial}{\partial y}(-\rho\overline{u'v'})+\frac{\partial}{\partial z}(-\rho\overline{u'w'})+\rho g_x \qquad \ldots. (4\text{-}2)$$

Y.direction (V.momentum):

$$\frac{\partial}{\partial x}(\rho uv)+\frac{\partial}{\partial y}(\rho vv)+\frac{\partial}{\partial z}(\rho vw)=-\frac{\partial p}{\partial y}+\frac{\partial}{\partial x}(\mu\frac{\partial v}{\partial x})+\frac{\partial}{\partial y}(\mu\frac{\partial v}{\partial y})+\frac{\partial}{\partial z}(\mu\frac{\partial v}{\partial z})$$
$$+\frac{\partial}{\partial x}(-\rho\overline{u'v'})+\frac{\partial}{\partial y}(-\rho\overline{v'v'})+\frac{\partial}{\partial z}(-\rho\overline{v'w'})+\rho g_y \quad \text{…. (4-3)}$$

Z.direction (W.momentum):

$$\frac{\partial}{\partial x}(\rho uw)+\frac{\partial}{\partial y}(\rho vw)+\frac{\partial}{\partial z}(\rho ww)=-\frac{\partial p}{\partial z}+\frac{\partial}{\partial x}(\mu\frac{\partial w}{\partial x})+\frac{\partial}{\partial y}(\mu\frac{\partial w}{\partial y})+\frac{\partial}{\partial z}(\mu\frac{\partial w}{\partial z})$$
$$+\frac{\partial}{\partial x}(-\rho\overline{u'w'})+\frac{\partial}{\partial y}(-\rho\overline{v'w'})+\frac{\partial}{\partial z}(-\rho\overline{w'w'})+\rho g_z \quad \text{…. (4-4)}$$

Where the terms

$(\frac{\partial}{\partial x}(-\rho\overline{u'u'})+\frac{\partial}{\partial y}(-\rho\overline{u'v'})+\frac{\partial}{\partial z}(-\rho\overline{u'w'}))$, $(\frac{\partial}{\partial x}(-\rho\overline{u'v'})+\frac{\partial}{\partial y}(-\rho\overline{v'v'})+\frac{\partial}{\partial z}(-\rho\overline{v'w'}))$ and

$(\frac{\partial}{\partial x}(-\rho\overline{u'w'})+\frac{\partial}{\partial y}(-\rho\overline{v'w'})+\frac{\partial}{\partial z}(-\rho\overline{w'w'}))$ represented the turbulent Reynolds stress for flow in X, Y and Z direction respectively.

3- Conservation of thermal energy

The energy equation per unit volume for a three dimensional flow is,[8]:

$$\frac{\partial}{\partial x}(\rho UT)+\frac{\partial}{\partial y}(\rho VT)+\frac{\partial}{\partial z}(\rho WT)=\frac{\partial}{\partial x}\left(\Gamma\frac{\partial T}{\partial x}\right)+\frac{\partial}{\partial y}\left(\Gamma\frac{\partial T}{\partial y}\right)+\frac{\partial}{\partial z}\left(\Gamma\frac{\partial T}{\partial z}\right) \quad \text{…. (4-5)}$$

Where:

(Γ) the diffusion coefficient (diffusivity) and it's given by:

$$\Gamma=\frac{\mu}{\mathrm{Pr}} \quad \text{…. (4-6)}$$

$$\mathrm{Pr}=\frac{\upsilon}{\alpha}=\frac{\mu C_p}{k} \quad \text{…. (4-7)}$$

Where (Pr) the Prandtl number

4.1.3 The turbulence model

To Determining the Flow Regime (turbulent or laminar flow) Airpak computes the Rayleigh number (Ra) and the Prandtl number (Pr), which are also dimensionless. The Prandtl number measures the relative magnitude of molecular diffusion to thermal diffusion. The Rayleigh number is a measure of the importance of the buoyancy effects.

If the Rayleigh number value in a certain lower range denotes laminar flow; a value in a higher range, turbulent flow. In the present study the Rayleigh number was more than (10^6).

The turbulence model used in present study is defined as two equation eddy viscosity model. Renormalization Group Method (RNG k- ε) was a good choice for users in numerical analysis for a ventilation system, **[81,102,103]**.

The (RNG k- ε) equations were distinguished from the other turbulence models, **[104]**:

–Additional term in dissipation equation for connecting between mean shear and turbulence dissipation.

–Treated the swirl effects on turbulence flow.

–The analytical formula for Prandtl number in turbulent flow.

–Effective viscosity analysis by differential formula.

The RNG k-ε equations are given by, [**99]**

Turbulent kinetic energy:

$$\rho U_i \frac{\partial k}{\partial x_i} = \mu_t S^2 + \frac{\partial}{\partial x_i}(\alpha_k \mu_{eff} \frac{\partial k}{\partial x_i}) - \rho\varepsilon \qquad \text{…. (4-8)}$$

Convection term — Generation term — Diffusion term — Dissipation term

Where $S \equiv \sqrt{2S_{ij}S_{ij}}$, $S_{ij} \equiv \frac{1}{2}\left(\frac{\partial U_j}{\partial x_i} + \frac{\partial U_i}{\partial x_j}\right)$ …. (4-9)

Dissipation rate equation:

$$\rho U_i \frac{\partial \varepsilon}{\partial x_i} = C_{1\varepsilon}\left(\frac{\varepsilon}{k}\right)\mu_t S^2 + \frac{\partial}{\partial x_i}\left(\alpha_\varepsilon \mu_{eff} \frac{\partial \varepsilon}{\partial x_i}\right) - C_{2\varepsilon}\rho\left(\frac{\varepsilon^2}{k}\right) - R \quad \text{…. (4-10)}$$

Convection term — Generation term — Diffusion term — Destruction term — Additional term related to mean strain and turbulence quantities

The (R) term in the dissipation equation (4-10) is given by:

$$R = \frac{C_\mu \rho \eta^3 \left(1 - \frac{\eta}{\eta_o}\right)\varepsilon^2}{(1+\beta\eta^3)k} \quad \text{…. (4-11)}$$

Where $\eta = \frac{Sk}{\varepsilon}$

The model constants were the following values: $C_{1\varepsilon}$=1.42 and $C_{2\varepsilon}$=1.68, β=0.012, η_0=4.38, C_μ=0.0845

4.1.4 AIRPAK software structure

The structure of AIRPAK software includes four main stages, its:

1- **Build model**: Building objects based on the predefined objects as (rooms, person, blocks, fans…etc) and gives the boundary conditions for the model.
2- **Generate mesh**: The model is divided into discrete elements. Airpak software will solve the equations which govern the heat transfer and flow within these elements.

3- **Calculate solution**: When the solution being, the Airpak software check the model and saves a project and starts performs several operations preprocessing to solve the governor equations at each node in the model.
4- **Examine results**: After the solution is fished, the results can be examined as (air temperature, air velocity, PMV, PPM, ADPI,….etc)

Fig.(4-1) shows the basic AIRPAK software structure.

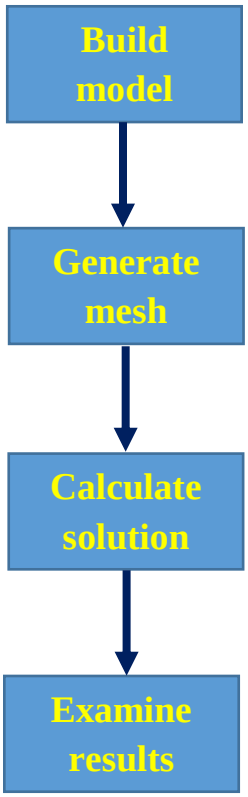

Fig.(4-1) Basic AIRPAK software structure

4.1.5 Validation of AIRPAK software

To ensure the accuracy of the results of the AIRPAK software to work in the field of (DV/CC) system, it was validated with another experimental study. The validation of software was done by comparing the numerical results (with RNG k-Ɛ turbulence model) with experimental results obtained in an office with (DV/CC) system which conducted by **(Rees and Haves), [6]**.

The experimental tested chamber at dimensions (5.43×3.08×2.78m) as shown in Fig.(4-2) located in Hong Kong with isolated walls. Internal heat sources were simulated by using cuboid boxes with light bulbs. The experimental test done with large cooling load (72W/m^2) by four heat sources puts on the tables seated symmetrically inside tested chamber. The air supply temperature, and air change per hour were (20 ^{o}C) and (5 1/h) respectively supplied by semi-circle diffuser at dimension (70cm high and 40cm diameter).

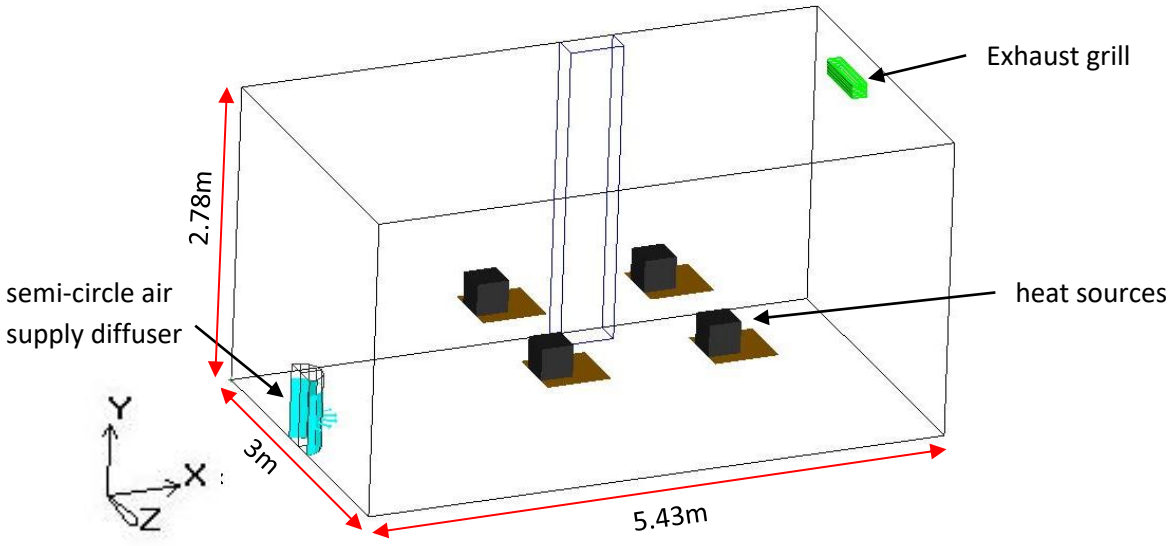

Fig.(4-2) Test chamber **by Rees and Haves, [6]**

The comparison depends on the air temperature which was measured at a different heights for the vertical line at points (0.7, 1.54) on the XZ- plane as shown in Fig.(4-3). The comparison gave an acceptable agreement between experimental data, [**6]** and numerical results. The average percentage error between the numerical and experimental results was about (±3.27%). The maximum deviation occurred at the height level between (0.2-1.2m) approximately, this level range was within the zone of heat sources location, led to that the temperature disturbance between the heat sources and the supply cold air, which leads to an error rate in some reading between the numerical and experimental results, addition to the accuracy of measuring devices and humans errors.

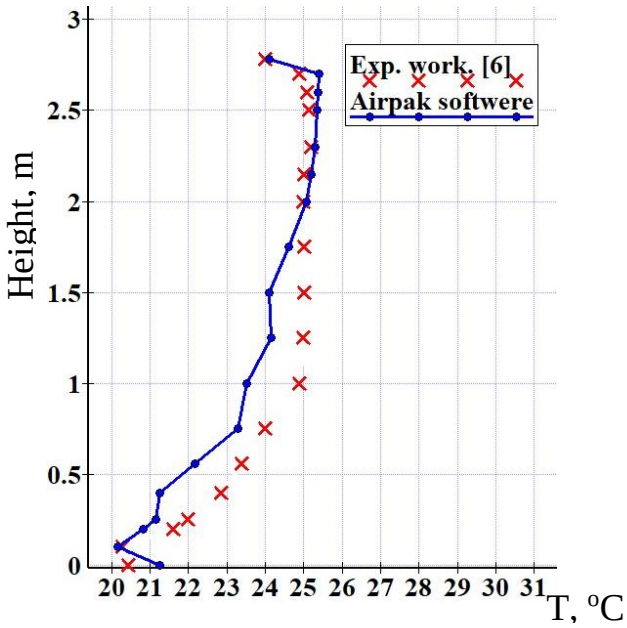

Fig.(4-3)Validation of the AIRPAK software with the experimental result by (Rees and Haves **[6]**)

4-2 Numerical Cases Study

To validate (DV/CC) system, numerical results with experimental measurements are compared for four tests under (Case-I) and four tests under (Case-II) which were described in chapter three (Section 3.1).

To generate further sets of data for (DV/CC) system under Hilla (Iraq) climate, non-insulated office room and classroom are studied as other room geometries. For non-insulated office room (Case-III under rectangular diffuser and Case-IV under semi-circle diffuser) and for the classroom (Case-V under rectangular diffuser and Case-VI under semi-circle diffuser). Numerical results for non-insulated office room cases are compared with insulated office room cases. Also, the results for classroom cases are compared with ASHRAE standard data. The AIRPAK.3.0.16 software is used to generate simulation models for each case.

4.3 Numerical Validation for Experimental Cases

4.3.1 Case-I (insulated office room with rectangular supply diffuser)

Figure (4-4) shows the geometry used in the tested room (Case-I), which is drawn by using AIRPAK.3.0.16, more details of the room can be seen in chapter three. The airflow is discharged horizontally from the front surface of the DV system. The supply air velocity and air flow rate are fixed at (0.25 m/s) and (35 L/s (74.1cfm)) respectively.

The chilled ceiling draw as two walls represented (80%) of the floor area.

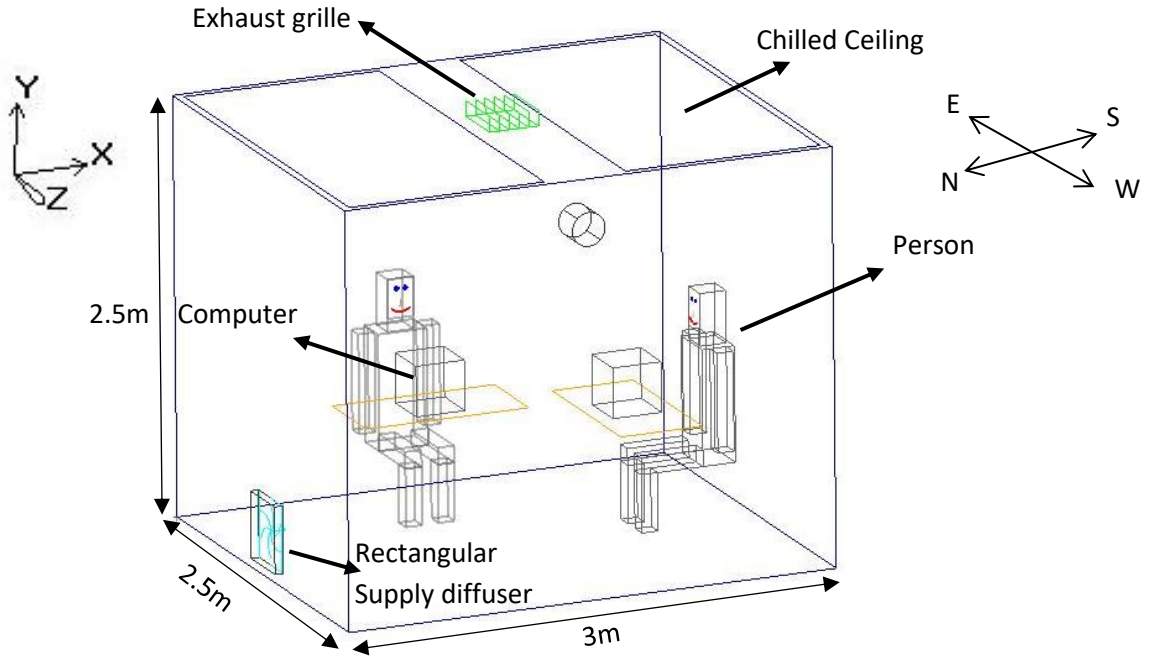

Fig.(4-4) Schematic diagram for the tested room, (case-I)

4.3.2 Case-II (Insulated office room under semi-circle supply diffuser)

The specific properties of this test room are the same as properties in Case-I. Figure (4-5) shows the geometry used in the tested room (Case-II), which is drawn by using AIRPAK.3.0.16, more details of the room can be seen in chapter three.

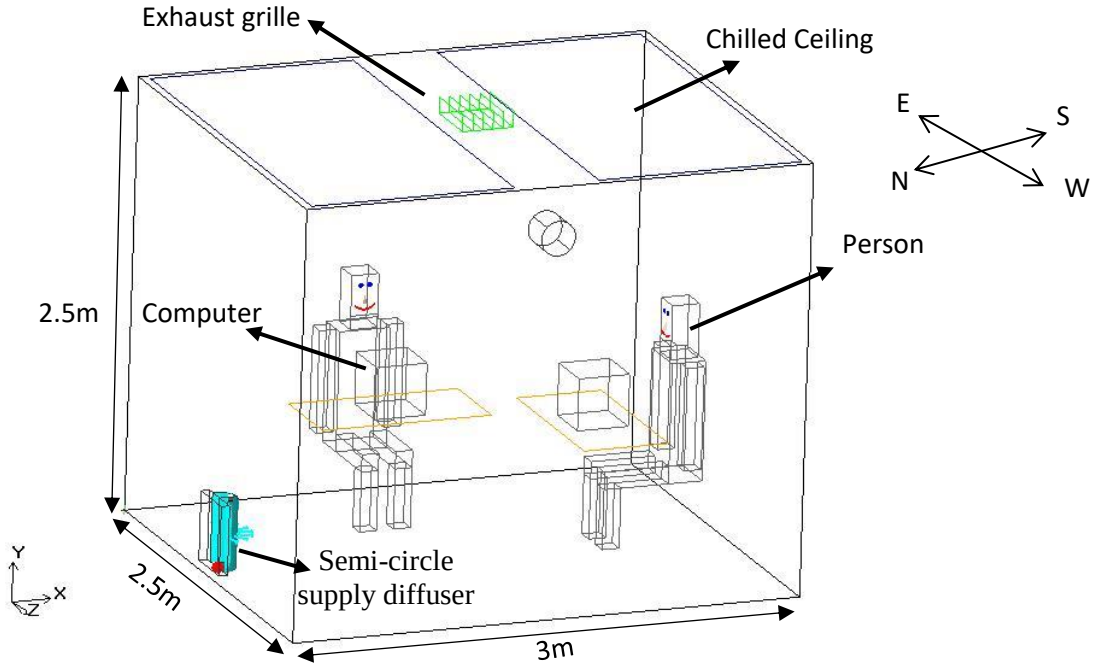

Fig.(4-5) Schematic diagram for the tested room, (Case-II).

4.3.3 Boundary conditions

Table(4-2) shows the boundary conditions for the two insulated office room cases (Case-I and Case-II).

Table(4-2) The boundary conditions for the (Case-I and Case-II)

Parts	Boundary condition	Equation
rectangle air supply diffuser	inlet velocity	$\vec{u}=\vec{u}_x$
semi-circle air supply diffuser	inlet velocity	$\vec{u}=\vec{u}_x+\vec{u}_z$
Walls	no penetration and no slip condition	u=0
sidewalls, ceil and floor	zero heat flux	$\frac{dq}{dx}=\frac{dq}{dy}=\frac{dq}{dz}=0$
exhaust grill	constant air flow rate	$\dot{V}_{in}=\dot{V}_{out}$
Occupants, computers and lights	constant heat sources	q=constant
chilled ceiling	constant temperature	T=constant

4.3.4 Generate mesh strategy

The flow solution field problems (air age, pressure, temperature, etc.) are analyzed by (CFD) software at nodes for each cell. The accuracy of the numerical solutions are governed by numbers of cell and node in the geometry grid. In general, the accuracy of the numerical solution depends on the acceptable number of nodes.

The cost and the accuracy of the solution are closely related to each other in term of good computer hardware and time of calculation, **[100]**. For choosing the best mesh strategy, many testing meshes at different node numbers were made and described in section (4.3.4.1).

4.3.4.1 Mesh independence study

The initial step for making any numerical simulation studies is to use an appropriate grid to obtain accurate results.

Grid independent tests depend on five mesh strategies (221315, 29805,318907, 360530, and 425725 nodes). Four positions were chosen to capture the age of air and temperature simulating results, i.e. P_1 (0.5, 0.5, 1.25), P_2 (0.5, 1.8, 1.25), P_3 (0.75, 1.1, 0.5) and P_4 (2.75, 1.1, 0.5). (P_1 and P_2) are two positions in front of the supply diffuser with two different heights, while, (P_3 and P_4) are two positions at breathing zone near two occupants. Figs.(4-6) and (4-7) show air age and temperature profiles for five different selected node numbers.

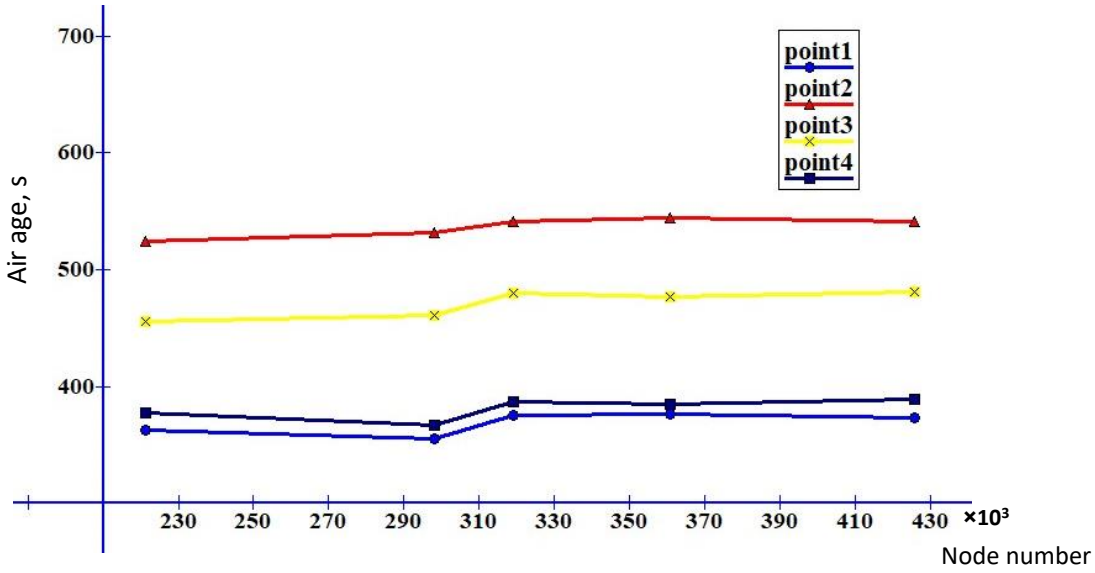

Fig.(4-6) Air age profile for five different node numbers

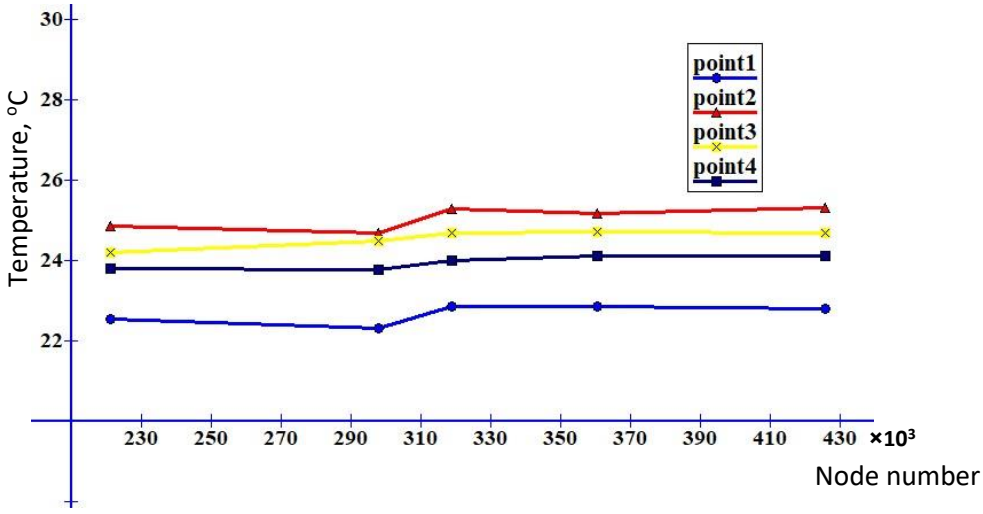

Fig.(4-7) Temperature profiles for five different node numbers

After testing many mesh strategy the size of cells which acceptable for all types listed in Table (4-3). Figs.(4-8) and (4-9) show the part of the meshed model for case-I and case-II respectively.

Table(4-3) Mesh strategy for insulated office room (case-I)

Part	Mesh Strategy
Edge line	The edges of room in (x, y and z dimensions) meshed as interval size of (0.07) and the double side ratio is (1.16). Edges of exhaust grill and air supply diffuser are meshed as interval size of (0.05).
Faces	The surfaces meshed as Hexa Cartesian type.
Volume	Meshed as Hexa Cartesian type for interval size (0.07) in X and Z-direction, 0.05 in Y-direction.

After the mesh strategy applied, the number of elements and nodes for the model simulated by the Airpak software are shown in Table(4-4) for each case.

Table(4-4) Number of element and node for Case-I and Case-II

	Tests	η%	Element No.	Node No.
CASE-I	Test-1	0	302507	318907
	Test-2	25	313699	330446
	Test-3	50	313699	330446
	Test-4	80	313699	330446
CASE-II	Test-5	0	377954	397226
	Test-6	25	402064	422011
	Test-7	50	402064	422011
	Test-8	80	402064	422011

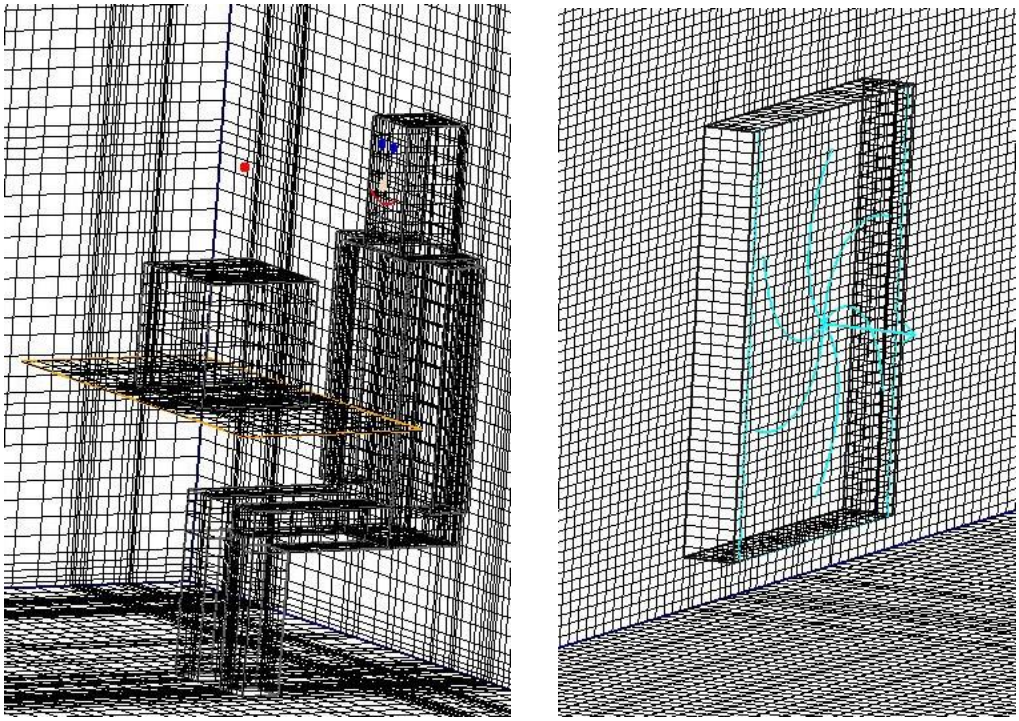

a-Meshed person with computer b-Meshed air supply diffuser

Fig.(4-8) Parts of meshed model (case-I)

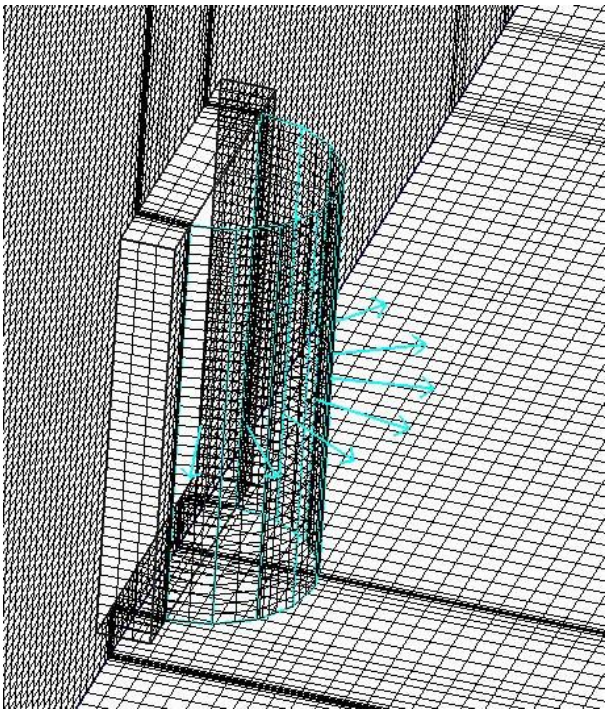

Fig.(4-9) Part of meshed model (semi-circle diffuser) (case-II)

4.3.5 Error calculation for validated cases

The experimental results compared with the simulated results by calculating the average error using the following equation, **[105]**:

$$E = \sum_{i=1}^{n} \frac{\left| X_{CFD}^{\,i} - X_{EXP}^{\,i} \right|}{X_{EXP}^{\,i}} * 100 \qquad \text{…. (4-12)}$$

Where (X) is any variable and ($\left| X_{CFD}^{\,i} - X_{EXP}^{\,i} \right|$) is the absolute difference between the simulated and the experimental values for variable X and (n) is number of measurements.

4.4 Numerical Study for Non- insulated Office Room (Cases-III &IV)

This section presents a numerical study for non-insulated office room to predict the indoor age of air, temperature distribution, CO_2 concentration and thermal comfort parameters by adopting a displacement ventilation combined with chilled ceiling system. Two cases were studied with different types of supply diffuser (Case-III under rectangular diffuser and Case-IV under semi-circle diffuser) each case has four tests at different (η) ratio (from 0 to 80%). The results are compared with the numerical results found by insulated office room (Case-I and Case-II).

4.4.1 Cases description

The non-insulated office room has the same details for insulated office room as shown in section (3.2.2) but in these cases, the walls are not insulated by assuming the wall with a window (1.25m width × 1m height) at the north side is exposed to outside conditions (at maximum summer temperature in Hilla city (47^{o}C), **[106]**). West wall with door (2×1m) oriented to the inside corridor. Other walls assumed as adiabatic (Adjacent to another room with the same temperature). The room ceiling area cover by (80%) chilled ceiling surface as shown in Fig.(4-10).

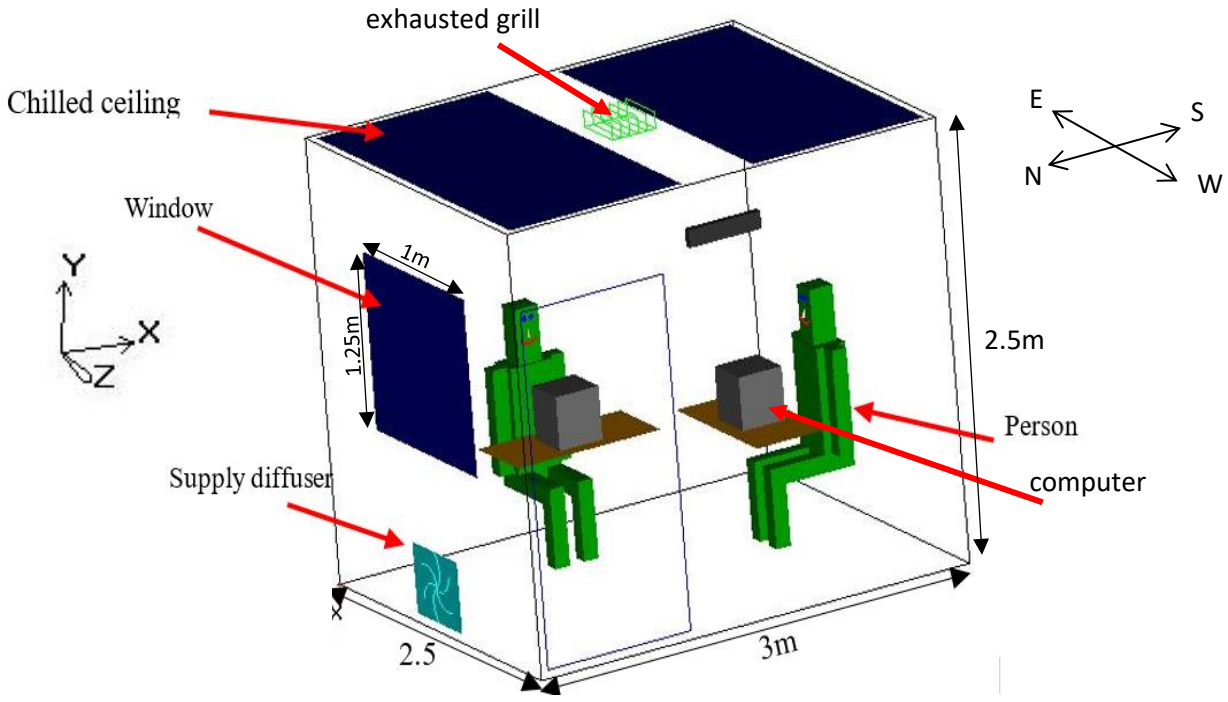

Fig.(4-10) Schematic diagram for the non-insulated office room (Case-III)

4.4.1.1 Side wall description

In Iraqi buildings, the walls are mainly formed from multi-materials. The thickness of the wall is (30 cm) and consists of four layers from inside to outside (gypsum plaster (2cm), cement plaster (2cm), common brick (24cm) and cement plaster (2cm)) as shown in Fig.(4-11). Details of materials and thickness are described in Table(4-5).

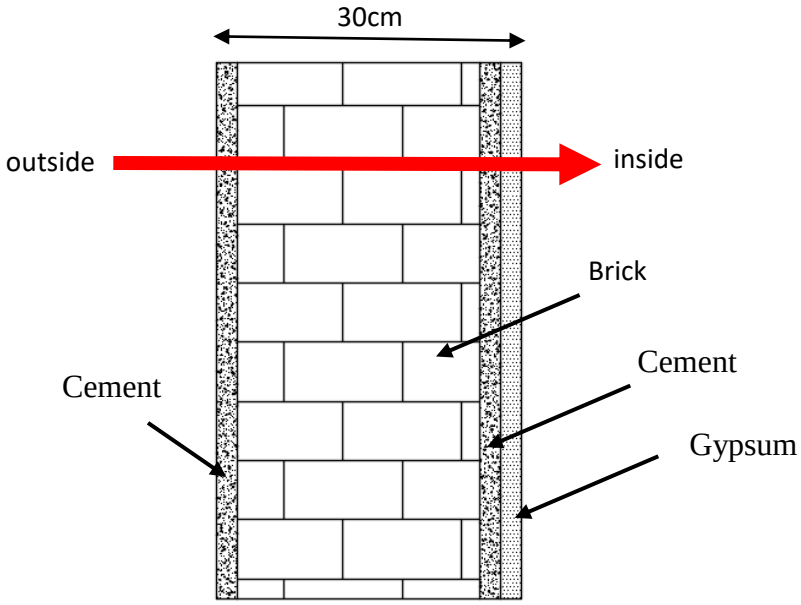

Fig.(4-11) Heat transfer through the side walls and their components

Table(4-5) Details of materials and their thickness for non-insulated room walls

Material	**Thickness (cm)**	**K, [107] (W/m.ºC)**
Brick	24	0.69
Gypsum	2	0.48
Cement	2	1.16
Wood	5	0.28
glass	0.6	0.78

4.4.2 Theoretical analysis

4.4.2.1 Calculating of non-insulated office room cooling load

The cooling load was calculated by using the methods outlined in ASHRAE handbook 2013, [**46]**. Heat gain due to occupants, lamps, computers and others. Outside heat gain due to heat transfer through the windows, walls and door from outside to inside. The calculated supply air temperature and air flow rate depend on the overall load as shown below.

In present study, the heat transfer in walls, door and windows are calculated by cooling load temperature different method (CLTD) as described in ASHRAE Handbook, 2013, [**46]** by using the following equations:

$$Q=U\times A\times CLTD_c \quad \text{…. (4-13)}$$

Where

$$U=\frac{1}{R_{th}} \quad \text{…. (4-14)}$$

$$R_{th}=\frac{1}{h_i}+\frac{x_1}{k_1}+.....+\frac{x_n}{k_n}+\frac{1}{h_o} \quad \text{…. (4-15)}$$

The ($CLTD_C$) calculated as follows:

For walls:

$$CLTD_C=(CLTD+LM)\times K+(25.5-T_i)+(T_m-29.4) \quad \text{…. (4-16)}$$

$$T_m=T_o-\frac{DR}{2} \quad \text{…. (4-17)}$$

Where (DR) is daily rang temperature between day and night.

For the door and window:

$$CLTD_C=CLTD+(25.5-T_i)+(T_m-29.4) \quad \text{…. (4-18)}$$

The heat gain due to radiation heat transfer through the window that generated by solar energy, obtained as:

$$Q_r = A \times SC \times SHG \times CLF \quad \text{…. (4-19)}$$

To calculate the temperature of the corridor, the following equation is used, [**108]**.

$$T_{corridor} = T_i + \frac{2}{3}(T_i - T_o) \quad \text{…. (4-20)}$$

The total cooling load for non-insulated office room was calculated by used (HAP-4.5) software as shown in Appendix-A2. The total cooling load was found about (800 W).

4.4.2.2 HAP-4.5 software

Carrier's Hourly Analysis software (HAP) is a tool that helps engineers in designing heating, ventilation and air conditioning systems. (HAP) had two tools. First, it is a tool for calculation cooling or heating load and design systems. The second tool used to simulate building costs and energy.

4.4.2.3 Supply air temperature and flow rate supply for (DV) System.

The air flow rate and supply air temperature (T_s) determined as mentioned in chapter three, section (3.3.1.1 and 3.3.1.2) by using Eqs.(3-1 and 3-2), [**91]**.

The supply flow rate (V_{DV}) is fixed at (52 L/s (110.2 cfm)) for each test and the diffuser supply air temperature (T_s) varied depending on the amount of cooling load covered by displacement ventilation (CL_{DV}) at constant flow rate.

The indoor air conditions for office room design as dry bulb temperature (T_{rd}) of (25^{o}C) and relative humidity (50%) due to ASHRAE standard 2011, [**92]**.

4.4.2.4 Calculation of chilled ceiling temperature

To calculate the temperature of (CC) system surface, the following empirical equation is used, **[49** and **109]**.

$$T_{CC}=T_{rd}-\left(\frac{CL_{CC}}{8.92.f.A_f}\right)^{0.9} \quad \text{….. (4-21)}$$

Where, (T_{rd}) and (T_{CC}) are the room design indoor air temperature and temperature of the chilled ceiling surface respectively, (*f*) is the rate of chilled ceiling area to the floor area (equal to 0.8).

When (CL_{CC}) is known, Eq.(4-21) is used to calculate the required surface temperature of the chilled ceiling system (T_{CC}).

As shown in chapter three (section (3.2.2)), the chilled ceiling surface temperature (T_{CC}) should be at least (1°C) higher than the dew point temperature of indoor room air to avoid condensation on the chilled ceiling surface.

Table(4-7) shows the values of calculated air supply temperature (T_s) and calculated chilled ceiling surface temperature (T_{CC}) at different ratio of cooling load (η) for non-insulated office room cases (case-III and IV).

Table(4-6) Operating conditions for Case-III and IV (non-insulated office room)

η (%)	**CL_{DV} (W)**	**CL_{CC} (W)**	**V_{DV} (L/s)**	**T_{amp} (°C)**	**T_s (°C)**	**RH_s (%)**	**T_{cc} (°C)**
0	800	0	52	47	18	75	-
25	600	200	52	47	20.5	70	21.5
50	400	400	52	47	23	60	19
80	160	640	52	47	24.5	55	16

4.4.3 Selection of air supply diffuser

In using displacement ventilation system, there are some goals can be achieved as low air speed, thermal comfort, clam operation, low noise and provide good indoor air quality (IAQ). Depending on the value of air flow rate (52 L/s (110.2cfm)), and to satisfy low air velocity (0.25 m/s), diffuser with area (0.208m^2) at dimensions

(50cm width, 42cm height) is selected for one way flow rectangular diffuser (Case-III) and (32cm diameter, 42cm height) is selected for semi-circle diffuser (Case-IV) to give air velocity about (0.25 m/s) as shown in Fig.(4-12).

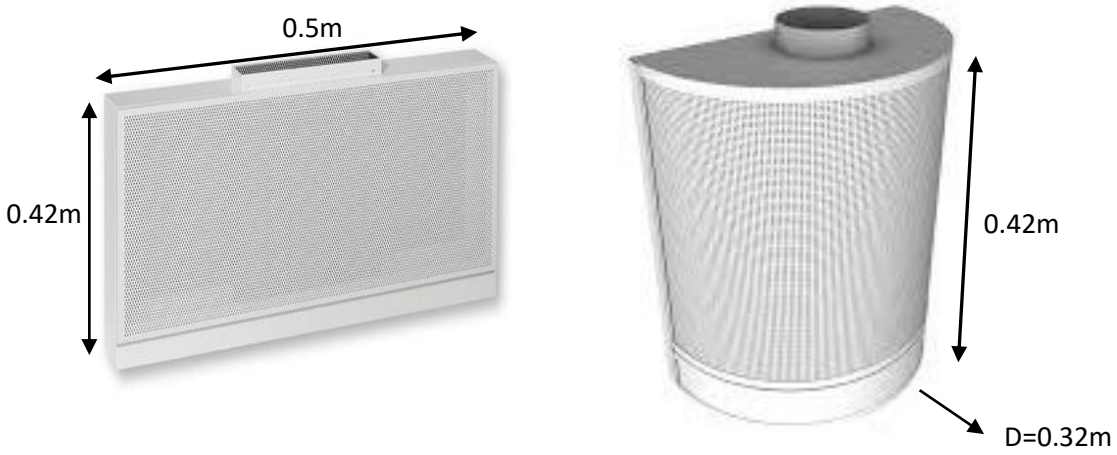

a-One way rectangle diffuser b-Semi-circle diffuser

Fig.(4-12) Diffuser dimensions for one way rectangular and semi-circle diffusers related to non-insulated office cases

4.4.4 Boundary conditions

Table(4-7) shows the boundary conditions for the two non-insulated office room cases (Case-III and Case-IV).

Table(4-7) The boundary conditions for (Case-III and Case-IV

Parts	Boundary condition	Equation
rectangle air supply diffuser	inlet velocity	$\vec{u}=\vec{u}_x$
semi-circle air supply diffuser	inlet velocity	$\vec{u}=\vec{u}_x+\vec{u}_z$
East, south floor and ceil Walls	no penetration and no slip condition	u=0
North and west walls, window and door	constant heat flux	$\frac{dq}{dx}=\frac{dq}{dy}=\frac{dq}{dz}=C$
sidewalls, ceil and floor	zero heat flux	$\frac{dq}{dx}=\frac{dq}{dy}=\frac{dq}{dz}=0$
exhaust grill	constant air flow rate	$\dot{V}_{in}=\dot{V}_{out}$
Occupants, computers and lights	constant heat sources	q=constant
chilled ceiling	constant temperature	T=constant

Calculated results by (HAP program) of heat for each side wall, windows and door of the tested cases shown in Table(4-8).

Table(4-8) Heat gain for the side wall, windows and door, Case-III and Case-IV

Wall	West	East	North	South	Ceiling	Window		Door
						conduction	Radiation	
Heat, W/m^2	18.4	0	20	0	0	55.2	70.4	31

4.4.5 Mesh Strategy

The method in section (4.3.4.1) was used to find suitable grid numbers for these study cases, independent test based on five mesh methods of case study depend on five strategies (285460, 305631, 330044, 354122 and 391811 Nodes). Figs.(4-13) and (4-14) show air age and temperature profiles for five different selected node numbers.

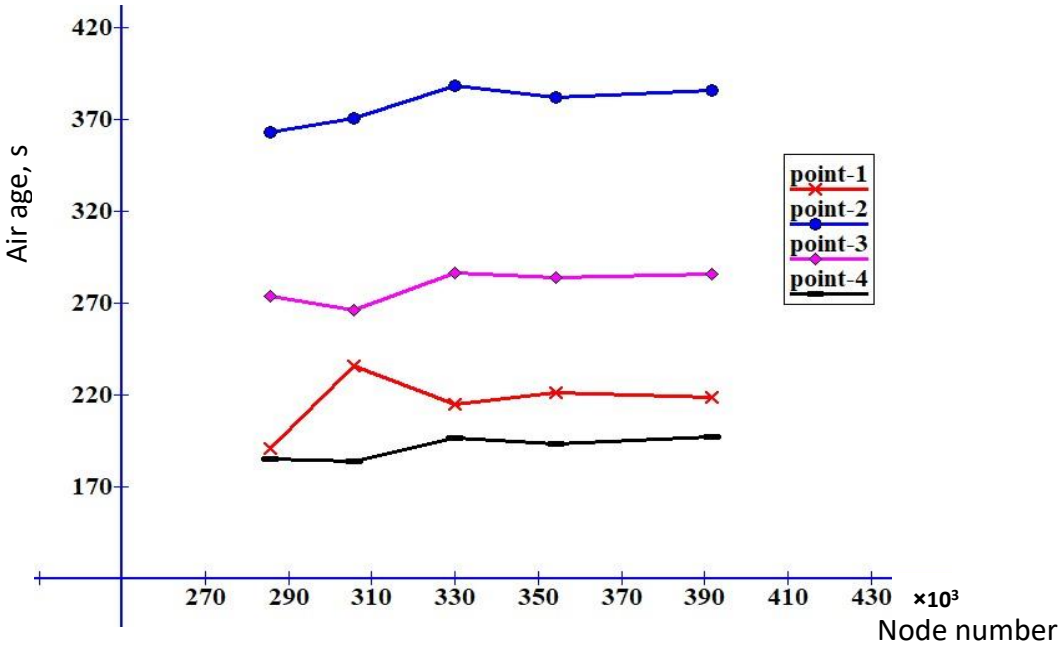

Fig.(4-13) Air age profiles for five different node numbers

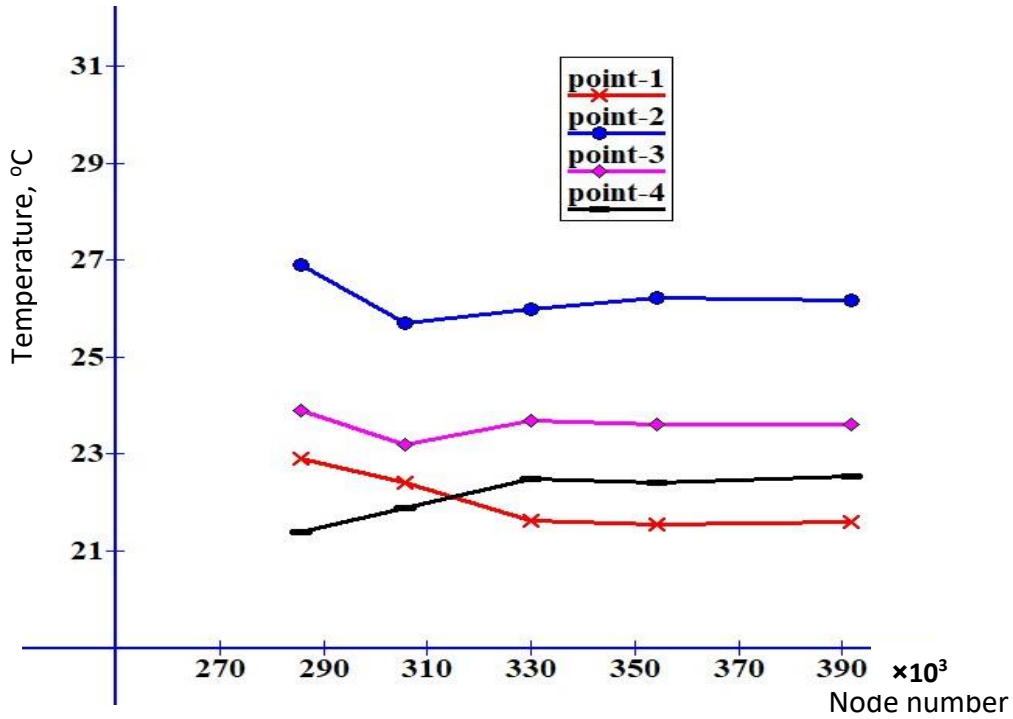

Fig.(4-14) Temperature profiles for five different node numbers

After applying the meshing strategy shown above, the number of elements and nodes for the model simulated by (AIRPAK) software are shown in Table(4-9) for each test cases.

Table (4-9) Number of elements and node for Case-III and Case-IV

	Tests	η%	**Element No.**	**Node No.**
CASE-III	Test-1	0	291615	307663
	Test-2	25	313289	330044
	Test-3	50	313289	330044
	Test-4	80	313289	330044
CASE-IV	Test-5	0	358837	377442
	Test-6	25	373221	392274
	Test-7	50	373221	392274
	Test-8	80	373221	392274

4.5 Numerical Study for Classroom (Cases-V and VI)

This section presents a numerical study for predicting the indoor age of air, temperature distribution and CO_2 concentration by adopting a displacement ventilation system combined with a chilled ceiling within non-insulated classroom. Many of the studies concerned with the ventilation of closed places focused on studying the office rooms. Few studies dealt with the study of classroom ventilation, although some studies proved that (50%) of school students suffer from asthma and allergies as a result of air pollution. The results of the office ventilation studies cannot be reversed in the classroom due to the classroom have high occupancy density than the office room, **[110]**. Thus, there is a need for more study of the classroom ventilation system.

Two cases are studied numerically for the classroom to satisfy thermal comfort under Hilla (Iraq) climate inside a space for a different type of supply diffuser (Case-V and Case-VI). Each case have four tests at different (η) ratio (from 0 to 80%). The results were compared with ASHRAE standard data.

4.5.1 Cases description

The age of air, air temperature, air velocity distribution and CO_2 concentration are predicted inside the classroom with dimensions of (9×5×2.5m) as shown in Fig.(4-15) for (case-V) and Fig.(4-16) for (case-VI). There are twenty one (21) persons (students and teacher), nine tables, six overhead lights (three lights at each side), one (T.V) show and one computer simulated inside the occupied region. Table(4-10) shows the details of the equipment and occupants in the classroom. Fig.(4-17) presents the plane view of a classroom with a floor area ($28m^2$) by assuming that the south wall has three windows which exposed to outside conditions (at a maximum temperature in Iraqi summer (47^oC), **[106]**). North-wall with doors orient to inside corridor. The other wall is a partition among rooms at same designed

indoor-air temperatures for classroom (25ºC due to ASHRAE.2011, **[92]**). The chilled ceiling covers (80%) of ceil area.

Table(4-10) Dimensions and heat convective for different indoor items

Items	No.	Dimensions, (m)			Heat, (W)
		Δx	Δ**y**	Δ**z**	
Person	21	0.125	1.15	0.4	75 W per person
Student desk	10	0.5	0.7	1.25	-
Window	3	1.5	1	0	-
Door	1	1	2	0	-
Rectangular diffuser	2	0.05	0.5	1	-
Semi-circle diffuser	2	0.4m Diameter at 0.8m height			-
Exhaust grill	2	0.6	0	0.6	-
Lights	6	0.75	0.05	0.05	480
T.V	1	0.1	0.6	1	150
Computer	1	0.3	0.3	0.3	60
Chilled ceiling	3	2.5	0	3	-

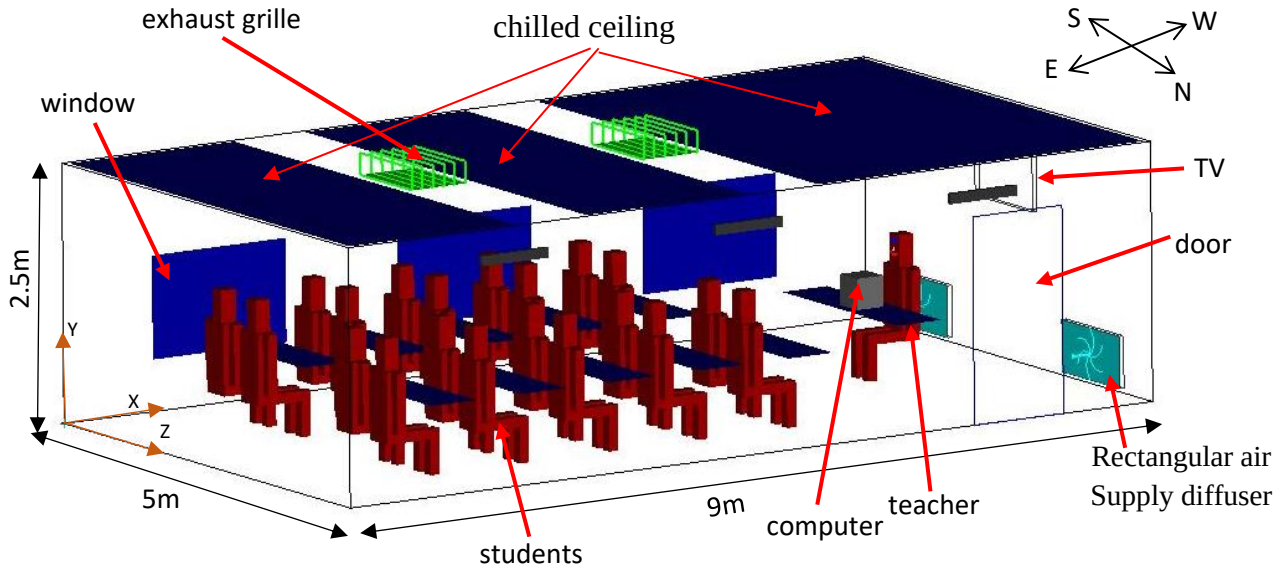

Fig.(4-15) Schematic diagram for the tested classroom under one way rectangular supply (case-V)

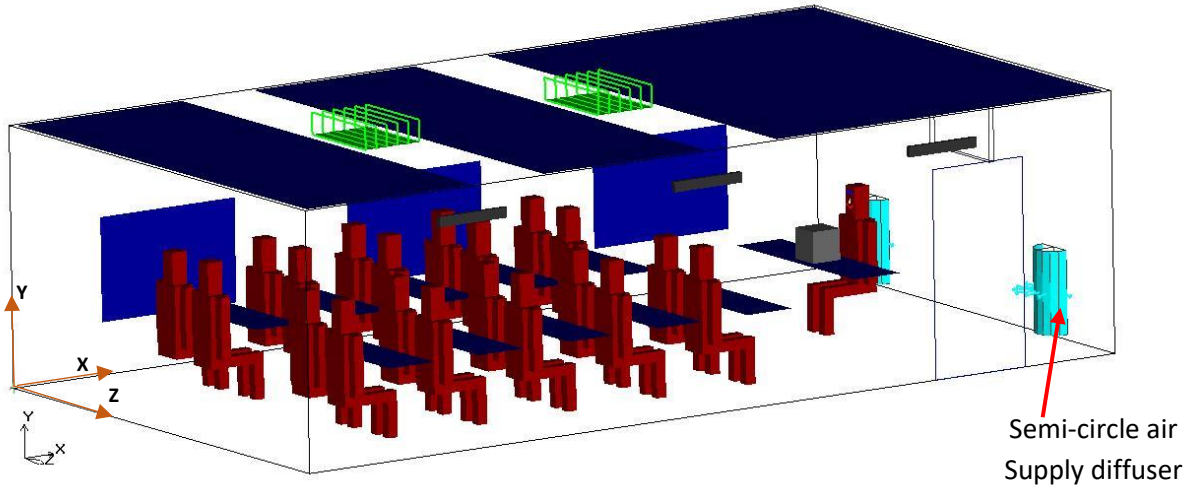

Fig.(4-16) Schematic diagram for the tested room under semi-circle air supply diffuser, (case-VI)

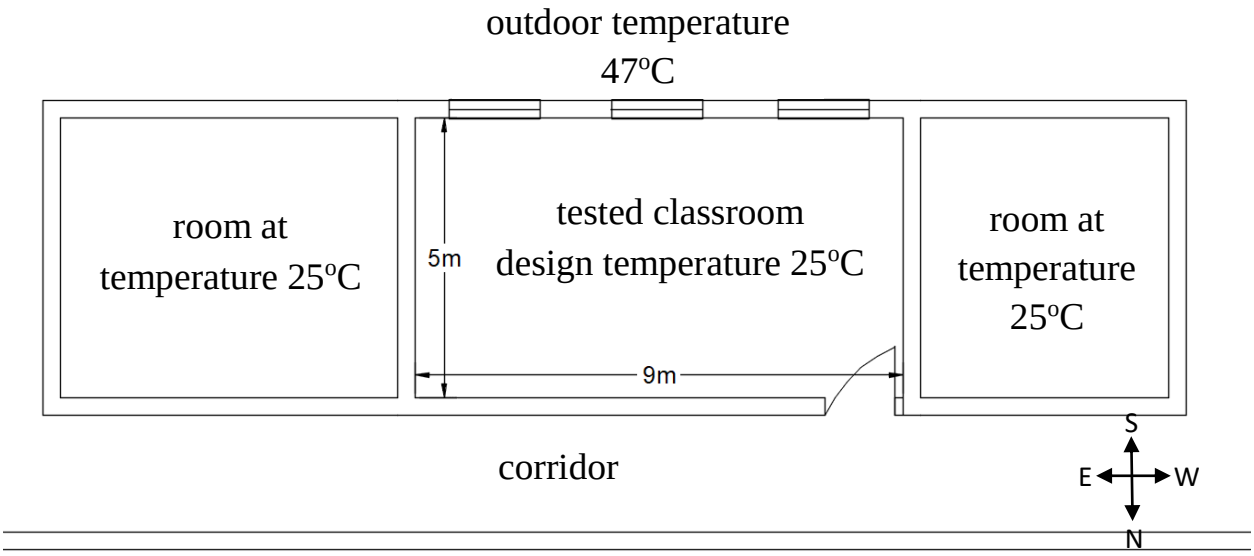

Fig.(4-17) Plane view of a classroom model

4.5.1.1 Side walls description

The side walls are assumed to be formed from multi-materials at (30cm) thickness and consists of (gypsum plaster (2cm), cement plaster (2cm), common brick (24cm) and cement plaster (2cm)) as is common in Iraqi buildings. It's perversely described in section (4.4.1.1).

4.5.2 Theoretical analysis

4.5.2.1 Calculation of classroom cooling load

In this case, the heat transfer in walls, door and windows are calculated by cooling load temperature difference method as shown in section (4.4.2.1).

The total cooling load for classroom was calculated by using (HAP) program as shown in Appendix-A2. The total cooling load was found about (3808 W, 84.6W/m^2).

4.5.2.2 Supply air temperature and flow rate for (DV) System.

The air flow rate and supply air temperature(T_s) determined as mentioned in chapter three, section (3.2.1.1 and 3.2.1.2) by using Eqs.(3-1to 3-4), **[91]**.

The supply air flow rate (V_{DV}) is fixed at (300 L/s (635.5 cfm)) for each test and the diffuser supply air temperature (T_s) varied depending on the amount of cooling load covered by displacement ventilation (CL_{DV}) at constant flow rate. Calculated method for air flow rate and supply air temperature was shown in Appendix-A.

The indoor air conditions for classroom design as dry bulb temperature (T_{rd}) of (25ºC) due to ASHRAE standard 2011), **[92]**.

4.5.2.3 Calculation of chilled ceiling temperature

The chilled ceiling temperature calculated by the same method described in section (4.4.2.4) by using Eq.(4-21).

From the psychometric chart, as shown in Fig.(4-18), the dew point temperature of indoor air for classroom at (25ºC) dry bulb temperature and (50%) relative humidity is (14ºC), then the chilled ceiling surface temperature must be large than (15ºC).

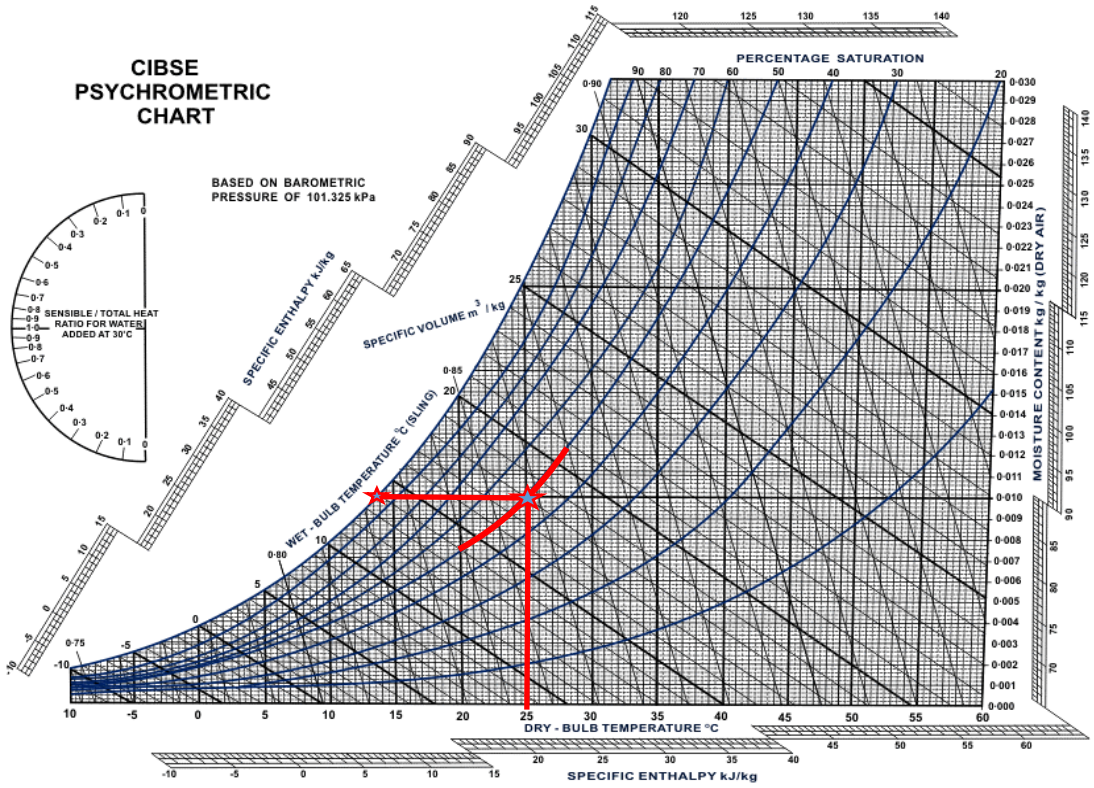

Fig.(4-18) Psychometric chart **[92]**

Table(4-11) shows the value of calculated air supply temperature (T_s) and calculated chilled ceiling surface temperature (T_{CC}) by using Eqs.(3-2) and (4-21) respectively at deferent ratio of cooling load (η) for case-V and VI.

Table(4-11) Operating conditions for (Case-V) and (Case-VI)

η (%)	**CL_{DV} (W)**	**CL_{CC} (W)**	**ACH (1/h)**	**V_{DV} (m^3/s)**	**T_{amp} (^oC)**	**T_s (^oC)**	**RH_s (%)**	**T_{cc} (^oC)**
0	3808	0	9.6	0.3	47	19.5	70	-
25	2856	952	9.6	0.3	47	21.5	65	22
50	1904	1904	9.6	0.3	47	23.5	60	20
80	761.6	3046.4	9.6	0.3	47	24.5	55	17.5

4.5.3 Selection of air supply diffuser

Depending on the value of the total air flow rate ($0.3m^3/s$) and to satisfy low air velocity (0.3 m/s), two diffusers with the area ($0.5m^2$) at dimensions (1m width, 0.5m height) for one way flow rectangle diffuser (Case-V) and (0.4m diameter, 0.8m height) for semi-circle diffuser (Case-VI)as shown in Fig.(4-19) to give air velocity about (0.3 m/s).

The surrounding classrooms are typically arranged with the teacher's desk at one side of the room, and students sit in rows facing the teacher. The most common diffuser arrangement for this room layout requires spreading on each side of the wall near a teacher. Each diffuser supply flow rate is (150 L/s (317.8cfm)).

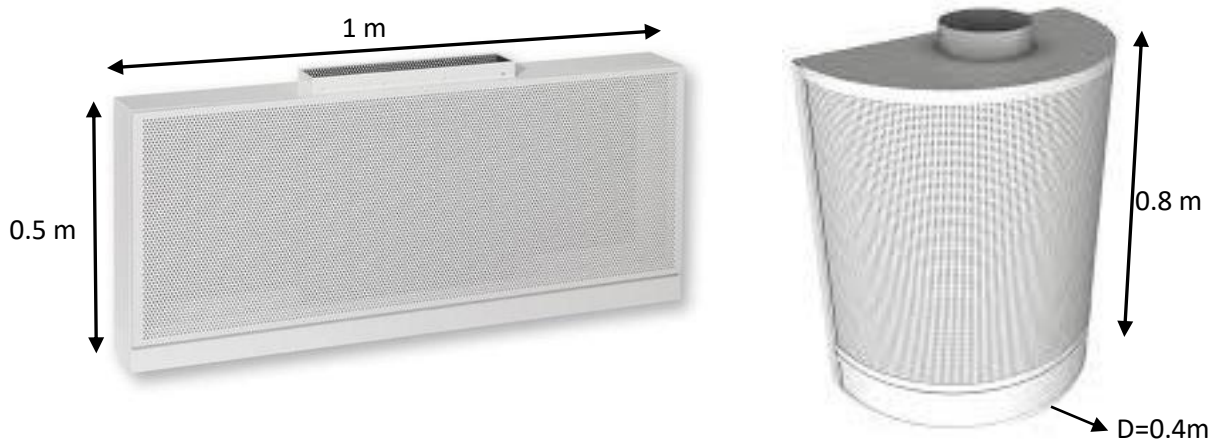

a- One way rectangle diffuser b- Semi-circle diffuser

Fig.(4-19) Diffusers dimensions for classroom case study

4.5.4 Boundary conditions

Table(4-12) shows the boundary conditions for the two classroom cases (Case-V and Case-VI).

Table(4-12) The boundary conditions for the (Case-V and Case-VI)

Parts	Boundary condition	Equation
rectangle air supply diffuser	inlet velocity	$\vec{u}=\vec{u}_x$
semi-circle air supply diffuser	inlet velocity	$\vec{u}=\vec{u}_x+\vec{u}_z$
East, west, floor and ceil Walls	no penetration and no slip condition	u=0
North and south walls, window and door	constant heat flux	$\frac{dq}{dx}=\frac{dq}{dy}=\frac{dq}{dz}$=constant
sidewalls, ceil and floor	zero heat flux	$\frac{dq}{dx}=\frac{dq}{dy}=\frac{dq}{dz}=0$
exhaust grill	constant air flow rate	$\dot{V}_{in}=\dot{V}_{out}$
Occupants, computers, TV and lights	constant heat sources	q=constant
chilled ceiling	constant temperature	T=constant

Calculated results of heat gain by (HAP program) for each side wall, windows and door of the tested classroom are shown in Table(4-13).

Table(4-13) Heat gain for the side wall, windows and door (Case-V and Case-VI)

Surface	West	East	North	South	Ceiling	Window		Door
						conduction	radiation	
Heat, W	0	0	390	338	0	410	338	67

4.5.5 Mesh strategy

As the same method used in section (4.4.5.1), acceptable mesh strategy depends on compared among six mesh type (962531, 1133262, 1214510, 1351966, 1564681 and 1806426 Nodes). Five positions were chosen to acquire the age of air and temperature simulating results: P_1(6,0.4,4), P_2(7,1.8,2.5), P_3(2,1.1,2.5), P_4(3,1.8,3.5) and P_5(4,1.1,2.5). P_1 at the position in front of the supply diffuser, P_2 at front of the teacher, P_3, P_4 and P_5 are three positions at breathing zone in space among student's rows. Figs.(4-20) and (4-21) show air age and temperature profiles for six selected different node numbers.

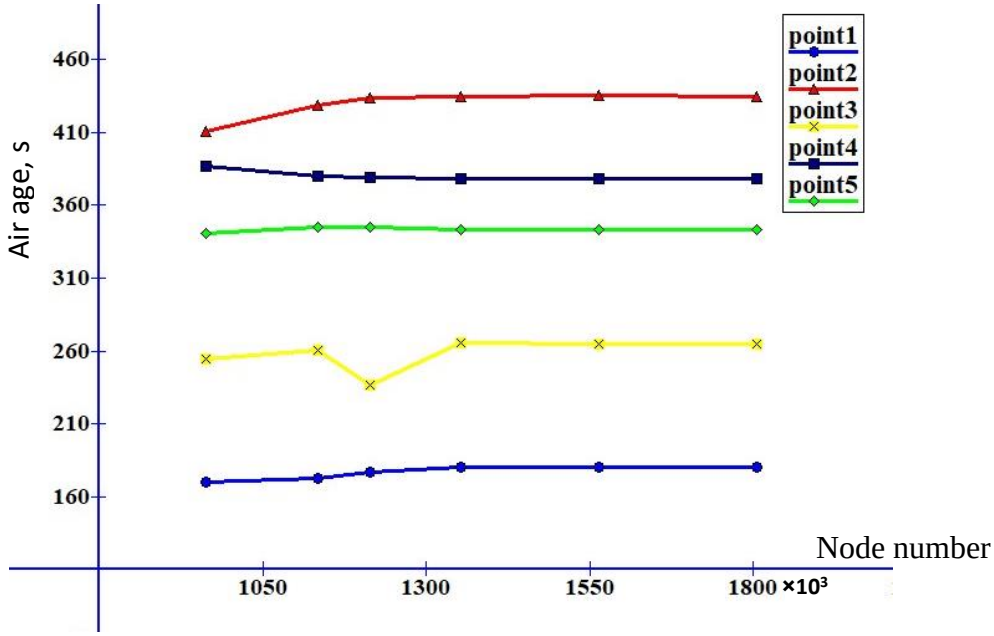

Fig.(4-20) Air age profiles for six different node numbers

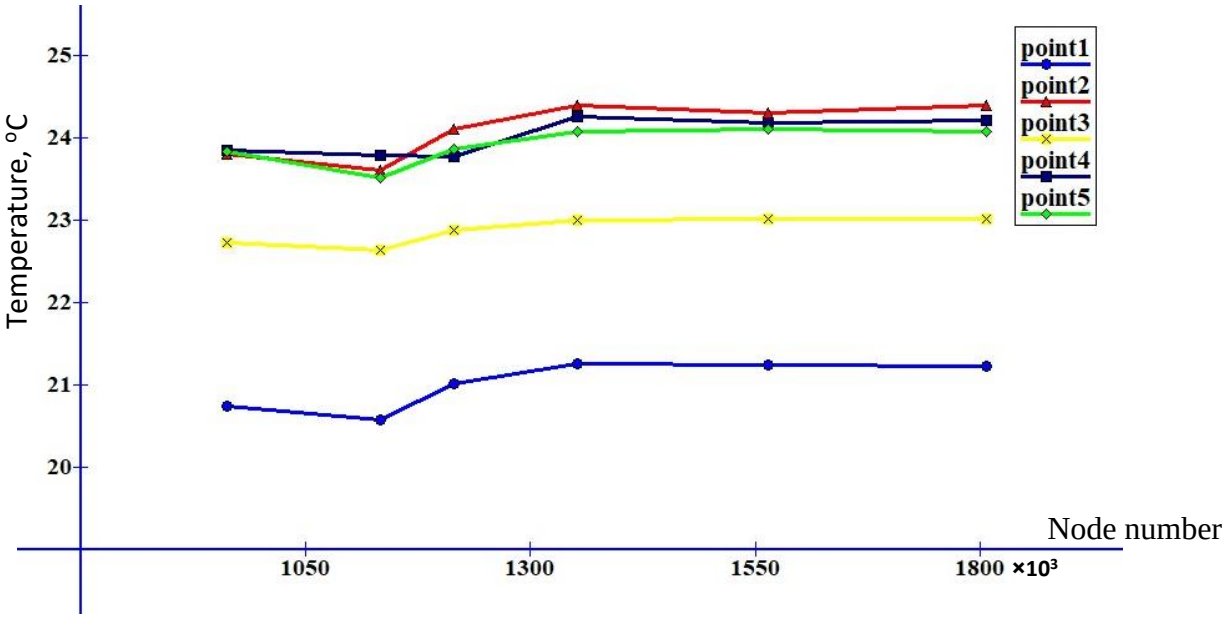

Fig.(4-21) Temperature profiles for six different node numbers

After testing six different mesh strategy the size of cells which acceptable for all types listed in Table(4-14). Figs.(4-22) and (4-23) show part of the meshed model for case-V and case-VI respectively.

Table(4-14) Mesh strategy for classroom cases

Part	**Mesh Strategy**
Edge line	The edges of classroom in (x, y and z) dimensions are meshed as interval size (0.12, 0.08 and 0.1) respectively, the double side ratio is (1.1). Edges of supply diffuser, exhausted grill are meshed as interval size (0.07).
Faces	All surface meshed as Hexa Cartesian type.
Volume	Meshed as Hexa Cartesian type for interval size (0.12) in X-direction, (0.1) in Z-direction, 0.08 in Y-direction.

After applying the above grid strategy, the number of elements and nodes for the model simulated by (AIRPAK) software are shown in Table(4-15) for each case.

Table(4-15) Number of elements and nodes for (Case-V and Case-VI)

	Tests	η %	**Element No.**	**Node No.**
CASE-V	Test-9	0	1284268	1351966
	Test-10	25	1313235	1380951
	Test-11	50	1313235	1380951
	Test-12	80	1313235	1380951
CASE-VI	Test-13	0	1577919	1655221
	Test-14	25	1600105	1679187
	Test-15	50	1600105	1679187
	Test-16	80	1600105	1679187

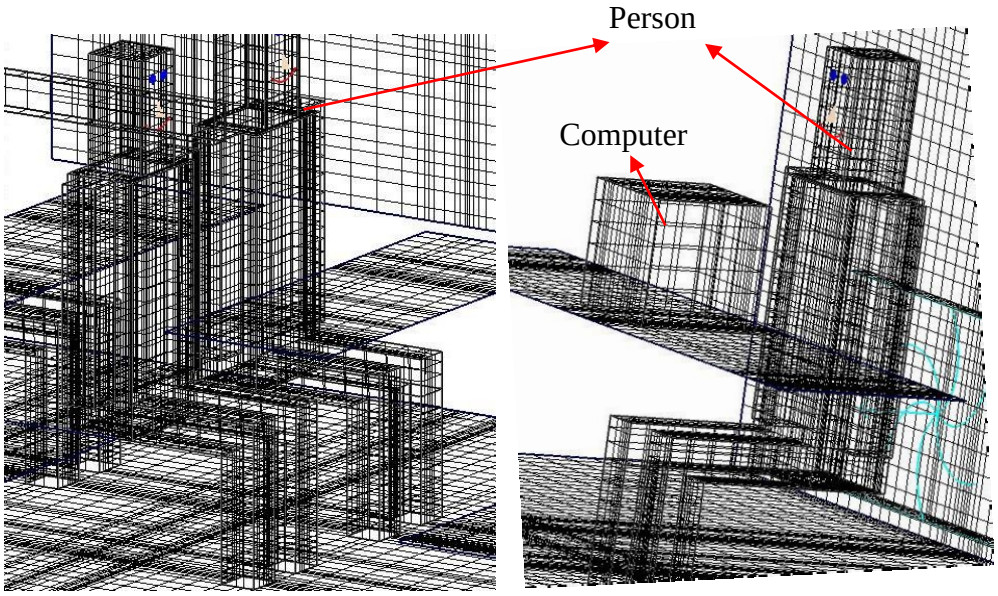

a- Students mesh b- Meshed teacher with computer

Fig.(4-22) Part from meshed model for case-V

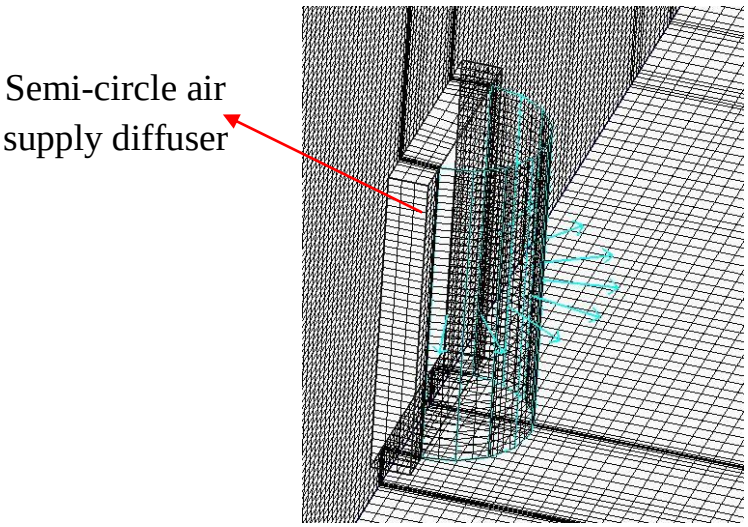

Fig.(4-23) Part from meshed model for Semi-circle diffuser (case-VI)

4.6 Numerical Solution Procedures

This section provides detailed information about the procedures adopted in the numerical solution for six considered cases (Case-I, II, III, IV, V and VI).

4.6.1 Working fluid properties

The working fluid is three phases. The main fluid is air and the other are CO_2 and H_2O as relative humidity. The air and CO_2 properties are shown in Table(4-16).

Table (4-16) Air and CO_2 properties, [**107]**.

Parameter	**Air**	**CO_2**
density, $\rho(T)$, (Kg/m^3)	1.225	1.7878
Thermal Conductivity (k), (W/m.K)	0.0242	0.0166
Specific Heat (C_p), (J/kg.K)	1005	871
Viscosity (μ), (kg/m.s)	1.7894×10^{-5}	1.495×10^{-5}

4.6.2 Momentum boundary conditions

Table (4-17) shows the momentum boundary conditions for the parts of the model tested room for the six cases (Case-I, Case-II, Case-III, Case-IV, Case-V and Case-VI). The equations of general boundary conditions are given in Table (4-18).

Table(4-17) Momentum boundary conditions.

Part	Type	Momentum condition	
		Wall Motion	Shear condition
Persons, computer, side wall, tables and lights	Wall	Stationary	No slipping
Rectangle air supply diffusers	velocity inlet	magnitude (normal with X-direction)	
Semicircle air supply diffusers	velocity inlet	magnitude, normal with X.Z-direction	
Extract grills	out flow	flow rate weighting ($\frac{\dot{V}_{in}}{\dot{V}_{out}}$)=1	

Table(4-18) Boundary conditions equations

Boundary	Velocities (m/s)		Temperature (^oC)	Heat flux (W/m^2)
Inlet	$U = u_s$		$T=T_s$	-
Outlet	$U=u_s \frac{A_{in}}{A_{out}}$		$\frac{\partial T}{\partial X}=0$	-
No slip at wall	For six cases	U=0, V=0, W=0	-	q_{wall}/A_{wall}

4.6.3 Solution control

Turbulent kinetic energy, momentum, turbulent dissipation rate and energy equations are defined as convection terms for solution control. These terms are described by using the second order upwind. When Second order is used, quantity at cell face are compute and higher order accuracy was achieved at a faces of cells through a Taylor series expansion, [99]. Pressure describe as PRESTO (PREssure Staggering Option) is used with body force weighted. This option compute the pressure on face by assumed the normal acceleration of fluid results from the pressure gradient is continuous through each face. This option was good for high Rayleigh number (natural convection flows), [99]. The SIMPLEC (Semi-

Implicit)scheme is used for the pressure-velocity coupling. It's used as relationship between pressure and velocity to enforce mass conservation and obtain the pressure field.

Under relaxation factor (α) used to control update of the variables value (ϕ) which computed at each iteration by used the following equation:

$$\phi_n = \phi_{\text{old}} + \alpha \Delta \phi \quad \text{…. (4-22)}$$

This means that all equations have under relaxation factor associate with them. In (Airpak) software there are a default under relaxation factor for each variable, these default value are near optimal and suitable for many problems for largest numbers of cases [99]. The under relaxation factor used are listed in Table(4-19).

Table(4-19) Under relaxation factors

Item	Under-relaxation factors
Pressure	0.3
Temperature	1
Body Force	0.1
Momentum	0.7
Turbulent Kinetic Energy	0.5
Turbulent Dissipation Rate	0.5
Turbulent Viscosity	1
Carbon dioxide	0.8
H_2O	1

4.6.4 Convergence criteria

The residual error (R_E) for each variable (ϕ) is computed at end of each iteration by used the following equation:

$$R_E = \phi_n - \phi_{n.old} \quad \text{…. (4-23)}$$

The solve will stop after the residual error reach to the values shown in Table(4-20) for continuity, velocities, energy, H_2O, CO_2, turbulent dissipation rate and turbulent kinetic energy equations. The residual error is inversely proportional to the accuracy of the numerical results.

Table(4-20) Residual error for tested cases.

Equation	Continuity	X-velocity	Y-velocity	Z-velocity	Energy	K	ε	H_2o	Co_2
R. error	10^{-5}	10^{-5}	10^{-5}	10^{-5}	10^{-6}	10^{-5}	10^{-5}	10^{-5}	10^{-5}

4.7 Prediction of Thermal Comfort Parameters

The completion of analysis by AIRPAK software, the thermal comfort parameters can be predicted, such as the mean age of air, air temperature and velocity distributions, (ADPI), (PMV), (PPD) and temperature distribution effectiveness (ε_t). The (PMV), (PPD) and (ε_t) can be calculating by using the following equations respectively, **[8, 44 and 45]**:

$$PMV = [0.303\exp(-0.036M) + 0.028]L \quad (4\text{-}24)$$

$$PPD = 100 - \exp-[0.03353(PMV)^4 + 0.2179(PMV)^2] \quad (4\text{-}25)$$

$$\varepsilon_t = \frac{T_e - T_s}{T_{av} - T_s} \quad (4\text{-}26)$$

The mean air age (τ) and air exchange efficiency (η_ε) calculated by used the following equations, **[28]**:

$$f(\tau_r) = \frac{dF(\tau_r)}{d\tau} \quad (4\text{-}27)$$

$$F(\tau_r)=1-\int_0^{\tau} f(t_r)dt \qquad (4\text{-}28)$$

If assume $f(\tau_r)$ is the age of air particles that arriving at a given location is between (τ) and (τ +dτ) and $F(\tau_r)$ that the air age larger than (τ).

The local mean air age at (r) point was defined by the average age of all the air particles arriving at that point, **[28]**.

$$dF(\tau_r) = \int_0^{\infty} tf_r(t)dt = \int_0^{\infty} F_r(t)dt \qquad (4\text{-}29)$$

If assumed $\langle\tau\rangle$ as the room mean air age. The nominal time constant (τ_n) of a ventilated zone (the ratio of zone volume to the air flowrate supply), **[8, 28,** and **29]**.

$$\tau_n = \frac{V}{q} \qquad (4\text{-}30)$$

Then the air exchange efficiency (η_a) represented as, **[29** and **30]**:

$$\eta_a = \frac{\tau_n}{2\langle\tau\rangle} \qquad (4\text{-}31)$$

Finally, to predict thermal comfort for different numerical cases under Hilla (Iraq) climate, (CBE) tool (Center for the Built Environment) is used. This tool was produced by building energy center to calculate the thermal comfort conditions according to ASHREA standard 55 -2017(https://comfort.cbe.berkeley.edu). The tool depends on the average room dry bulb temperature, mean radiant temperature, average air velocity, average relative humidity, the value of metabolic rate and clothing level as shown in Fig.(4-24).

The mean radiant temperature (MRT) can be define as “the uniform temperature of an imaginary enclosure in which the radiant heat transfer from the human body equals the radiant heat transfer in the actual non-uniform enclosure”. The (MRT) is

calculated by using the results of the radiant heat transfer calculations in (Airpak). The (MRT) is a main parameter has a high effect on the comfort level. It has strong influence on comfort indexes such as (PMV) and (PPD) [99].

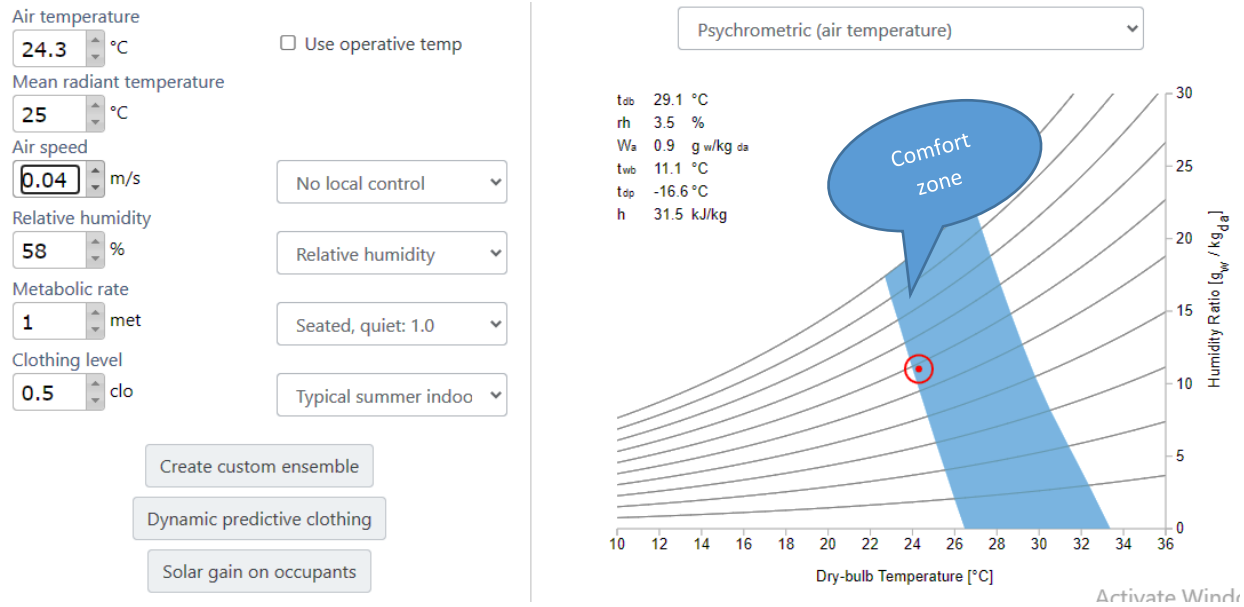

Fig.(4-24) CBE thermal comfort tool

CHAPTER FIVE

Results
&
Discussion

Chapter Five
Results and Discussion

Displacement ventilation with chilled ceiling system was studied experimentally and numerically in an office room and a classroom located in Hilla city (Iraq) under summer periods (hot and dry climate). This chapter is divided into four parts to achieve the objectives of this study. The first part deals with the experimental results for insulated office room. The behavior of each cooling system has been evaluated and compared with available data in previous studies. The second part dealt with the numerical results for insulated office room by using (ANSYS AIRPAK.3.0.16). The results were evaluated and then compared with the experimental results. The third part focuses on the comparison between numerical results for insulated and non-insulated office rooms. The fourth part deals with the numerical results for classroom by using (ANSYS AIRPAK.3.0.16) software.

5.1 Experimental Results (insulated office room)

Displacement ventilation with chilled ceiling system was studied experimentally in the office room as indicated in the third chapter. The experimental work of the office room was done in (August) and (September) under Hilla city climate. The ambient temperature in (August and September) varied between (40-50^{o}C) in Hilla city, **[106]**. This work made in (July) as primary test to treat the side problems that appear during laboratory work.

The experimental study divided into two cases depending on the shape of air supply diffuser by using rectangular diffuser for (case-I) and semi-circular diffuser for (case-II). Each case had four tests based on the portion of cooling load treated by chilled ceiling (η) as (0%, 25%, 50%, and 80%). The temperature for displacement ventilation air supply is varied as (20, 21.5 and 23 and 24^{o}C) which cover (100%, 75%, 50% and 20%) of cooling load respectively at a constant air flow rate for the two cases (35L/s (74.1 cfm)).

The experimental results are divided into four parts (air age results, air temperature distribution results, carbon dioxide removing results and predicting thermal comfort). Table.(5-1) listed the main measuring parameters collected in the experimental tested days.

Table(5-1) The main measuring parameters obtained in the experimental tests

						Displacement ventilation			Chilled ceiling				
	Test	**η (%)**	**Test day**	**T_{av} (^oC)**	**RH_{av} (%)**	**CL_{DV} (W)**	**T_s (^oC)**	**T_e (^oC)**	**CL_{CC} (W)**	**T_{ws} (^oC)**	**T_{wr} (^oC)**	**Q_{ws} (m^3/h)**	**T_{cc} (^oC)**
Case-I	Test-1	0	10/8/2020	25.2	55.4	370	20	27.4	0	-	-	0	-
	Test-2	25	12/8/2020	24.9	55.9	277.5	21.5	26.2	92.5	19.7	20.25	0.144	22.5
	Test-3	50	17/8/2020	26	54	185	23	27.1	185	18.4	18.93	0.288	21.2
	Test-4	80	19/8/2020	26.27	56.9	74	24	26.8	296	17	17.56	0.5	19.4
Case-II	Test-5	0	24/8/2020	25.27	55.2	370	20	27.8	0	-	-	0	-
	Test-6	25	26/8/2020	25.3	59.2	277.5	21.5	26.85	92.5	19.2	19.8	0.144	22.3
	Test-7	50	2/9/2020	25.6	54.7	185	23	26.56	185	18.4	19.1	0.288	21.4
	Test-8	80	7/9/2020	26.1	53.5	74	24	26.75	296	16.8	17.27	0.5	19.5

The results obtained at the interval between (1:00PM.) and (2:30PM.) O'clock at steady state after four hours from being the (DV/CC) system started.

5.1.1 Local air age results

Figures (5-1) to (5-3) show the mean local air age at steady state conditions for three measurements stand at different values of (0%, 25%, 50% and 80%) for the two cases (at breathing zone level (1.1 m) for setting condition and (1.8 m) for standing condition person in each measuring stand). The air age values were measured by using the decay method as indicated in the third chapter. The local air age at (1.8 m) level is higher as compared with the level at (1.1 m) in the two cases for different values of (η). That's mean the local air age increases with height regardless of the shape of diffuser and the value of cooling load treated by chilled ceiling due to an increased distance from the air supply diffuser.

Measuring stand-2 that located between the two occupants (between heat sources as shown in Fig.(3-19)). The local air age at (1.8 m) level (Fig.(5-2)) for the two cases is minimum as compared with the air age values in the same level at other stands regardless of portion of the load treated by the chilled ceiling (η) and type of diffuser as shown in Figs.(5-4) and (5-5). These figures presents the values of air age at level (1.8 m) for stand-2 with rectangular and semi-circle diffusers respectively. Since, the air in this zone is hotter than other zones in office room (location of heat sources), that cause base of the plumes leads to increase in air velocity. The increase in air velocity leads to decrease air age and air contaminants concentration.

The maximum value of local air age at (1.8 m) in stand-2 with using semi-circle diffuser is (415 sec) at (η=80%) while its (441 sec) with using rectangular diffuser. This result gives a good idea about the effect of air supply distribution on the local air age.

Figs.(5-6) and (5-7) present the relation between the average age air at breathing levels (1.1 m) and (1.8 m) respectively for the two cases at different (η). The average air age in each level in office room increases with the increase portion of cooling

load treating by chilled ceiling (η). This is because of mixing between hot air rise from the lower zone and cold air down from upper zone after it cold by chilled ceiling due to convection and leads to reduce the air speed. For each level, the local air age when using rectangular diffuser is higher than of air age when using semi-circle diffuser at each value of (η) although the airflow was constant in each test. This is due to the effect of the uniform and redial air distribution supplied by the semi-circle diffuser, addition to fresh air diffusion speed in the room led to reducing the air age. These results show that the semi-circle diffuser is more efficient in air exchange than rectangular diffuser. The effect of the diffuser shape on the air age being decrease the further away from the air supply diffuser, that's clearly in the Fig.(5-7), the difference in average air age at level (1.8 m) between the two cases is low compared with average air age different at (1.1 m) (Fig.(5-6)).

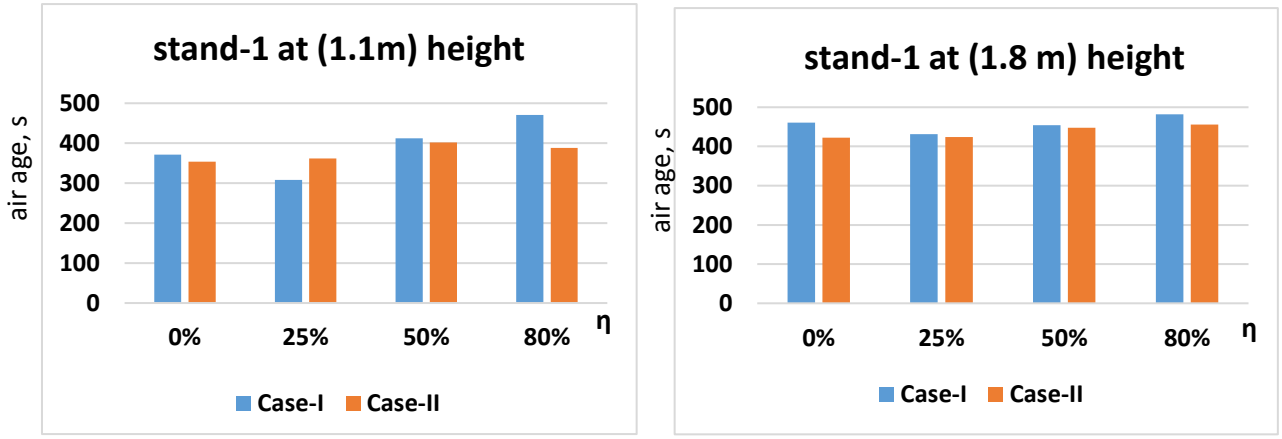

Fig.(5-1) Local air age at (1.1 m) and (1.8 m) height for instrument stand-1 at different values of (η) for the two cases (case-I and II)

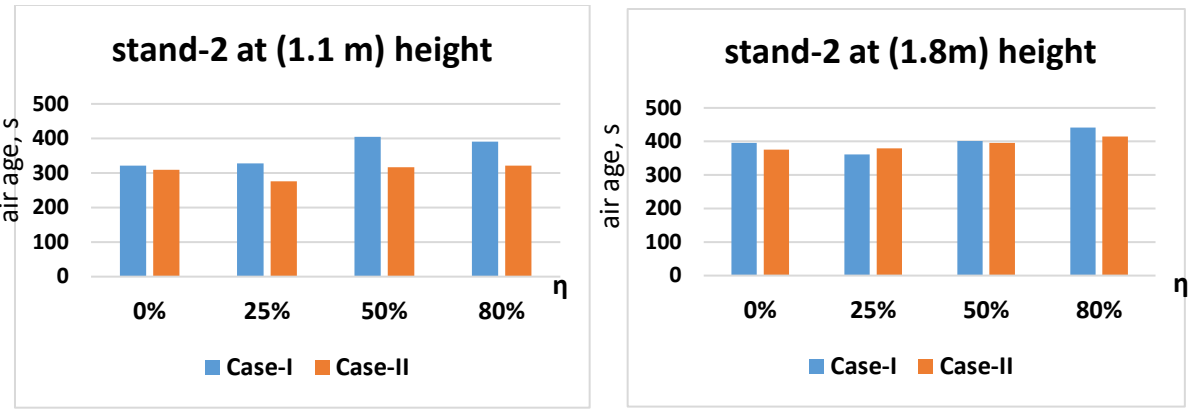

Fig.(5-2) Local air age at (1.1 m) and (1.8 m) height for instrument stand-2 at different values of (η) for the two cases (case-I and II)

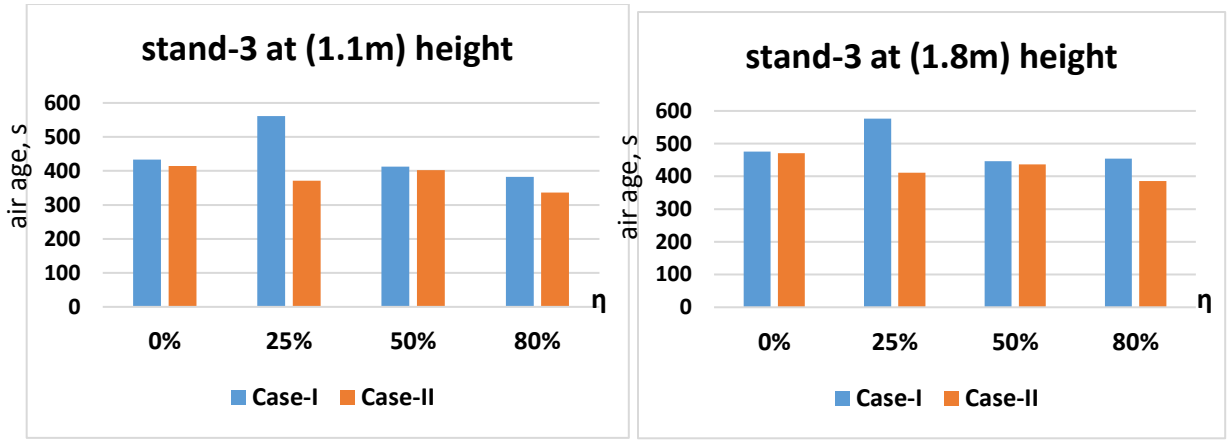

Fig.(5-3) Local air age at (1.1 m) and (1.8 m) height for instrument stand-3 at a different values of (η) for the two cases (case-I and II)

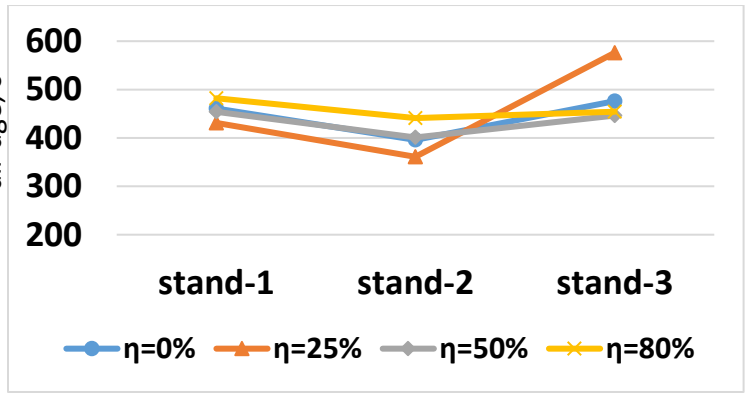

Fig.(5-4) Local air age at 1.8m level at each instrument stand for four testes with rectangular diffuser (case-I)

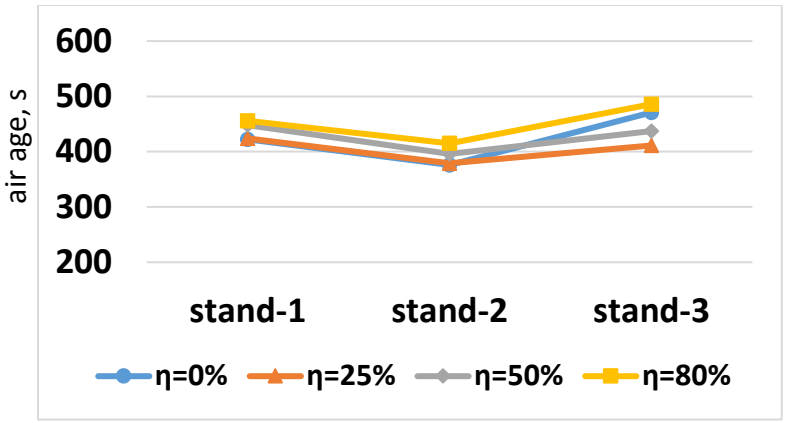

Fig.(5-5) Local air age at 1.8m level at each instrument stand for four tests with semi-circular diffuser (case-II)

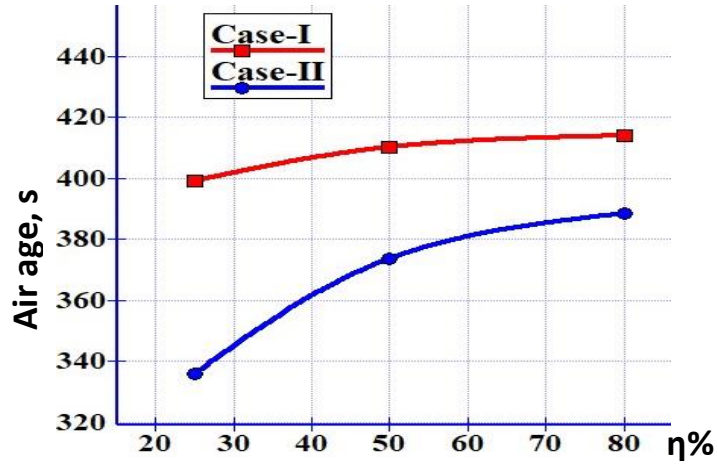

Fig.(5-6) Average air age at level (1.1 m) for the two cases (I and II) at different values of (η)

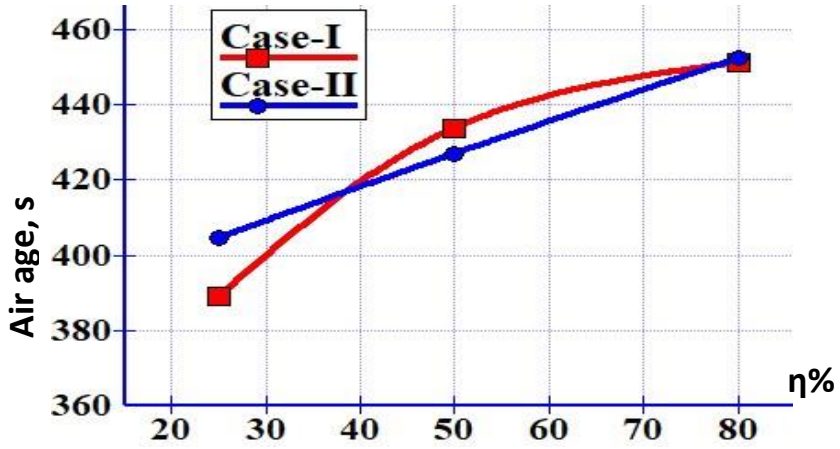

Fig.(5-7) Average air age at level (1.8 m) for the two cases (I and II) at different values of (η)

5.1.2 Temperature distribution results

Figs.(5-8) and (5-9) show the temperature distribution with room height for each measuring stand at different values of (η) with rectangular diffuser and semi-circle diffuser respectively. Layer stratified was one of the hallmarks of displacement ventilation. Supply air at low temperature flows along the floor, after that the air is heated when it passes through the heat sources and moving up due to the effects of buoyancy. For the two studied cases and for three measuring stands shown temperature rise with height at each value of (η). Also the temperature stratification decreases with increase portion of load treated by chilled ceiling due to its low temperature. The air temperature at the upper zone (above 1.8m height) will be decreasing due to convection with chilled ceiling and then the air being moves to the lower zone lead to minimize the air temperature in the zone below (1.8 m) height and causes a decrease in temperature difference with height. These results are similar to that founding by **Schiavon et. al., [37]** for a room air temperature stratification with (DV/CC) system by using corner displacement diffuser at different numbers of ceiling panel as shown in Fig.(5-10).

When compared air temperature distribution with a height between the two cases (for the two diffuser types), the air temperature distribution with height (at three measuring stands) by using semi-circle diffuser (case-II) is lower compared with rectangular diffuser (case-I) when chilled ceiling was used regardless of (η) value especially at the measuring stand-1 that located near of air supply diffuser as shown in Figs.(5-11) to (5-13). This is an additional advantage of the uniform and redial air distribution for the semi-circular diffuser, which lead to uniform air temperature distribution in the room zone. After that (at the zone over 1.8 m) height the air temperature begins to be affected by the chilled ceiling temperature and fade the effect of diffuser shape, that's led to converging the air temperature values in the upper zone for the two cases. For the stands-2 and 3, the effect of diffuser shape was

smaller because the far distance from the air supply diffuser and it location between the heat sources.

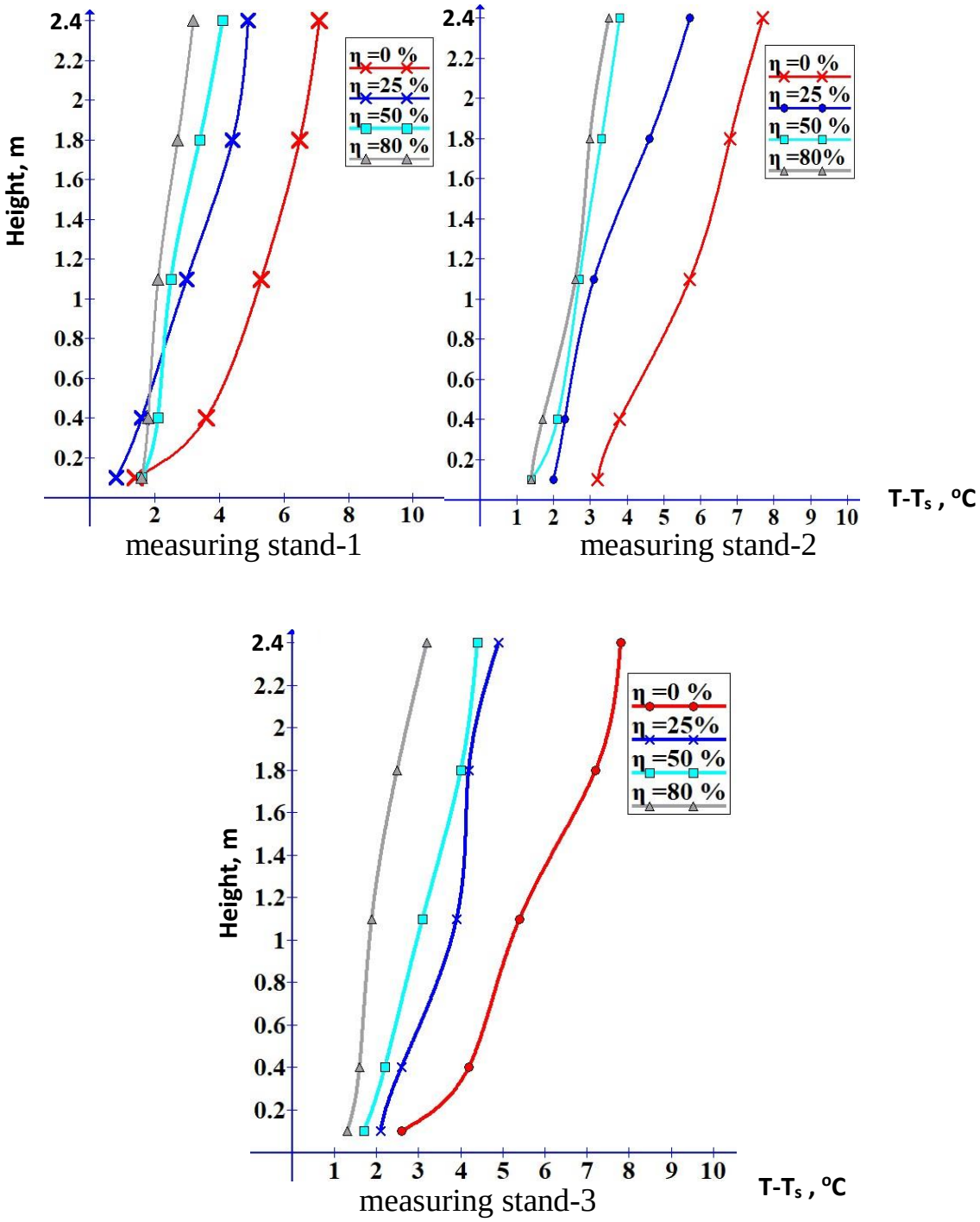

Fig.(5-8) Temperature distribution with height at different value of (η) for three measuring stands (case-I)

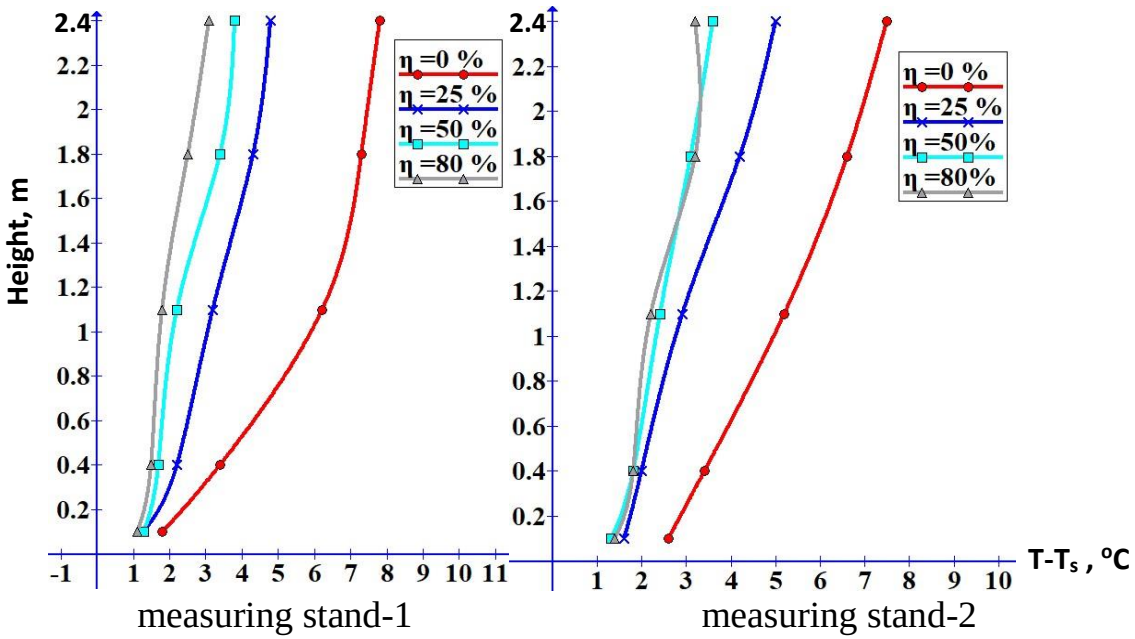

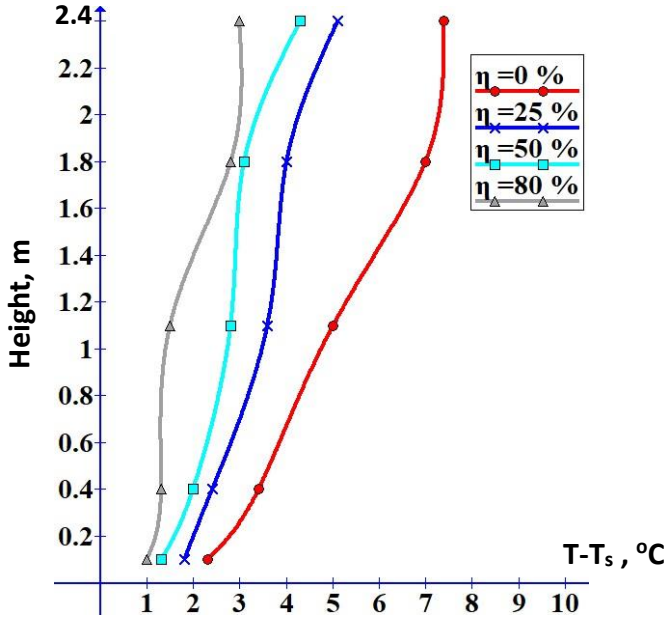

Fig.(5-9) Temperature distribution with height at different value of (η) for three measuring stands (case-II)

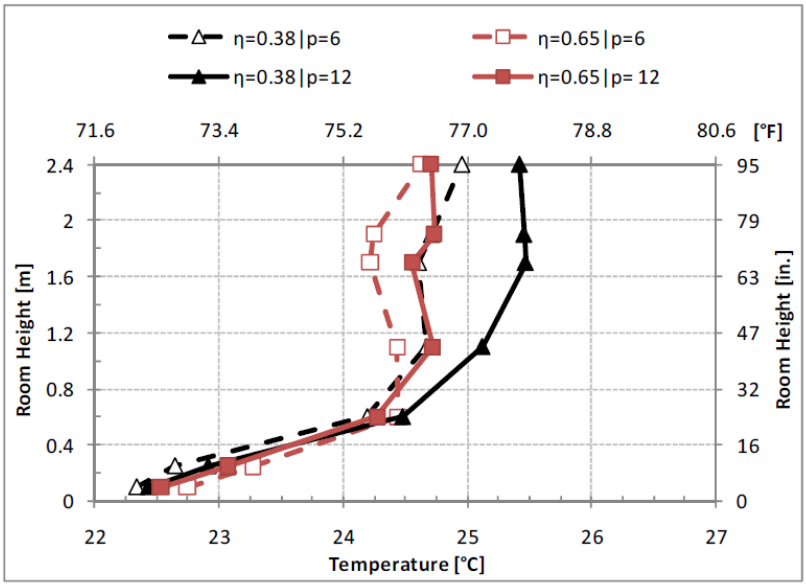

Fig.(5-10) Temperature profiles for test η=0.38 and η=0.65, **[37],**

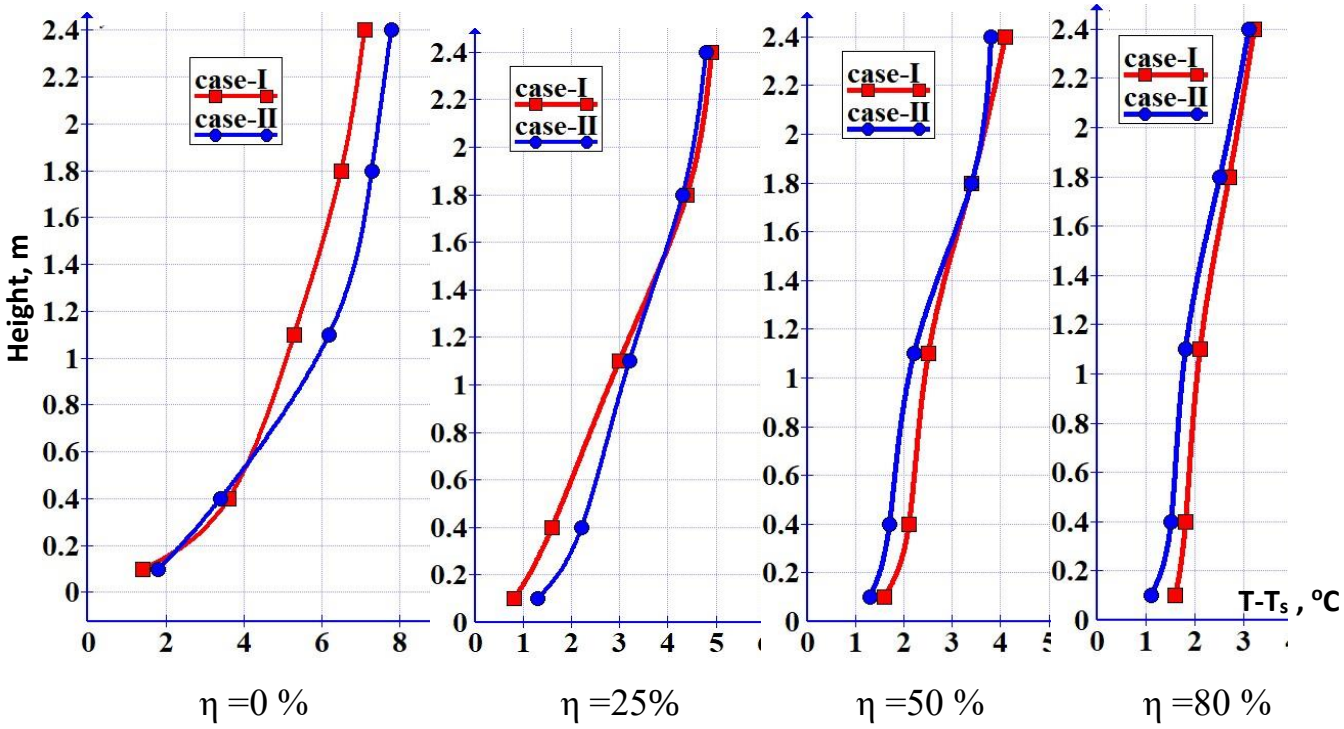

Fig.(5-11) Temperature gradient with height for the two cases at different (η) at measuring stand-1

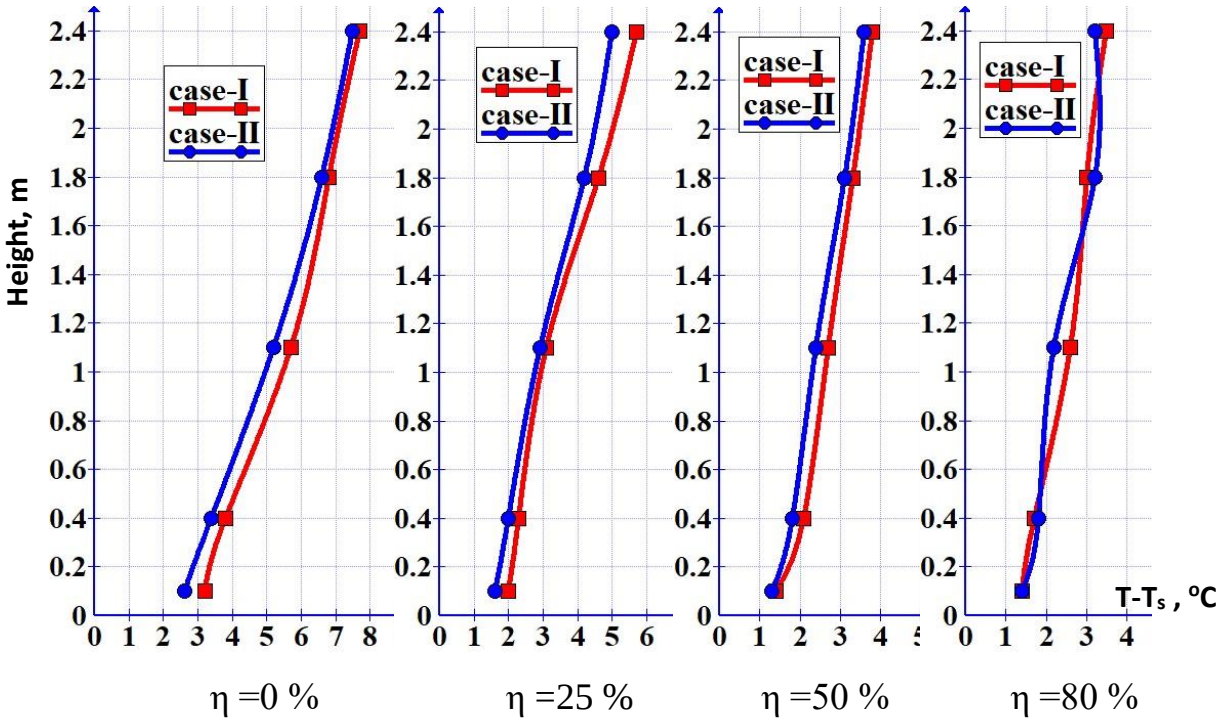

Fig.(5-12)Temperature gradient with height for the two cases at different (η) at measuring stand-2

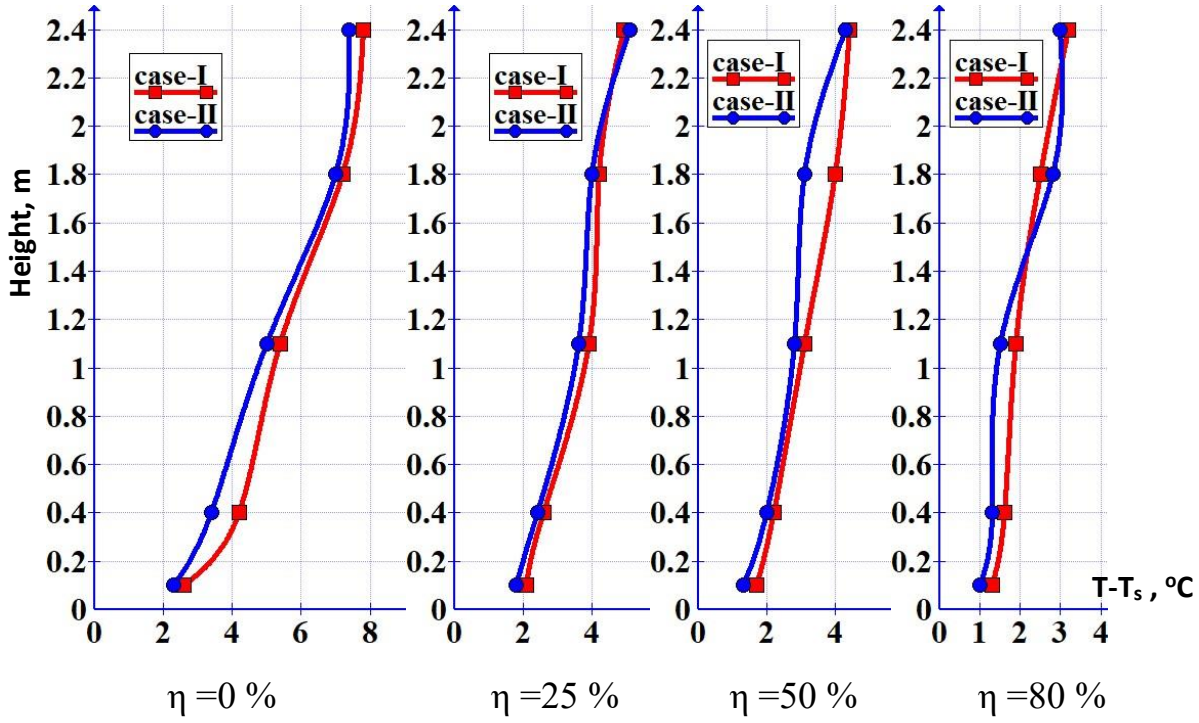

Fig.(5-13)Temperature gradient with height for the two cases at different (η) at measuring stand-3

The temperature difference between head and foot for a seated person (between 0.1-1.1m level) was specified by ASHRAE standard was between (2-3^{o}C). The study finds that the value of temperature difference between head to foot for a seated person decreasing with increase portion of cooling load treated by chilled ceiling as shown in Fig.(5-14). The decrease in air temperature gradient with (η) between (0-80%) leads to decreasing in temperature difference between head to foot of a seated by (1.14^{o}C) when using rectangular diffuser while its decrease by (1^{o}C) when using semi-circle diffuser. The temperature difference between head to foot by using rectangular diffuser is lower when compared with semi-circle diffuser at test without chilled ceiling (η =0) while at other tests (η value equal to 25-80%) indicated that the values of (ΔT_{fh}) by using semi-circle diffuser is lower when compared with the rectangular diffuser due to the ability of semi-circle diffuser to reduce the air age. Thus, cold air arrives faster to the human body. This means that increasing the value of (η) tends to reduce the temperature stratification for the two cases. This result explains clearly the effect of chilled ceiling temperature on thermal comfort.

Fig.(5-15) shows the temperature difference between head to foot as a function of chilled ceiling temperature for the two cases. The (ΔT_{hf}) directly proportional with chilled ceiling temperature (increase chilled ceiling temperature means decrease in the portion of cooling load treated by chilled ceiling). Then it agrees with the results mentioned in Fig.(5-14). These results are consistent with design diagram developed by **Tan,** [**111]**, Fig.(5-16).

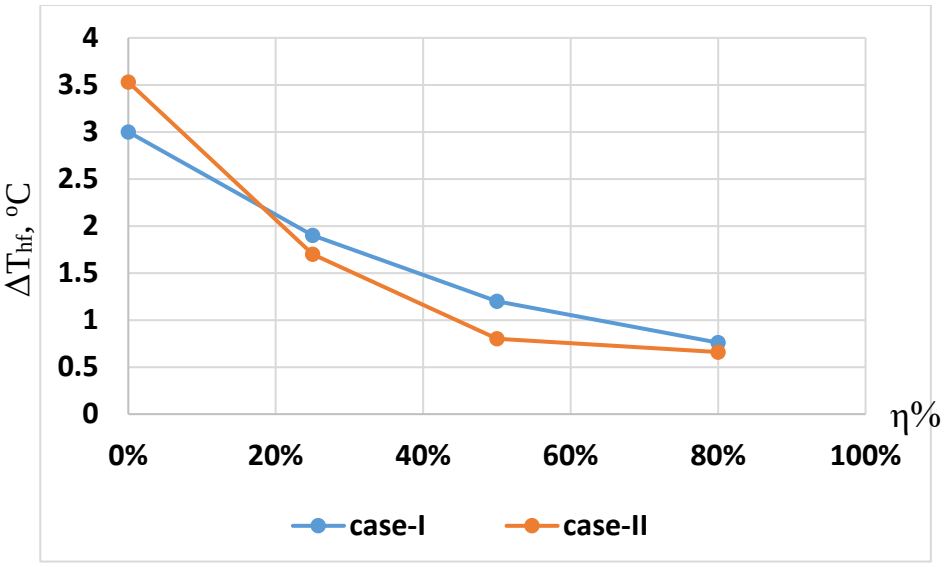

Fig.(5-14) Temperature difference calculated between head to foot for seated occupant (0.1-1.1 m) as a function of the chilled ceiling cooling load ratio (η)

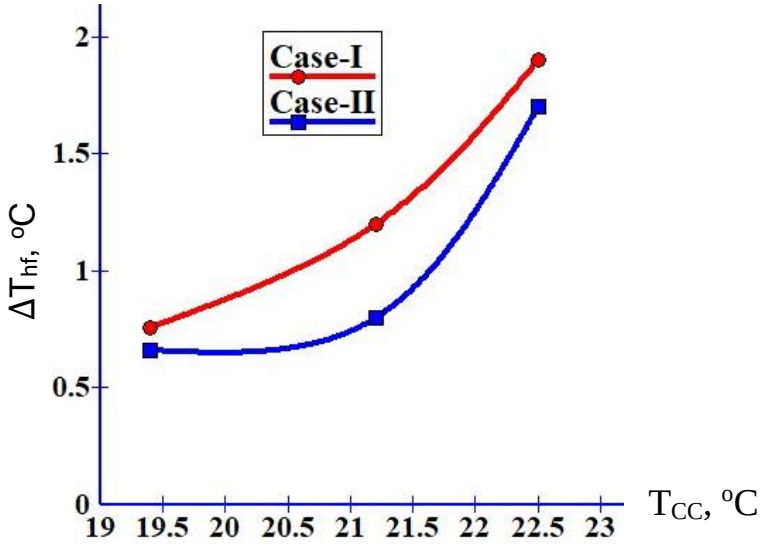

Fig.(5-15) Air temperature difference between head and foot for set person as a function of chilled ceiling temperature

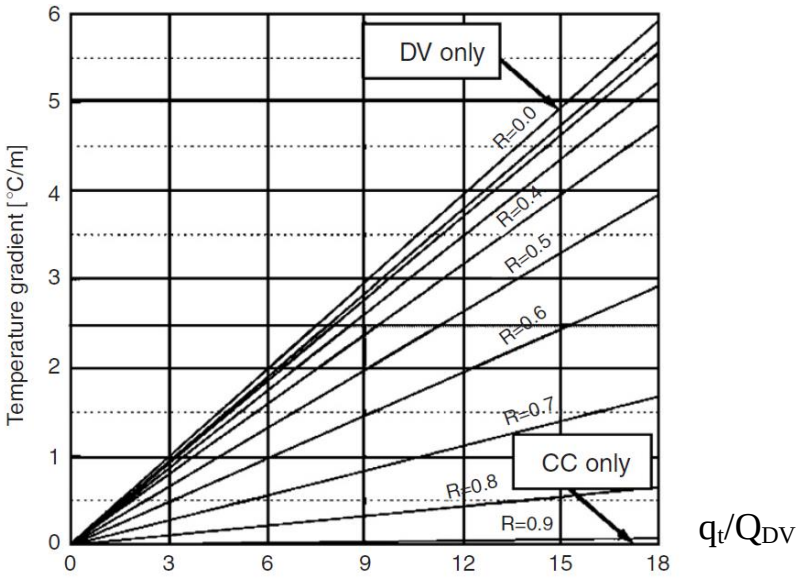

Fig. (5-16) Design diagram developed by **Tan et. al. [111]**, (R= η)

Fig.(5-17) shows the relation between cooling load ratio (η) and temperature distribution effectiveness (ε_t) for the two cases. In general the increase in cooling load treated by chilled ceiling means low temperature of chilled ceiling surface. A decrease in chilled ceiling surface temperature leads to decrease air temperature which contact with it. Due to that the exhaust air temperature decreases with increase value of cooling load ratio (η) as shown in table(5-1). This leads to a decrease in temperature distribution effectiveness based on Eq.(4-26)**.**

The advantage of air age value by used semi-circular diffuser (as shown in the previous figures) gives more chance to contact between cooled fresh air and heat sources. That led to improve the heat transfer by convection process. Due to this the exhaust temperature by using semi-circle diffuser (Table(5-1)) is higher compared with rectangular diffuser at each value of (η). This results give preference to semi-circle diffuser in term of temperature distribution efficiency and explain the effect of supply air flow diffusion method by (180^o) with semi-circle diffuser while the air supply flows in one way with the rectangular diffuser. Due to this the Fig.(5-17) shows clearly that the temperature distribution effectiveness (ε_t) by using semi-

circular diffuser is high when compared with rectangular diffuser especially at (η=0% and 80%) which is about (0.06) and (0.08) respectively. While the difference between the two cases decreases at (η=25% and 50%) which is about (0.02) and (0.01) respectively. This is due to the air supply temperature is minimum at (η=0%) and the chilled ceiling surface temperature is minimum at (η=80%) led to a greater effect of the air diffuser shape. That gives a good idea about the advantage of the semi-circle diffuser.

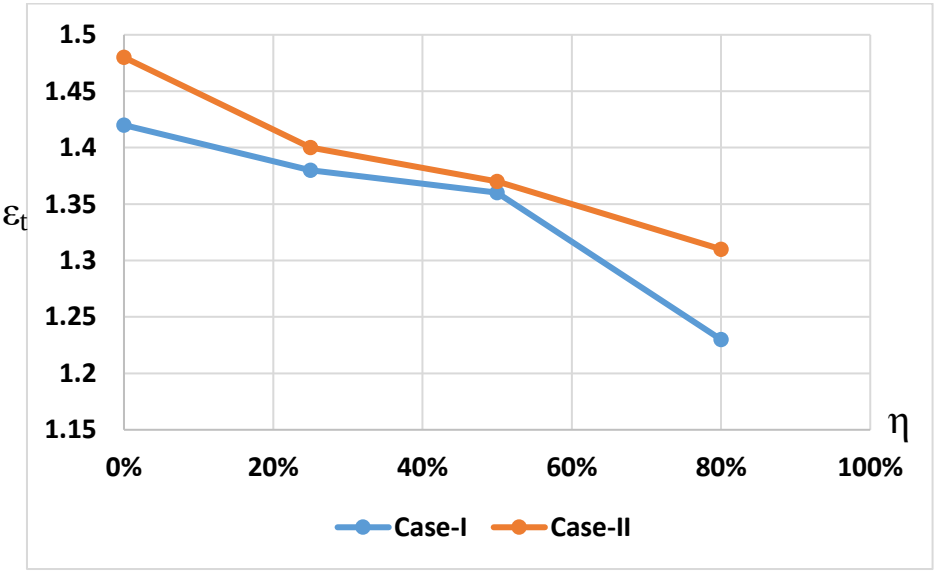

Fig.(5-17) Temperature distribution effectiveness varies with (η) for the two cases.

5-1-3 Carbon dioxide decay results

Figs.(5-18) to (5-21) present average measured of carbon dioxide concentrations varies with time at the two height levels for breathing zone at sitting and standing person (at 1.1m height level and 1.8m height level) for the two cases respectively at a different values of (η). All eight tests show variations in carbon dioxide concentration with the value of (η).

At the time between (0-500 sec), the CO_2 concentration between (1000- 800 ppm) respectively. For this interval the value of (η) have been little effect on the CO_2 concentration decay. This is due to the time needed for fresh air to reach to the zone above (1.1 m) and leads to a delay in the remove of CO_2 in high zone. The CO_2 concentration removing with time decrease with increase portion of cooling load treated by chilled ceiling until it reaches to the concentration in fresh air supply. The decay of CO_2 concentration with time associated with air movement in room zone. The decrease chilled ceiling temperature (increase value of η) leads to decrease air temperature by convection and it move down, cause's decrease in air age (as shown in section (5.1.1)) and obstruction of air removal from the exhaust and decreases CO_2 remove. Then the maximum time needed to remove CO_2 from the room occurs at (η=80%) for two cases at each measuring stand regardless of diffuser shape.

Variation in CO_2 concentration with office room height for the two cases are shown in Figs.(5-22) to (5-25) at (η) equal to (0%, 25%, 50% and 80%) respectively. At the values of (η) between (0-25%) for the two cases, the CO_2 concentration at (1.8 m) height is higher by about (10-20 ppm) than the concentration at (1.1 m) height because of the precedence of the arrival of fresh air to the (1.1 m) level. While at (η=80) the difference between concentration at the two breathing zone levels (1.1m and 1.8 m) be fading away, this is due to cooled air in the upper zone as a result of low chilled ceiling temperature.

It is noticed from these figures the clear effect of the diffuser shape in accelerating the removal of CO_2, which gave advantage to the semi-circular due to it has minimum air age compared with rectangular shape. This led to faster fresh air diffusion and reduce the removal Co_2 time.

These results compared with the results found by **Hormigos (2018),** [**58]**, it showed an acceptable converge as shown in Fig.(5-26)

The shape of the air supply diffuser has a direct effect on the remove Co_2 from space, that clearly in Figs.(5-22) to (5-25), the CO_2 remove by using semi-circle diffuser is faster by about (10 ppm/s) than rectangular diffuser at any value of (η).

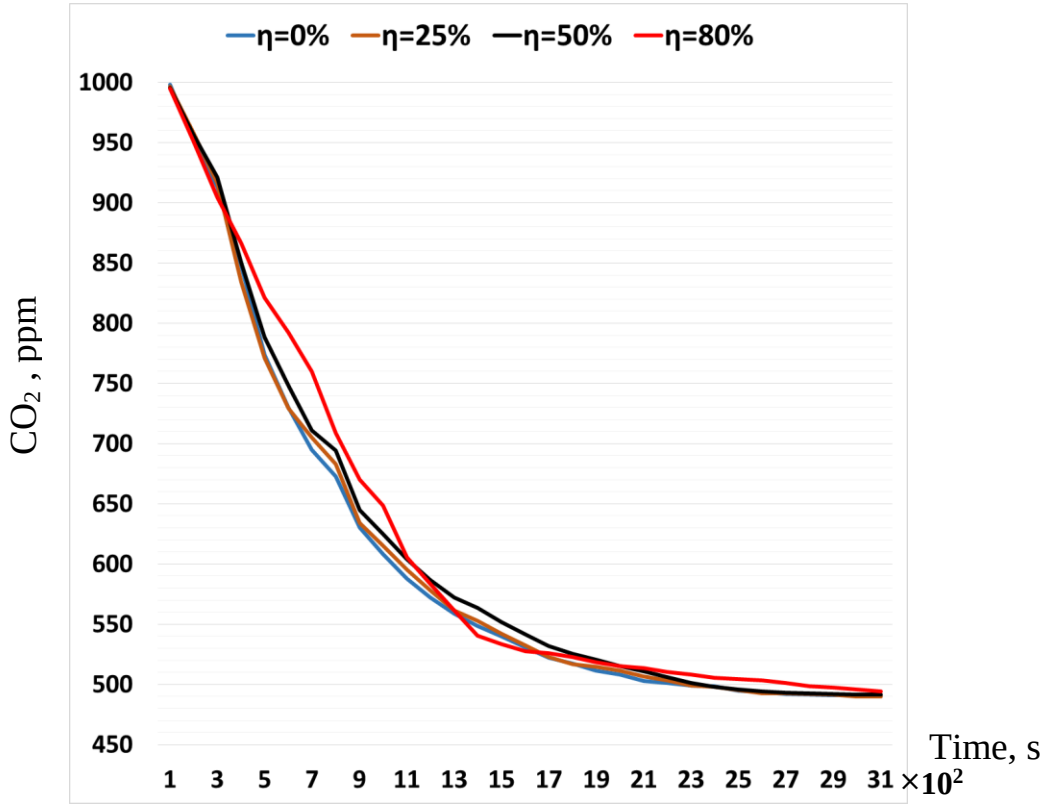

Fig.(5-18) Average CO_2 concentration with time at different values of (η) at (1.1 m) height, case-I

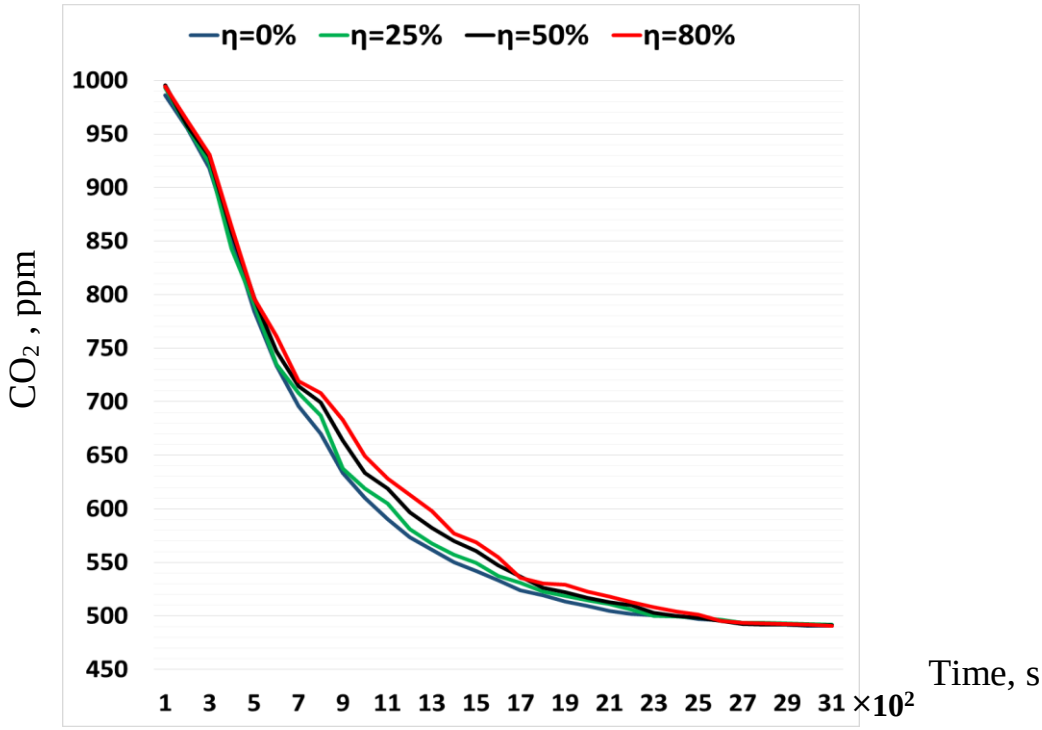

Fig.(5-19) Average CO_2 concentration with time at different values of (η) at (1.8m) height , case-I

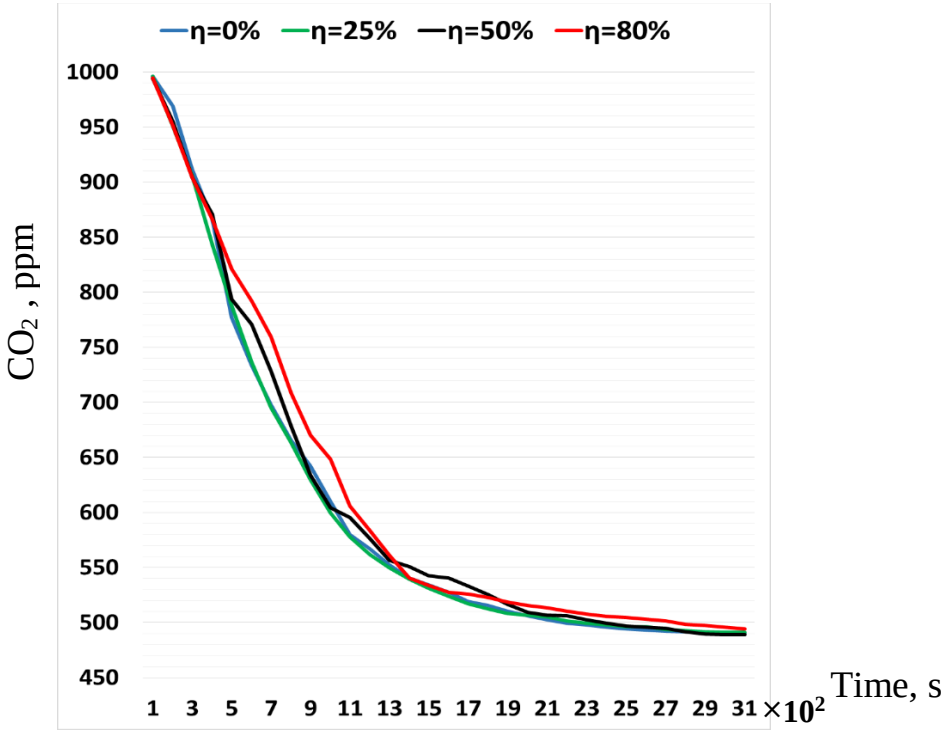

Fig.(5-20) Average CO_2 concentration with time at different value of (η) at (1.1m) height, case-II

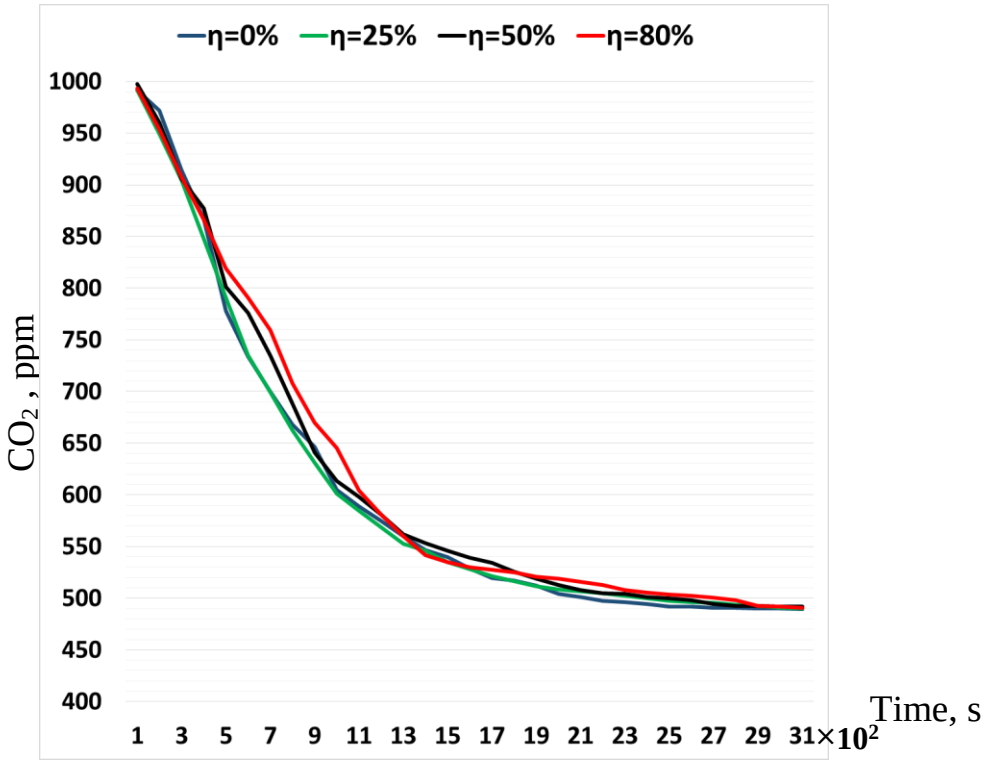

Fig.(5-21) Average CO_2 concentration with time at different values of (η) at (1.8m) height, case-II

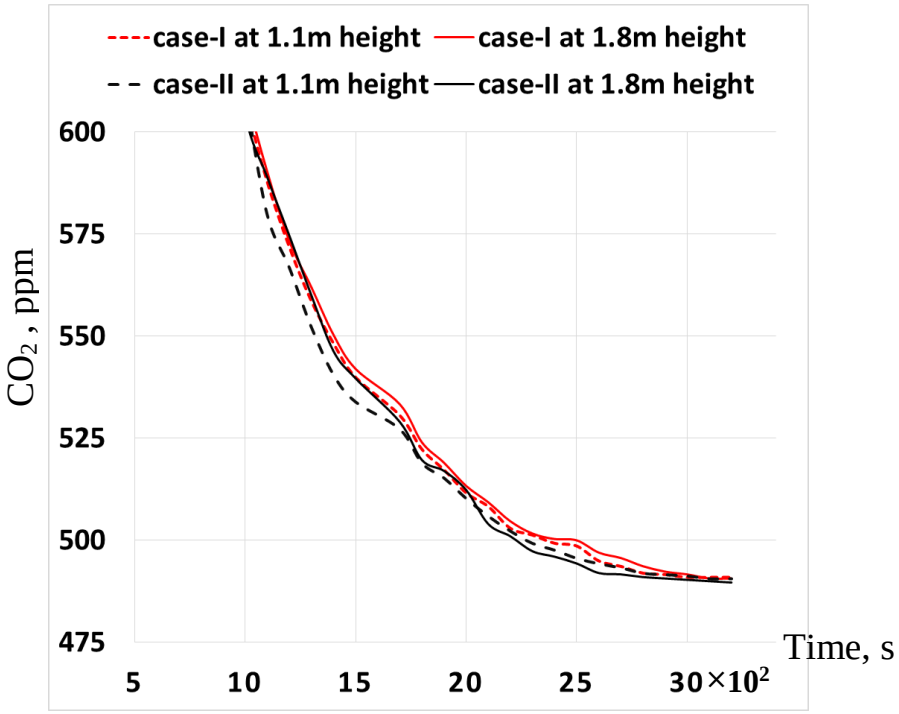

Fig.(5-22) Average CO_2 concentration with time at two height levels (1.1m and 1.8 m) for the two cases at η = 0%

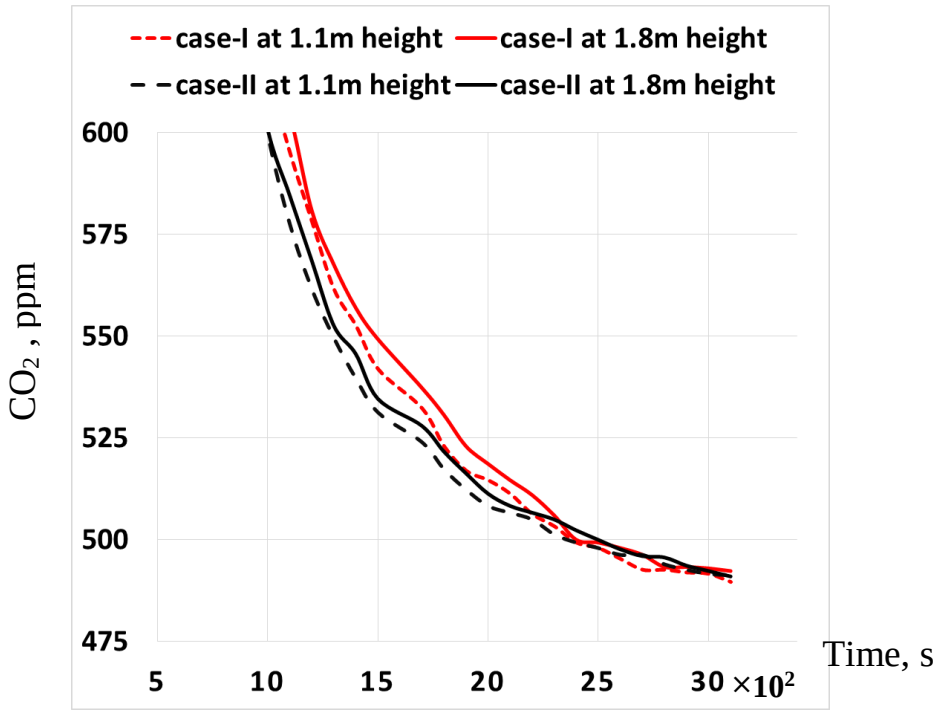

Fig.(5-23) Average CO2 concentration with time at two height levels (1.1m and 1.8 m) for the two cases at η = 25%

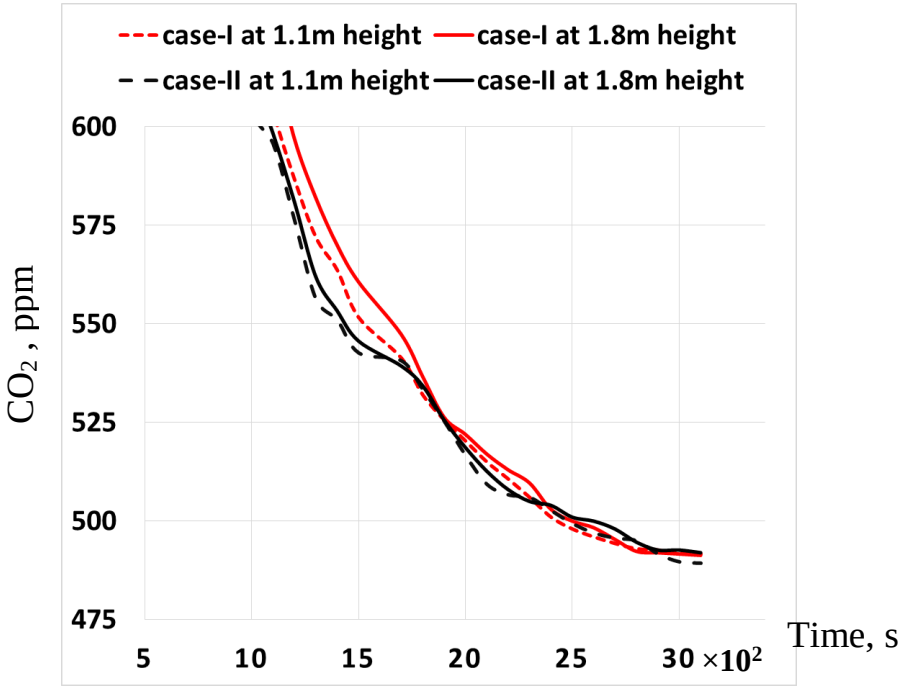

Fig.(5-24) Average CO_2 concentration with time at two height levels (1.1m and 1.8 m) for the two cases at η = 50%

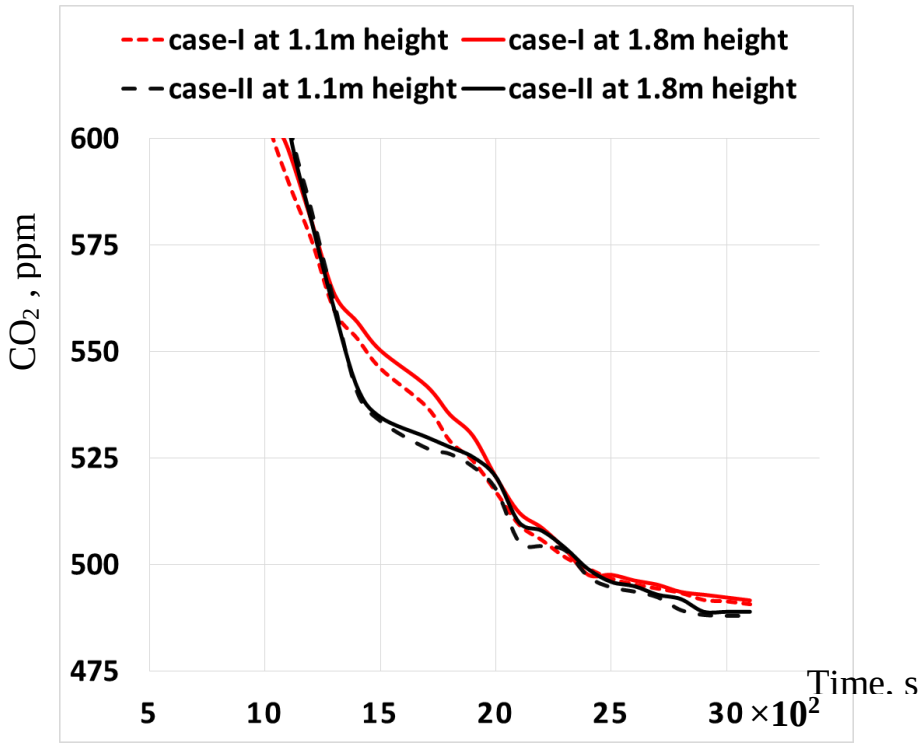

Fig.(5-25) Average CO_2 concentration with time at two height levels (1.1m and 1.8 m) for the two cases at η = 80%

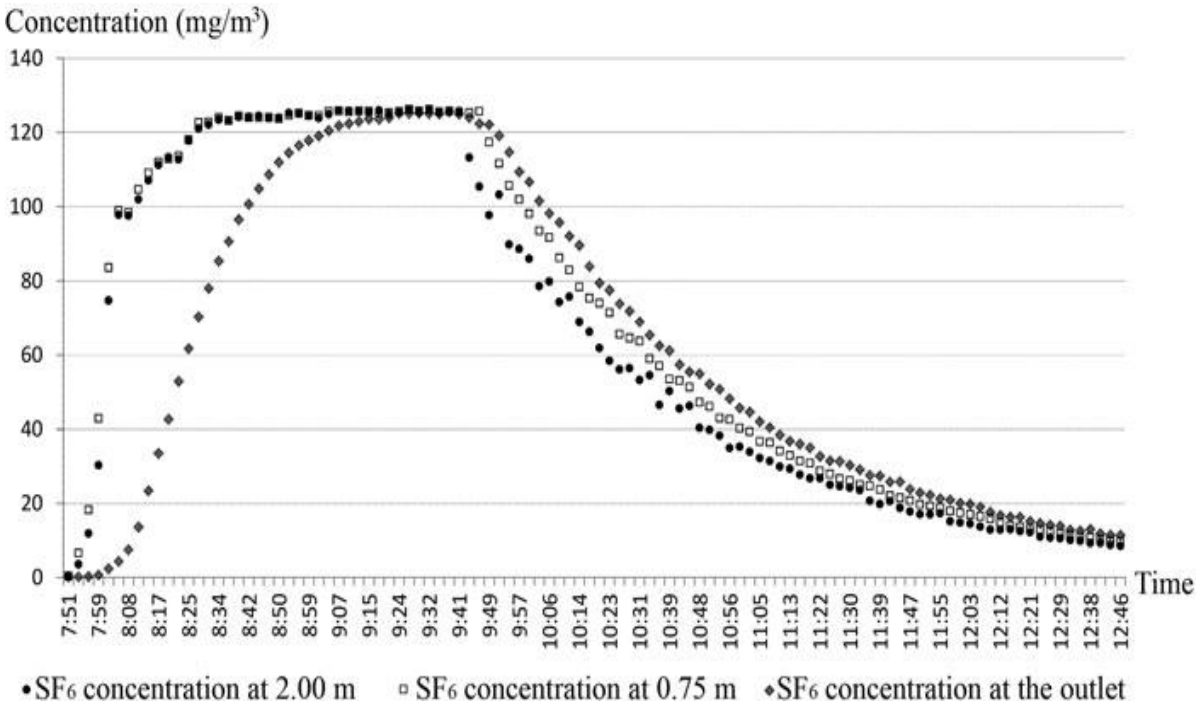

Fig.(5-26) Decay SF_6 concentration with time at different height levels**, [58]**.

5.2 Numerical Results

5.2.1 Numerical results for insulated office room cases

The two insulated office room cases at different supply diffuser shape (one way rectangular diffuser and semi-circle diffuser) are modeling by the ANSYS AIRPAK software, each case divided into four testes based on the ratio of cooling load treated by chilled ceiling as indicated in the fourth chapter, section (4.4). Boundary conditions for numerical analysis depending on the parameters obtain from experimental work. Numerical study aiming to get more results to study air age and thermal comfort parameters in further details as explain below:

Fig.(5-27) shows the mean local air age distribution contours of the insulated office room for the two cases at plane (z=1.25m, which pass through air supply diffuser and human body) with different values of (η). The mean local age of air within air supply diffuser is fresher than that inside room zoon. The mean local age of air starts from zero time and increasing after moving air in indoor zone. For the two cases, the breathing zone (between 0.1-1.1m height) is filled by fresher air more than other zone due to the air moving from down to up direction providing good air quality for the occupant. The air age at (1.1 m) height (breathing zone level) and at each value of (η) is fresher with using semi-circle diffuser compared with rectangular diffuser. This result show clearly the effect of air distribution method on the occupant comfort. For the two cases, the age of air is increasing with room height and the maximum value of mean air age at zone up to the diffuser location. That's mean low air movement in this zone leads to increase in pollution concentration and occupant discomfort. Increase value of (η) leads to increase age of air due to interchange the cool air coming from the chilled ceiling by convection and the hot air rise. The increasing in air temperature near the heat sources (person and computer…etc) by convection leads to decrease the age of air in this zone due to increase air velocity around the human body.

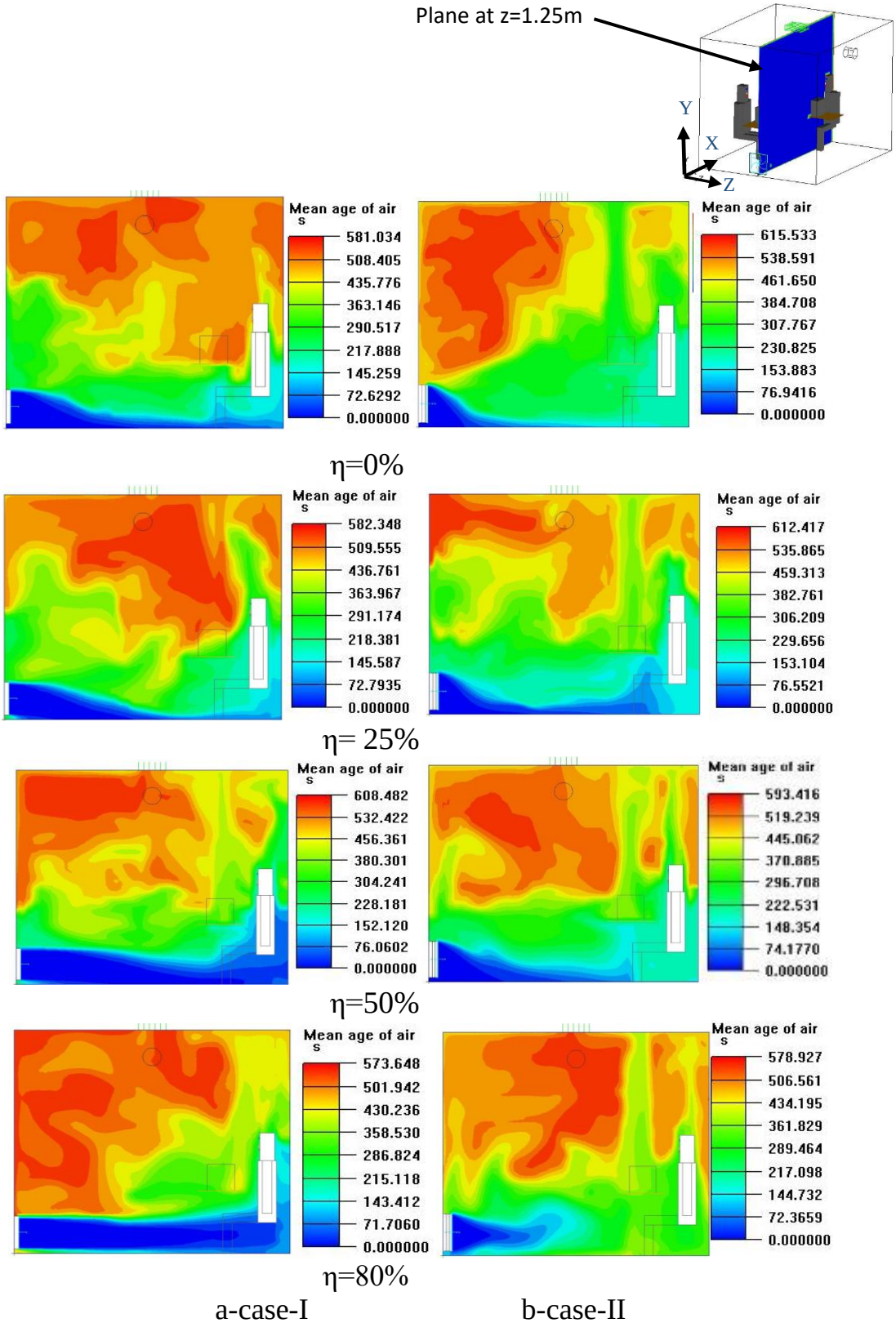

Fig.(5-27) Age of air contours with different (η) for the two cases (case-I and II) at plane z=1.25m

Figs.(5-28) and (5-29) show the air particle trace from the beginning at the supply air diffuser to the exhaust air for the two cases (case-I and case-II) respectively at different values of (η). A particle trace explain the path of a particle through the room and provides information about the time required for particle to exit from the office room. For the two cases the air age for air particle increase with increase portion of load treat by chilled ceiling (η). This result can be linked with the previous results, which showed the increase in air age with an increase in (η) as a result of the decrease in temperature of air falling from the ceiling. This results give idea about effect portion of cooling load treated by child ceiling on the air exchange efficiency. When used rectangular diffuser (Fig.(5-28)) the age of air particle at (η=80%) increase by (140 sec) compared with (η=0%). While with used semi-circle diffuser (Fig. (5-29)) the age of air particle difference between (η=0% and 80%) is (99 sec). This is due to the air particles movement is freer in the semi-circular diffuser and in all directions, unlike the rectangular diffuser in which the air particles movement is in one bundle and one direction.

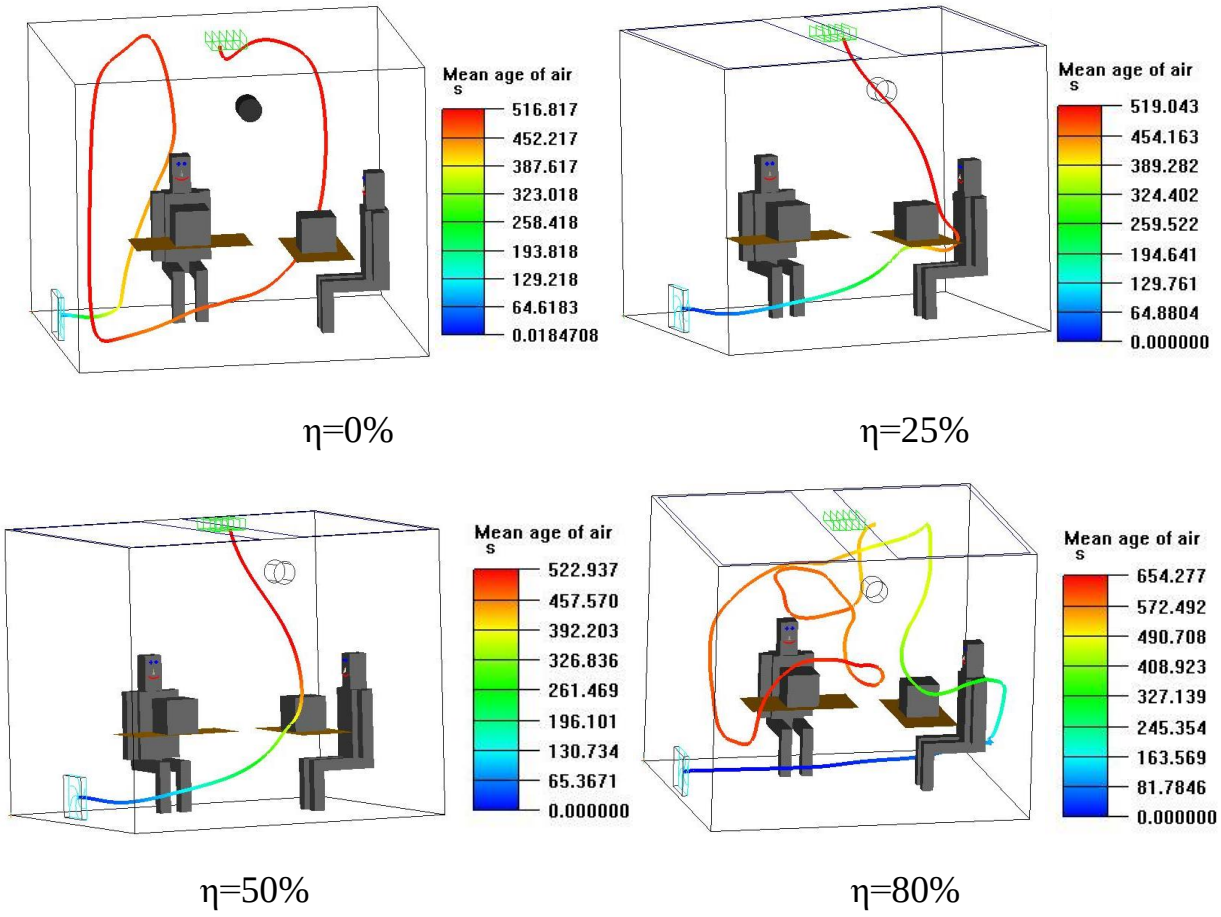

Fig.(5-28) Air particle trace from the inlet to outlet air at different (η), case-I.

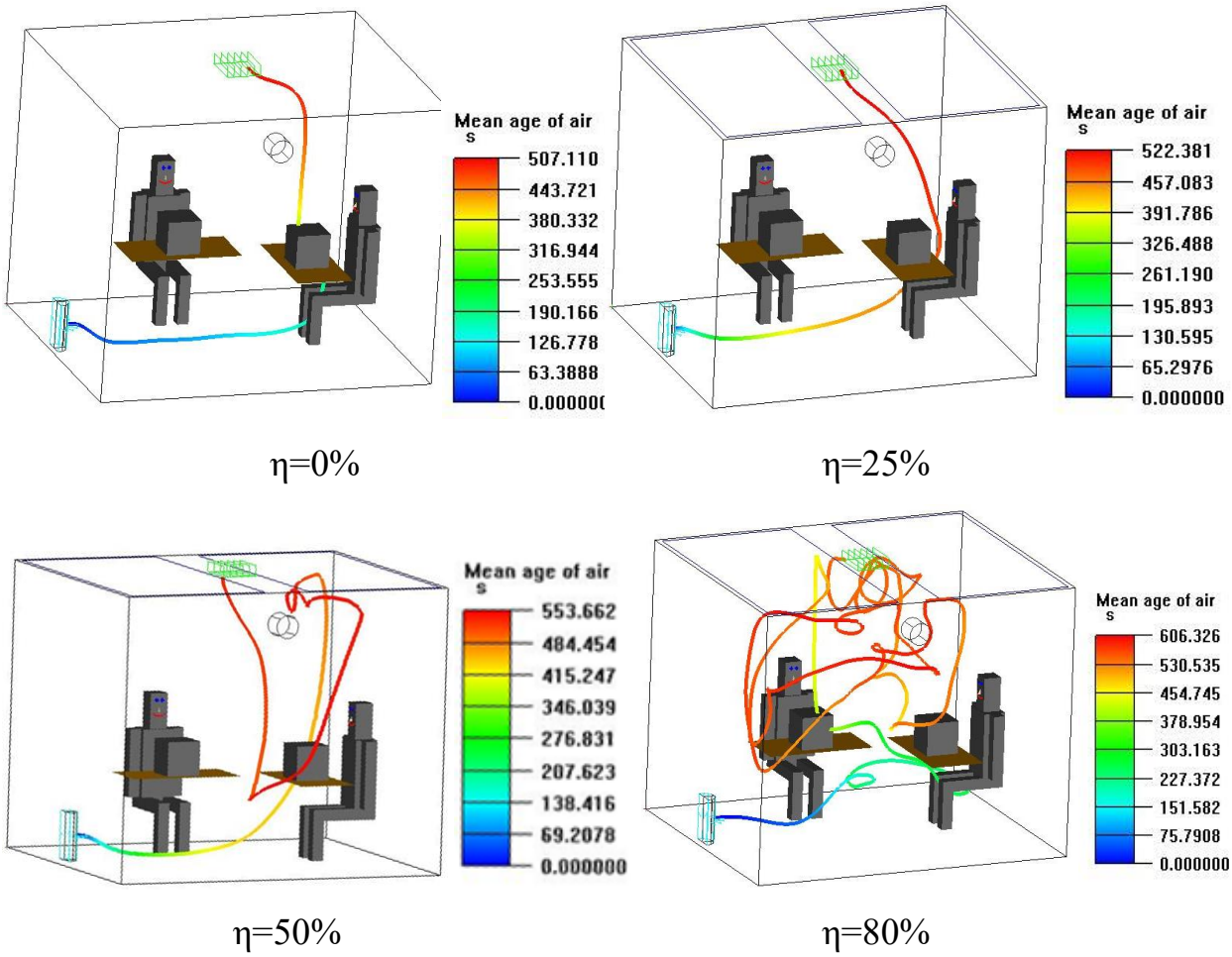

Fig.(5-29) Air particle trace from the inlet to outlet air at different (η), case-II

Fig.(5-30) shows vectors distribution plane of air velocity for the two cases at plane (z=1.25 m). The maximum value of air velocity located at the supply diffuser, which equal to (0.25 m/s) for the two cases. After that, the velocity reduces to reach zero in most point in indoor zone. The cooled air near the supply diffuser have been effected by buoyant force and this effect decreases with increase in air supply temperature. This due to that the air velocity near the floor (between 0.1m to 0.5 m height) will be increase with increase air supply temperature and it travels further in the horizontal direction.

The heat transfer by convection between the supply cooled air and the heat sources lead to increase in the velocity of the air, which is clearly in the zone near and above heat sources (over 1.1 m). At different (η) the air velocity above the occupant decreases with increase (η) due to the effect of cooled air near the ceiling which comes from convection between hot air and chilled ceiling. If compared this figure with air age contour (Fig.(5-27)) indicates that the increase in local air velocity leads to a decrease in mean local air age due to decrease the time needed to replace old air by fresher air indoor zone. While the air velocity in the zone over the supply diffuser is between (0-0.05 m/s) for the two cases leads to increase in air age in this zone, then these results showed there is a relation between air age, air velocity, and temperature. The cold air has a higher density than warmer air, and thus creates upward convective flows, then the warm air exits from the room by extracting grille.

The different methods of air distribution between rectangular and semi-circle diffuser lead to different air distribution in the room between the two cases especially at the zone near the floor (under 0.5m height). The high air supply momentum by using rectangular diffuser due to one-way flow in X-direction causes the air to flow further in the forward direction, in contrast to a semi-circle diffuser in which the direction of the supply air is radial flow direction as shown in Fig.(5-31). The radial flow direction by semi-circle diffuser gives an advantage to air exchange at room walls locate on the diffuser sides.

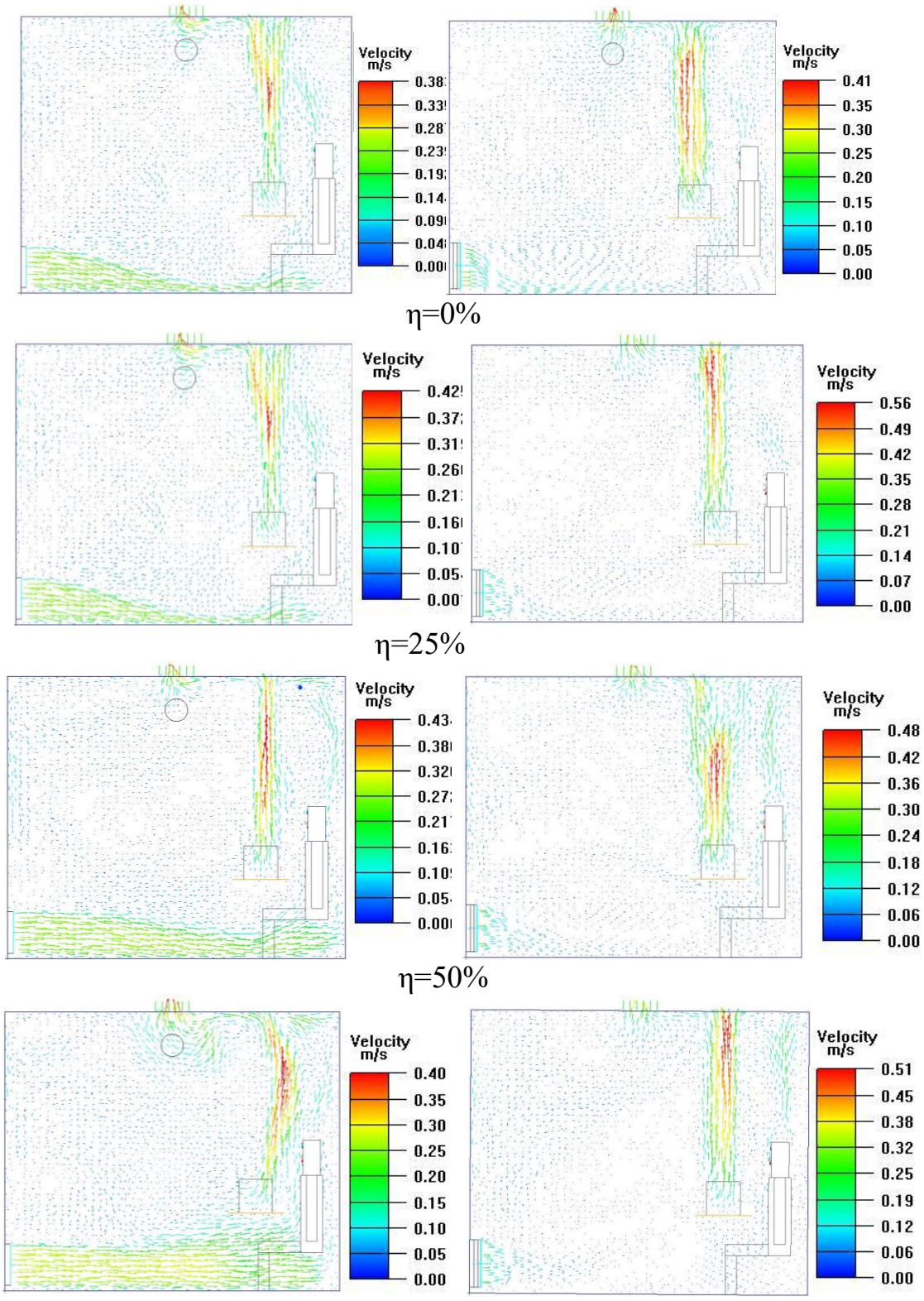

a-case-I b-case-II

Fig.(5-30) Velocity vector at different (η) for the two cases, plane z=1.25m

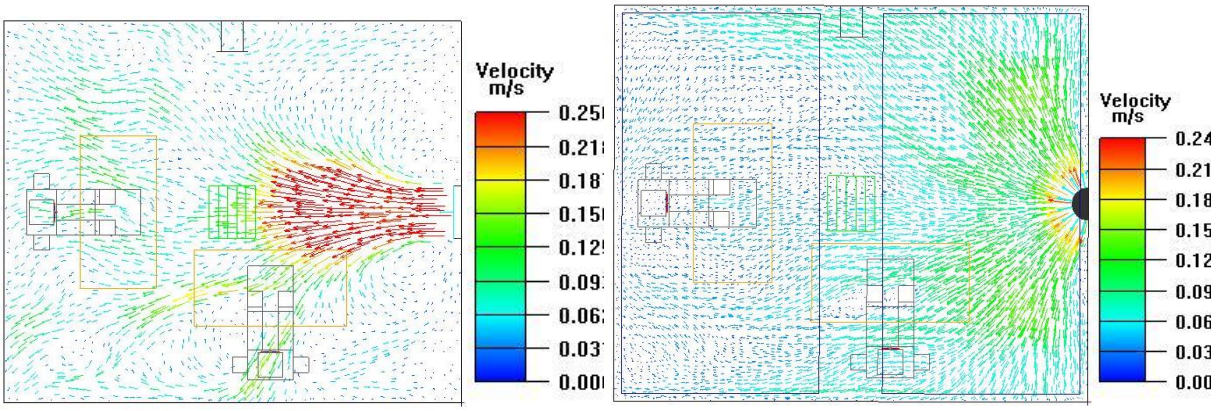

a-Rectangular diffuser b-Semi-circle diffuser

Fig.(5-31) Air distribution method by using rectangular and semi-circle diffusers at plane (y=0.2 m)

Fig.(5-32) presents the relation between portion of cooling load treated by chilled ceiling and air exchange efficiency for the two cases. Increase in air age with increase (η) for the two cases as shown in Figs.(5-27) to (5-29) leads to decrease air exchange efficiency (η_a) for the two cases. Reduces in air exchange efficiency (η_a) means increase in time required for fresh air to replace the old air in a room zone and reduce in occupants performance. The air exchange efficiency for (DV/CC) system in an office room by using semi-circle diffuser is higher by about (6%) at (η=0%) compared with rectangular diffuser (η), while it's reduce to (2%) with increase (η) to (80%). This is due to low chilled ceiling temperature at (η=50% and 80%) and cold air in upper zone which causes obstruction to old air movement outside office room from exhausted grill. This is leads to increase the time required to exit old air and reduces the effect of the diffuser shape. That's mean the semi-circle diffuser distributes fresh air more uniformly and faster than the rectangular diffuser. Also the shape of supply air diffuser have slightly effect on the air exchange efficiency at (η=50%) and (80%) due to decrease in chilled ceiling surface temperature and decrease velocity for hot air moving up.

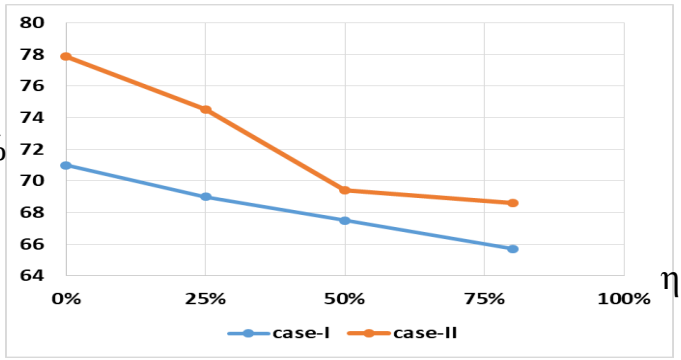

Fig.(5-32) Air exchange efficiency at different (η) for the two cases (case-I and II)

Fig.(5-33) shows air temperature distribution contours for the two cases with different (η) at plane (z=1.25 m). For the two cases, the air temperature increasing with increase height of the office room and creating a stratified layers due to convection between heat sources and cooled air. Stratified layers is one of the principles of displacement ventilation.

The temperature stratification for the two cases decrease with increase value of (η) and becomes unclear at (η=80%) due to the cold air coming down from the chilled ceiling, which leads to a decrease in the temperature difference between the layers. The supply air at low temperature flows along the floor, after that the temperature of air is rise when it passes through the heat sources and moves upward due to effects of buoyancy. The effect of gravity is very clear, especially near diffuser supply when air is supplied with a low temperature due to high air density. At same value of (η) for two cases, the air at high room level with semi-circle diffuser is colder than air with use rectangular diffuser especially with chilled ceiling. This is due to uniform fresh air distribution supplied by semi-circular diffuser. It is clear that the air temperature distribution is more uniform when increases (η), especially at (50% and 80%), and there is an advantage for the semi-circular diffuser.

The air temperature increases with height, after that the air being touch with the chilled ceiling and its temperature decrease by convection due to lower chilled ceiling surface temperature. Then the air tends to move down cause increase in

average air age. This phenomenon is evident in Fig.(5-34) which showed the effect of the cooled ceiling surface on the air temperature in contact with it for case-I at (η=50%) as example.

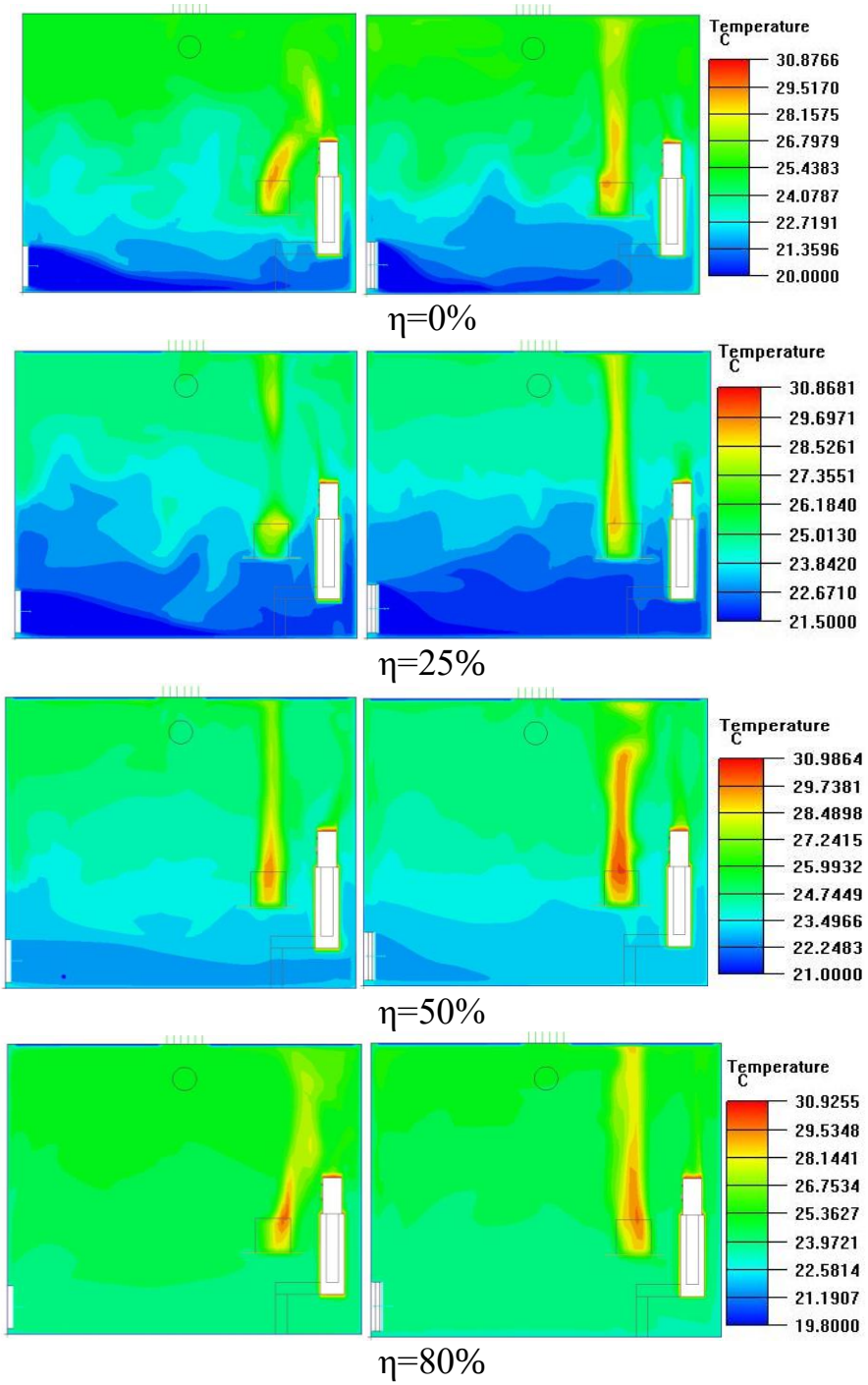

a-case-I b-case-II

Fig.(5-33) Air temperature distribution contours at different (η), (cases-I and II), plane z=1.25m

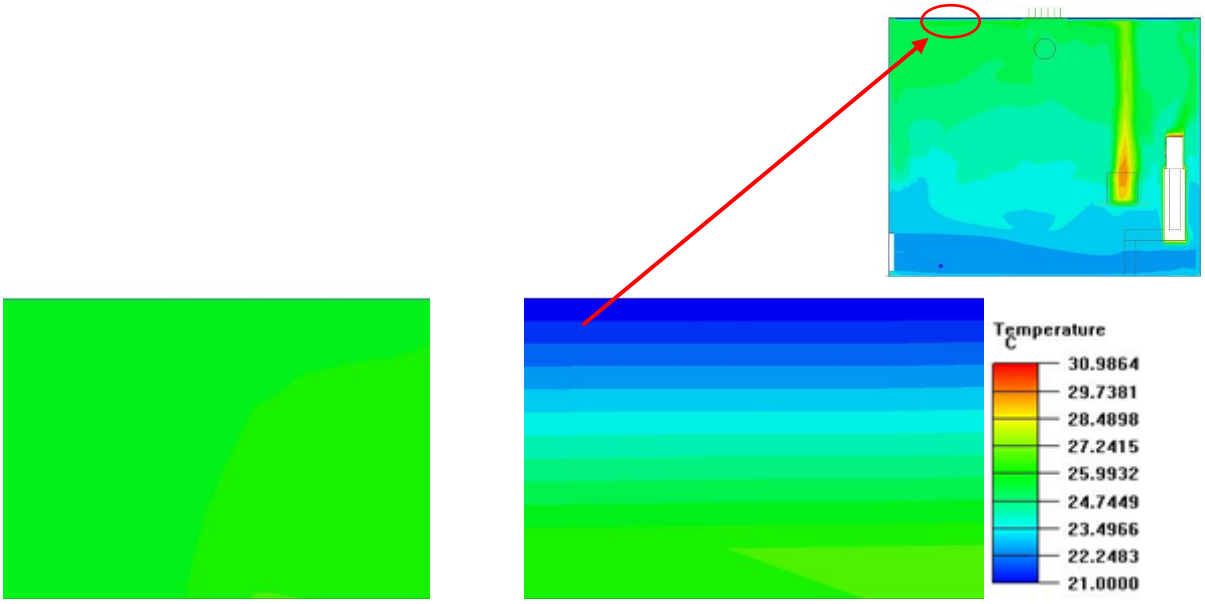

a-case without chilled ceiling b-case with chilled ceiling (η=50%)

Fig.(5-34) Effect of chilled ceiling on the air temperature in contact with it.

To predict human thermal comfort, three parameters are studied in this study, predicted mean vote (PMV), predicted percentage dissatisfied (PPD) and air diffusion performance index (ADPI).

Figs.(5-35) and (5-36) show the profiles of (PMV) and (PPD) respectively for the two cases at different value of cooling load treated by chilled ceiling (η). The (PMV) and (PPD) values are improving with increase value of (η) in the two cases and converge to the comfort values that specified by ASHRAE standard 2017 (-0.5≤ PMV ≤ 0.5 and PPD=10%,). At value of (η) change from (0% to 80%) the (PMV) decrease from (0.473 to 0.355) when using rectangular diffuser (case-I) and from (0.472 to 0.31) when using semi-circle diffuser (case-II).

(PPD) percentage values decreases with increase (η) also from (11.52 to 8.5) when using rectangular diffuser (case-I) and from (10.7 to 8.37) when using semi-circle diffuser (case-II). That's mean the increase in portion of load treated by chilled ceiling lead to improve thermal comfort. This is due to low child ceiling surface temperature lead to improve the heat transfer by radiation between heat sources and

the ceil wall. The values of (PMV) and PPD for the combined system (DV/CC) for case-II at different (η) is less than from its values for case-I and more converge from standard values specified by ASHRAE standard 2017. This is a result of the superiority of the semi-circular diffuser in distributing fresh cold air around the human body, which provided more thermal comfort. This result indicates that using a semi-circular diffuser gives a better thermal comfort than a rectangular diffuser with (DV/CC) system.

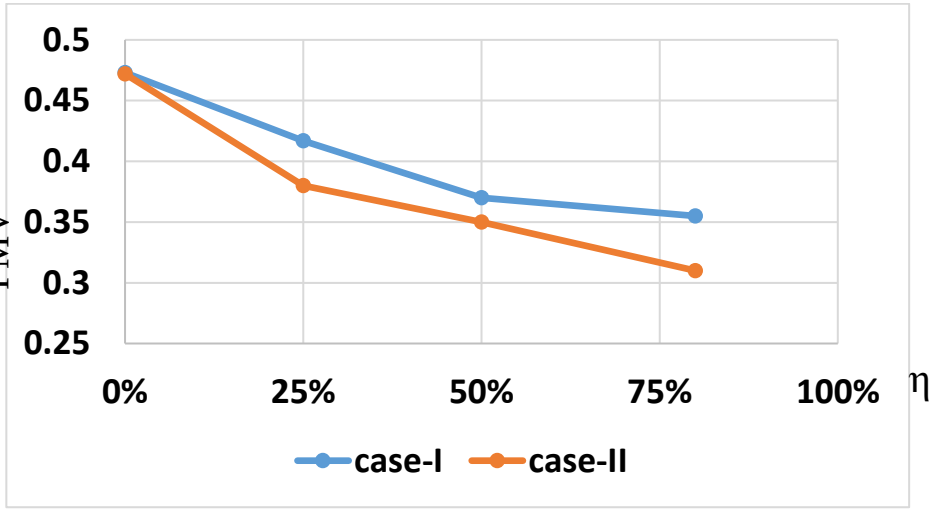

Fig.(5-35) PMV profile for the two cases at different (η)

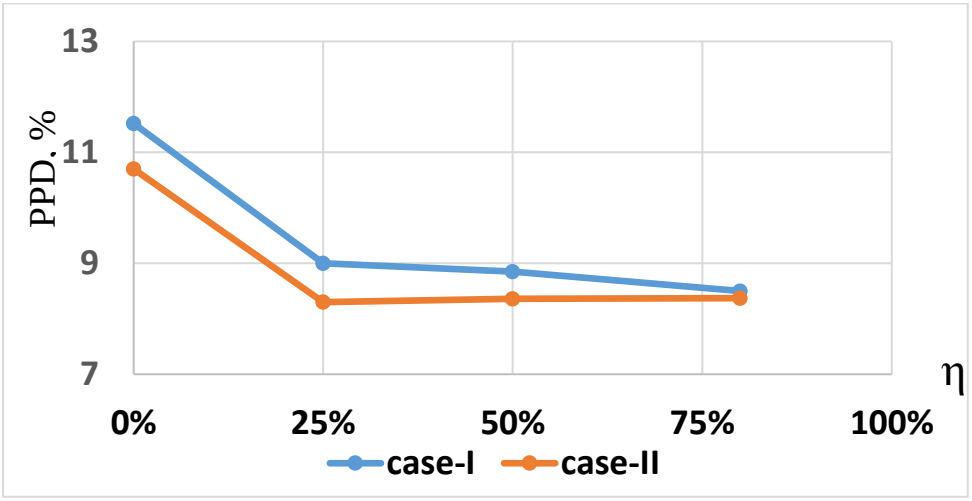

Fig.(5-36) (PPD) profile for the two cases at different (η)

Fig.(5-37) shows the percentage values of (ADPI) for the two cases (case-I and case-II) at different (η). (ADPI) is a factor used to predict air circulation system and the balance between air temperature and velocity in indoor, increase in (ADPI) percentage gives a good indication of occupants comfort. The (ADPI) increase with increase (η) in the two cases. This mean that the increasing in portion load treated by chilled ceiling leads to improve thermal comfort due to increase (ADPI) value due to increase (η) helps to reduce the temperature difference between the indoor stratified layers as shown in Fig.(5-33) .

The value of (ADPI) for (DV/CC) system by using semi-circle diffuser is slightly higher than from its value when used rectangular diffuser at different value of (η). This is due to uniform fresh air distribution supply by semi-circle diffuser gives more balance between air temperature and velocity. This result shown that the semi-circle diffuser has advantage of improving indoor thermal comfort more than rectangular diffuser.

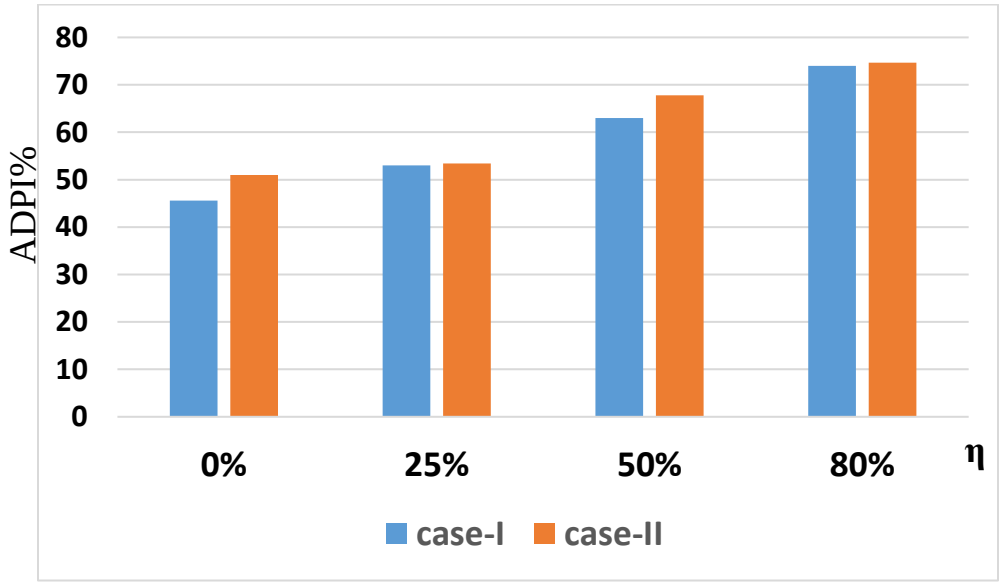

Fig.(5-37) (ADPI) profile for the two cases at different (η)

5.2.2 Percentage average deviation between experimental and numerical results

The deviation between experimental and numerical results is a possibility due to multiple reasons as the error in measurement devices, irregular in air supply temperature and velocity from the diffuser, and usual errors in CFD software running.

The three parameters obtain from experimental work for the office room at three measurement stands are used to find the percentage average error between experimental and numerical results (local air age, temperature distribution with height and CO_2 removing with time) by using Eq.(4-12).

5.2.2.1 Percentage average error for local mean air age (LMA)

Six points used to find the percentage average error locate on three measurement stands each stand have the two points at breathing zone for set and stand person (1.1m and 1.8 m) height represented the level of breathing zone at seated and standing person.

Figs.(5-38) to (5-41) and Figs.(5-42) to (5-45) show the comparison between experimental and numerical results at three measurement stands with different value of cooling load treated by chilled ceiling (η=0, 25, 50 and 80%) at (1.1m and 1.8 m) high for Case-I and case-II respectively.

The percentage average error in case-I (with rectangular diffuser) was (13%) as a minimum error at test-4 (η=80%) and (24%) as a maximum error at tests-1 (η=0%). For Case-II the maximum error was (25.2%) at test-7 and minimum error was (11.6%) at test-8. These percentage average error are reasonable due to the irregular in air supply velocity and supply carbon dioxide by diffuser which used to measured local air age by decay method. Table (5-2) shows the value of percentage average error for case-I and case-2 at different value of (η) (four tests in each case with (η=0, 25, 50 and 80%) respectively.

Table(5-2) Percentage average error between experimental and numerical results for local air age in the two cases at different value of (η)

	Test	η%	Average error %
Case-I	test-1	0	±24
	test-2	25	±17.7
	test-3	50	±17.3
	test-4	80	±13
Case-II	test-5	0	±18.4
	test-6	25	±21.8
	test-7	50	±25.2
	test-8	80	±11.6

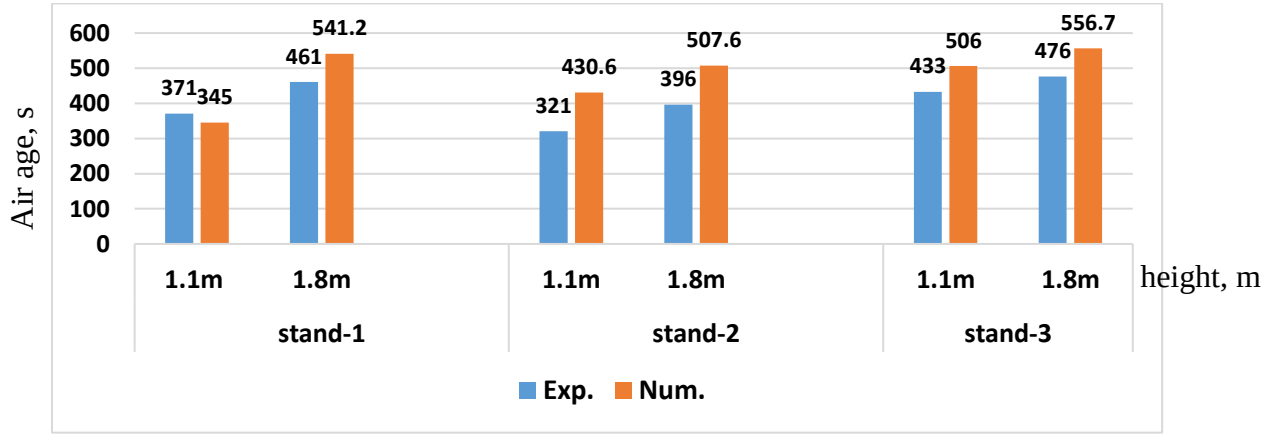

Fig.(5.38) Comparison of experimental with numerical results for (LMA) at three instrument stands in Case-I, η= 0% at high 1.1m and 1.8m

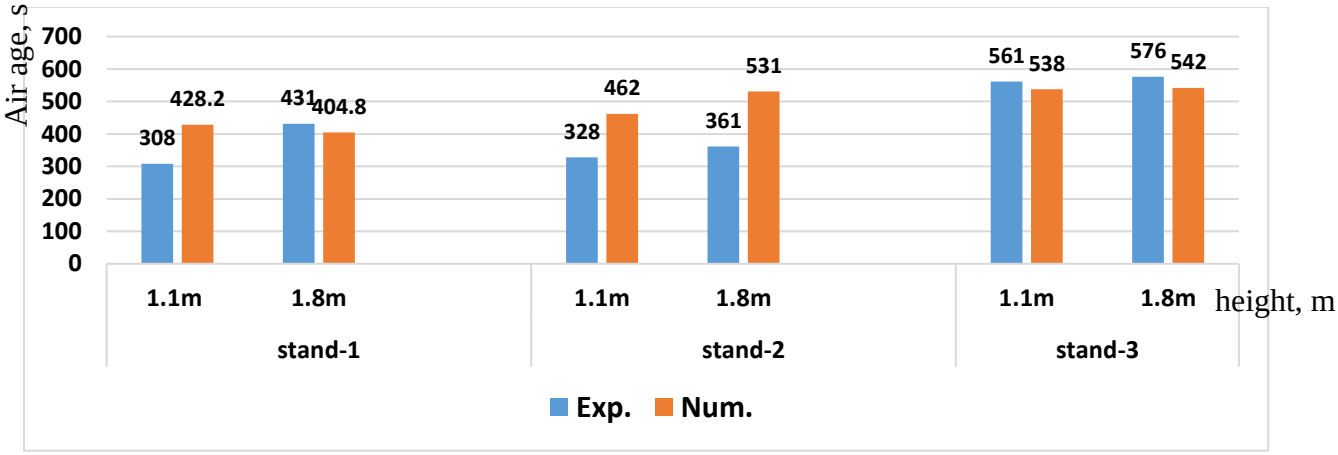

Fig.(5.39) Comparison of experimental with numerical results for (LMA) at three measurement stands in Case-I, η= 25% at high 1.1m and 1.8m

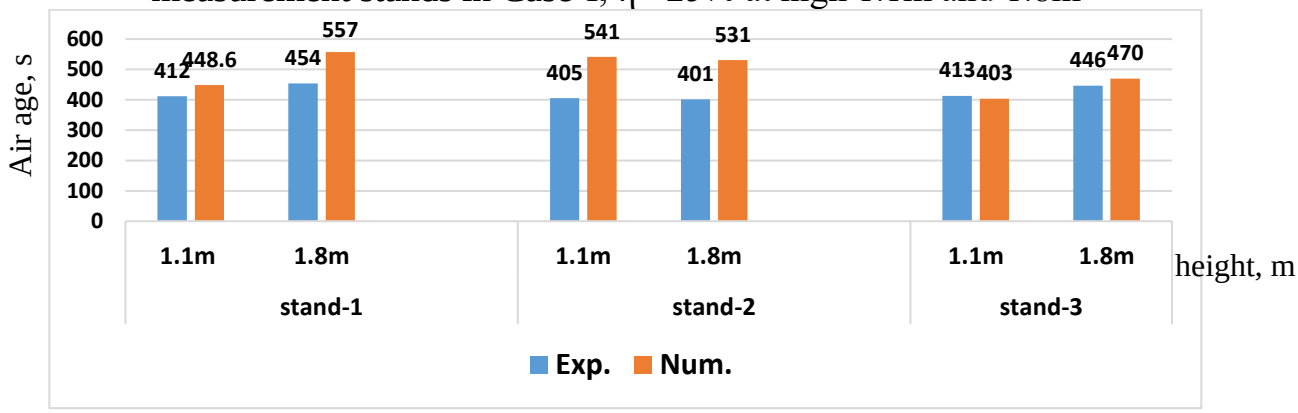

Fig.(5.40) Comparison of experimental with numerical results for (LMA) at three measurement stands in Case-I, η= 50% at high 1.1m and 1.8m

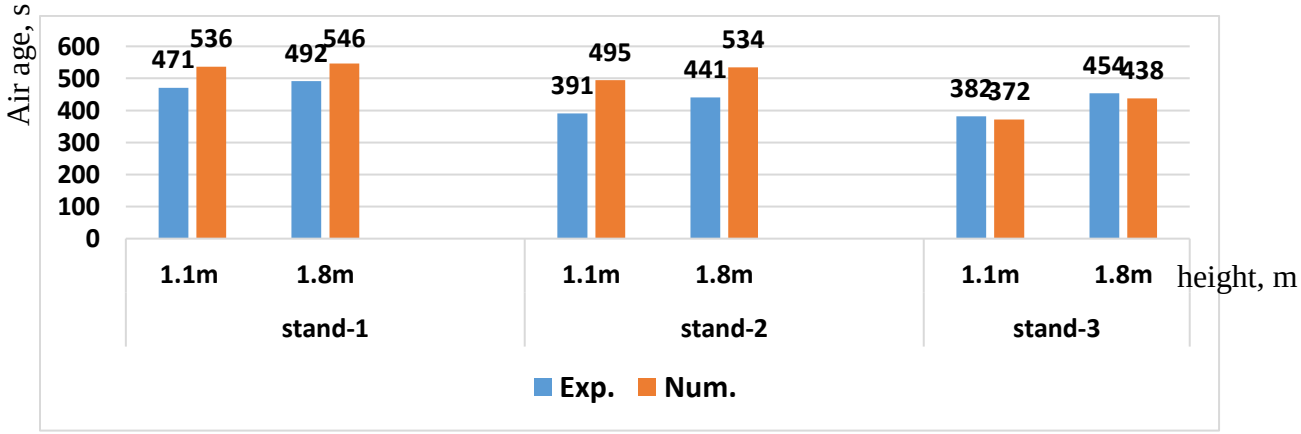

Fig.(5.41) Comparison of experimental with numerical results for (LMA) at three measurement stands in Case-I, η= 80% at high 1.1m and 1.8m

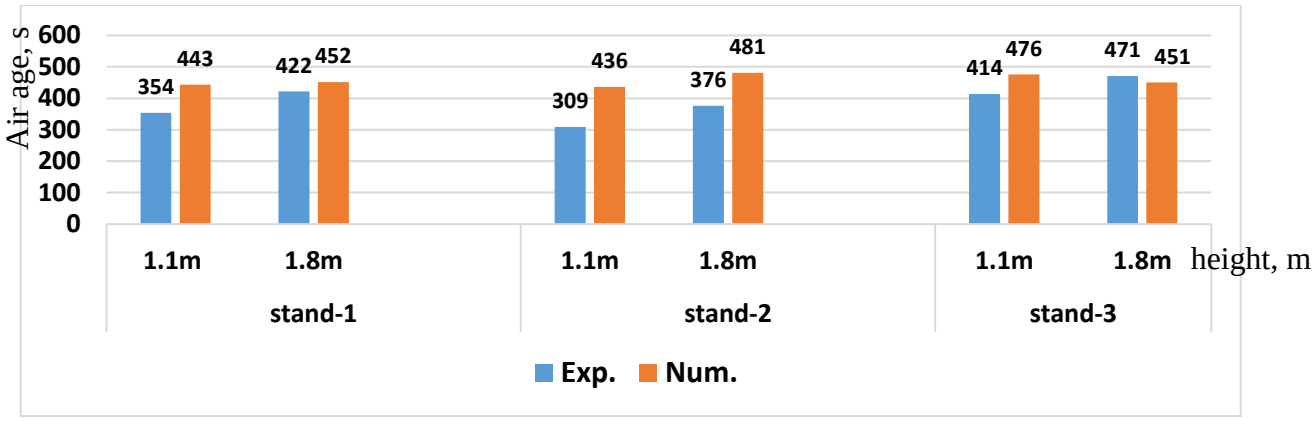

Fig.(5.42) Comparison of experimental with numerical results for (LMA) at three measurement stands in Case-II, η= 0% at high 1.1m and 1.8m

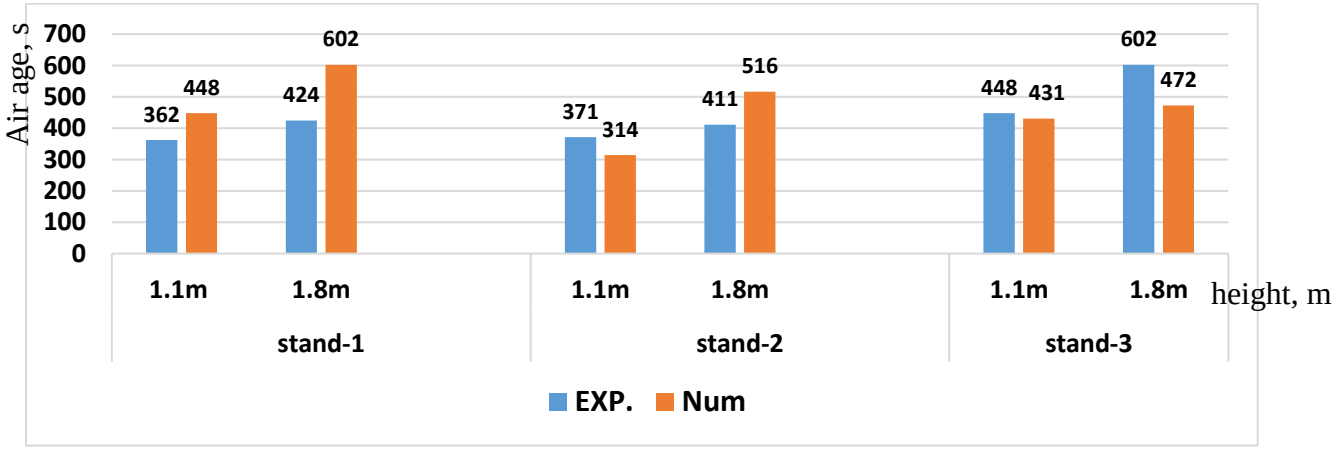

Fig.(5.43) Comparison of experimental with numerical results for (LMA) at three measurement stands in Case-II, η= 25% at high 1.1m and 1.8m

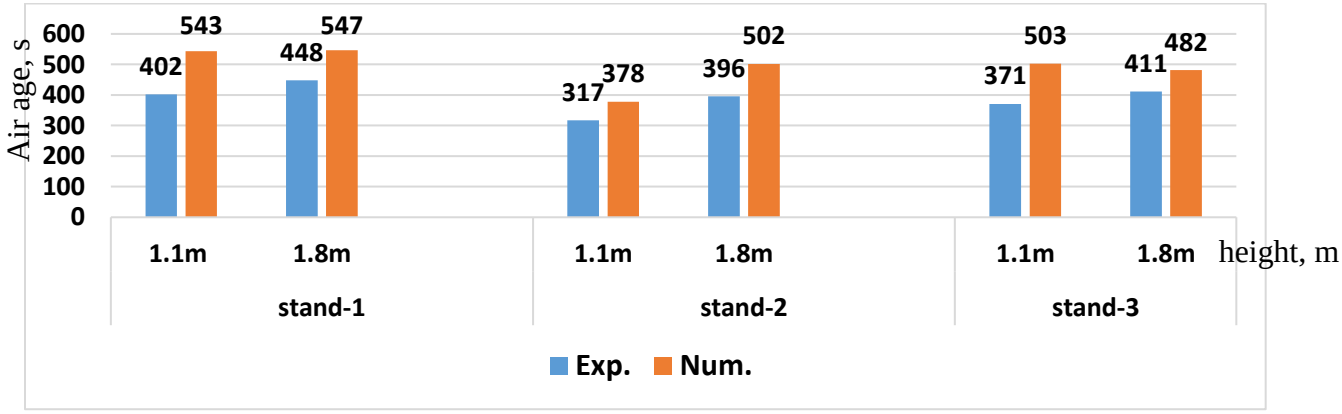

Fig.(5.44) Comparison of experimental with numerical results for (LMA) at three measurement stands in Case-II, η= 50% at high 1.1m and 1.8m

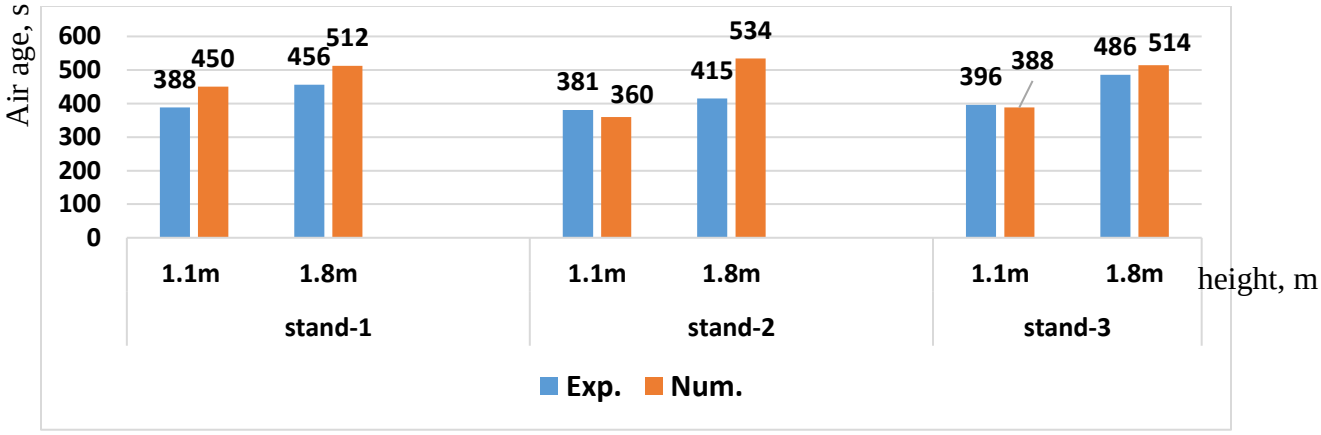

Fig.(5.45) Comparison of experimental with numerical results for (LMA) at three measurement stands in Case-II, η= 80% at high 1.1m and 1.8m

5.2.2.2 Percentage average error for temperature distribution

The percentage average error between experimental and numerical results for temperature distribution is calculated by using Eqn.(4-12). Fifteen points used to find the percentage average error located on the three measurement stands. Each stand have five points at height (0.1, 0.4, 1.1, 1.8 and 2.4 m).

Figs.(5-46) to (5-49) and Figs.(5-50) to (5-53) show the comparison between experimental and numerical results at three stands with different values of cooling load treated by chilled ceiling (η=0, 25, 50 and 80%) at level (0.1, 0.4, 1.1, 1.8 and 2.4 m) for Case-I and case-II respectively.

The percentage average error in case-I (with rectangular diffuser) was between (4.6-6.4%), the minimum error at test-2 (η=25%) and maximum error at tests-3 (η=50%). The percentage average error for Case-II found that the error between (5.2-6.7%), the maximum error at test-6 and minimum error at test-7. These percentage average errors in temperature distribution are acceptable due to the irregular in air supply velocity and temperature by supply diffuser. Table(5-3) shows the value of percentage average error for case-I and case-II at different value of (η) (four tests in each case with η=0, 25, 50 and 80% respectively).

Table(5-3) percentage average error between experimental and numerical results for air temperature distribution with height in the two cases at different value of (η)

	Test	η%	Average error %
Case-I	test-1	0	±6
	test-2	25	±4.6
	test-3	50	±6.4
	test-4	80	±6
Case-II	test-5	0	±6.07
	test-6	25	±6.7
	test-7	50	±5.2
	test-8	80	±6

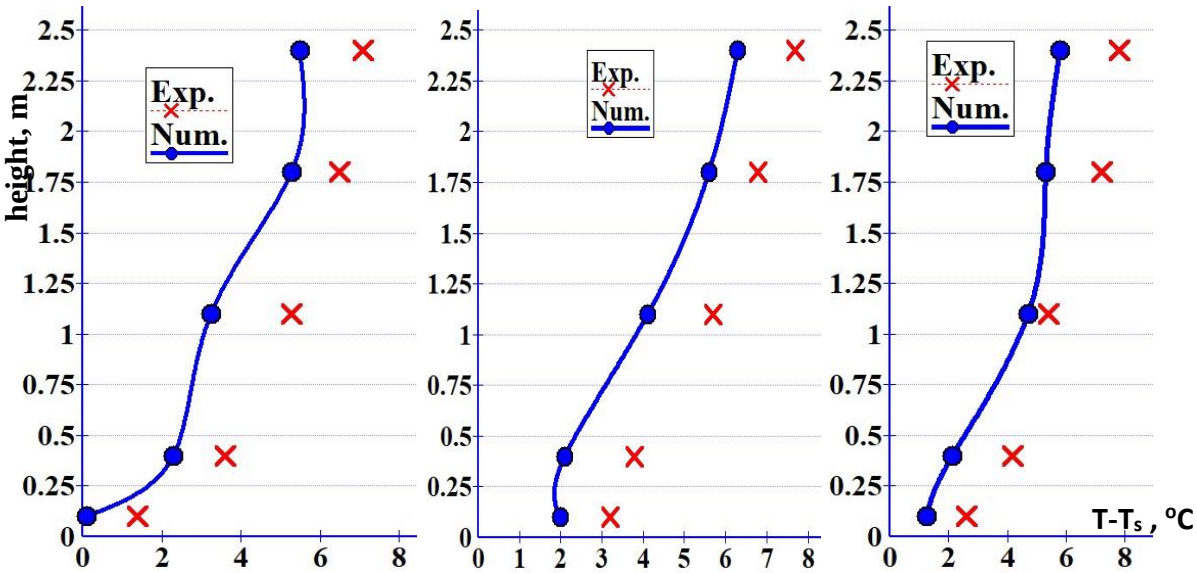

stand-1 stand-2 stand-3

Fig.(5-46) Air temperature distribution comparison between exp. and num. results at different indoor levels at three measurement stands, Case-I, η=0%

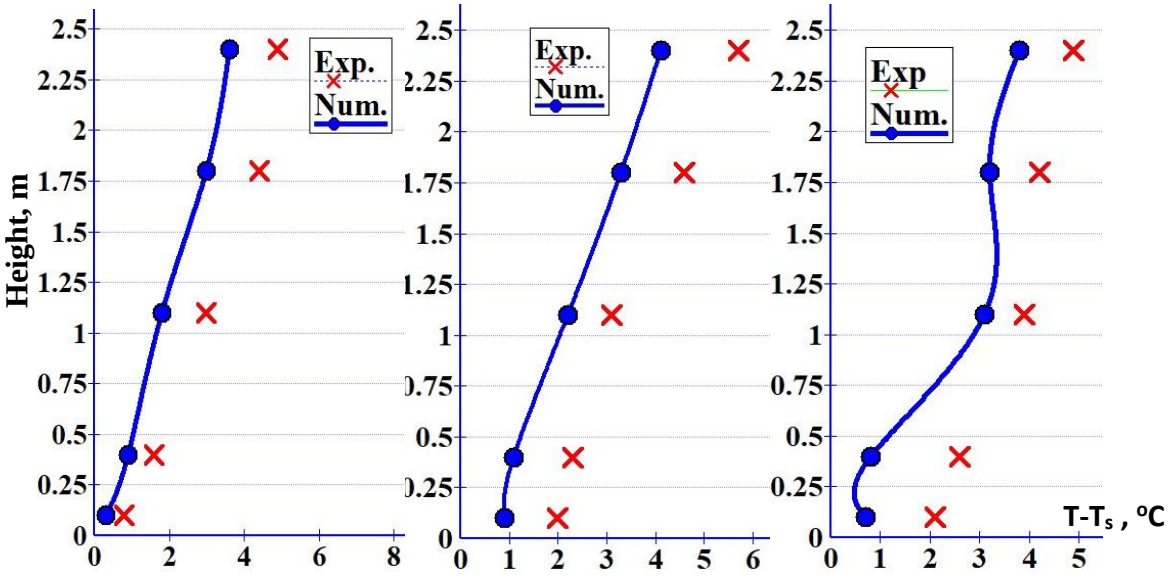

stand-1 stand-2 stand-3

Fig.(5-47) Air temperature distribution comparison between exp. and num. results at different indoor levels at three instrument stands, Case-I, η=25%

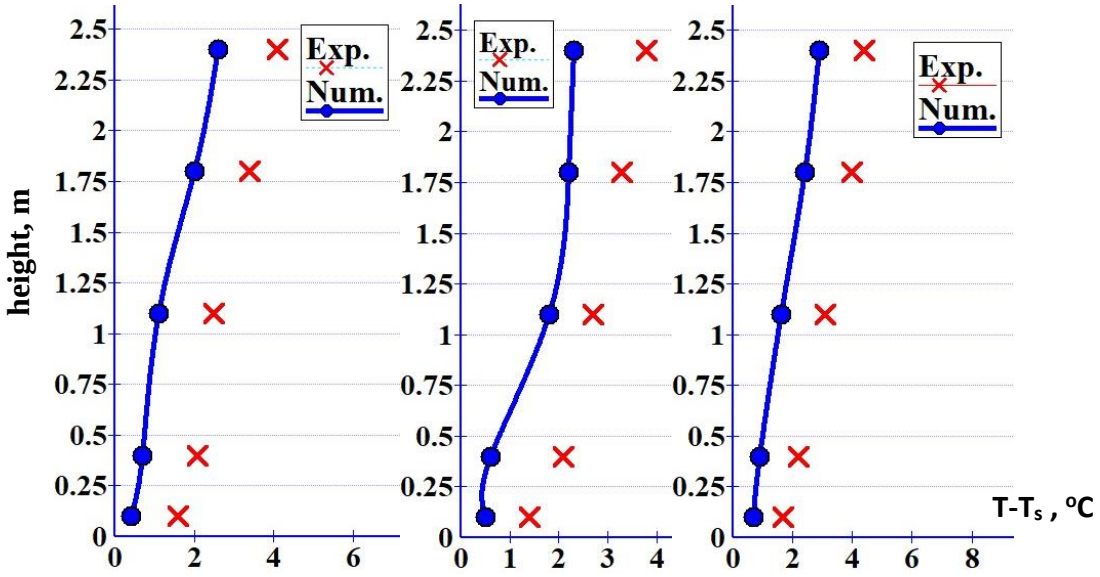

stand-1 stand-2 stand-3

Fig.(5-48) Air temperature distribution comparison between exp. and num. results at different indoor levels at three instrument stands, Case-I, η=50%

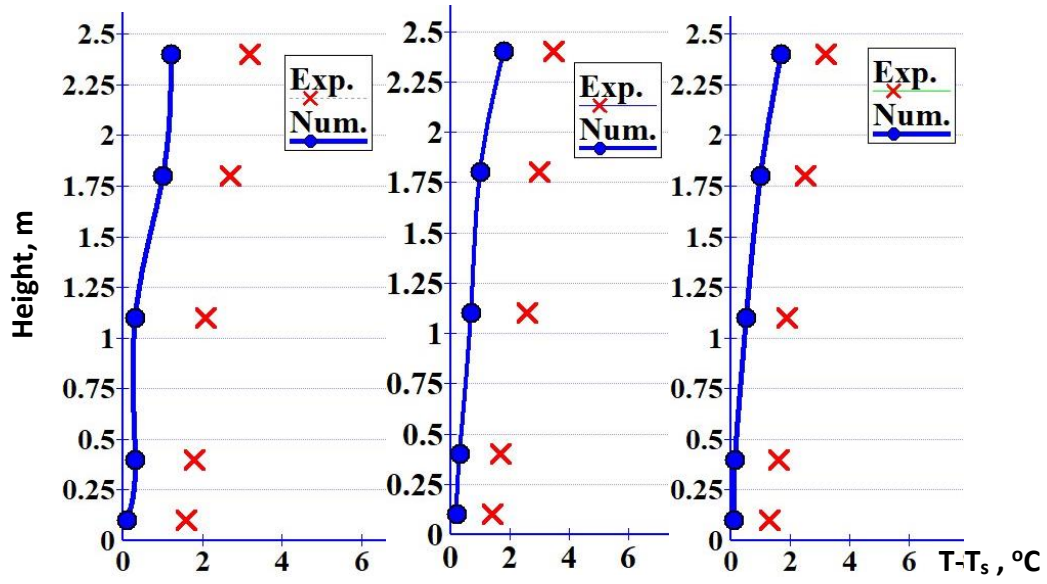

stand-1 stand-2 stand-3

Fig.(5-49) Air temperature distribution comparison between exp. and num. results at different indoor levels at three instrument stands, Case-I, η=80%

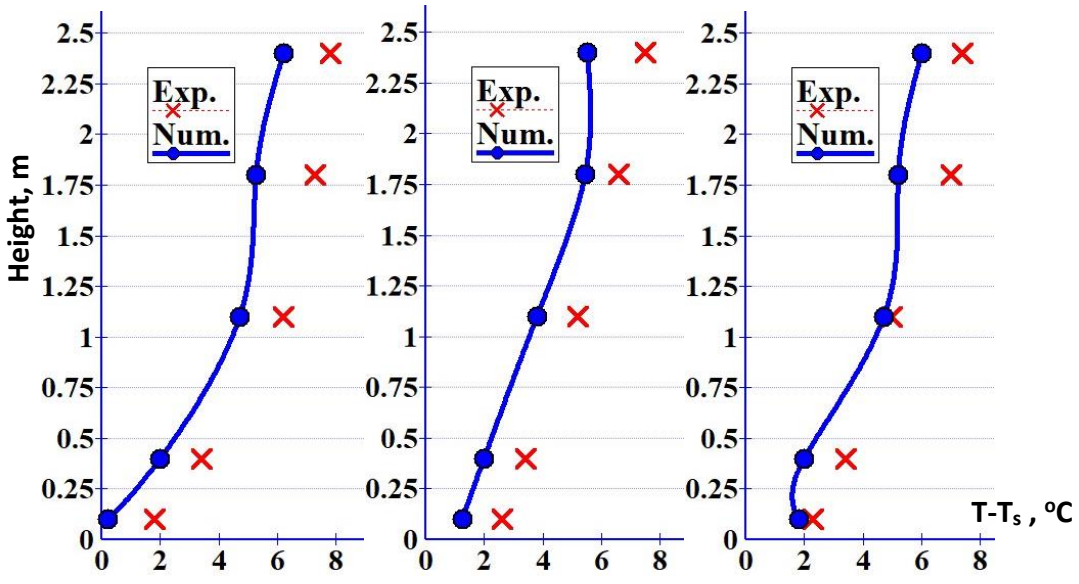

stand-1 stand-2 stand-3

Fig.(5-50) Air temperature distribution comparison between exp. and num. results at different indoor levels at three instrument stands, Case-II, η=0%

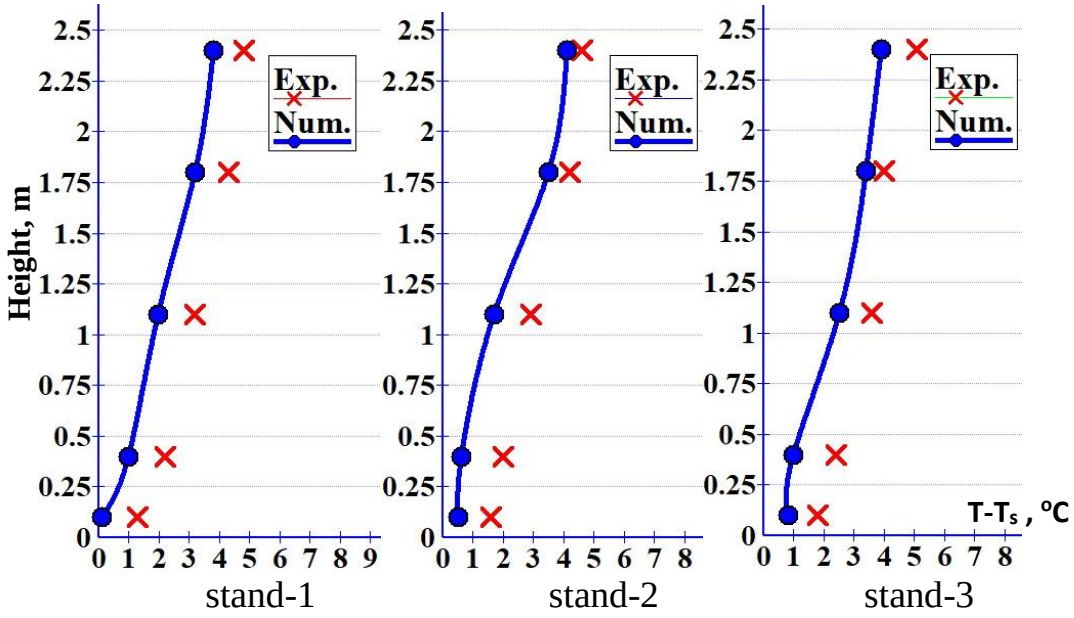

Fig.(5-51) Air temperature distribution comparison between exp. and num. results at different indoor levels at three instrument stands, Case-II, η=25%

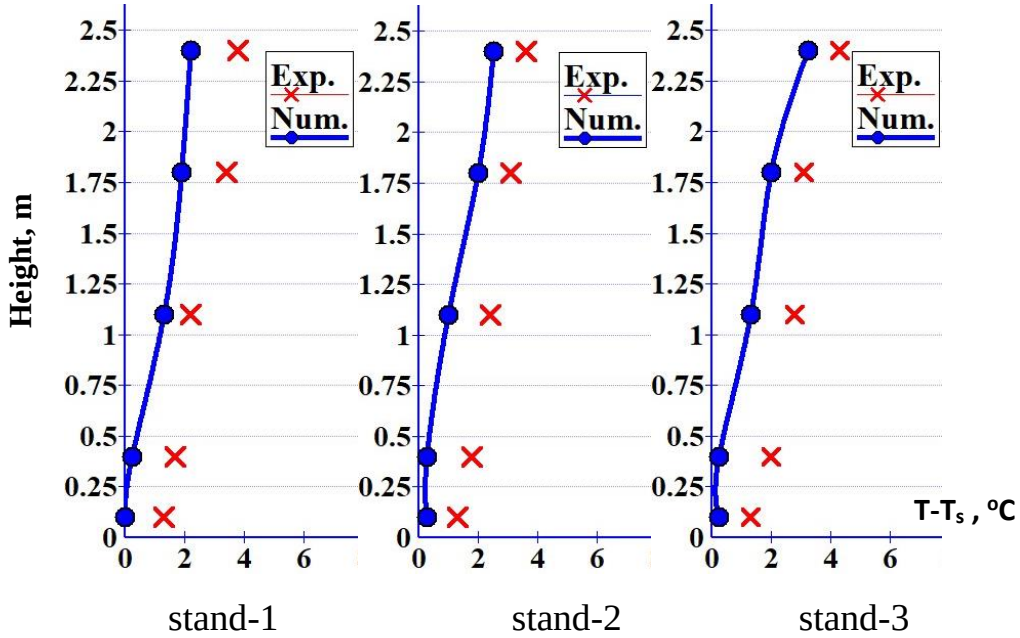

Fig.(5-52) Air temperature distribution comparison between exp. and num. results at different indoor levels at three instrument stands, Case-II, η=50%

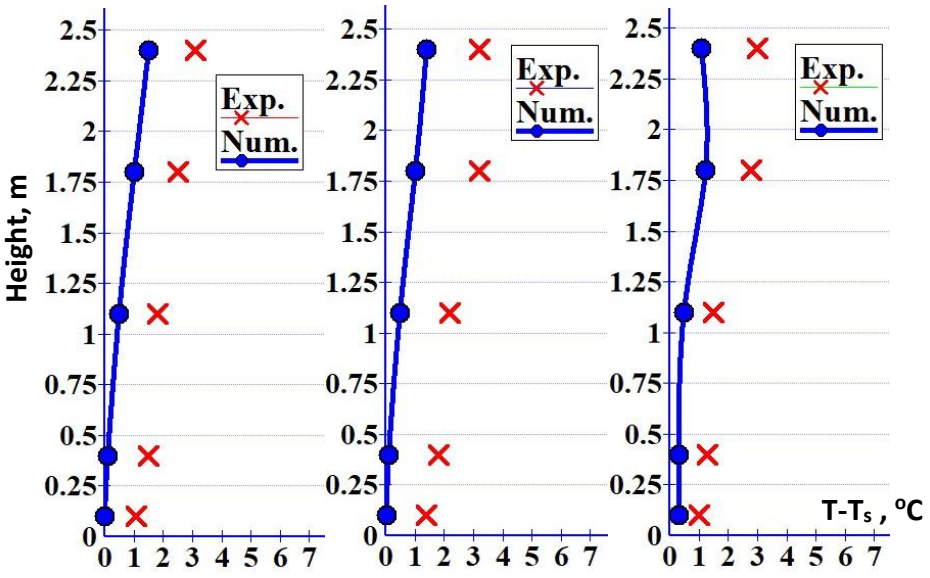

Fig.(5-53) Air temperature distribution comparison between exp. and num. results at different indoor levels at three instrument stands, Case-II, η=80%

5.2.2.3 Percentage average error for CO_2 removing with time

The percentage average error between experimental and numerical results for CO_2 decay with time is calculated by using Eq.(4-12). Six points located on the three measurement stands. Each stand have two points at (1.1m and 1.8 m) height represented the level of breathing zone at seated and standing person used to find the percentage average error at steady state.

Figs.(5-54) to (5-56) show the comparison between experimental and numerical results for case-I at (stand-1, η=0), (stand-2, η=25%) and (stand-3, η=80%) respectively . Figs.(5-57) to (5-59) show the compared experimental and numerical results for case-II at (stand-1, η=0), (stand-2, η=50%) and (stand-3, η=80%) respectively.

The percentage average error for CO_2 decay in case-I was between (5.5-7.1%). The minimum error found in test-3 (η=50%), while the maximum error found in tests-4 (η=80%). The percentage average error for Case-II found that the error between (4.5-8.4%). The maximum error at test-6 (η=50%) and minimum error at

test-8 (η=80%). These percentage average errors in CO_2 remove are less than (10%). Table(5-4) shows the value of percentage average errors for case-I and case-II at different values of (η) (four tests in each case with η=0, 25, 50 and 80% respectively).

Table(5-4) Percentage average error between experimental and numerical results for Co_2 decay with time in the two cases at different value of (η)

	Test	η%	Average error %
Case-I	test-1	0	5.7
	test-2	25	6.1
	test-3	50	7.1
	test-4	80	5.5
Case-II	test-5	0	6.3
	test-6	25	4.5
	test-7	50	7
	test-8	80	8.4

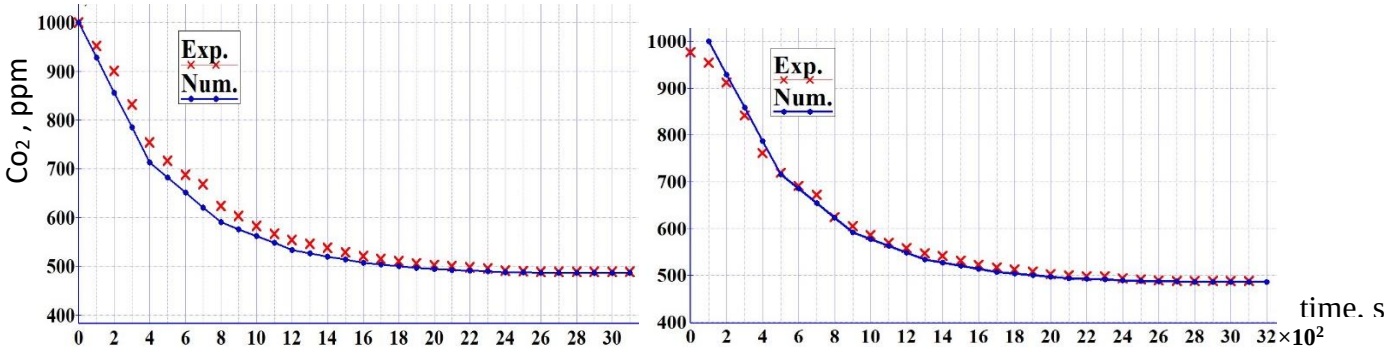

level 1.1m level 1.8m

Fig.(5-54) Comparison between experimental and numerical results for CO_2 removing at instrument stand-1, Case-I, η=0%

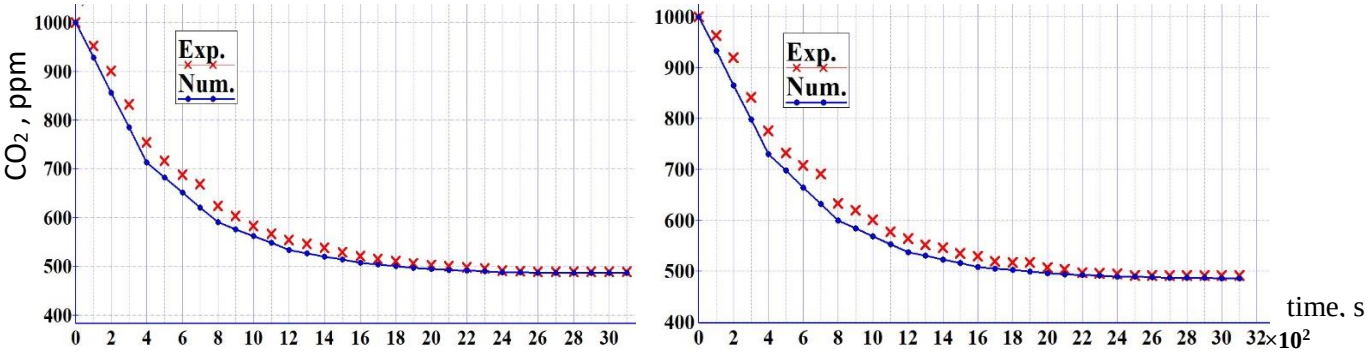

level 1.1m level 1.8m

Fig.(5-55) Comparison between experimental and numerical results for CO_2 removing at instrument stand-2, Case-I, η=25%

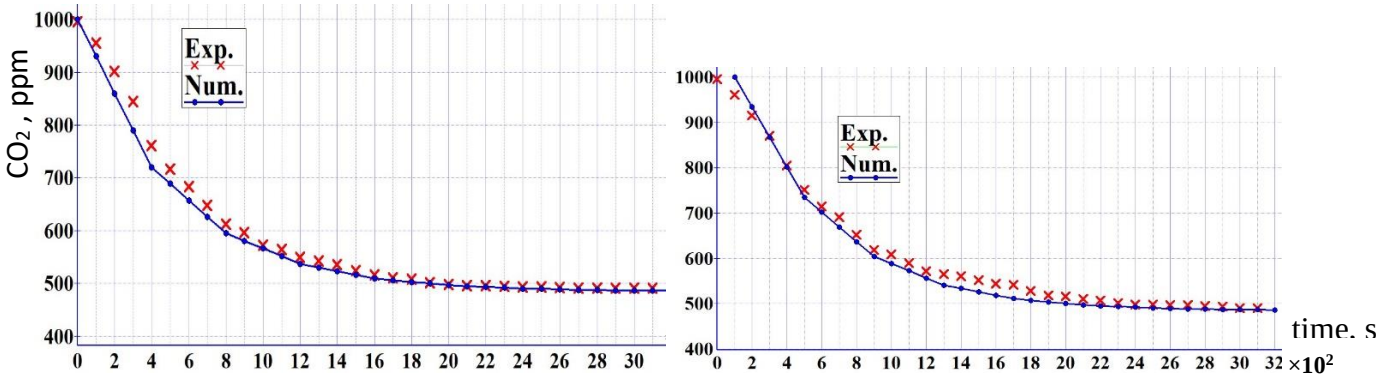

level 1.1m level 1.8m

Fig.(5-56) Comparison between experimental and numerical results for CO_2 removing at instrument stand-3, Case-I, η=80%

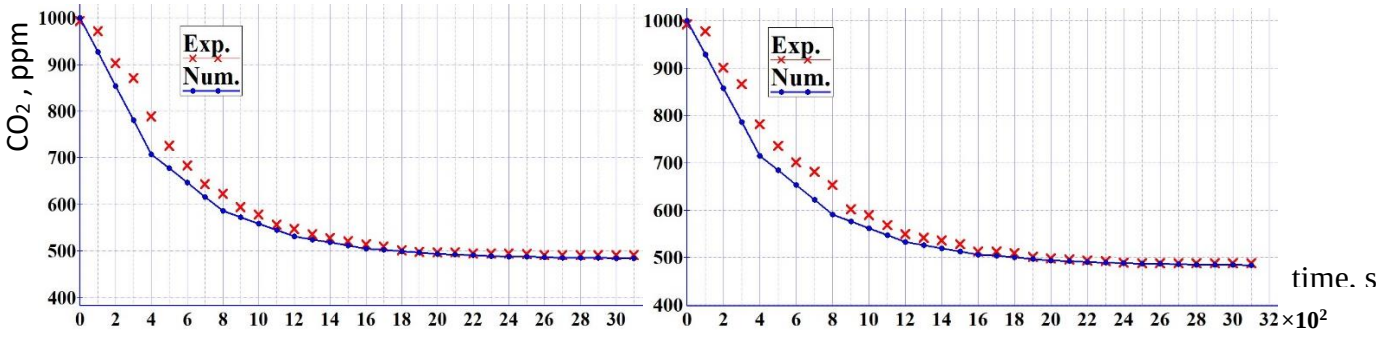

level 1.1m level 1.8m

Fig.(5-57) Comparison between experimental and numerical results for CO_2 removing at instrument stand-1, Case-II, η=0%

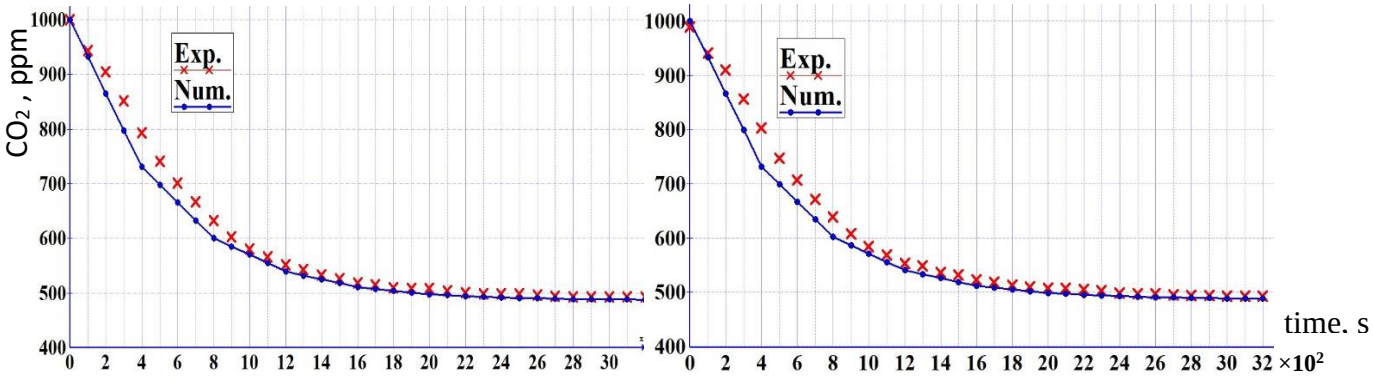

level 1.1m level 1.8m

Fig.(5-58) Comparison between experimental and numerical results for CO_2 removing at instrument stand-2, Case-II, at η=50%

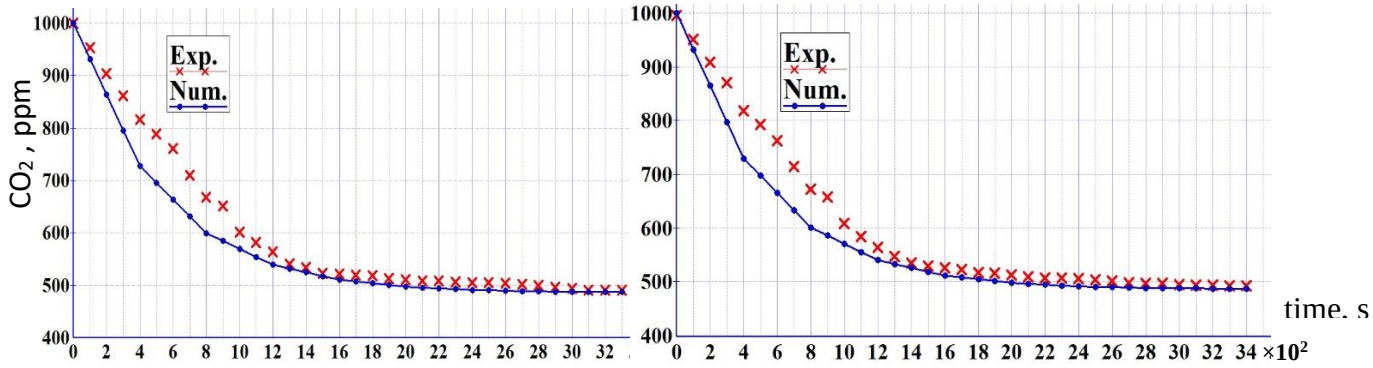

level 1.1m level 1.8m

Fig.(5-59) Comparison between experimental and numerical results for CO_2 removing at instrument stand-3, Case-II, η=80%

5.3 Numerical Comparison between Insulated and Non- Insulated Office

To understand more details about (DV/CC) system in a hot and dry climate (as like Hilla climate), numerical analysis for non- insulated office room with one window and exterior wall was simulated as described in chapter four section (4.4.1).

The numerical results for non- insulated office room (case-III and IV with rectangular and semi-circular air supply diffuser respectively) are compared numerically with insulated office room (case-I and II with rectangular and semi-circular air supply diffuser respectively) to examining the air age and thermal comfort parameters in these climate. Each case has four tests depending on the portion of cooling load treated by chilled ceiling. Tables (5-5) and (5-6) show the main numerical results for non- insulated office (case-III and IV) and insulated office (case-I and II) respectively.

Table(5-5)Main numerical results for non-insulated office room (case-III and IV)

Cases	**η (%)**	**T_{av} (ºC)**	**u_{av} (m/s)**	**MRT (ºC)**	**RH_{av} (%)**	**ADPI (%)**	**PMV**	**PPD (%)**	**ΔT_{hf} (ºC)**	**η_a (%)**	ε_t
Case-III	0	25.3	0.061	30.1	57.8	38	1.26	42.3	4.1	76.3	1.28
	25	25.8	0.062	28.1	60.2	42	1.24	39.6	3.2	71.4	1.22
	50	26.6	0.063	29.7	57	45	1.17	37.1	2.6	68.9	1.11
	80	26.9	0.073	28.1	58.8	61	1.15	35.3	1.9	66.6	1.1
Case-IV	0	24.8	0.045	30	59.5	42.7	0.81	23.6	3.6	79	1.32
	25	26	0.057	28.8	59.8	48.3	0.74	21.3	2.9	77.2	1.25
	50	26.6	0.047	28.2	51.8	56.6	0.54	15.9	2.1	72.6	1.16
	80	26.2	0.051	28	50.4	72.6	0.536	15.7	1.7	69.3	1.15

Table.(5-6) Main numerical results for insulated office room (case-I and II)

Cases	η (%)	T_{av} (°C)	u_{av} (m/s)	MRT (°C)	RH_{av} (%)	ADPI (%)	PMV	PPD (%)	ΔT_{hf} (°C)	η_a (%)	ε_t
Case-I	0	24.6	0.05	25.3	55.4	45.6	0.473	11.5	2.3	71	1.34
	25	24.8	0.054	24.4	56.2	53	0.417	9	2.1	69	1.24
	50	25.1	0.054	24.2	52.2	63	0.37	8.85	1.6	67.5	1.19
	80	25.4	0.06	24.1	54.8	74	0.355	8.5	0.6	65.7	1.14
Case-II	0	23.7	0.046	25.2	57	51	0.427	10.7	2.7	77.9	1.48
	25	24.3	0.04	24.3	58	53.4	0.38	8.3	1.8	74.5	1.39
	50	24.9	0.041	24.13	53	67.8	0.35	8.36	1.2	69.4	1.26
	80	25.2	0.044	24.5	52.3	74.7	0.31	8.37	0.6	68.6	1.16

5.3.1 Air age profile comparison.

Figs.(5-60) and (5-61) show the average air age variation with height level for insulated and non-insulated office room at different (η) with rectangular diffuser (case-I and case-III) and semi-circular diffuser (case-II and case-IV) respectively. The figures show that the average air age increase with height in each cases. If compared between the two office rooms (insulated and non-insulated), the average air age in non-insulated office room under (0.4 m) is less than by about (75 sec) compared with insulated room regardless of the shape of diffuser. This difference reaches to about (150 sec) in the zone over (1 m). This is due to the effects of heat gain from window and wall. This heat gain leads to increase in air temperature and velocity, that's lead to decrease in average air age in the zone over (1 m) height level.

The average air age values at the (0.1 m) height level (near of floor) has a minimum difference value between insulated and non-insulated office room especially at (η) between (0-50%). This due to the supply cooled air moving near the

floor and it's not yet affected by the heat gained from the non- insulated walls and window. This phenomena clearly appears with semi-circular diffuser due to regular supply air distribution. At (η=80), the average air age for the two office rooms at height level (0.1 m) has high difference from other values of (η) at the same level. Because the supply air temperature was (24°C and 24.5°C) for insulated and non-insulated office room respectively. These supply air temperature is near of average room design temperature (25°C) and the effects of buoyancy force is little, then the air supply temperature has more effective on the air age.

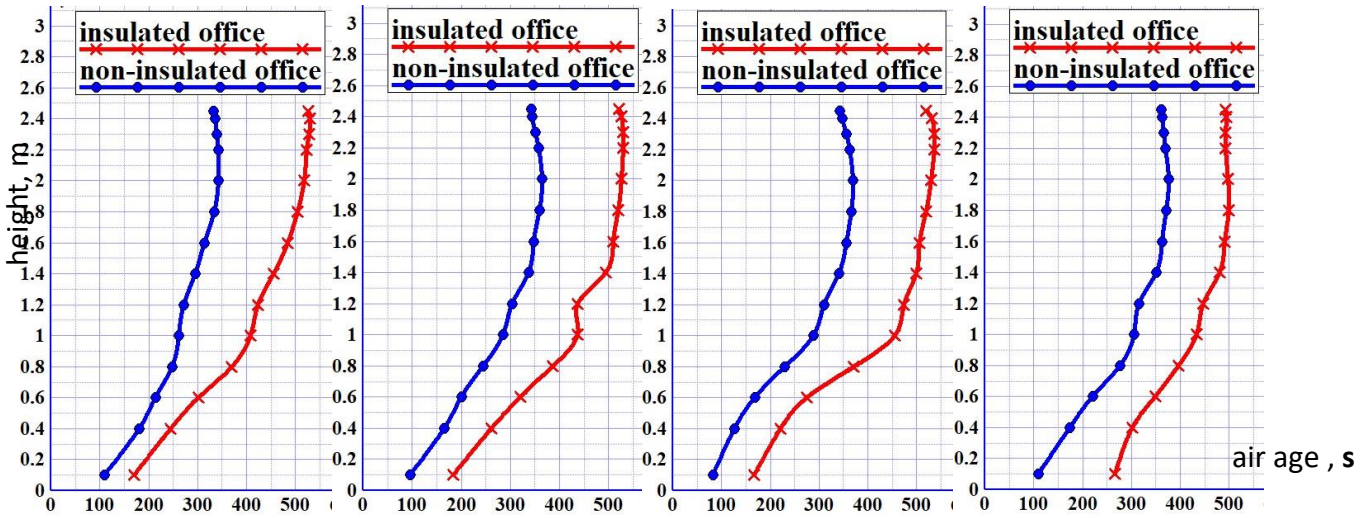

Fig.(5-60) Comparison between mean air age with height for insulated and non-insulated office, (cases-I and III) at different (η)

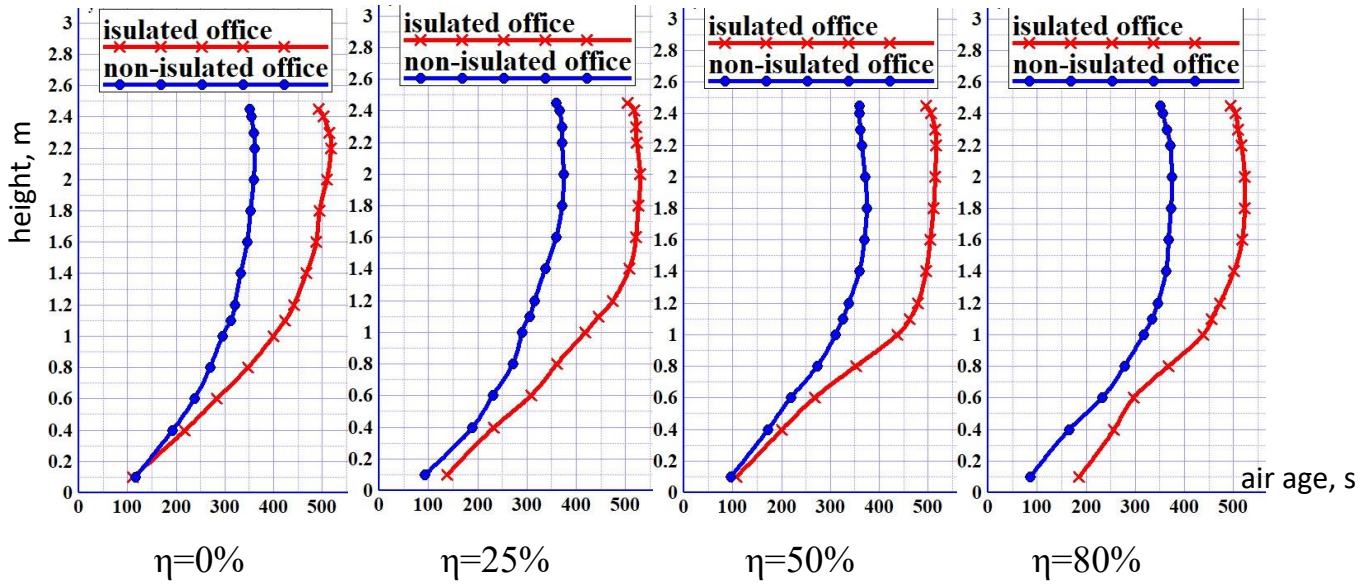

Fig.(5-61) Comparison between mean air age with height for insulated and non-insulated office, (cases-II and IV) at different (η)

Fig.(5-62) shows the comparison of air exchange efficiency between insulated and non-insulated office rooms with rectangular and semi-circular diffusers at different value of (η).

The air exchange efficiency for non-insulated office room is higher compared with insulated office, regardless of shape of diffuser. This is due to the large supply flowrate to cover heat gain from walls and window. Also, the heat gain from walls and window tend to rise indoor air velocity and decrease age of air. The air exchange efficiency for non-insulated office room with used rectangular diffuser is higher by (5%) compared with insulated office at (η=0). This value being decreases with increase value of (η) to reach to (1%) at (η=80). This is due to maximize air age by decreasing chilled ceiling surface temperature, while the air exchange efficiency difference between the two rooms with semi-circular diffuser is almost stable with an increase (η) about (2%) as average due to the uniform air distribution (radial distribution).

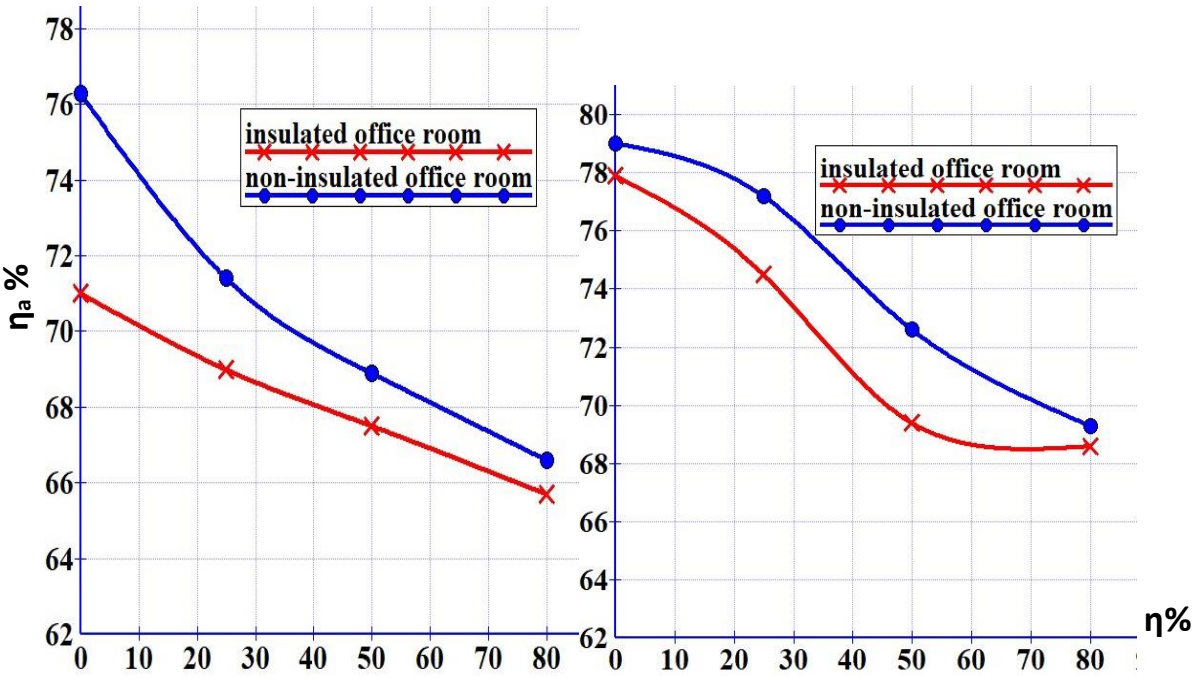

a- DV/CC with rectangular diffuser b-DV/CC with semi-circular diffuser

Fig.(5-62) Comparison between air exchange efficiency for insulated and non-insulated office at different (η)

To understand more details about the mean local air age in non-insulated office room, Figs.(5-63) and (5-64) show the mean age of air contours in it for three planes at (x=2.75m, y=0.1m and z=0.25) with rectangular and semi-circular diffuser respectively at different (η). These planes chosen to pass through two persons and supply air diffuser. The comparison based on the maximum value of air age at (η=80) which equals (346s and 312 sec) with rectangular and semi-circular diffusers respectively.

The air age (represented by red area) near the ceil increases with increase (η) for two types of diffuser due to the air cools by convection near the chilled ceiling and moves down, lead to decrease velocity of the rising hot air.

If comparison between rectangular and semi-circular diffusers at (y=0.1 m) plane, the air age (represented by blue area) with rectangular diffuser decreases with

horizontal direction. While with semi-circular diffuser decreases with radial direction. This difference gives more advantage to semi-circular diffuser to reduce the mean local air age along the non-insulated wall which located at the north side (same side of diffuser location).

The heat transfer by convection between occupants (heat sources) and the air around them caused increase in air temperature near the heat sources and leads to decrease the age of air in this zone (represented by green area). This is due to increase air velocity around the human body. This green area being reduce with increase portion of cooling load treated by chilled ceiling due to increase in air age and approaching the red area.

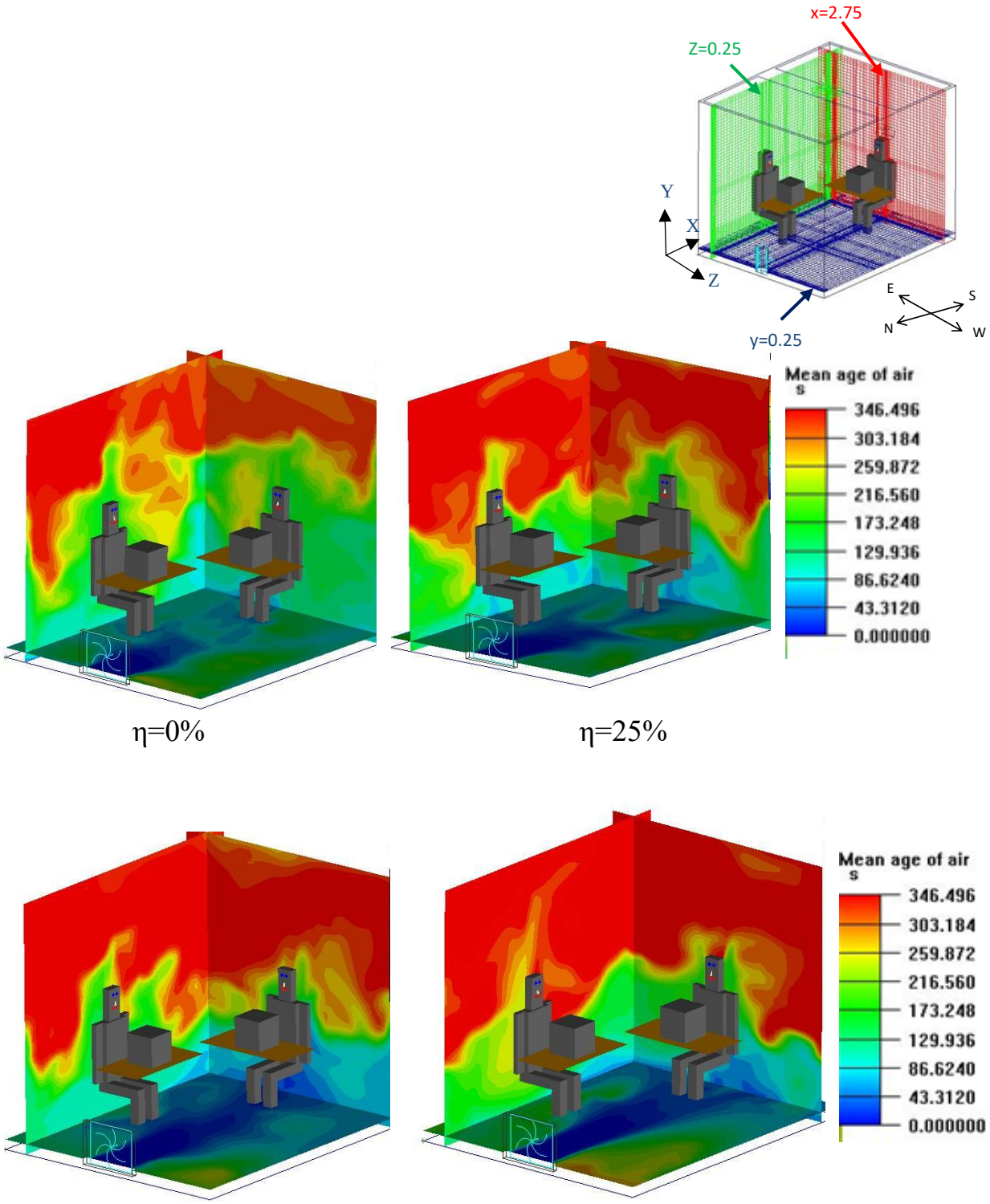

Fig.(5-63) Age of air contours for non-insulated office room cases for three planes at (x=2.75 m), (y=0.1 m) and (z=0.25 m) with rectangular diffuser at different (η)

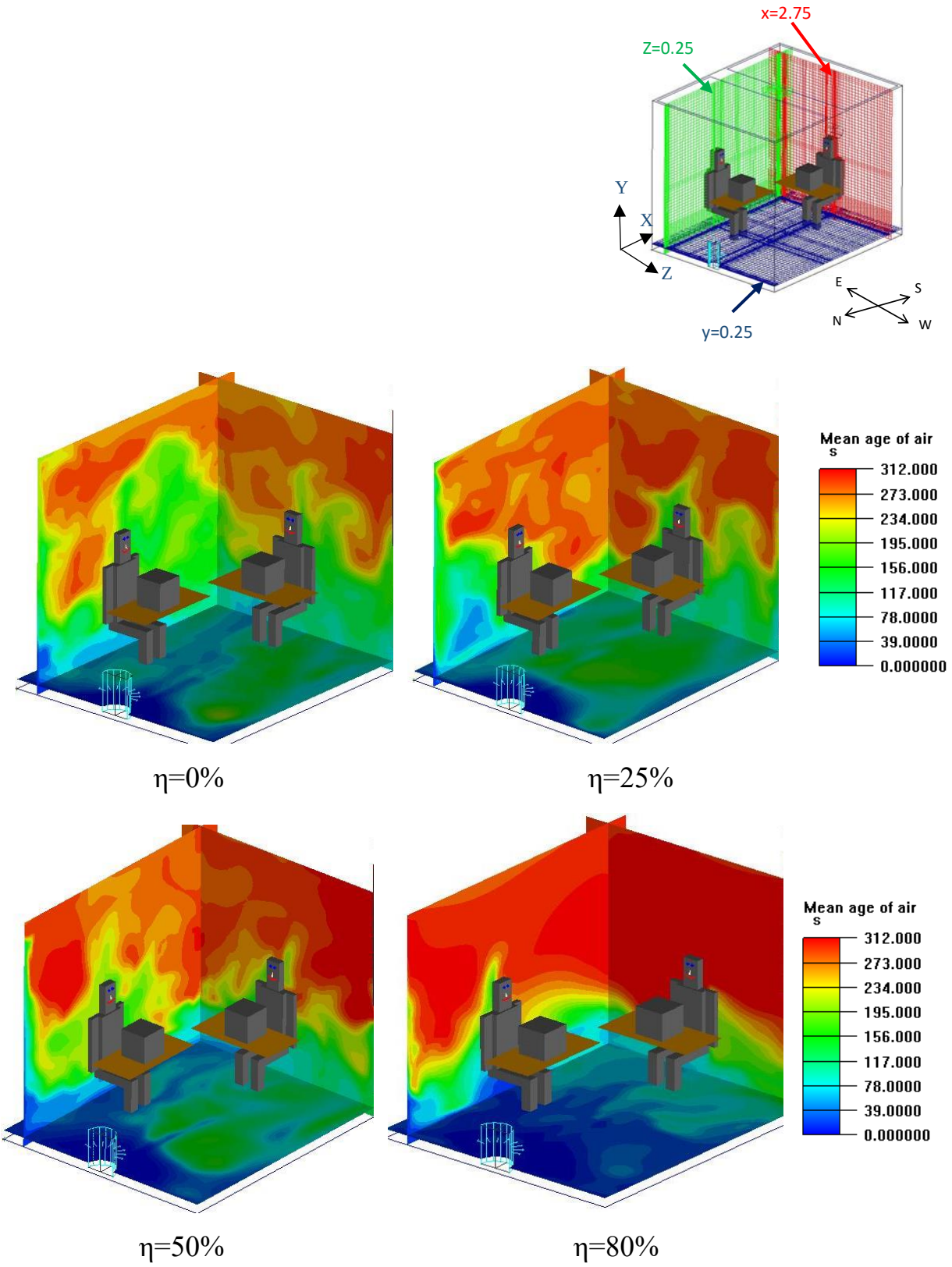

Fig.(5-64) Age of air contours for non-insulated office room cases for three planes at (x=2.75 m), (y=0.1 m) and (z=0.25 m) with semi-circular diffuser at different (η)

5.3.2 Air temperature distribution comparison.

Figs.(5-65) and (5-66) show comparison air temperature with height for the different case studies with rectangular diffuser (case-I and case-III) and semi-circular diffuser (case-II and case-V) respectively at different (η). The comparison based on the temperature difference between indoor air and air supply temperatures to understand the indoor air temperature rising with height.

The air temperature increases with height in each case and at each value of (η). This phenomena is one of the features that are unique to the displacement ventilation system. If compared between insulated and non-insulated office rooms, the non-insulated walls and window lead to raise indoor air temperature. This effect being at level about of (0.8 m). The temperature difference between the two cases reduces from (3 to 1.5^{o}C) with increase portion of load treated by chilled ceiling from (0% to 80%) regardless of the diffuser shape because effect of decrease chilled ceiling surface temperature.

Under (0.8 m) level the difference in rising indoor air temperature (compared with supply air temperature) between non-insulated and insulated office rooms does not exceed (1^{o}C) especially with increase value of (η). The reason for that is due to the air near the floor is colder than other zone and it has not yet been affected by the heat gain from walls and window, then the air temperature near the floor is almost identical in insulated and non-insulated office rooms regardless shape of diffuser. These result is more clearly in cases with semi-circular diffuser compared with rectangular diffuser due to regular distribution for air supply.

The rising in air temperature is maximum in the zone near of ceil and air temperature difference in this zone decreases with increase portion of load treated by chilled ceiling. This is due to increase in chilled ceiling surface temperature. After that the air goes outside room by exhaust grille which located in the middle of

ceiling. The decrease in exhaust air temperature leads to decrease in temperature distribution effectiveness (ε_t) according to Eqn.(4-26) as shown in Fig.(5-67).

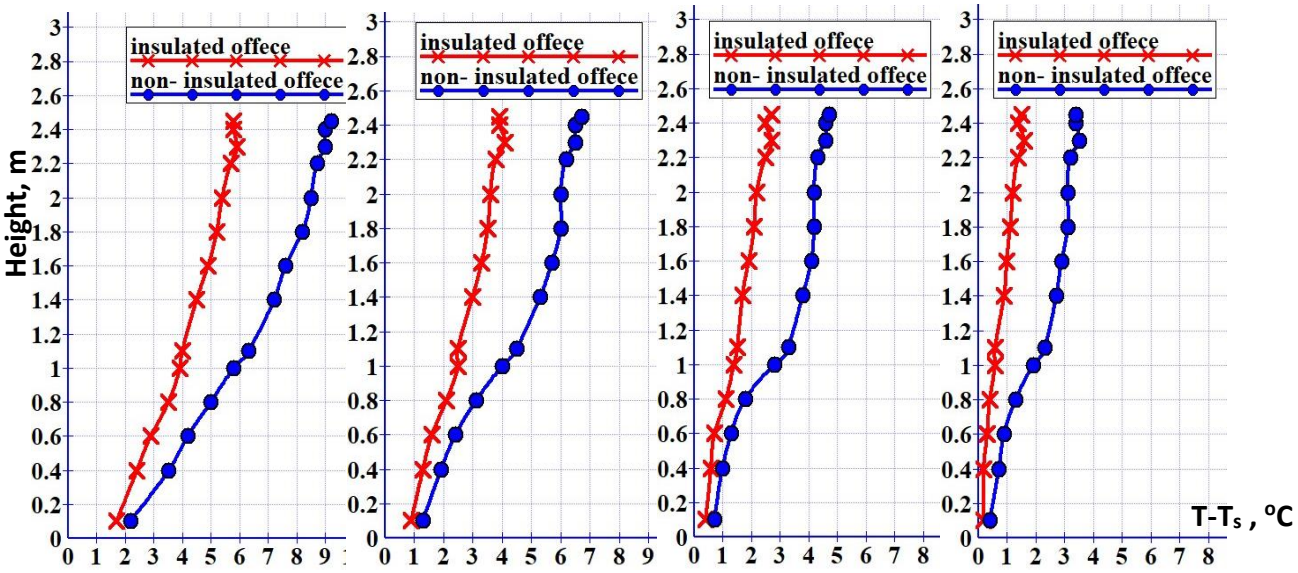

η=0% η=25% η=50% η=80%

Fig.(5-65) Air temperature distribution comparison between insulated and non-insulated office with rectangular diffuser, (cases-I and III) at different (η)

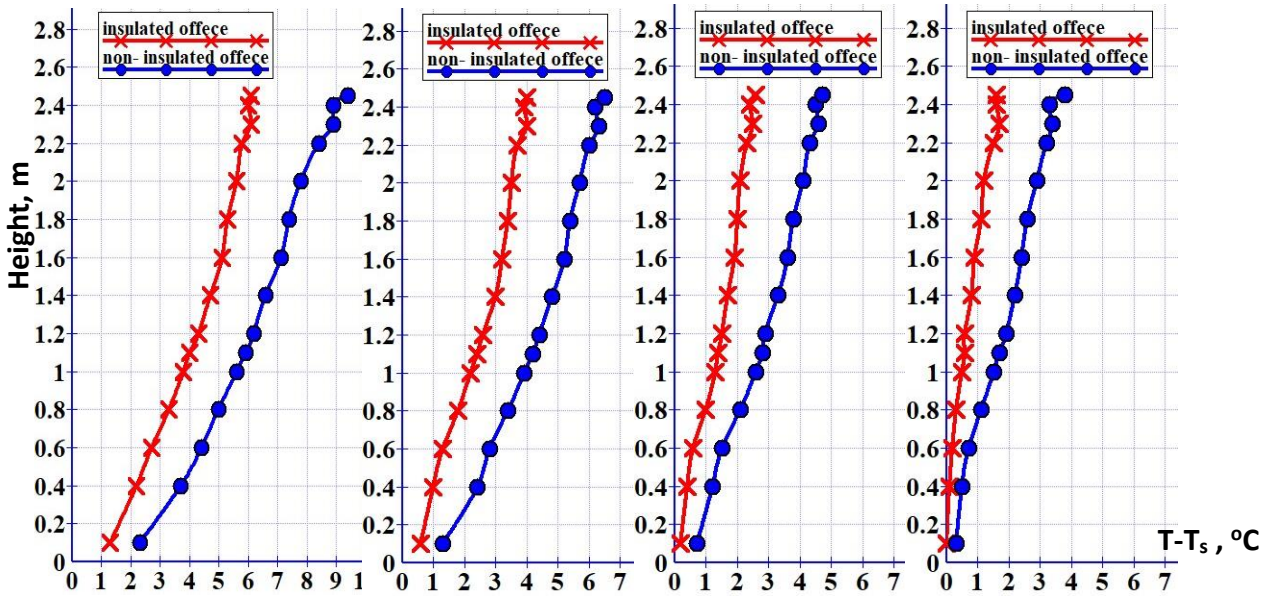

η=0% η=25% η=50% η=80%

Fig.(5-66) Air temperature distribution comparison between insulated and non-insulated office with semi-circular diffuser, (cases-II and IV) at different (η)

Fig.(5-67) shows the comparison of air temperature distribution effectiveness (ε_t) at different (η) between insulated and non-insulated office rooms with rectangular and semi-circular diffusers. The (ε_t) in non-insulated room is less than insulated room at each value of (η) regardless shape of diffuser. This is due to increase the average room temperature (T_{av}) (according to Eqn.(4-26)) in non-insulated room compared with insulated room as shown in tables (5-5) and (5-6). This result gives more advantage to the insulated office room to satisfy human thermal comfort.

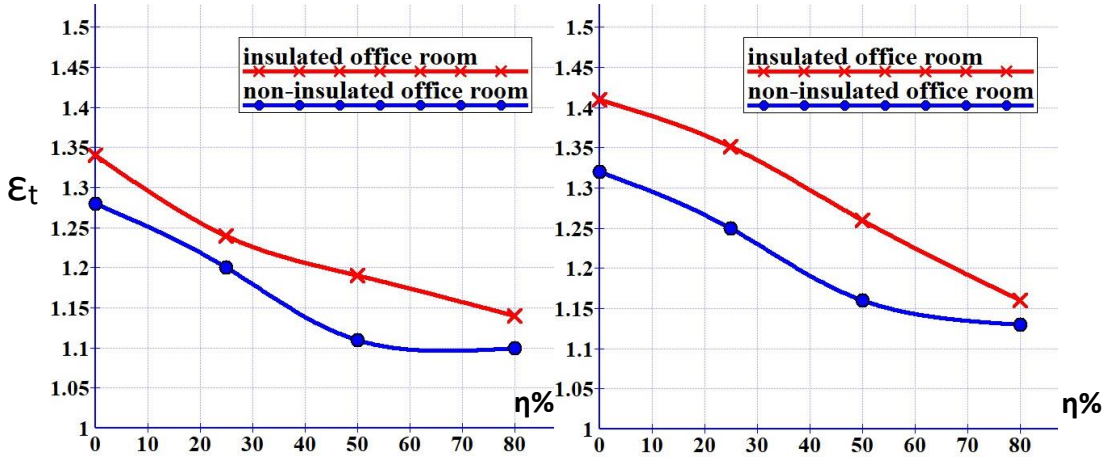

a-cases with rectangular diffuser b-cases with semi-circular diffuser

Fig.(5-67) Air temperature effectiveness comparison between insulated and non-insulated office rooms at different (η)

Fig.(5-68) shows the comparison of temperature difference between head (at level 1.1 m) to foot (at level 0.1 m) at different (η) between insulated and non-insulated office rooms with two types of diffuser. This factor represented locally specific condition which affected on thermal comfort. For non-insulated office room, the temperature difference between head to foot (ΔT_{hf}) decreases with increase value of (η) due to the same reasons explained in (Fig.5-14) which shown the temperature difference between head to foot for insulated office room. The (ΔT_{hf}) in non-insulated office room (at each value of η) is higher by about (1.5°C) with rectangular

diffuser and by about (1°C) with semi-circular diffuser compared with insulated office room. This is due to the faster rising in indoor air temperature as a result of heat gain from non-insulated wall and window. This increase in (ΔT_{hf}) caused discomfort for occupants. The (ΔT_{hf}) for non-insulated office room at (η=0, 25 and 50%) with rectangular and semi-circular diffusers is more than (2°C), thus, thermal comfort is not achieved according to (ASHRAE standard 55, 2010) which specified (2°C) for sitting person. While at (η=80%) the thermal comfort related with (ΔT_{hf}) is achieved for two rooms due to low child ceiling surface temperature caused decrease in indoor air stratified layers.

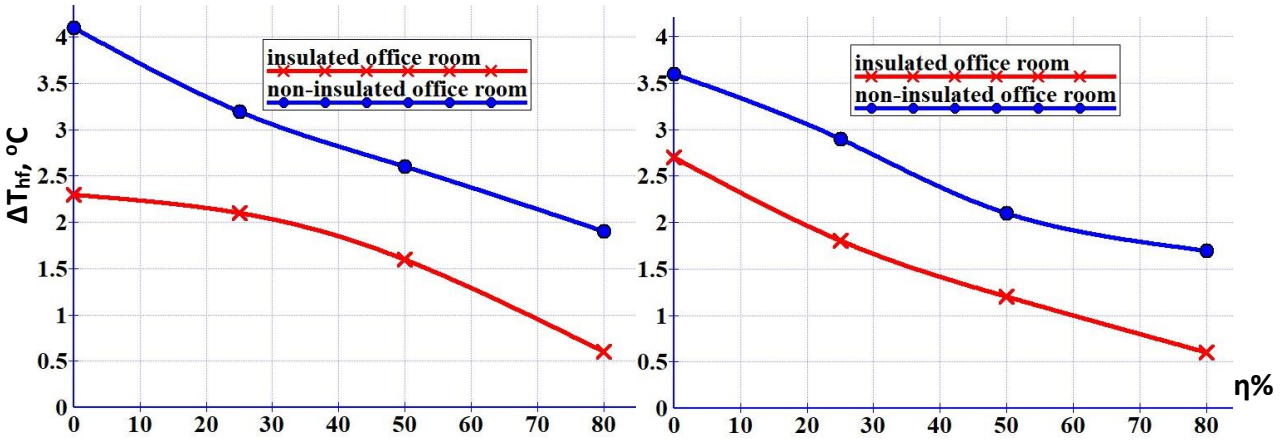

a-cases with rectangular diffuser b-cases with semi-circular diffuser

Fig.(5-68) Temperature difference between head to foot comparison at different (η) between insulated and non-insulated office rooms

5.3.3 Thermal comfort parameters

Fig.(5-69) shows the comparison of average Predicted Mean Vote (PMV) between insulated and non-insulated office rooms with rectangular and semi-circular diffusers at different (η). The average value of mean (PMV) for non-insulated room has the same behavior for insulated office room. Its decreases by increasing value of portion load treated by chilled ceiling. This is due to the increase heat transfer by radiation between heat sources and chilled ceiling. If it is compared between insulated and non-insulated room room, the (PMV) value in non-insulated room is higher compared with insulated room. It's between about (0.6-0.4) with rectangular diffuser and between about (0.4-0.2) with semi-circular diffuser for (η) between (0-80%) respectively. This is a result of the warmer indoor air in non-insulated room as compared with it in insulated room which leads to decrease heat transfer by convection with heat sources. Also the semi-circular diffuser performance is due to the uniform distribution of cool fresh air provided, which increase heat transfer by convection with heat sources.

The values of (PMV) for non-insulated office room are between (1.14 to 0.76) with rectangular diffuser for (η) between (0-80%) respectively. These values don't achieve with the (PMV) value specified by ASHREA slandered (2013) (-0.5<PMV<0.5), while with semi-circular diffuser the (PMV) values is between (0.81-0.53) respectively. It is near of (PMV) value specified by ASHREA slandered.

The average value of (PPD) is related with the average (PMV) value, then it decreases with increase value of (η) also, as shown in Fig.(5-70). The values of (PPD) for non-insulated office room are between (32.3% to 20.8%) with rectangular diffuser for (η) between (0-80%) respectively. While with semi-circular diffuser the its between (23.6% to 15.7%) respectively. These values don't achieve with the (PPD) value specified by ASHREA slandered (PPD<10%). The value of (PPD) for

non-insulated office is higher compared with insulated office room regardless of value of (η) and shape of diffuser due to the same reason above related with (PMV).

The (PPd) values for insulated room are less than about (10%) as compared with non-insulated room with rectangular or semi-circular diffuser in each cases. These above results for (PMV) and (PPD) give more thermal comfort advantages for insulated office room and semi-circular diffuser.

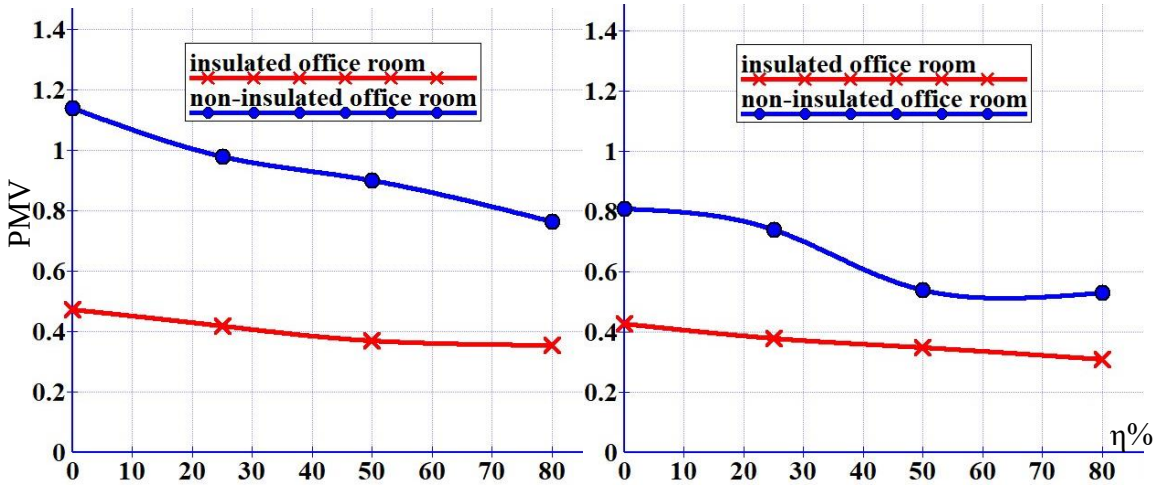

a-cases with rectangular diffuser b-cases with semi-circular diffuser

Fig.(5-69) Average Predicted mean vote (PMV) comparison between insulated and non-insulated office rooms at different (η)

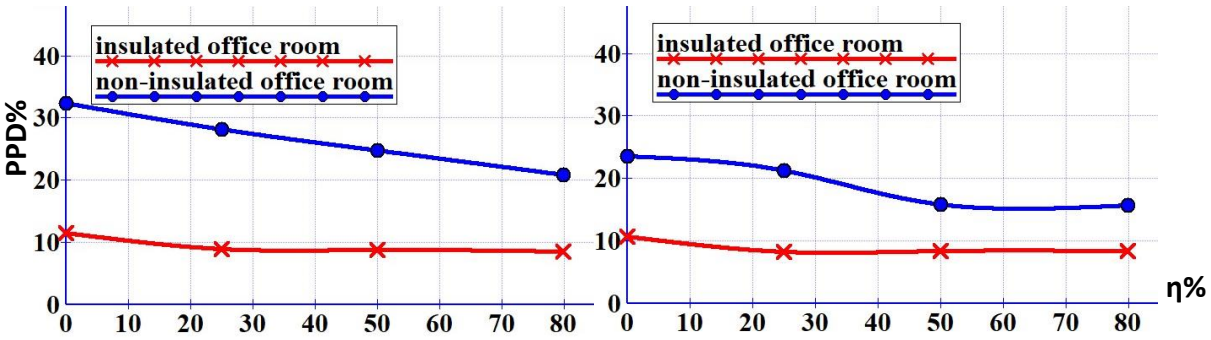

a-cases with rectangular diffuser b-cases with semi-circular diffuser

Fig.(5-70) Mean predicted percentage dissatisfied (PPD) comparison between insulated and non-insulated office rooms at different (η)

To understand the effect of non-insulated walls and window on the level of local thermal comfort in terms of Predicted Mean Vote (PMV). Figs. (5-71a-b) and (5-72a-b) show the (PMV) contours for non-insulated and insulated office rooms in three planes at (x=2.75m, y=0.1m and z=0.25) with rectangular and semi-circular diffuser respectively at different (η). In general, it is clearly that the (PMV) value of insulated room is less than its value in non-insulated office with the two type supply diffuser. This is due to warmer indoor average air temperature (T_{av}) in non- insulated room as compared with insulated room. This leads to decrease heat transfer by convection with heat sources, thus reduce human thermal comfort.

The (PMV) value in non-insulated room increase by about (1) compared with insulated room with rectangular diffuser. This difference recede to about (0.15) with semi-circular diffuser. These results mean that the indoor air in non-insulated room is warmer than insulated room (depending on the (PMV) values specified by ASHREA as shown in Fig.(1-8)). So, semi-circular diffuser is more suitable compared with rectangular diffuser.

From the (PMV) contour plane at (z=0.25) in non-insulated room, the maximum value of (PMV) is located in the zone over the occupant that sits near non-insulated wall and window in north side regardless of the diffuser type and value of (η). This is due to the increase air temperature in this zone that exposed to heat transfer from outside leads to decrease thermal comfort.

The value of (PMV) in indoor for two rooms decreases with increase (η) and get closer to the range specified by AHREA standard (-0.5<PMV<0.5). This is due to the decrease in air temperature that falls from chilled ceiling and indoor average air temperature. Then, increase value of (η) gives more thermal comfort.

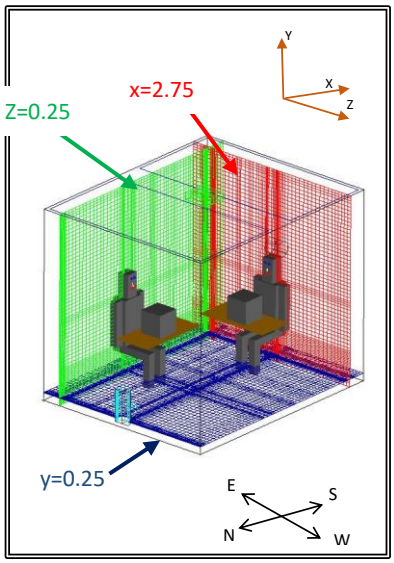

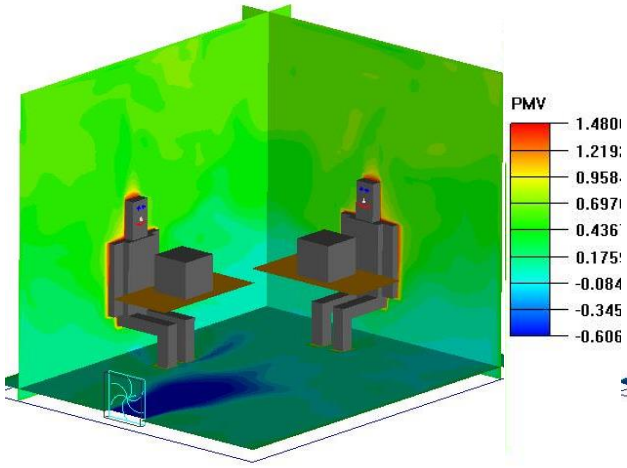

η=0%

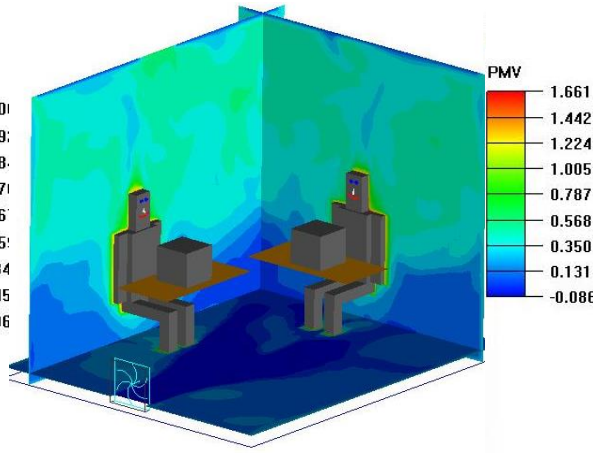

η=25%

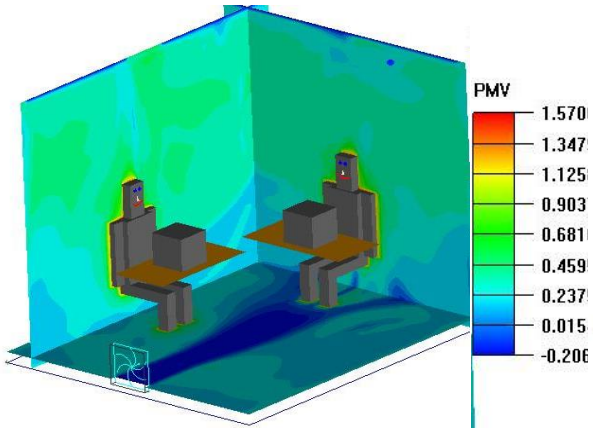

η=50%

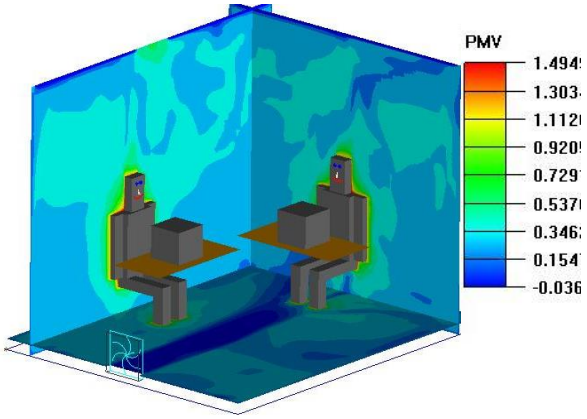

η=80%

Fig.(5-71a) PMV contours at three plane (x-2.75m, y=0.1m, z=0.25 m), case-I, at different (η)

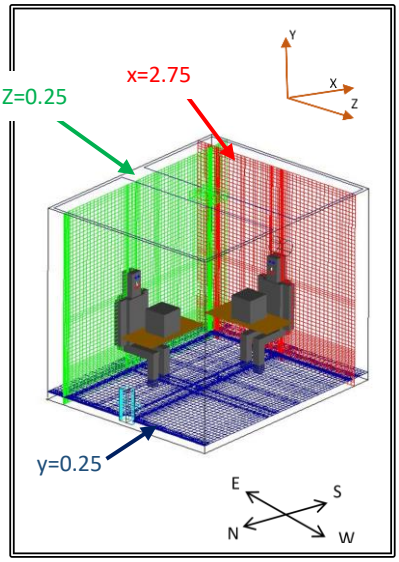

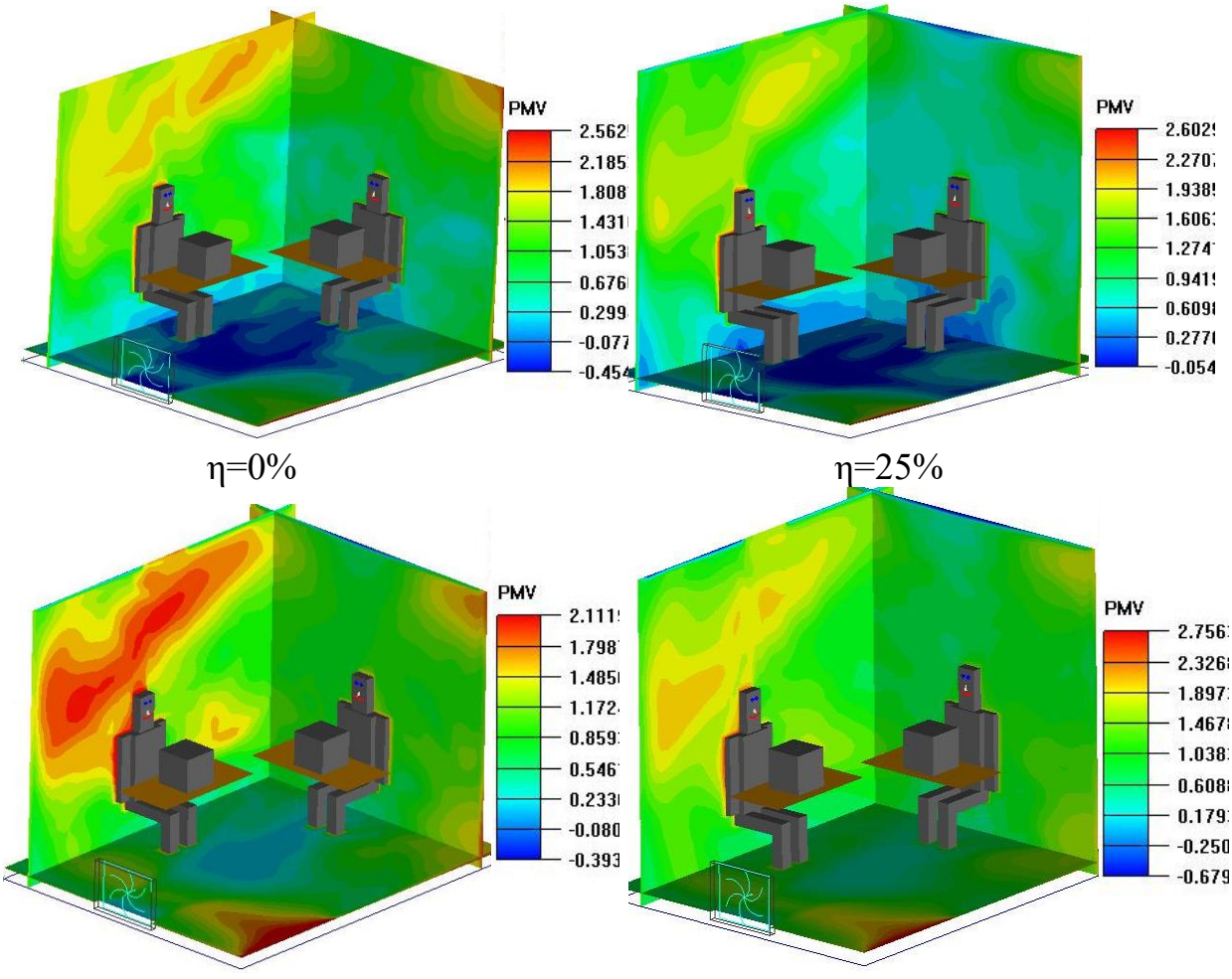

η=0% η=25%

η=50% η=80%

Fig.(5-71b) PMV contours at three plane (x-2.75m, y=0.1m, z=0.25 m) at different (η), case-III

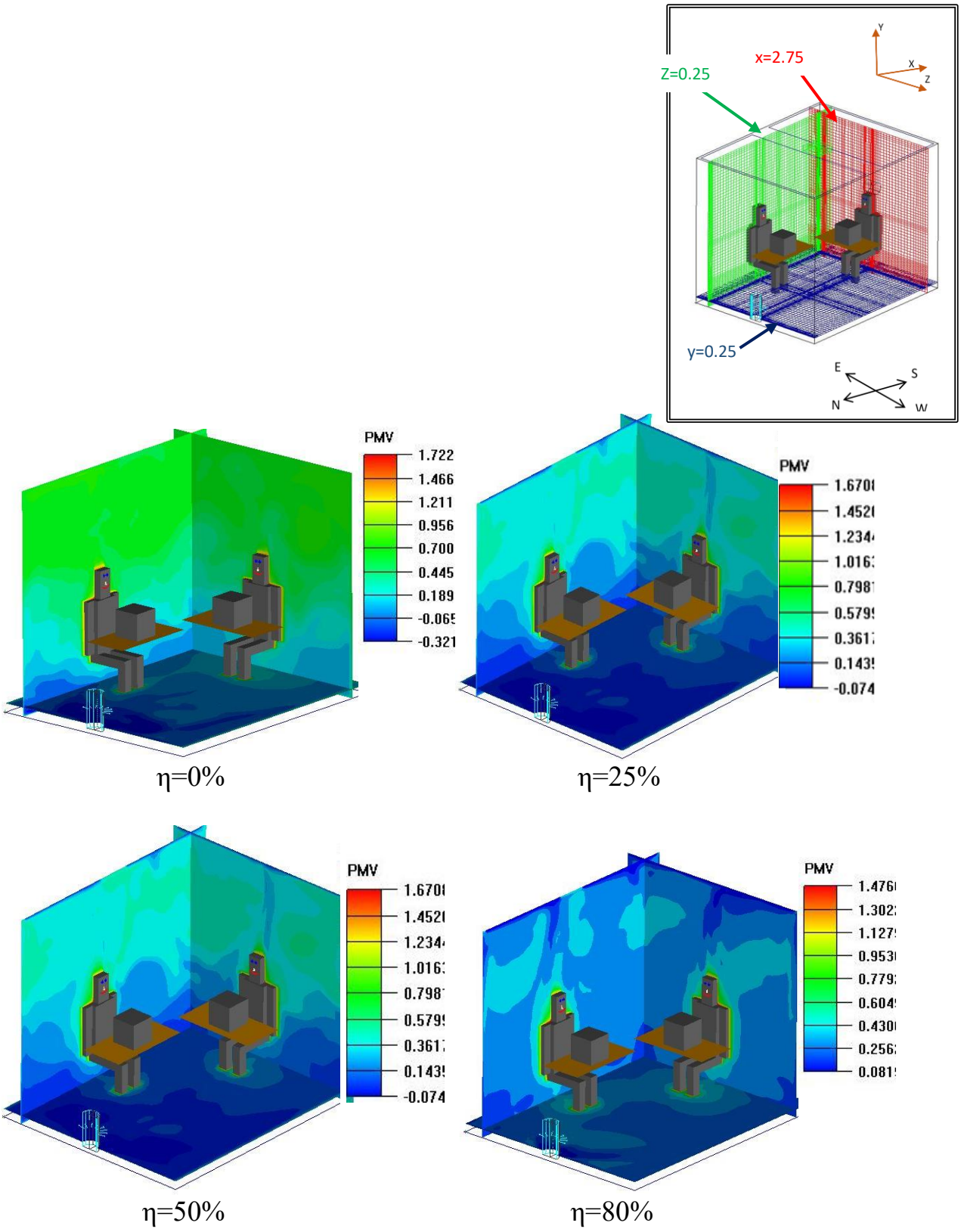

Fig.(5-72a) PMV contours at three plane (x-2.75m, y=0.1m, z=0.25 m) at different (η), case-II.

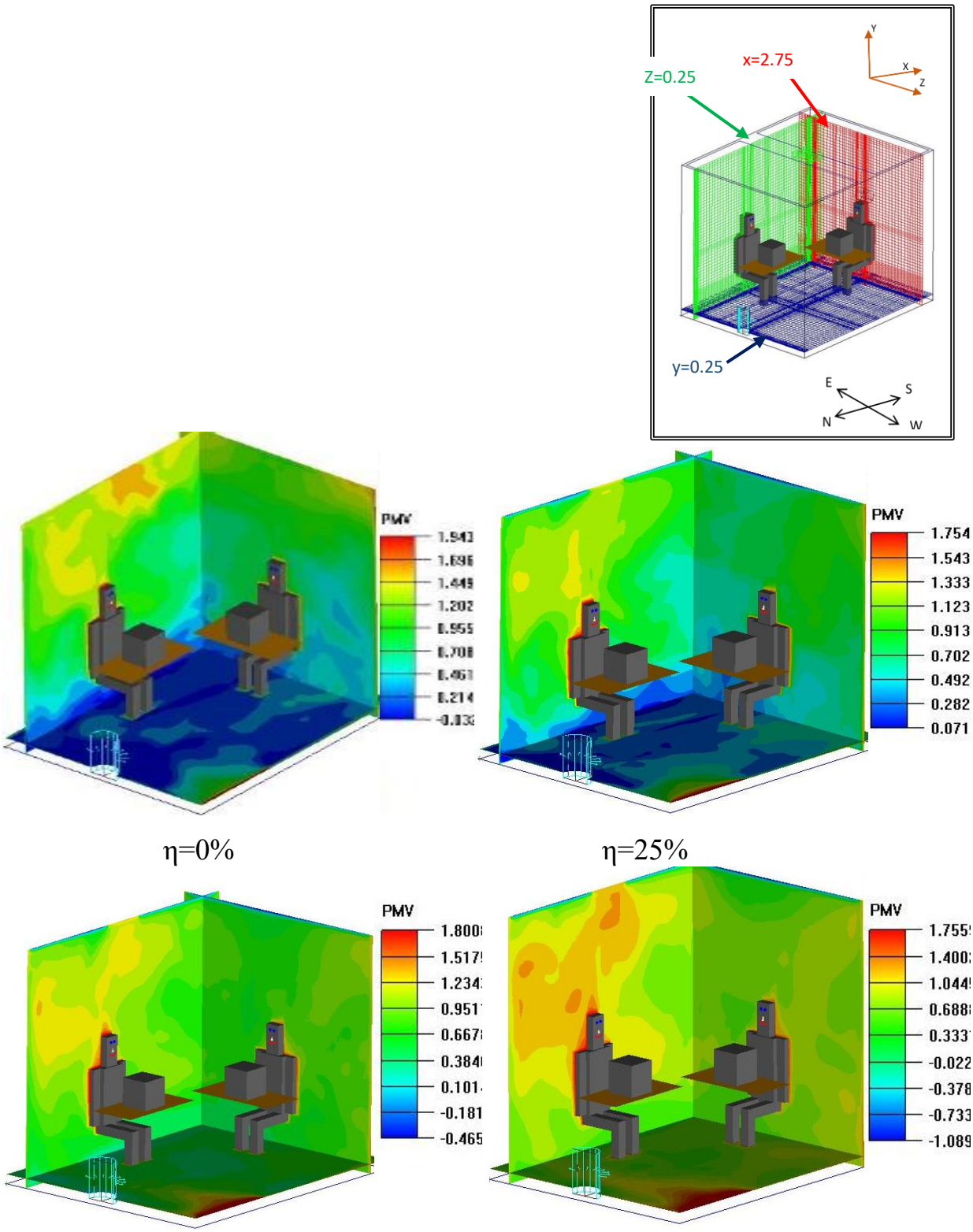

Fig.(5-72b) PMV contours at three plane (x-2.75m, y=0.1m, z=0.25 m) at different (η), case-IV.

Fig.(5-73) shows a comparison of air diffusion performance index (ADPI) at different (η) between insulated and non-insulated office rooms with rectangular and semi-circular diffuser. The (ADPI) in the two rooms cases increase with increase portion of cooling load treated by chilled ceiling by about (7%) as average with used rectangular or semi-circular diffuser. This increase in (ADPI) because of the cold air come back from the chilled ceiling, which make balance between air temperature and its velocity. The value of (ADPI) for insulated office room with rectangular diffuser is higher by about (between 10% to 15%) at different value of (η) compared with its value for non- insulated office room. This increase was a result of heat transfer from non-insulated walls and window which leads to increase indoor air temperature. (ADPI) with semi-circular diffuser for insulated office room is higher than non-insulated office by about (between 1% to 6%) at different value of (η) because it gives a suitable balance between air temperature and velocity.

The difference of (ADPI) between insulated and non-insulated room with semi-circular diffuser being fade at high value of (η), its reach to only about (1%) at (η=80%). These results gives addition advantage for semi-circular diffuser.

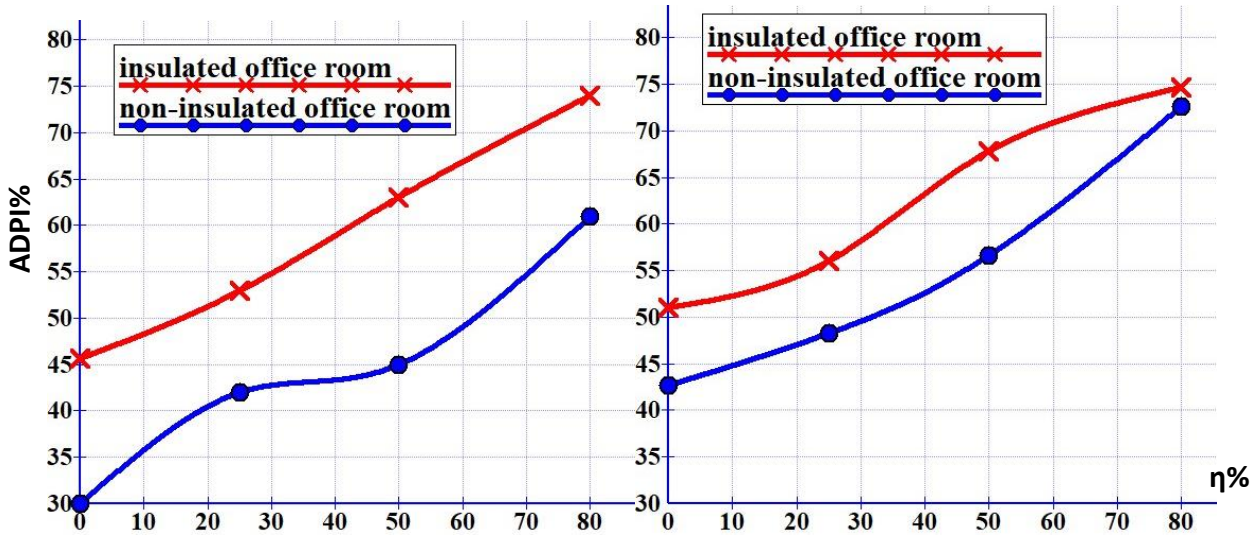

a- cases with rectangular diffuser b- cases with semi-circular diffuser

Fig.(5-73) Air diffusion performance index (ADPI) comparison between insulated and non-insulated office rooms at different (η)

Figs.(5-74) and (5-75) show the thermal comfort conditions by using (CBE) tool (which produced by building energy center) for non-insulated and insulated office rooms with rectangular and semi-circular diffusers respectively at different (η).

By observing the location of the red circular point respect to thermal comfort zoon (blue color zoon), the thermal comfort don't achieve in non-insulated office room with rectangular and semi-circular diffuser and its approach to the warm area. While with semi-circular diffuser the red point more converge to the comfort zone spatially at (η=80%) compared with rectangular diffuser. This is due to the thermal comfort zone presents by the combined indoor average air temperature (T_{av}) with mean radiation temperature (MRT) for which satisfy the (PMV) between (-0.5 and +0.5) according to the ASHREA standard. Average indoor air temperature (T_{av}) and (MRT) have main effect to satisfied thermal comfort. Increase it leads to the red point go out comfort zone, this clear in the non- insulated room which has warmer air. It was noted from figures that the mean radiant temperature (MRT) is important factor to specify the thermal comfort zone. The thermal comfort zone tend to right side with decrease mean radiant temperature and rise the dry bulb temperature range which satisfy thermal comfort. This is due to the decrease in (MRT) leads to improve the heat transfer by convection with heat sources, thus improving (PMV and PPD). As shown in tables (5-5) and (5-6), the increase in (η) led to decrease in (MRT), then the red point getting close to the thermal comfort zone with increase (η)

The difference in average indoor air velocity among the cases has a slight effect on the thermal comfort zone because it's very low in the displacement ventilation system. Adding to that, the effects of chilled ceiling which causes reduce it. In this study, no direct effect was observed for the change in relative humidity between cases, as its change was slight.

These results give advantage to the insulated office room to use (DV/CC) system in hot and dry climate (as Hilla climate).

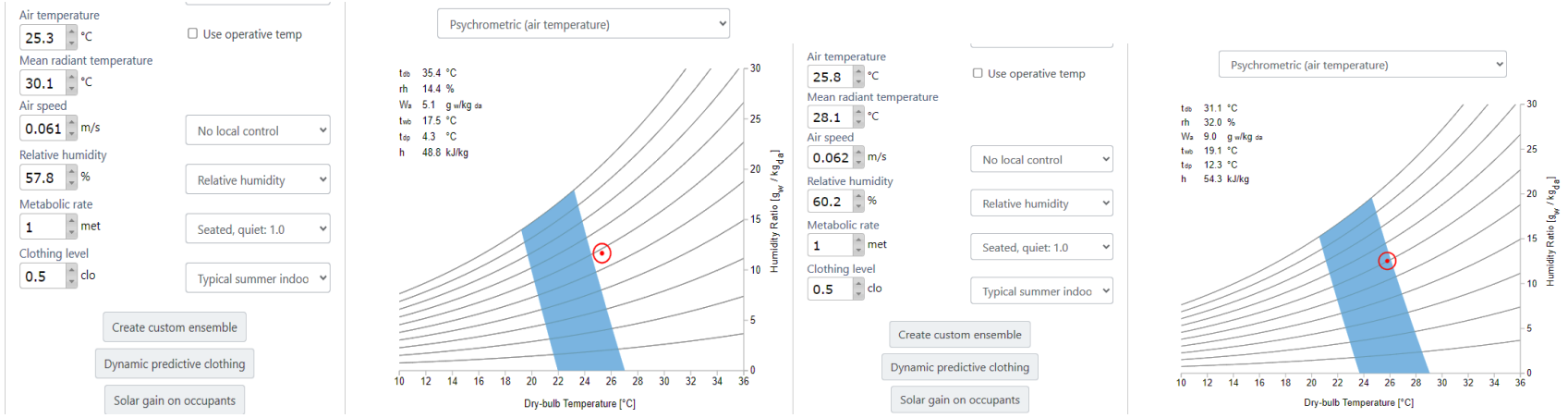

0% 25%

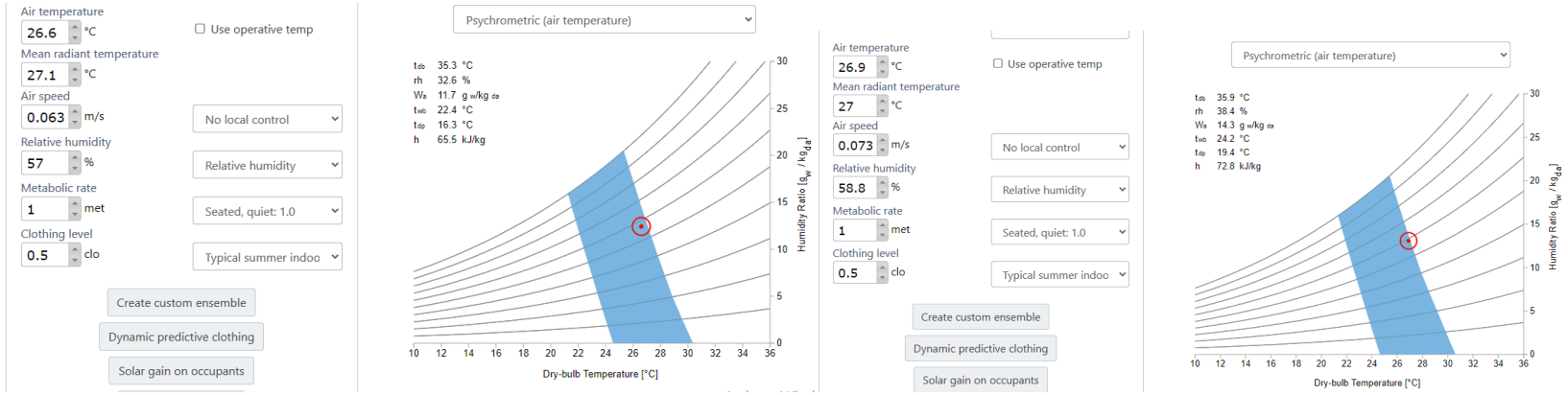

50% 80%

Fig.(5-74a) Thermal comfort conditions by using CBE tool for non-insulated office room, case-III, at different (η).

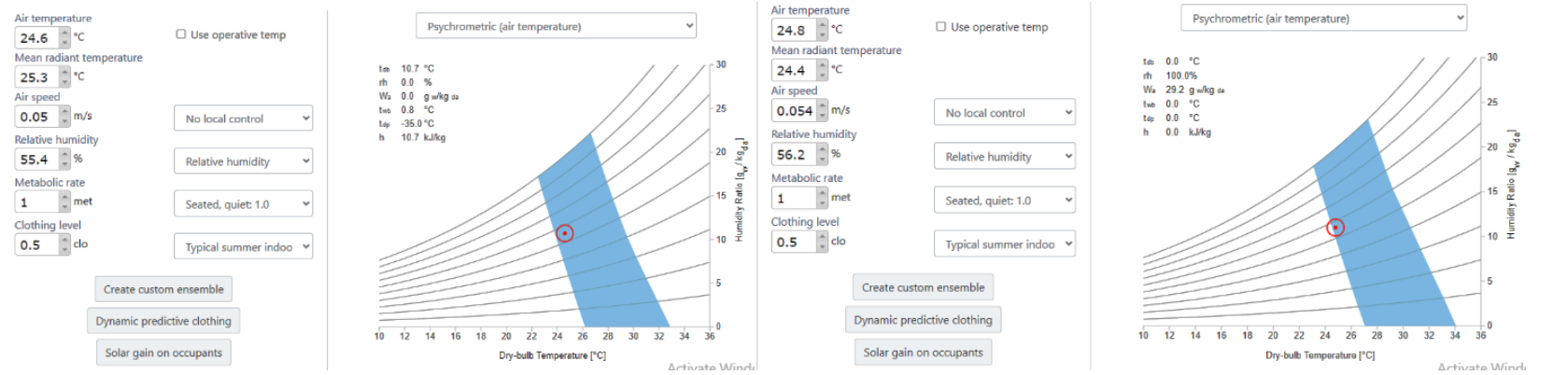

η=0% η=25%

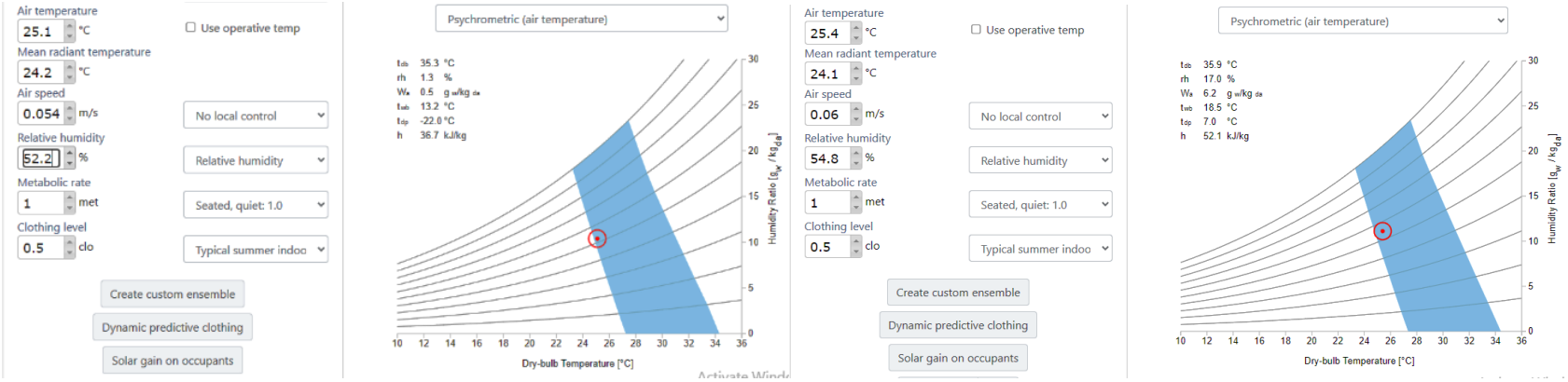

η=50% η=80%

Fig.(5-74b) Thermal comfort conditions by using CBE tool for insulated office room, case-I, at different (η).

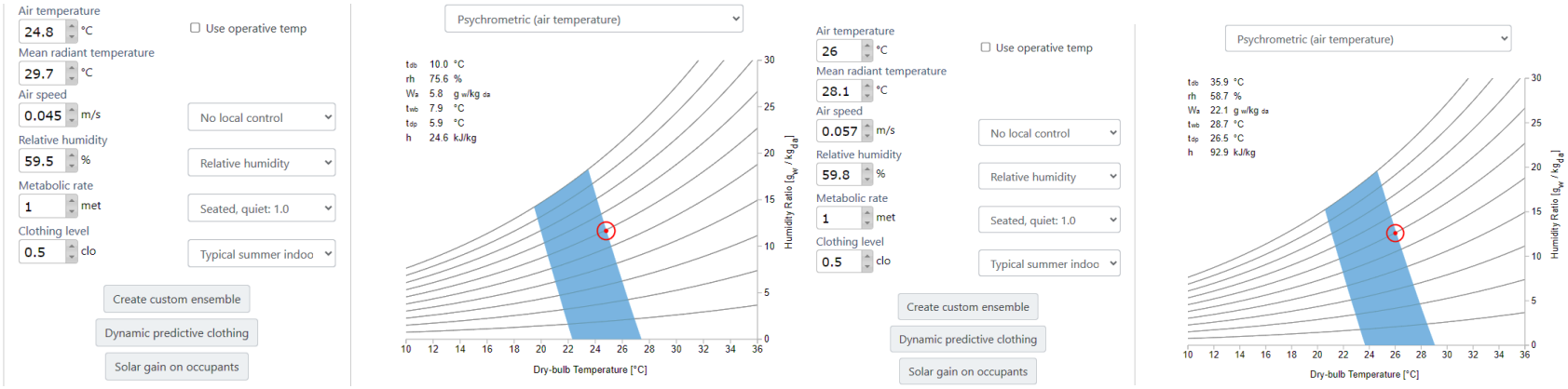

η=0% η=25%

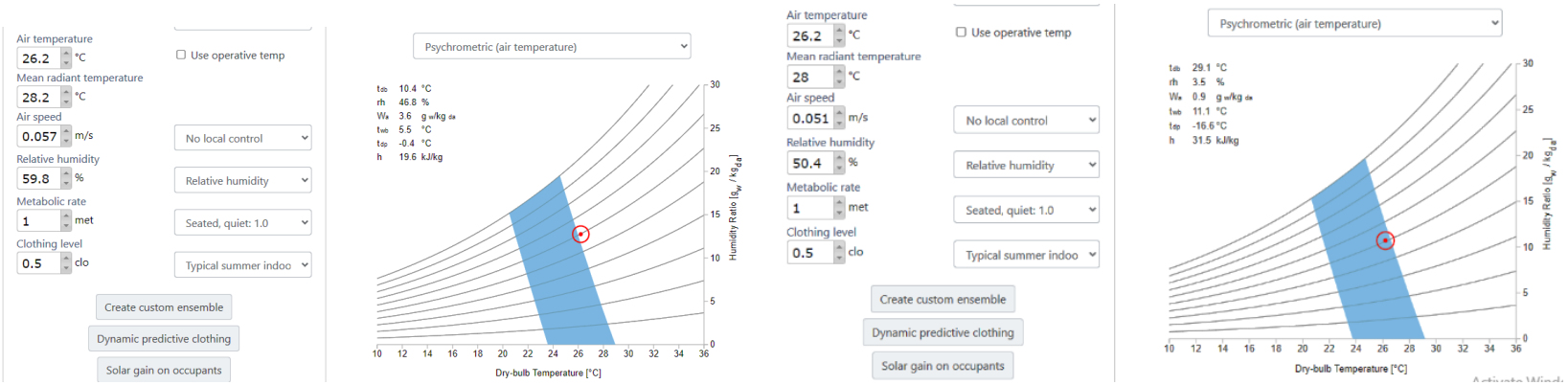

η=50% η=80%

Fig.(5-75a) Thermal comfort conditions by using CBE tool for non-insulated office room, case-IV, at different (η).

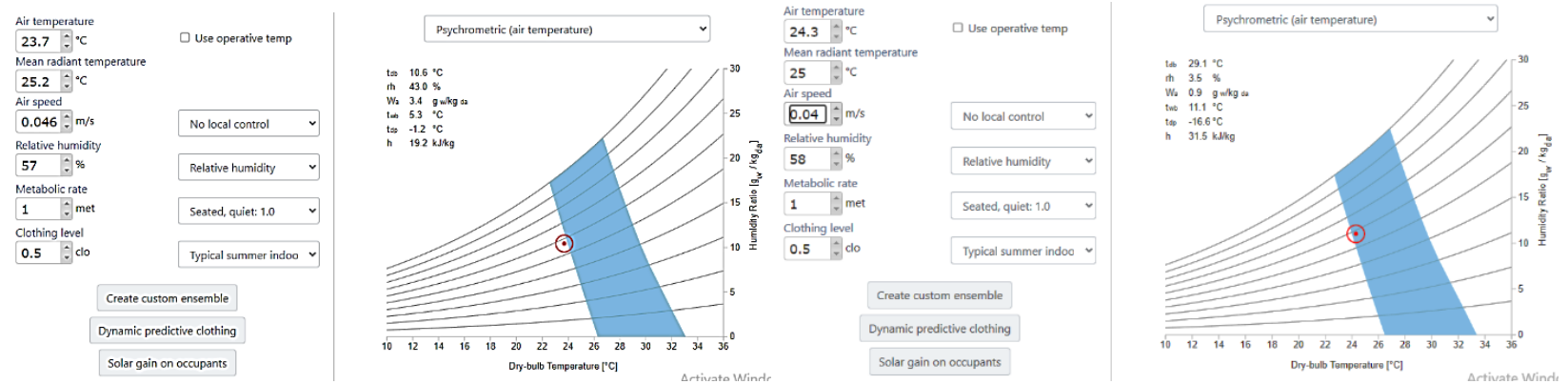

η=0% η=25%

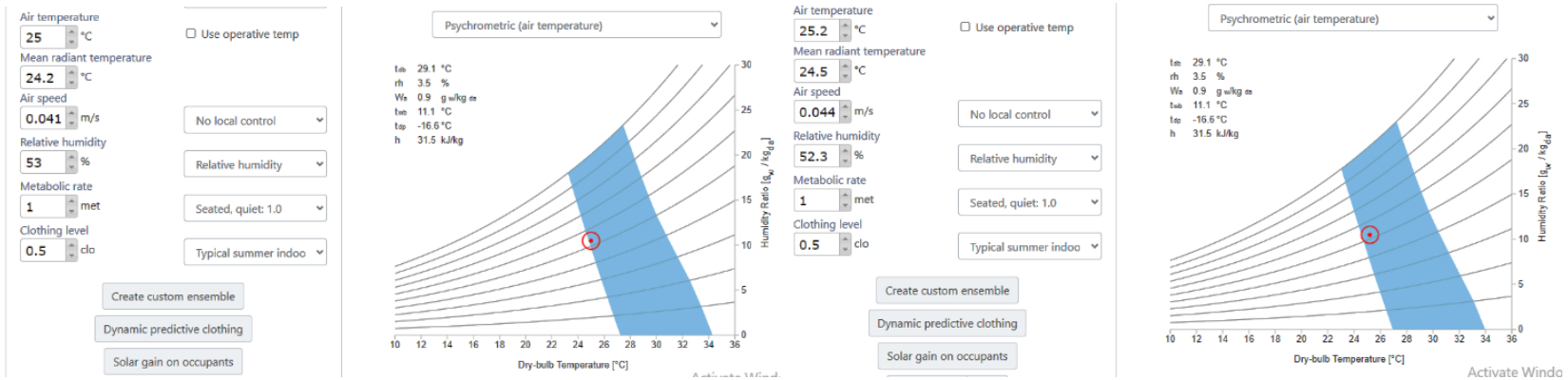

η=50% η=80%

Fig.(5-75b) Thermal comfort conditions by using CBE tool for insulated office room, case-II, at different (η).

5.4 Numerical Results for Classroom (Case-V and VI)

(DV/CC) system is studied numerically in a classroom under Hilla city (Iraq) climate at maximum summer temperature (47°C). The study are identified based on the different cooling load chilled ceiling ratio (η). The displacement ventilation supply air temperature varied as (19.5, 21.5, 23.5, 24.5°C) and the chilled ceiling temperature varied as (22, 20 and 17.5°C) at (η) equals to (25%, 50% and 80%) respectively. The airflow rate is fixed at ($0.3m^3/s$) (9.6 air changes per hour) divided on the two one way rectangular air supply diffusers for case-V and the two semi-circular air supply diffuser for case-VI as shows in chapter four. The main results parameters obtained in the numerical analyses are summarized in Table (5-7).

Table(5-7) numerical results for classroom (case-V and case-VI)

Cases	**η (%)**	**V_{DV} (m^3/s)**	**T_{av} (°C)**	**T_s (°C)**	**T_{CC} (°C)**	**MRT (°C)**	**ADPI (%)**	**PMV**	**PPD (%)**	**ΔT_{hf} (°C)**	**η_a (%)**	ε_t
Case-V	0	0.3	23.7	19.5	-	31.29	50.14	0.815	19.5	2.2	72.8	1.38
	25	0.3	24.2	21.5	22	30.2	50.17	0.783	19.1	1.4	70.7	1.31
	50	0.3	25.2	23.5	20	29.3	58.97	0.765	18.7	0.9	69.93	1.28
	80	0.3	25.3	24.5	17.5	29.1	81.54	0.69	17	0.4	57.2	1.25
Case-VI	0	0.3	23.6	19.5	-	30.5	57.6.	0.76	20	2.1	74.2	1.37
	25	0.3	24	21.5	22	28.7	59.7	0.66	15.9	1.3	72.4	1.36
	50	0.3	25	23.5	20	29.7	61.3	0.62	13.1	0.8	71.8	1.31
	80	0.3	25.2	24.5	17.5	28.6	80.7	0.58	12.7	0.5	64.7	1.28

5.4.1 Mean air age and air exchange efficiency results

Fig.(5-76) shows mean air age distribution contours of the classroom for case-V (with rectangular diffuser) and case-VI (with semi-circular diffuser) in plane at (z=1.1 m) for different values of (η). This plane passes through the supply diffuser and row of students to observe changes in air age for each case.

The air age starts from zero at the air supply diffuser and increasing with horizontal distance from the supply diffuser, especially with semi-circular diffuser due to low momentum compared with rectangular diffuser.

The temperature of the chilled ceiling surface decreases with increase (η) and reduces the air temperature contact with it by convection, which leads to increase the air age with increase (η). This phenomenon is clear by noting the increase in red and yellow colors in upper area of the figures with increase (η) in both cases. With rectangular diffuser, the maximum and minimum values of air age are (686s and 483 sec) at (η=80% and 0%) respectively. While with semi-circular diffuser the maximum and minimum values are (521s and 486 sec) at (η=80% and 0%) respectively. This result shows that the semi-circular diffuser led to a reduction age air compared with rectangular diffuser. This is due to the performance of semi-circular diffuser to supply fresh air in multiple directions indoor.

For the two cases, the zone locates over diffuser has a maximum value of air age compared with other zones in a classroom. That's mean the fresh air in this zone is very little and has a high concentration of pollution. This result is found also in the office room as shown above. Decrease the air age around students in each case is due to increase air temperature by convection with the human body causes decrease in air density and increase velocity of air moving and causes decrease in air age.

Fig.(5-77) shows mean air age distribution contours of the classroom for (case-V) and (case-VI) in plane at (x=4 m) for different values of (η). This plane touches the non-insulated walls (north and south walls) and passes through the students

sitting on the same desk. For the two cases, the minimum air age value is near of the floor (blue area) due to supply cold fresh air by the two displacement diffusers.

The maximum air age locates in the upper zone near the wall without windows (north wall) because the air temperature near the wall with windows increases by heat radiation and convection through windows (yellow color at the left said of the figures). This causes increase in air velocity, which leads to decrease in air age in this zone. The figure also shows the effects of chilled ceiling in increasing the air age, and this effect increases with the increase (η) as shown above.

As shown in Figs. (5-76) and (5-77), the air age increases with increase (η), and its values with the semi-circular diffuser are lower compared with the rectangular diffuser for the same reasons that were demonstrated in the office room discussion.

The vertical mean age of air profiles in a classroom with height for the two cases at different values of (η) is shown in Fig.(5-78). This figure depends on the average mean air age in different horizontal planes at several heights. The mean air age increases with height. For the two cases with each value of (η), the increase of (η) leads to increase in mean air age. This is due to the reduction in air velocity due to meeting the rising warm air with the falls cold air after it contacts with chilled ceiling surface. This leads to decrease air temperature by convection.

The above results can be confirmed by knowing the time taken by the air particle to travel from the air supply diffuser to the exhaust grille as shown in Figs.(5-79) and (5-80) for case-V (with rectangular diffuser) and case-VI (with semi-circular diffuser) respectively. The air particle travel time from the air inlet to the outlet increases with increase (η) for the two cases, because its velocity reduction by the cold air coming down from chilled ceiling. The travel time with rectangular diffuser (Fig.5-79) is between (365 to 471 sec) at (η=0% to 80%) respectively, while with semi-circular diffuser (Fig.5-80) it's between (328 to 436 sec) at (η=0% to 80%) respectively. This result shows that the old indoor air is expelled faster from the

room when using a semi-circular diffuser, due to ability to distribute fresh air more uniform than rectangular as shown in office room discussion.

As indicated in Eqn.(4-31), the air exchange efficiency depending on the value of mean air age. Then it decreases with increase in mean air age as shown in Fig.(5-81). This figure shows the relation between air exchange efficiency with (η) for the two cases. The air exchange efficiency decreases with increase (η) regardless of the shape of the diffuser. The air exchange efficiency at (η=80) decreases by about (15.6%) compared with the test at (η=0%) with rectangular diffuser, while with semi-circular diffuser the air exchange efficiency at (η=80) decreases by about (11.65%) compared with the test at (η=0%). The air exchange efficiency by used a semi-circular diffuser is higher by (4.6%) as average compared with a rectangular diffuser. This is due to advantage of semi-circular diffuser to reduce air age as discussed above. This result leads to the fact that the use of chilled ceiling reduces air exchange efficiency. The reduction of air exchange efficiency (η_a) means increase in time required for fresh air to replace the old air in a classroom zone, which affects student performance.

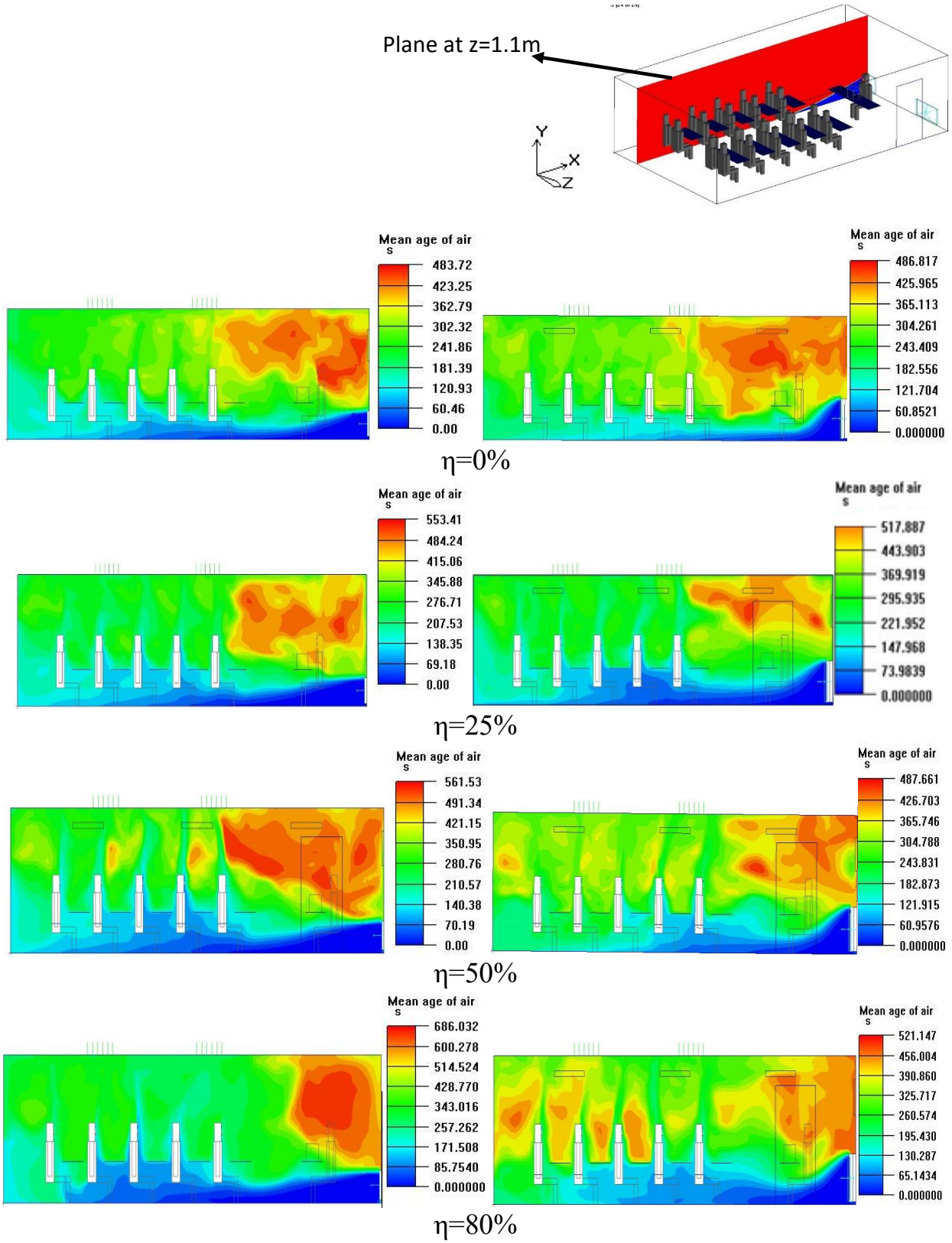

a-case-V b-case-VI

Fig.(5-76) Age of air contours at plane (z=1.1 m) for different (η), cases-V and VI

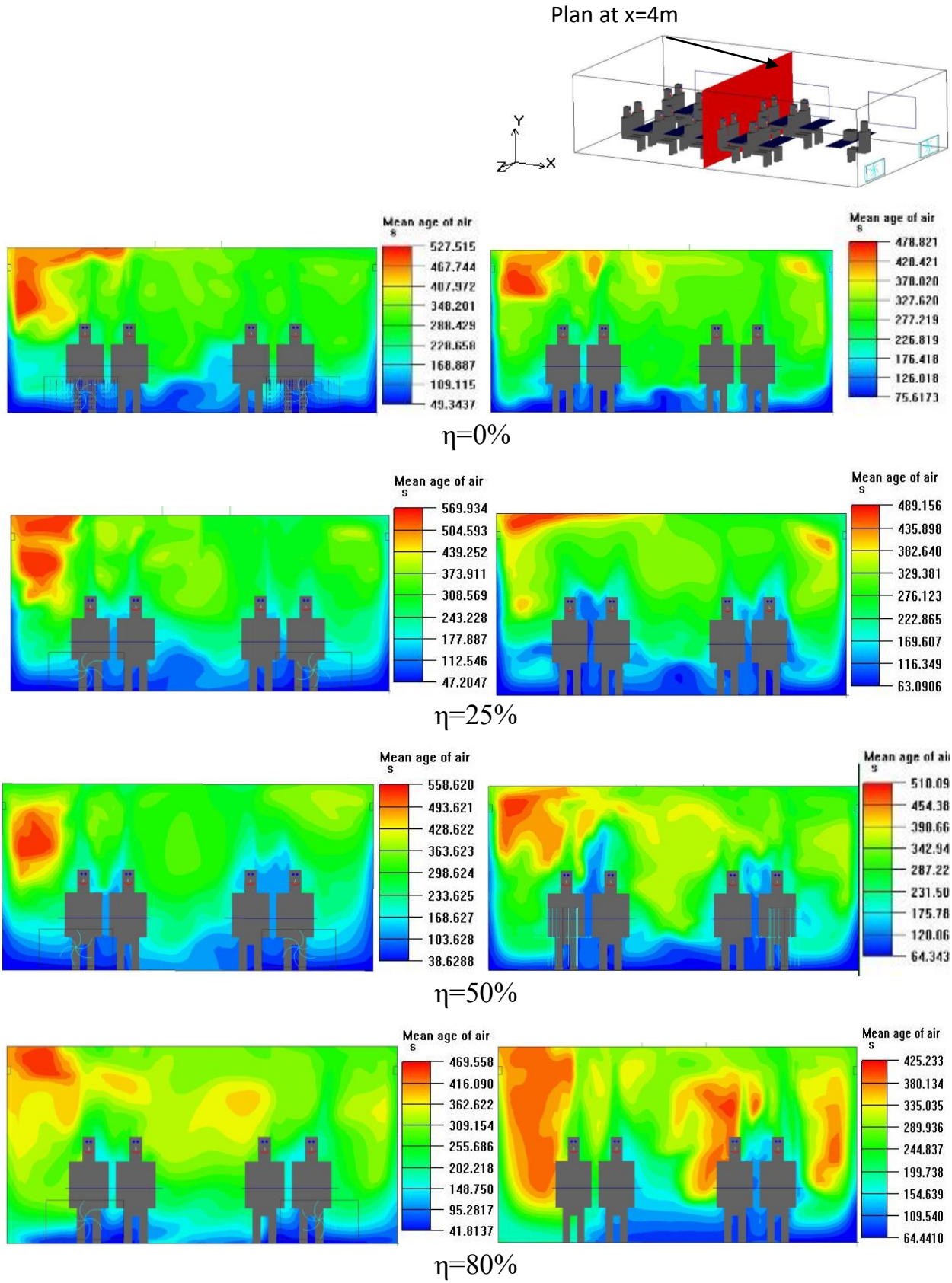

Fig.(5-77) Age of air contours at plane (x=4 m) for different (η), cases-V and VI

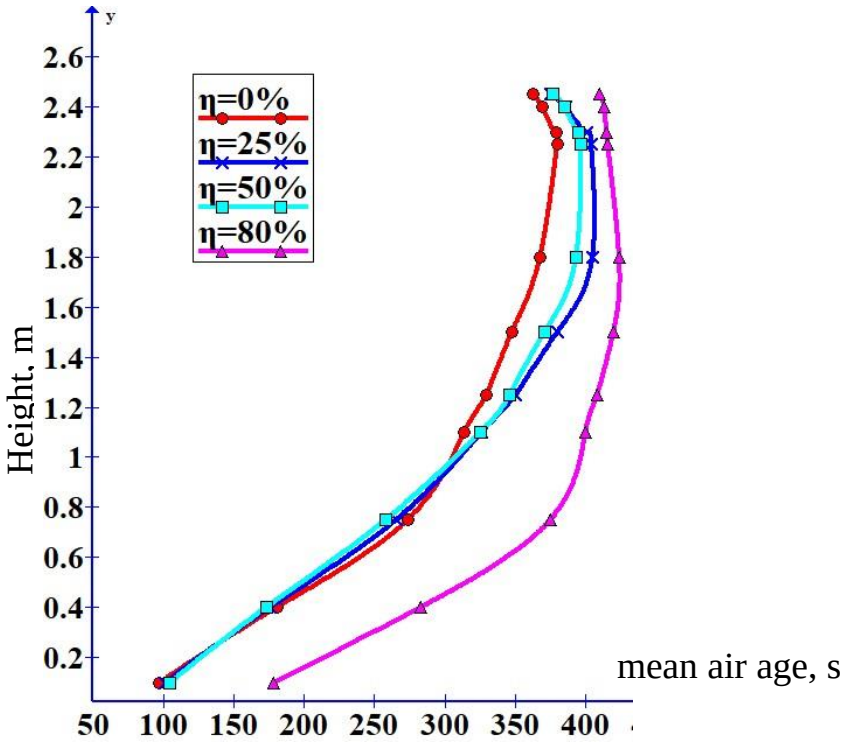

a-case-V

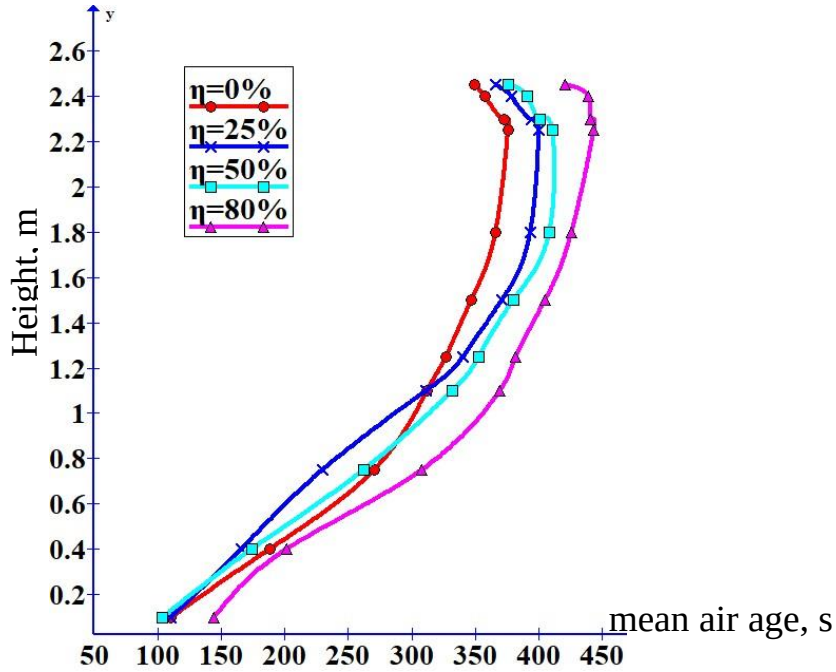

b-case-VI

Fig.(5-78) Mean air age profiles with height level for the two cases at different (η)

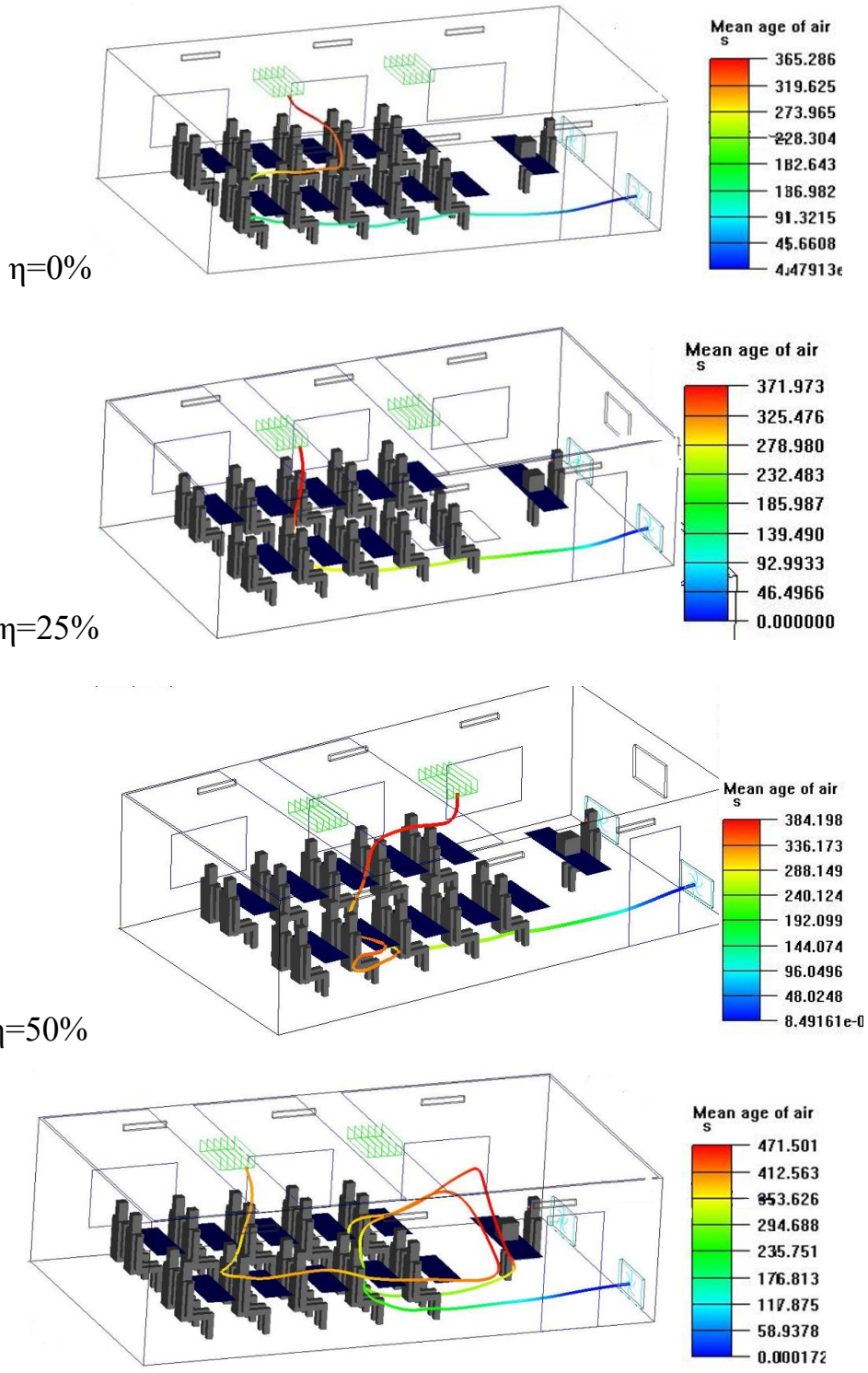

Fig.(5-79) Air particle trace from the inlet to the outlet air for case-V at different (η)

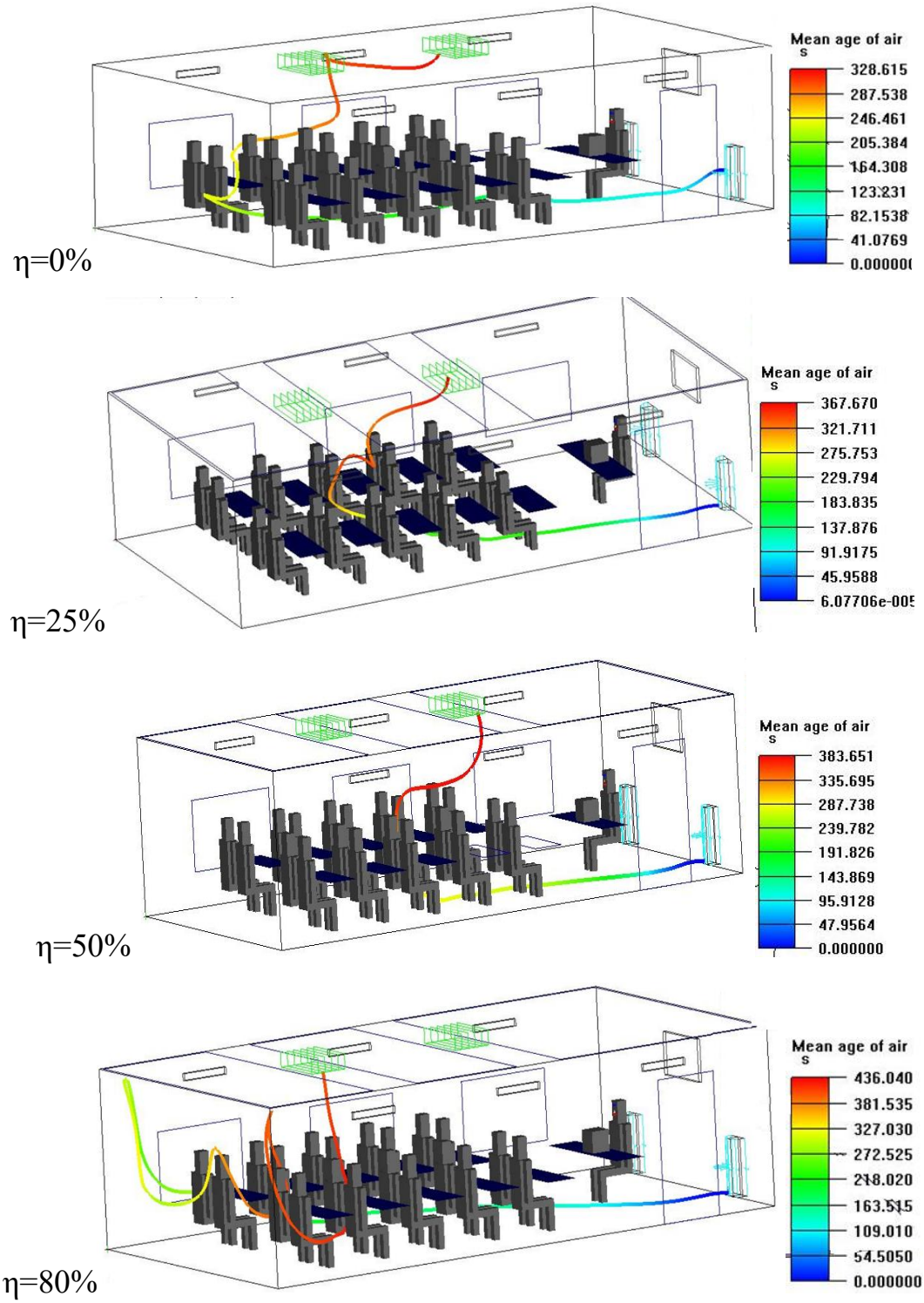

Fig.(5-80) Air particle trace from the inlet to the outlet air for case-VI at different (η)

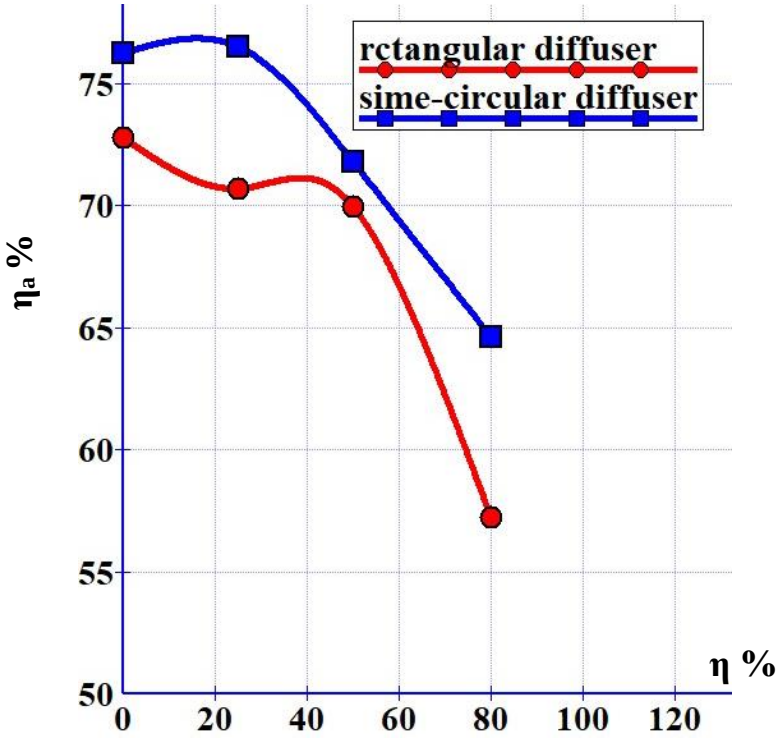

Fig.(5-81) Air exchange efficiency for the two cases at different (η)

5.4.2 Air Temperature and velocity distribution

Figs.(5-82) and (5-83) show the average air temperature distribution with height level at different (η) for case-V (with rectangular diffuser) and case-VI (with semi-circular diffuser) respectively. The air temperature increases with room height and being decrease near the chilled ceiling surface. In the test without chilled ceiling (η=0) (for the two cases) the temperature continues increase after (2 m) height, while with using it the air temperature above (2 m) decreases due to convection with chilled ceiling surface.

For the two cases, the temperature stratification decrease with increase (η) due to effect of low temperature of chilled ceiling surface causes decreasing in air temperature at upper zone and falls down. This is due to increase air density that leads to decrease in air temperature located in the lower layers.

The increase of air temperature near the chilled ceiling surface by convection as shown above causes some cold air to escape outside the classroom due to the location of exhausted grill near the ceil. The temperature of cold air which escape outside decreases with increase (η). This phenomenon caused a decrease in air temperature distribution effectiveness (ε_t) with increase (η) (with decrease chilled ceiling surface temperature) as shown in Fig.(5-84).

Fig.(5-84) shows air temperature distribution effectiveness for the two cases at different (η). The air temperature distribution effectiveness decreases by (0.13) and (0.08) with rectangular and semi-circular diffusers respectively at (η=0-80%).

The air temperature distribution effectiveness with semi-circular diffuser is higher by average (0.035) as compared with rectangular diffuser at (η) between (25%-80%). While without chilled ceiling (η=0), can be noted no different in temperature distribution effectiveness between the two types of supply diffuser. This is due to the high cooling load for classroom and the warmer air in the upper zone, leads to reduce the effect diffuser shape.

Fig.(5-85) shows the relation of average air temperature difference between head to foot for a seated student ($\Delta T_{hf,}$) with (η) for the two cases. The (ΔT_{hf}) decreases with increase (η) for the two cases. The decrease in air temperature gradient with (η) as shown above lead to decrease in temperature different between head to foot of a seated by 1.8^{o}C with rectangular diffuser and (1.78^{o}C) with semi-circular diffuser between (η=0-80%). ASHRAE Standard found that the value of temperature difference between foot and head for a seated person about (2^{o}C). While the (ΔT_{hf}) in the two cases at (η=50-80%) is less than (1^{o}C) due to effect of chilled ceiling in canceling the indoor air stratified layers. This value doesn't achieve the value specified by AHREA standard.

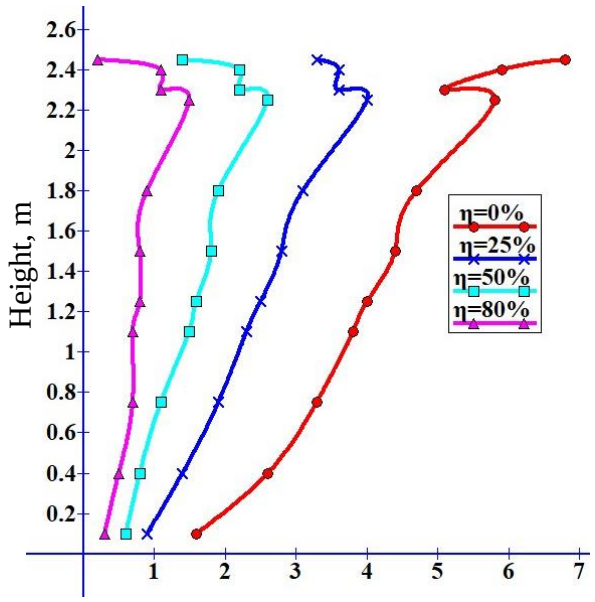

Fig.(5-82) Temperature gradient with height at different (η) for case-V

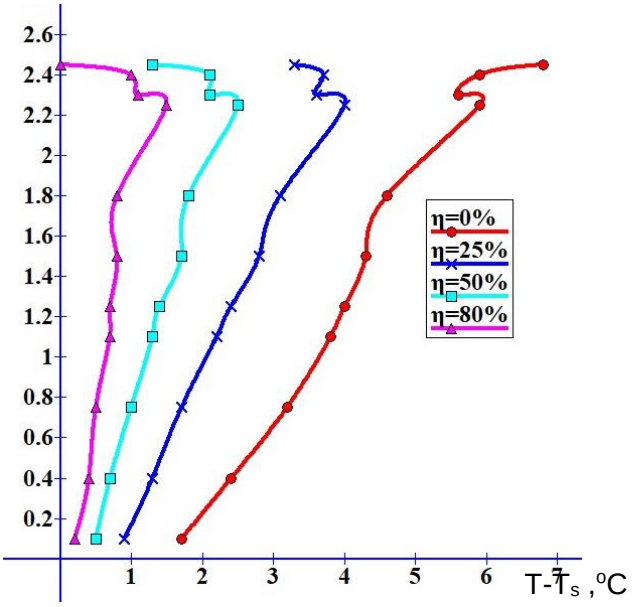

Fig.(5-83) Temperature gradient with height at different (η) for case-VI

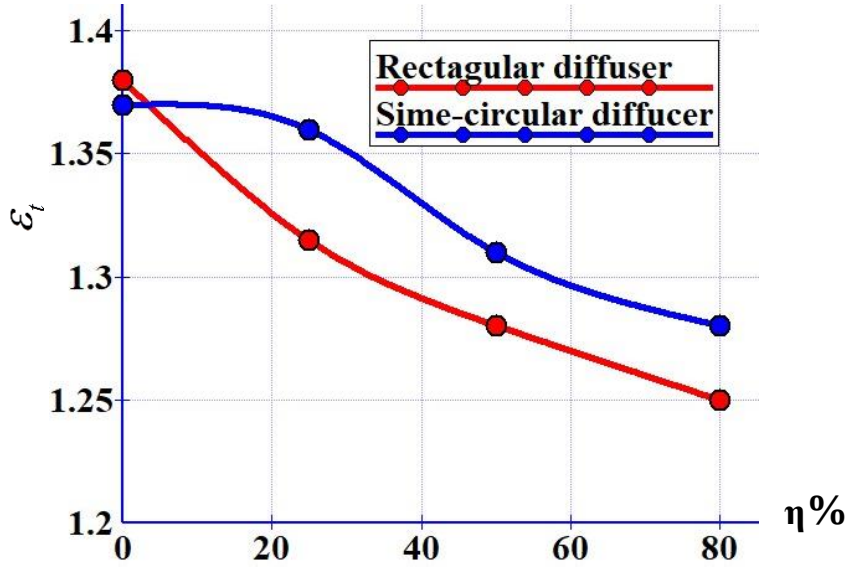

Fig.(5-84) Temperature distribution effectiveness for the two cases at different (η)

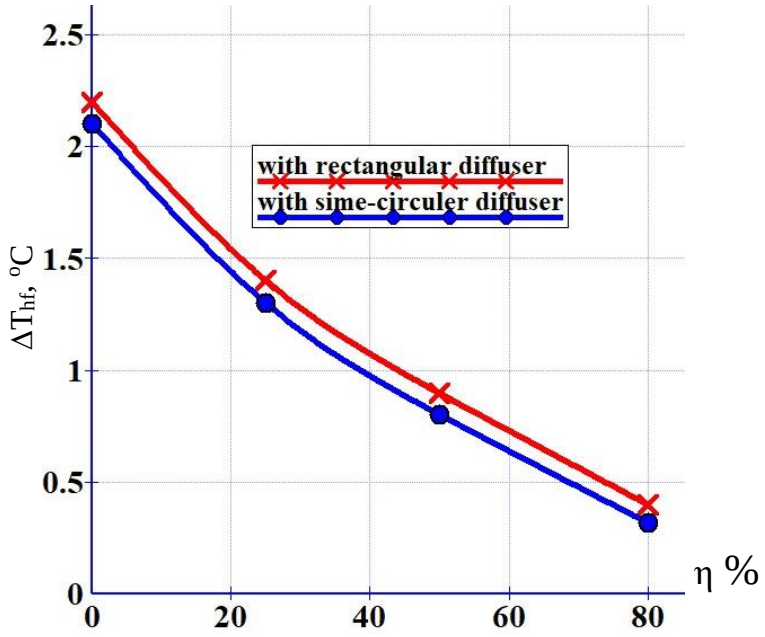

Fig.(5-85) ΔT_{hf} variation at different (η) for the two cases

Fig.(5-86) shows air temperature distribution contours for the two cases (case-V and VI) with different (η) at plane (z=1.1). The supply air temperature behavior same as shown in office room contours (Fig.5-33). The striking difference in the air temperature distribution contours is that the column of warm air appears more clearly over the students, especially when (η=0% and 25%), while at (η =50% and 80%) disappears because the cold air falling from the upper zone due to the low chilled ceiling temperature. The temperature stratification decreases with increasing value of (η) until it becomes unnoticeable at (η=80%).

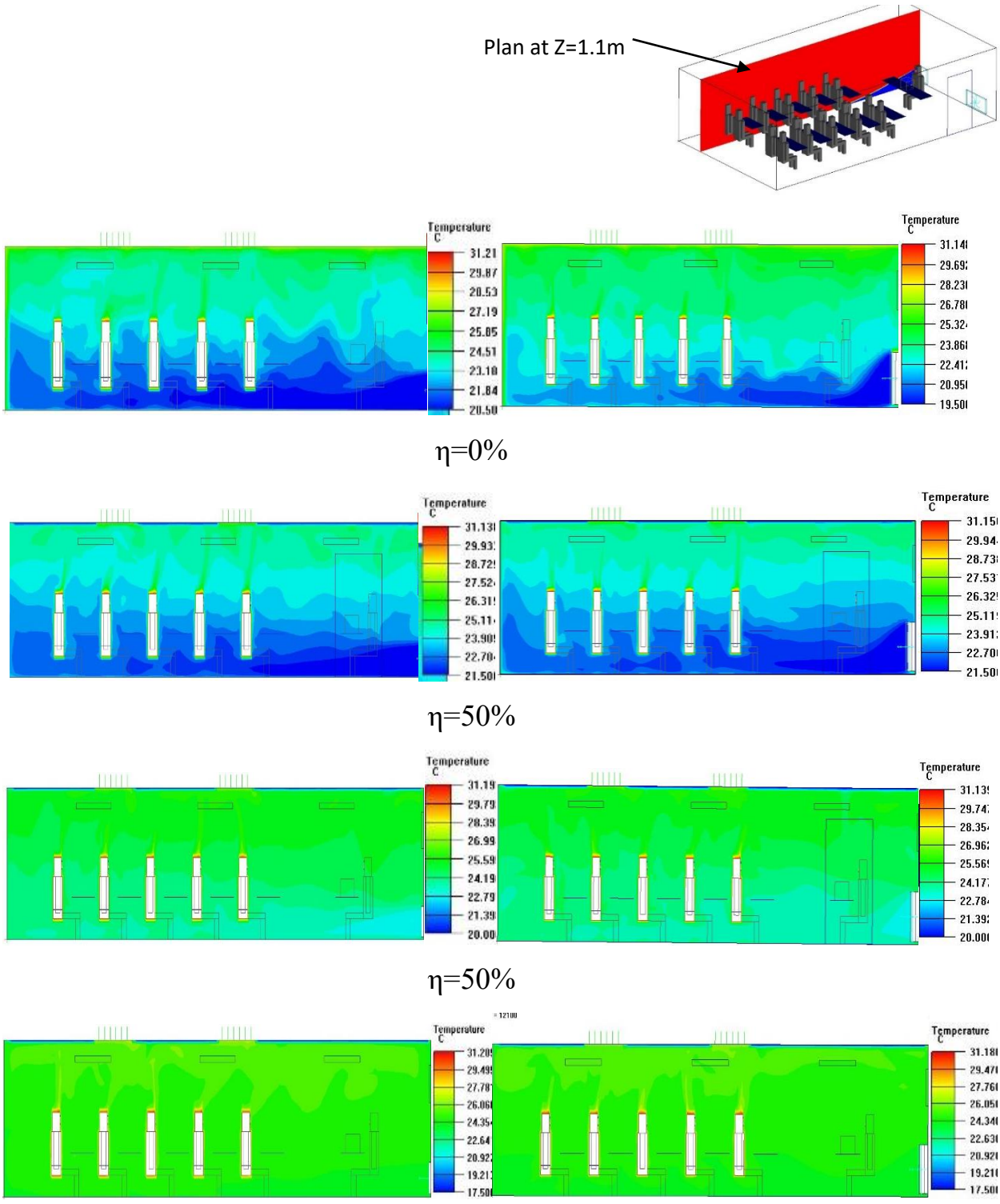

Fig.(5-86) Air temperature distribution contours at different (η) for the two cases at plane z=1.1m

Figs.(5-87) and (5-88) show the change in mean air velocity distribution with height at different value of (η) for (case-V an VI) respectively. The air velocity near the floor (ay=0.1 m) reduces with increase (η) due to the increase in air supply temperature and buoyancy force. This makes the air tends to rise up and decrease in air momentum near floor. In general, the air velocity reduces with height and at level (1.2 m) the velocity being increase due to the increase in air temperature as a result of heat sources effect. The air velocity continue in increase and the maximum value of it near of ceil at (η=80%). This because the zone has a high heat transfer between air and chilled ceiling by convection, in addition to the effects of exhaust grille which located at the ceil.

The comparison between air velocity distribution in the two cases is shown in Fig.(5-89) which indicated that the air velocity near floor was higher with rectangular diffuser as compared with semi-circular diffuser at each value of (η) due to deference in air distribution between two types of supply diffuser as shown above. In general, the difference in average air velocity between two diffusers types unnoticed due to low air supply in displacement ventilation.

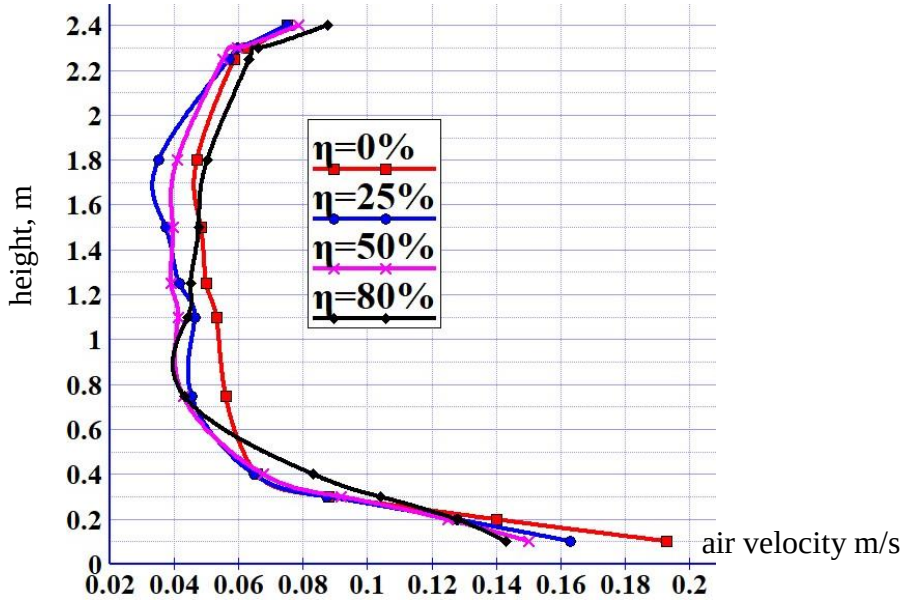

Fig.(5-87) Mean air velocity distribution with height for different (η), case-V

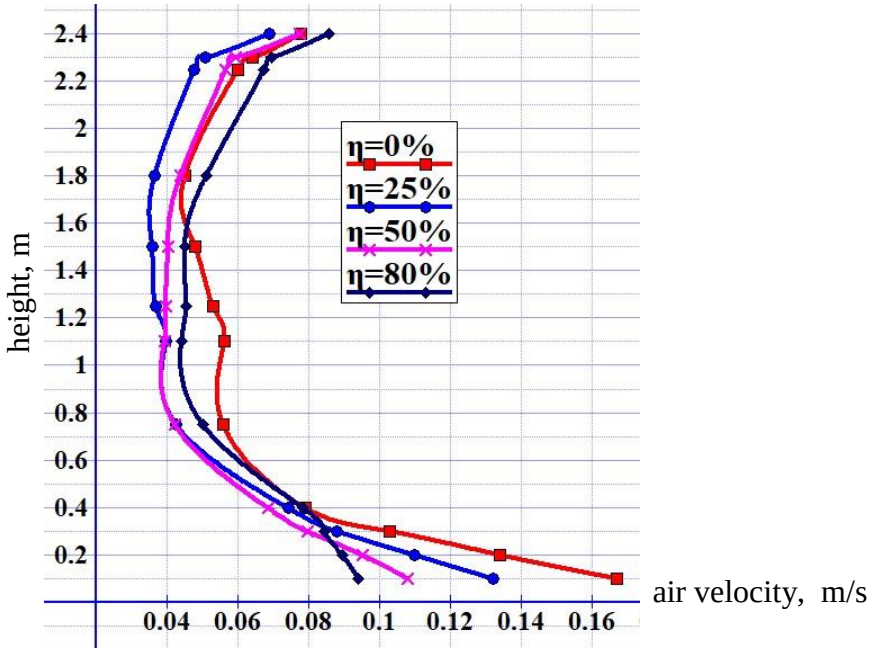

Fig.(5-88) Mean air velocity distribution with height for different (η), case-VI

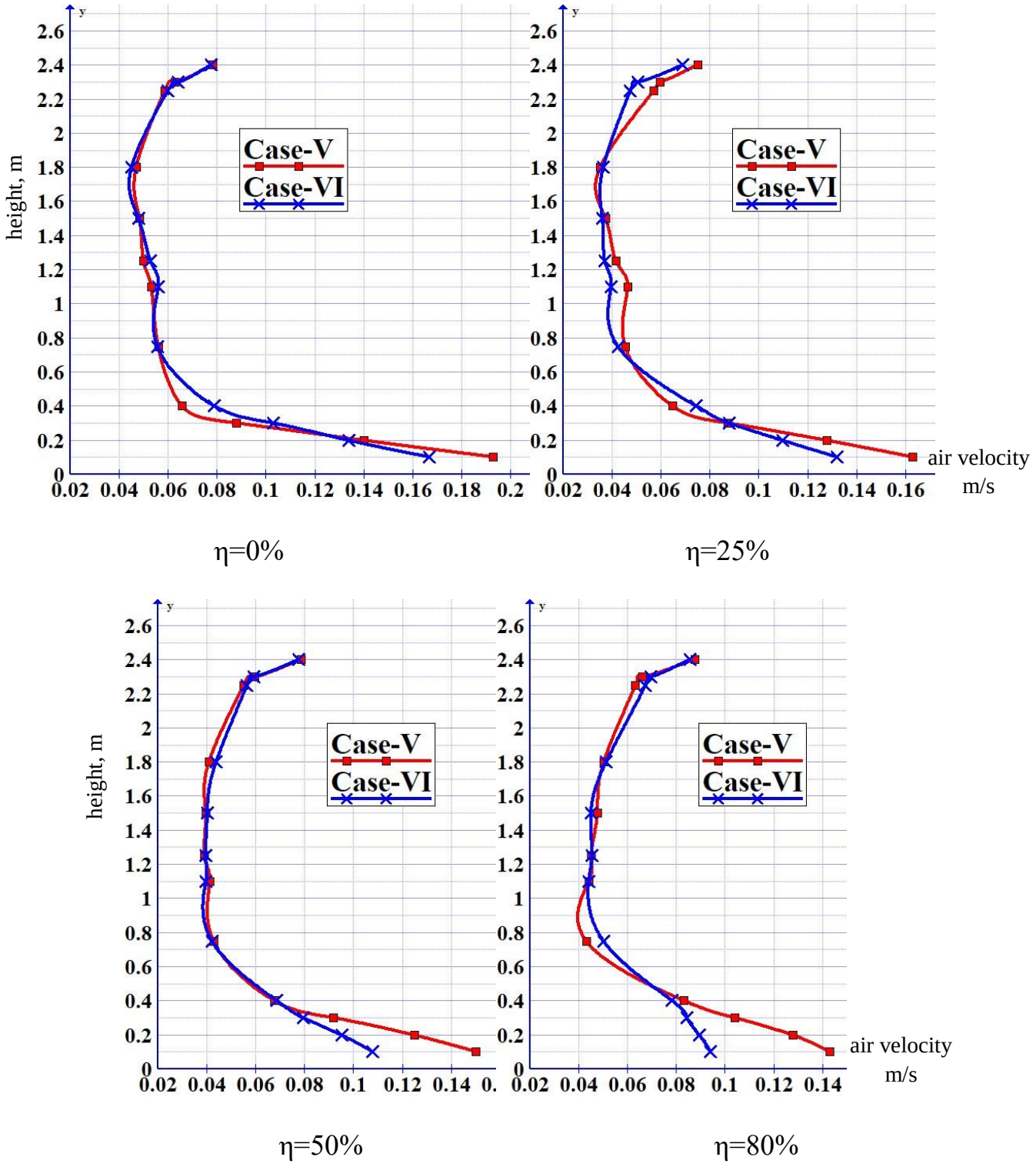

Fig.(5-89) Mean air velocity with height comparison between the two cases at different values of (η).

5.4.3 Thermal comfort and air quality results

In this section, three parameters are studied to give a good idea about thermal comfort in occupied zone for classroom. It's (PMV), (PPD) and (ADPI). The results for these parameters compared with ASHRA standard (2013).

Figs.(5-90) and (5-91) show the profiles of average (PMV) and (PPD) respectively with increase (η) for the two cases. The (PMV) and (PPD) values for the two cases decrease and improve with increase value of (η). It's more converge to values which specified by ASHRAE standard, 2013 (-0.5≤ PMV ≤ 0.5 and PPD ≤10%). As value of (η) increase from (0% to 80%) the (PMV) with rectangular diffuser decrease from (0.815 to 0.69) and (PPD) decreases from (19.5% to 17%) respectively. While, with semi-circular diffuser the (PMV) decreases from (0.75 to 0.62) and (PPD) decrease from (19.1% to 16.7%) as (η) increases from (0% to 80%) respectively. This is due to the increase (η) (decrease chilled ceiling surface temperature) leads to lowering air temperature in the upper zone, which allows for an increase heat transfer with heat sources by convection, thus improve (PMV and PPD). These results mean the increase in (η) leads to improve thermal comfort level ,but in the same time these values don't achieves the range specified by AHREA standard (-0.5≤ PMV ≤ 0.5 and PPD≤10%). Its approach the slightly warm weather (according to Fig.(1-8)) due to high mean radian temperature (MRT) as shown in Table(5-7). The values of (PMV) and (PPD) with semi-circular diffuser is less than their values with rectangular diffuser due to the uniform air temperature and velocity, which gives an indication of the preference to the semi-circular diffuser.

To explain more effects of chilled ceiling on the comfort level under Hilla (Iraq) climate. Fig.(5-92) shows the (PMV) distribution contours plane at breathing level for seating students (y=1.1 m) with different (η) for the two cases. This plane presents the breathing zone level. For each cases, and at different value of (η), the value of (PMV) near the windows is between (1 to 3). These are large values due to

heat transfer by conduction and radiation through window from hot outside climate in Hilla (Iraq) summer. This results lead to discomfort for occupants that sitting near the windows. According to the ASHRAE standard (2010), the occupied zone was (0.5-1.5 m) away from wall with windows. Then the chilled ceiling doesn't have any change to the range which is specified by ASHRAE standard. The (PMV) value in another indoor zones for the two cases is between (0.3 to 1). This means that the weather in this level is between natural and slightly warm. This range decreases with increase value of (η) for the same reason discussed above.

(ADPI) is another factor used as a parameter to predict the air circulation system of the indoor. The increase in the percentage of this factor gives a good indication of occupants comfort.

Fig.(5-93) shows the relation between (ADPI) and (η) for (cases-V and VI). The (ADPI) increases with increase value of (η) for the same reason discussed in office room (Fig.(5-73)). Its reach up to (75%) for each cases at (η=80%) and converges from design goal which specified by ASHRAE standard. While at (η) from (0% to 50%) it ranges from (50% to 60%). This means that the increase in (η) gives more equilibrium between air temperature and velocity with provide a good thermal comfort to the occupants. If it is compared between two types of the diffuser, no difference in (ADPI) (less than 1%) at (η=80%) can be noted. This is due to the high cooling load and increases in air temperature supply to approach room design temperature (25oC). In addition to the decrease in chilled ceiling surface temperature which gives more effect than supply diffuser to make a balance between indoor air temperature and velocity.

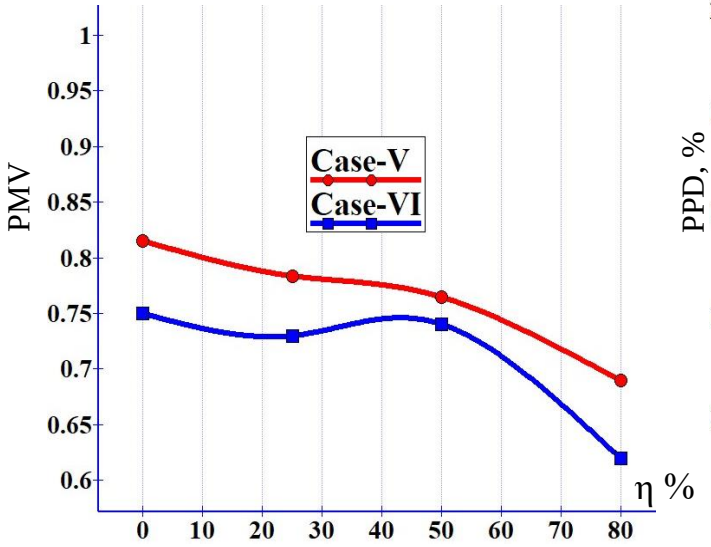

Fig.(5-90) PMV profile at different (η), cases-V and VI

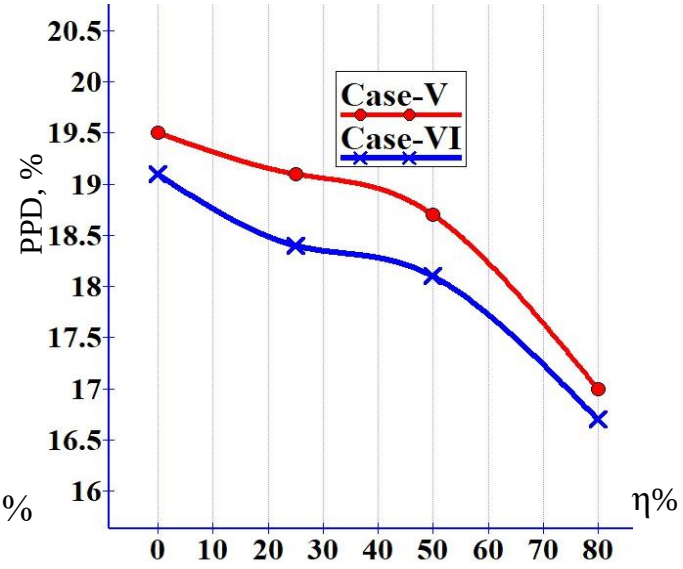

Fig.(5-91) PPD profile at different (η), cases-V and VI

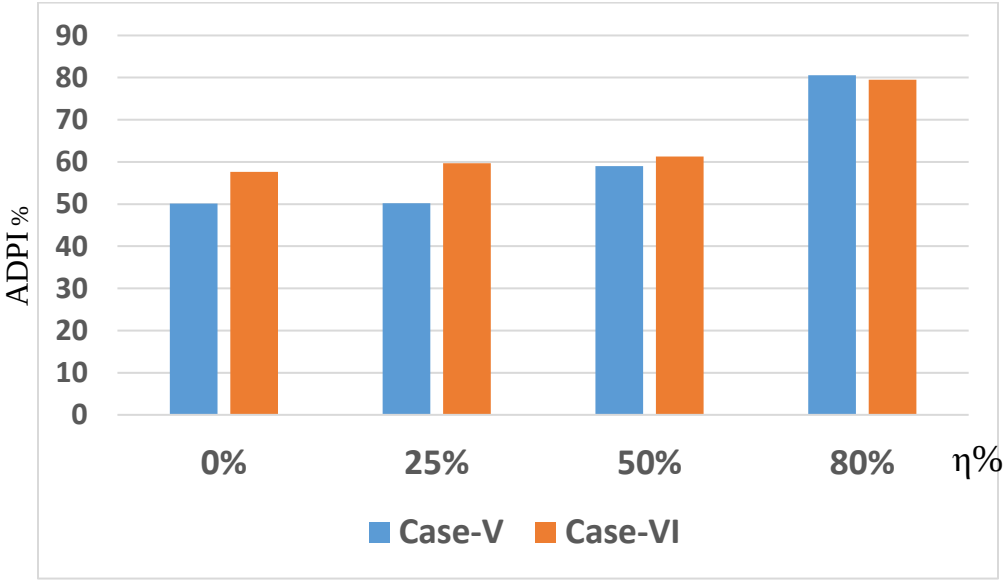

Fig.(5-92) ADPI profile at different (η), cases-V and VI

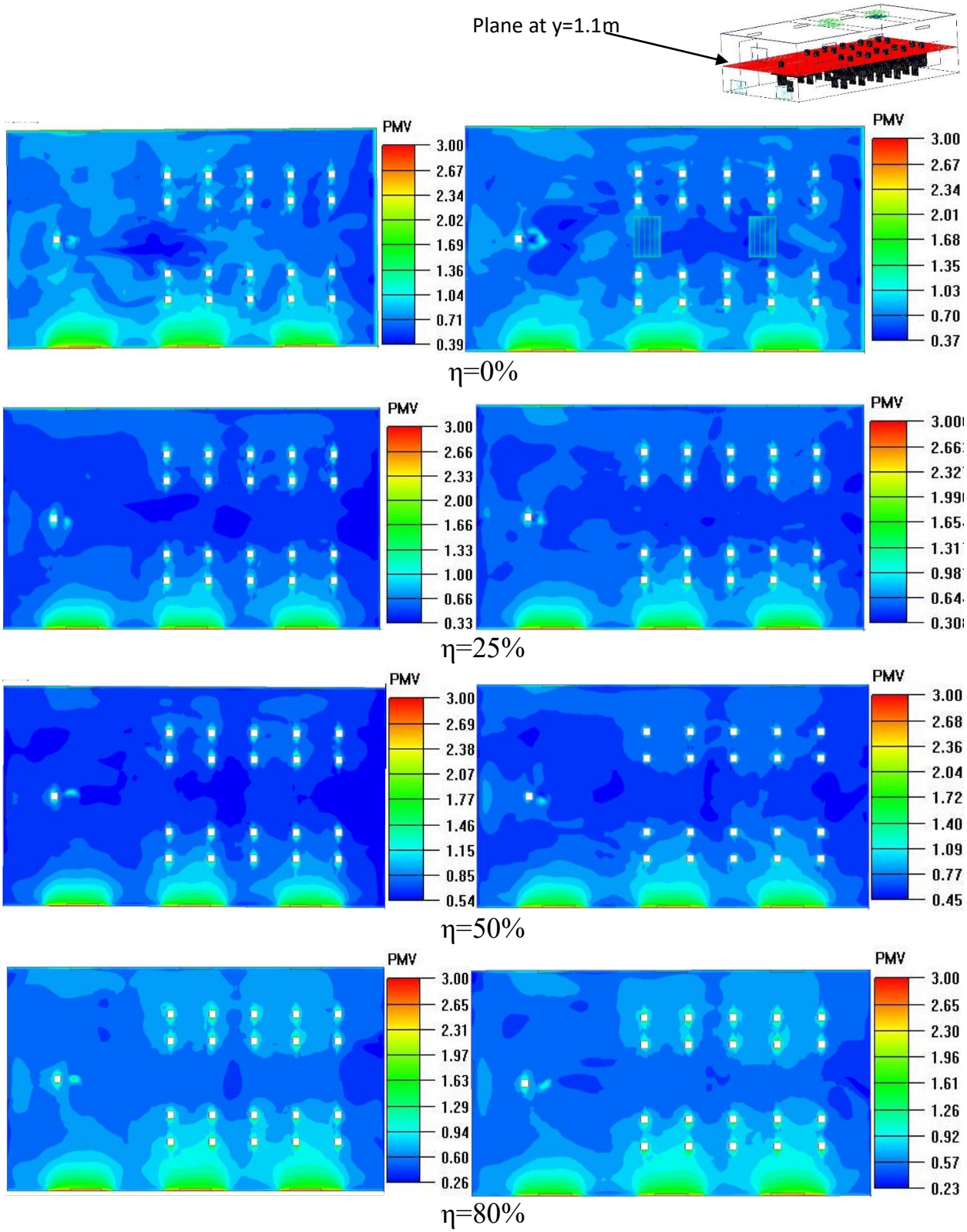

a- Case-V b-Case-VI

Fig.(5-93) PMV contours at plane (y=1.1 m) with different (η) for the two cases

Figs.(5-94) and (5-95) show the carbon dioxide decay with time starting from (1000ppm) to supply air concentration (400ppm) for case-V (rectangular diffuser) and case-VI (semi-circular diffuser) respectively at different (η).

For both cases, the CO_2 concentration decreases with time until reaches supply air concentration. The results show that the increase of the load treated by chilled ceiling at constant air supply flowrate has a slight effect on the carbon dioxide removal. This is due to the high fresh air supply flowrate (300L/s, 635.6cfm) as a result of high cooling load, leads to escape the old air from exhausted grills faster, and reduce chilled ceiling effect.

The CO_2 concentration takes about (2300 sec) at (η=0%) and about (2400 sec) at (η=80%) with a rectangular diffuser while with a semi-circular diffuser it takes about (2200 sec) at (η=0%) and about (2300) at (η=80%) to reach (400 ppm). If compared between the two types of diffuser, it can be found that the semi-circular diffuser is faster to remove carbon dioxide by about (100 sec) at constant air flow rate supply and this value doesn’t effected by air supply temperature.

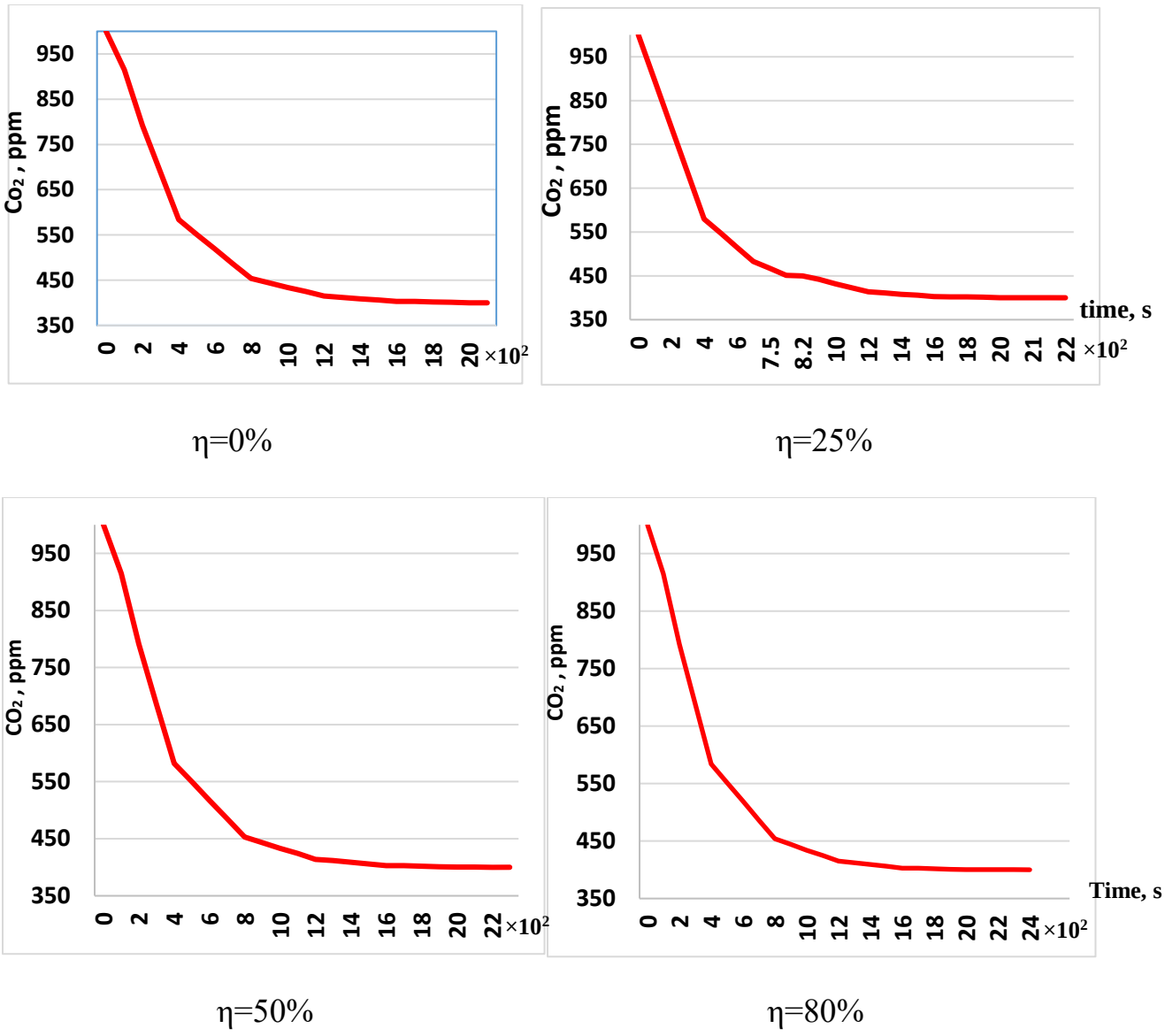

Fig.(5-94) Time required to remove carbon dioxide at different (η) and constant supply air flow rate, case-V.

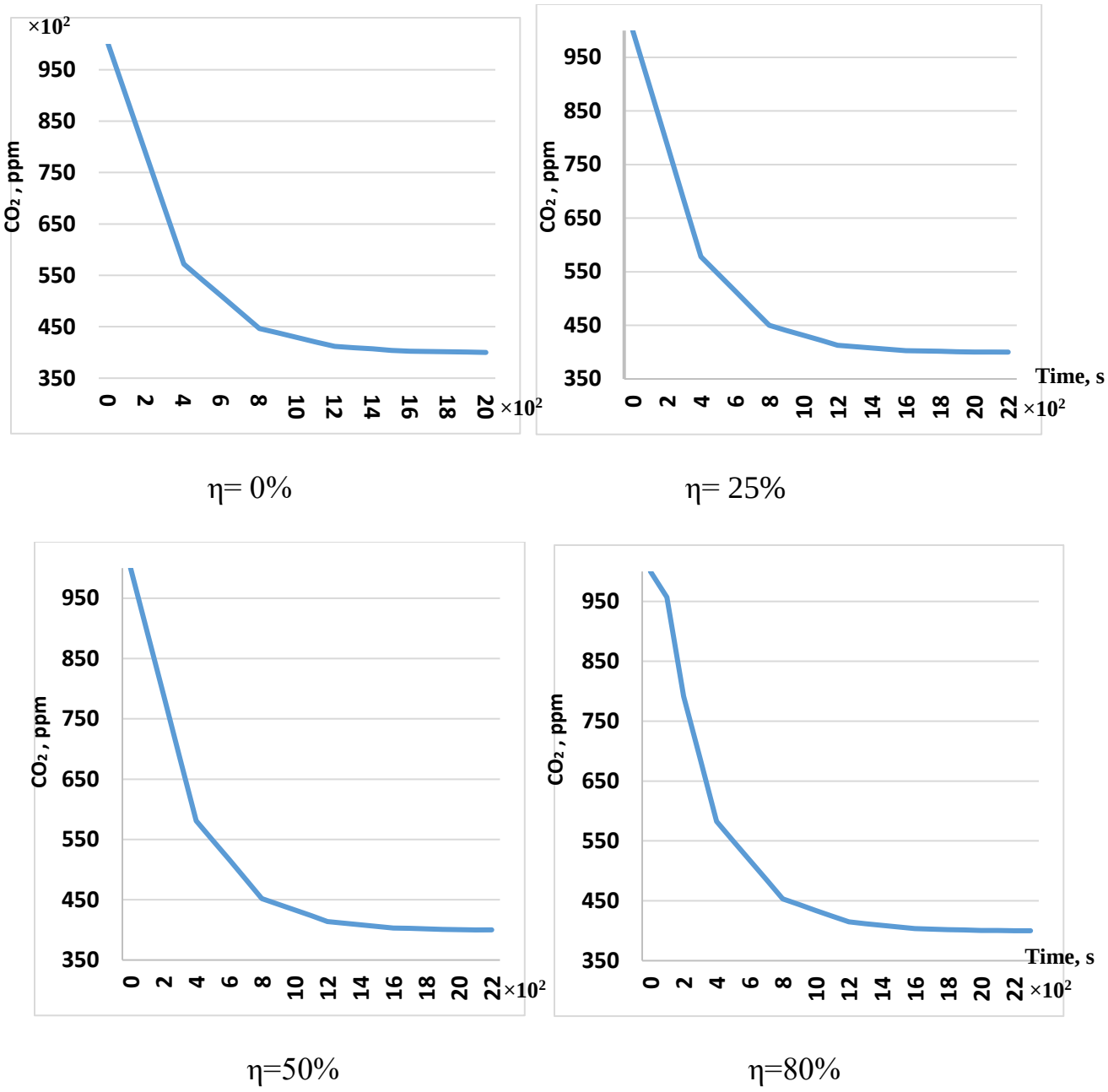

Fig.(5-95) Time required to remove carbon dioxide at different (η) and constant supply air flow rate, case-VI.

Figs.(5-96) and (5-97) show the thermal comfort conditions by using (CBE) tool for cases with rectangular and semi-circular diffusers respectively at different (η). By observing the location of the red circular point respect to thermal comfort zone (blue color zone), the thermal comfort was achieved with rectangular and semi-circular diffuser. The air conditions with semi-circular diffuser are more converge to the comfort zone compared with rectangular diffuser (the red point at the edge of the comfort zone). These results give advantage to the semi-circular diffuser.

The comparison between the results found by (CBE) tool for non-insulated office room cases (as shown in Figs.(5-74a) and (5-75a)) and classroom cases, indicates that the (DV/CC) system gives more thermal comfort conditions when used with classroom compared with non-insulated office room especially with semi-circular diffuser. This is because the mean radiant temperature (MRT) and indoor average temperature satisfied a good balance in non-insulated classroom due to large space and high air supply flowrate.

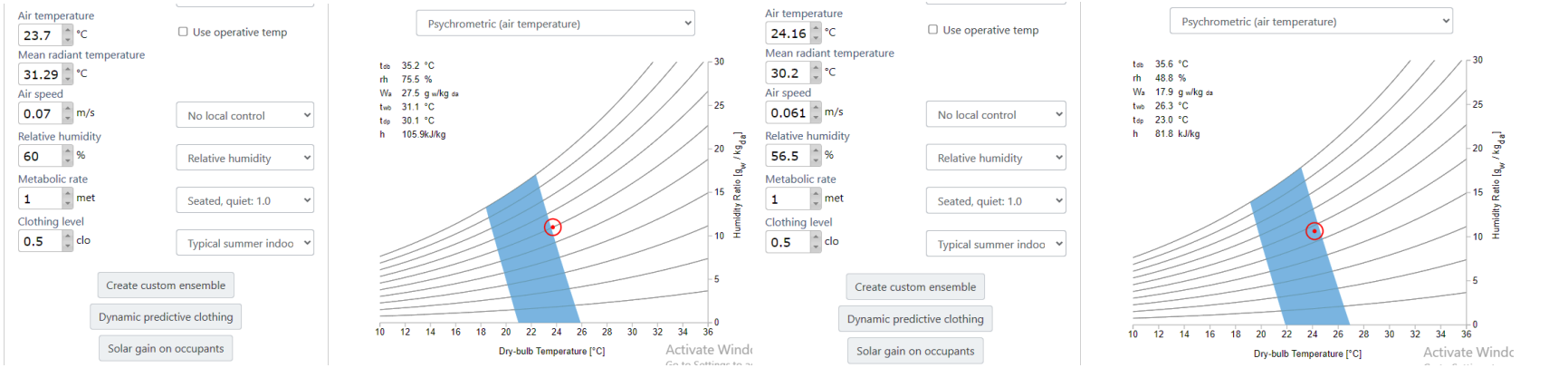

η=0% η=25%

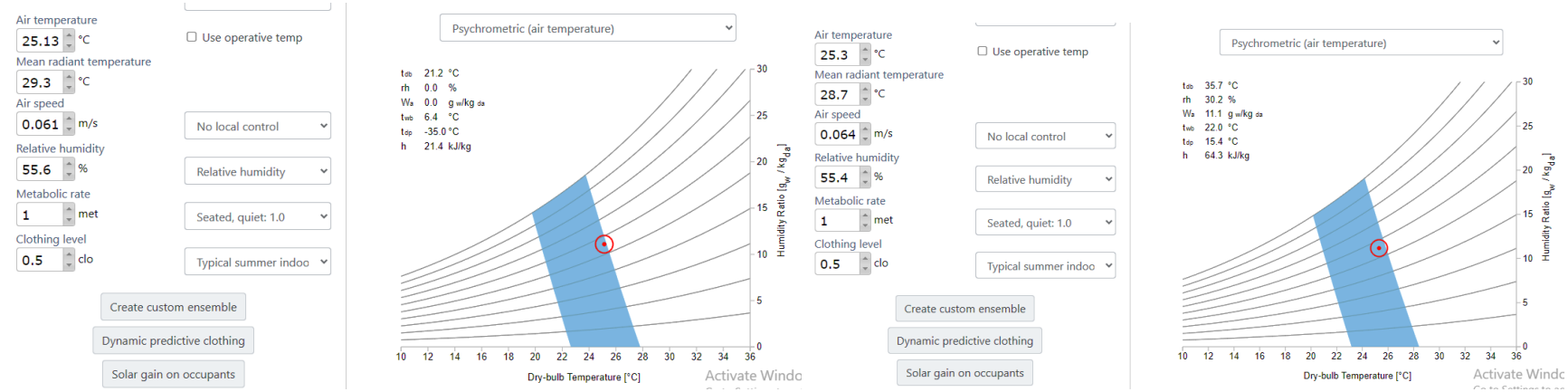

η=50% η=80%

Fig.(5-96) Thermal comfort conditions by using CBE tool for Case-V at different (η).

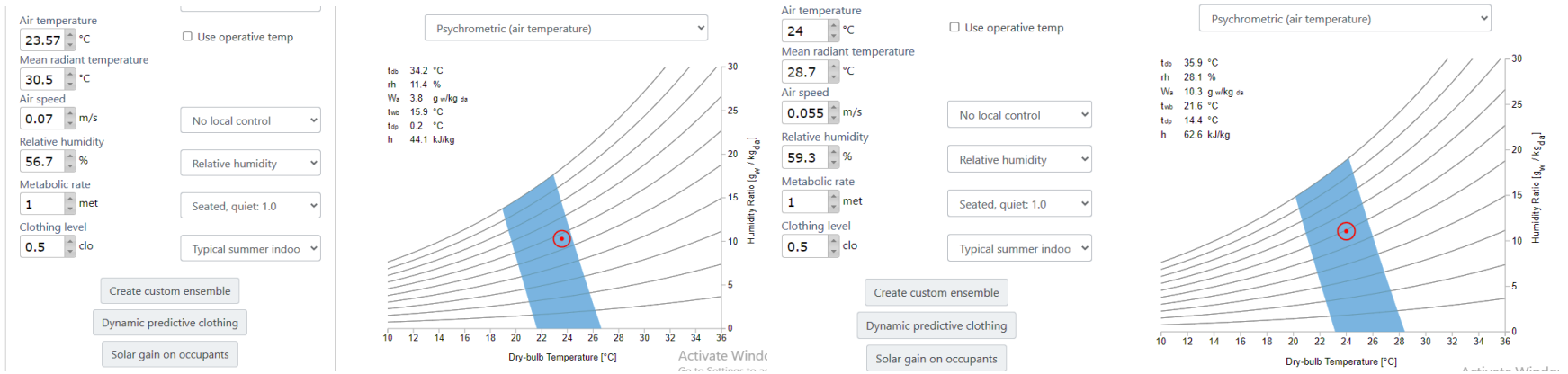

η=0% η=25%

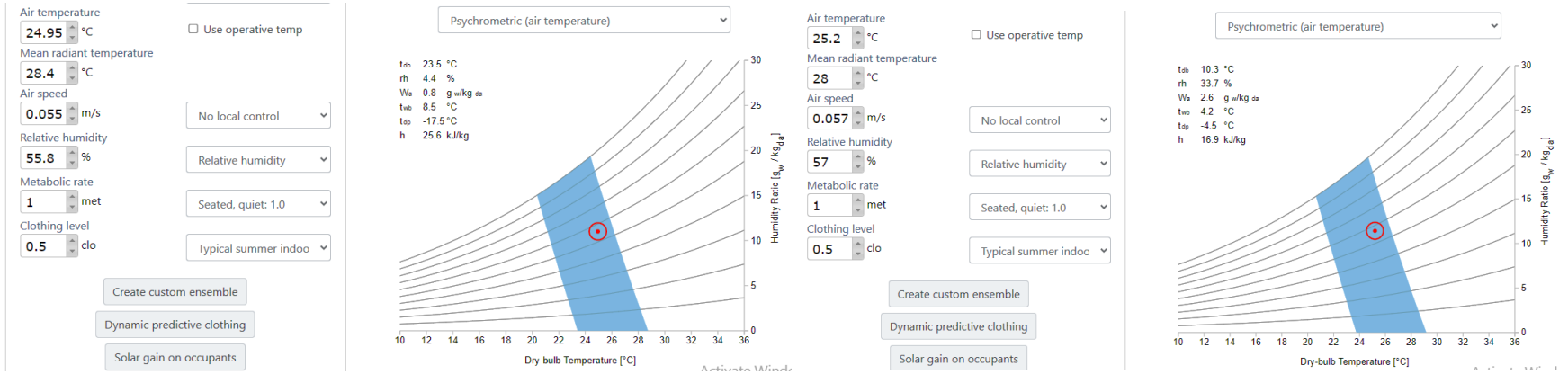

η=0% η=25%

Fig.(5-97) Thermal comfort conditions by using CBE tool for Case-VI at different (η)

CHAPTER SIX

CONCLUSIONS
&
SUGGESTIONS FOR FUTURE WORKS

Chapter Six

Conclusions and Suggestions for Future Work

6-1 Conclusions

The main conclusions can be summarized as follows:

6.1.1 General conclusions

1- The local air age increases with height regardless of the shape of the diffuser and value of cooling load treated by chilled ceiling.

2- The semi-circle diffuser gives advantages in reduce air age compared with rectangular diffuser. The effect of the diffuser shape on the air age is not noticeable in the upper zone of the room (over 1.8 m height).

3- The local air age increases with increase cooling load treated by chilled ceiling with rectangular or semicircle diffuser. The zone among the heat sources has a minimum value of air age due to high air velocity in this zone. The effect of the diffuser shape on the air age is not noticeable in the upper zone of the room (over 1.8 m height).

4- The temperature difference between head and foot for a seated person decreases with increase portion of cooling load treated by the chilled ceiling and it's directly proportional with chilled ceiling temperature.

5- The temperature distribution effectiveness decreases with increase portion of cooling load treated by the chilled ceiling and semicircular diffuser gives better effectiveness as compared with the rectangular diffuser.

6- CO_2 concentration in (CC/DV) system increases with height but this difference fading with increase portion of cooling load treat by the chilled ceiling. The CO_2 removed by using semi-circle diffuser was better compared with rectangular diffuser by about (25 sec) at any value of (η).

7- Semi-circle diffuser tends to improve (PMV), (PPD) and (ADPI) and gives a better thermal comfort than a rectangular diffuser when using with (CC/DV)

system and their values converge from standard values specified by (AHRAE-2013) with increase value of cooling load portion treated by chilled ceiling.

6.1.2 Insulated and non-insulated office room

1. The (CC/DV) system achieves thermal comfort conditions in insulated space, while in non- insulated space the thermal comfort depends on the mean radiant temperature as a main parameter. (PMV), (PPD) and (ADPI) in insulated room were more convergent from values specified by ASHREA-2013.
2. At breathing zoon, the air age in non-insulated office room was more than by about (100 sec), with semi-circular diffuser. While it is about (200 sec) with rectangular diffuser.
3. Average air exchange efficiency in insulated room was more by (3%) compared with insulated room with rectangular diffuser. While with semi-circular diffuser it was (2.6%).
4. Average air temperature effectiveness was best in insulated room by about (4.5%) with rectangular diffuser. While it was about (6%) with semi-circular diffuser.
5. The temperature difference between head and foot raised by (1.5^{o}C) with rectangular diffuser and (1^{o}C) with semicircle diffuser in non-insulated room compared with insulated room.

6.1.3 Non-insulated office room and classroom

1. The semi-circle diffuser gave advantage to reduce air age by about (10%) in classroom and about (6%) in office room compared with rectangular diffuser.
2. Semicircular diffuser gave better temperature distribution effectiveness by about (8%) in non-insulated office room, and (2.5%) with classroom compared with the rectangular diffuser.

3. For two offices, the chilled ceiling didn't effect on the occupied zone dimensions which specified by ASHREA-55, 2010.
4. The more balance between classroom average air temperature and mean radiant temperature gave more thermal comfort compared with office room, especially with semi-circular diffuser.

6.2 **Suggestions for Future Works**

To develop the current study, future works are recommended as follows:

1- Studying the efficiency and effectiveness of displacement ventilation in combined with chilled ceiling (DV/CC) system in a large halls such as commercial centers, theaters and cinemas under hot and dry climates.
2- Studying and analyzing the air flow distribution below chilled ceiling (thin layer). The analysis of air flow distribution is an important topic to predicting the thermal comfort in occupied zoon. The flow near chilled ceiling is unstable and it was affected greatly by internal and external heat sources. So, experimental or numerical study of air flow distribution field should considered in future studies.
3- Study another shape of air supply diffuser such as (circular diffuser and corner diffuser) and analyses its effect on thermal comfort parameters by using (CC/DV) system.
4- Calculating the optimal density for occupancy to reducing energy consumption in a hot and dry climate by adopting any type of ventilation devices in combined with chilled ceiling system.

REFRENCES

References

[1] Janssen, J. E.. The history of ventilation and temperature control: The first century of air conditioning. Ashrae Journal, 41(10), PP:47-52. (1999)

[2] Schulze, F., Gao, X., Virzonis, D., Damiati, S., Schneider, M. R., & Kodzius, R.. Air quality effects on human health and approaches for its assessment through microfluidic chips. Genes, 8(10), 244.PP:2-26. (2017)

[3] Awbi H. Ventilation of buildings. London: Taylor and Francis, first edition. (2003)

[4] Chen, H. Experimental and numerical investigations of a ventilation strategy–impinging jet ventilation for an office environment (Doctoral dissertation, Linköping University Electronic Press). (2014)

[5] Turiel, I.. Indoor air quality and human health. First edition, Routledge. (1985)

[6] Rees, S. J., & Haves, P.. An experimental study of air flow and temperature distribution in a room with displacement ventilation and a chilled ceiling. Building and Environment, 59, PP:358-368. (2013)

[7] Haghighat, F. Thermal comfort in housing and thermal environments. Sustainable built envrionment-Voll. (2009)

[8] Awbi, H. B.. Ventilation of buildings. Taylor & Francis. Second edition. (2008)

[9] Titus, the leader in air management, “displacement ventilation, application guide”, www.titus-energysolutions.com, (2008).

[10] Hashimoto, Y.. Numerical study on airflow in an office room with a displacement ventilation system. In Building Simulation (Vol. 1) PP:381-388. (2005).

[11] Cho, Y. Awbi H. B. & Karimipanah, T.. Theoretical and experimental investigation of wall confluent jets ventilation and comparison with wall displacement ventilation. Building and Environment, 43(6),PP:1091-1100. (2008)

[12] Aye, L., & Fuller, R. J. . The Ventilation System in the CH2 Building - Meeting Occupant Needs, paper, The University of Melbourne, Victoria, Australia. (2010)

[13] Kobayashi, N., & Chen, Q. Floor-supply displacement ventilation in a small office. Indoor and Built Environment, 12(4), PP:281-291. (2003).

[14] Skistad, H., Mundt, E., Nielsen, P. V., Hagström, K., & Railio, J. Displacement ventilation in non-industrial premises. American Society of Heating, (2002).

[15] Price engineer's HVAC Handbook. Engineering guide displacement ventilation. www.price-hvac.com; (2014).

[16] Hamilton K, Watkins D. Evidence-Based design for multiple building types. 1st Edition; (2009).

[17] Roth K. Westphalen D., Dieckmann J. Goetzler W. Energy consumption characteristics of commercial building HVAC Systems. Energy Savings Potential. Volume III; (2002).

[18] Waterloo Air Products plc. An introduction to chilled beams and ceilings. Version 1. (2012).

[19] Karmann, C., Bauman, F., Raftery, P., Schiavon, S., & Koupriyanov, M. Effect of acoustical clouds coverage and air movement on radiant chilled ceiling cooling capacity. Energy and Buildings, 158, PP:939-949. (2018).

[20] Stetiu, C. Energy and peak power savings potential of radiant cooling systems in US commercial buildings. Energy and buildings, 30(2), PP:127-138. (1999).

[21] Dieckmann, J., Roth, K. W., & Brodrick, J. Radiant ceiling cooling. ASHRAE journal, 46,PP: 42-43. (2004).

[22] Ho V. Radiant chilled ceiling system. Sustainable Building, Hong Kong Regional Conference Urban Density & Sustainability. (2013).

[23] Badenhorst S. Chilled ceilings and beams. AIRAH Energy Conference. (2003)

[24] Waterloo Air Products plc. An introduction to chilled beams and ceilings. Version 1. (2012).

[25] Price Industries Limited. Chilled sails. Printed in Canada. V1. (2018).

[26] Cao, G., Awbi, H., Yao, R., Fan, Y., Sirén, K., Kosonen, R., & Zhang, J. J. A review of the performance of different ventilation and airflow distribution systems in buildings. Building and Environment, 73, PP:171-186. (2014).

[27] Sandberg, M. Ventilation efficiency as a guide to design. ASHRAE transactions, 89, PP:455-479. (1983).

[28] Sandberg, M., & Sjöberg, M. The use of moments for assessing air quality in ventilated rooms. Building and environment, 18(4), PP:181-197. (1983).

[29] Mundt E, Mathisen H, Nielsen P, Moser A. Ventilation Effectiveness. Rehva guidebook No.2. (2004)

[30] Etheridge, D. W., & Sandberg, M. Building ventilation: theory and measurement (Vol. 50). Chichester: John Wiley & Sons. (1996).

[31] Awbi, H. B. Ventilation for good indoor air quality and energy efficiency. Energy Procedia, 112, PP:277-286. (2017).

[32] Meiss, A., Feijó-Muñoz, J., & García-Fuentes, M. A. Age-of-the-air in rooms according to the environmental condition of temperature: A case study. Energy and buildings, 67, PP:88-96. (2013).

[33] Xing, H., Hatton, A., & Awbi, H. B. A study of the air quality in the breathing zone in a room with displacement ventilation. Building and environment, 36(7),PP: 809-820.(2001).

[34] Feustel, H. E., & Stetiu, C. Hydronic radiant cooling—preliminary assessment. Energy and buildings, 22(3), PP:193-205. (1995).

[35] Laine, T. Cool ceiling system: for better control of office building indoor climate. Proceedings of 'Indoor Air, 93, PP:423-430. (1993).

[36] Keblawi, A., Ghaddar, N., Ghali, K., & Jensen, L. Chilled ceiling displacement ventilation design charts correlations to employ in optimized system operation for feasible load ranges. Energy and Buildings, 41(11), PP:1155-1164. (2009).

[37] Schiavon, S., Bauman, F., Tully, B., & Rimmer, J. Room air stratification in combined chilled ceiling and displacement ventilation systems. HVAC&R Research, 18(1-2), PP:147-159. (2012).

[38] Yuan, X., Chen, Q., & Glicksman, L. R. A critical review of displacement ventilation. ASHRAE Transactions-American Society of Heating Refrigerating Air-conditioning engine, 104(1), PP:78-90. (1998).

[39] Schiavon, S., Bauman, F. S., Tully, B., & Rimmer, J. Chilled ceiling and displacement ventilation system: Laboratory study with high cooling load. Science and Technology for the Built Environment, 21(7), PP:944-956. (2015).

[40] Chen, H. Experimental and numerical investigations of a ventilation strategy–impinging jet ventilation for an office environment (Doctoral dissertation, Linköping University Electronic Press). (2014).

[41] Novoselac, A., & Srebric, J. A critical review on the performance and design of combined cooled ceiling and displacement ventilation systems. Energy and buildings, 34(5), PP:497-509. (2002).

[42] ASHRAE. Standard 55. Thermal environmental conditions for human occupancy. Atlanta. (2010)

[43] Fanger, P. O.. Moderate thermal environments Determination of the PMV and PPD indices and specification of the conditions for thermal comfort. ISO 7730. (1984)

[44] Gao, S., Wang, Y. A., Zhang, S. M., Zhao, M., Meng, X. Z., Zhang, L. Y., ... & Jin, L. W. Numerical investigation on the relationship between human thermal comfort and thermal balance under radiant cooling system. Energy Procedia, 105, PP:2879-2884.. (2017).

[45] Hopfe C, Mcleod R. The passive house designer's manual. Routledge.2015.

[46] ASHRAE Fundamentals Handbook. (2013).

[47] Ayoub, M., Ghaddar, N., & Ghali, K. Simplified thermal model of spaces cooled with combined positive displacement ventilation and chilled ceiling system. HVAC&R Research, 12(4), PP:1005-1030. (2006).

[48] Wang Q, Zhen Z. Performance comparison between mixing ventilation and displacement ventilation with and without cooled ceiling. International Journal for Computer-Aided Engineering and Software; 23 (3), PP:218-237. (2006).

[49] Hao, X., Zhang, G., Chen, Y., Zou, S., & Moschandreas, D. J. A combined system of chilled ceiling, displacement ventilation and desiccant dehumidification. Building and Environment, 42(9), PP:3298-3308. (2007).

[50] Karadağ, R. The investigation of relation between radiative and convective heat transfer coefficients at the ceiling in a cooled ceiling room. Energy conversion and management, 50(1), PP:1-5. (2009).

[51] Mateus, N. & Graça, G. Simplified modeling of displacement ventilation systems with chilled ceilings. Energy and Buildings, 108, PP:44-54. (2015).

[52] Taki, A. H., Loveday, D. L., & Parsons, K. C. The effect of ceiling temperatures on displacement flow and thermal comfort—experimental and simulation studies. In 5th International Conference on Air Distribution in Rooms ROOMVENT 96, July 17-19, pp:307 (Vol. 314). (1996).

[53] Rees, S. J. Modelling of displacement ventilation and chilled ceiling systems using nodal models (Doctoral dissertation, Loughborough University). (2010).

[54] Itani, M., Ghali, K., & Ghaddar, N. Performance evaluation of displacement ventilation system combined with a novel evaporative cooled ceiling for a typical office in the city of Beirut. Energy Procedia, 75, PP:1728-1733. (2015).

[55] Teodosiu, C., Ilie, V., & Teodosiu, R. Numerical prediction of thermal comfort and condensation risk in a ventilated office, equipped with a cooling ceiling. Energy Procedia, 85(1), PP:550-558. (2016).

[56] Muslmani, M., Ghaddar, N., & Ghali, K. Performance of combined displacement ventilation and cooled ceiling liquid desiccant membrane system in Beirut climate. Journal of Building Performance Simulation, 9(6), PP:648-662. (2016).

[57] Yang, Y., Wang, Y., Yuan, X., Zhu, Y., & Zhang, D. Simulation study on the thermal environment in an office with radiant cooling and displacement ventilation system. Procedia Engineering, 205, PP:3146-3153. (2017).

[58] Hormigos-Jimenez, S., Padilla-Marcos, M. A., Meiss, A., Gonzalez-Lezcano, R. A., & Feijó-MuÑoz, J. Experimental validation of the age-of-the-air CFD analysis: A case study. Science and Technology for the Built Environment, 24(9), PP:994-1003. (2018).

[59] Shan, W., & Rim, D. Thermal and ventilation performance of combined passive chilled beam and displacement ventilation systems. Energy and Buildings, 158, PP:466-475. (2018).

[60] Tian, Y., Guo, S., Jin, G., Pang, Y., Wang, X., Wu, W., & Zhao, J. A two-step approach to solve the issue of dew condensation for displacement ventilation and chilled ceiling system. Energy Procedia, 158, PP:6527-6531. (2019).

[61] Guo, S., Tian, Y., Fan, D., Wu, W., Zhao, J., Jin, G., & Wang, X. A novel operating strategy to avoid dew condensation for displacement ventilation and chilled ceiling system. Applied Thermal Engineering, PP:115344. (2020).

[62] Amini, M., Maddahian, R., & Saemi, S. Numerical investigation of a new method to control the condensation problem in ceiling radiant cooling panels. Journal of Building Engineering, 32, 101707. (2020).

[63] Fonseca, N., Cuevas, C., & Lemort, V. Radiant ceiling systems coupled to its environment part 1: Experimental analysis. Applied Thermal Engineering, 30(14-15), P:2187-2195. (2010).

[64] Chakroun, W., Ghali, K., & Ghaddar, N. Energy saving using mixed air in rooms conditioned by chilled ceiling displacement ventilation system. ASHRAE Transactions, 117(2),PP:67-76. (2011).

[65] Andrés-Chicote, M., Tejero-González, A., Velasco-Gómez, E., & Rey-Martínez, F. J. Experimental study on the cooling capacity of a radiant cooled ceiling system. Energy and Buildings, 54, PP:207-214. (2012).

[66] Liu, Z., Zhang, L., & Gong, G. Experimental evaluation of a solar thermoelectric cooled ceiling combined with displacement ventilation system. Energy Conversion and Management, 87, PP:559-565.(2014).

[67] Kim, M. K., & Leibundgut, H. Advanced Airbox cooling and dehumidification system connected with a chilled ceiling panel in series adapted to hot and humid climates. Energy and buildings, 85, PP:72-78. (2014).

[68] Itani, M., Ghali, K., & Ghaddar, N. Increasing energy efficiency of displacement ventilation integrated with an evaporative-cooled ceiling for operation in hot humid climate. Energy and Buildings, 105, PP:26-36. (2015).

[69] Yuan, Y. L., Zhou, X., & Zhang, X. Experimental study of heat performance on ceiling radiant cooling panel. Procedia Engineering, 121, PP:2176-2183. (2015).

[70] Krajčík, M., Tomasi, R., Simone, A., & Olesen, B. W. Thermal comfort and ventilation effectiveness in an office room with radiant floor cooling and displacement ventilation. Science and Technology for the Built Environment, 22(3), PP:317-327. (2016).

[71] Cholewa, T., Anasiewicz, R., Siuta-Olcha, A., & Skwarczynski, M. A. On the heat transfer coefficients between heated/cooled radiant ceiling and room. Applied Thermal Engineering, 117, PP:76-84.(2017).

[72] Seblany, R., Ghaddar, N., Ghali, K., Ismail, N., Simonetti, M., Virgone, J., & Zoughaib, A. Humidity control of liquid desiccant membrane ceiling and displacement ventilation system. Applied Thermal Engineering, PP:144, 1-12. (2018).

[73] Wu, X., Gao, J., Lv, P., Wang, H., Wang, S., & Wang, F. Impact of chilled ceiling on indoor air distribution in a room with mixing ventilation. Science and Technology for the Built Environment, 26(3), PP:366-376. (2020).

[74] Li N., & Chen, Q. Study on dynamic thermal performance and optimization of hybrid systems with capillary mat cooling and displacement ventilation. International Journal of Refrigeration, 110, PP:196-207. (2020).

[75] Bahman, A., Saade, R., Chakroun, W., Ghali, K., & Ghaddar, N. Performance comparison of conventional and chilled ceiling/displacement ventilation systems in Kuwait. ASHRAE Transactions, 115(1). (2009).

[76] Taki, A. H., Jalil, L., & Loveday, D. L. Experimental and computational investigation into suppressing natural convection in chilled ceiling/displacement ventilation environments. Energy and buildings, 43(11), PP:3082-3089.(2011).

[77] Hui, S. C., & Leung, J. Y. Thermal comfort and energy performance of chilled ceiling systems. In Proceedings of the Fujian-Hong Kong Joint Symposium 2012. The Conference paper. (2012).

[78] Kim J. Evaluating the performance of passive chilled beams with respect to energy efficiency and thermal comfort. Purdue University. Phd. (2016).

[79] Ning, B., Chen, Y., Liu, H., & Zhang, S. Cooling capacity improvement for a radiant ceiling panel with uniform surface temperature distribution. Building and Environment, 102, PP:64-72. (2016).

[80] Yuan, Y., Zhang, X., Zhou, X., & Gao, J. An experiment-oriented simulation method for cooling capacity determination of cooling ceiling radiant panel system. Science and Technology for the Built Environment, 22(6), PP:831-844. (2016).

[81] Shbeeb A. and Mahdi A..Experimental and numerical investigation of displacement ventilation system with assessment of four turbulence models. Ms.C theses. Babylon University. (2016)

[82] Al Tuarihi M. and Mahdi A. Experimental and numerical investigation on air flow and temperature distribution under different geometries of displacement ventilation devices in an office room. Ms.C theses. Babylon University. (2017).

[83] AbdulGhafor I., Abdulrasool A., Mehdi Q. Theoretical and Experimental Study of Combined System: Chilled Ceiling and Displacement Ventilation. Universal Journal of Mechanical Engineering 7(3), PP: 118-138. (2019).

[84] Jin, W., Jing, J., Jia, L., & Wang, Z. The dynamic effect of supply water flow regulation on surface temperature changes of radiant ceiling panel for cooling operation. Sustainable Cities and Society, 52, 101765. (2020).

[85] Koju, S. M. Thermal behavior of expanded polystyrene based lightweight concrete sandwich panel at various temperatures. Journal of Science and Engineering, 4, PP:47-52. (2017).

[86] ASHRAE Fundamentals Handbook. (2001).

[87] Schiavon, S., Bauman, F., Tully, B., & Rimmer, J. Room air stratification in combined chilled ceiling and displacement ventilation systems. HVAC&R Research, 18(1-2), PP:147-159. (2012).

[88] Wilkins, C., & Hosni, M. H. Heat gain from office equipment. Ashrae Journal, 42(6), PP:33-39. (2000).

[89] ASHRAE/IES standard 90.1, part 11, (2010).

[90] Chen, Q., & Glicksman, L. System performance evaluation and design guidelines for displacement ventilation:[prepared under ASHRAE research project 949...]. American Society of Heating, Refrigerating, and Air-Conditioning Engineers, Incorporated, (2003).

[91] Skistad H., Mundt E., Nielsen P.V., Hagstrom K., Railo J. Displacement ventilation in nonindustrial premises. Guidebook, REHVA, (2002).

[92] ASHRAE-HVAC Applications, Atlanta, (2011).

[93] ASHRAE handbook. Heating, HVAC Systems and Equipment (SI). Panel heating and cooling; (2012).

[94] Waterloo Air Products plc. An Introduction to Chilled Beams and Ceilings. Version 1; (2012).

[95] ASHRAE Fundamentals Handbook. (2009).

[96] ASHRAE Fundamentals of water system design. (1999).

[97] ISO 16000–8: 2007. Indoor Air Part 8: Determination of Local Mean Ages of Air in Buildings for Characterizing Ventilation Conditions. Geneva, Switzerland: International Organization for Standardization.

[98] Bartak M, Cermak M, Clarke J A, Denev J, Drkal F, Lain M, Macdonald I A, Majer M, Stankov P. Experimental and numerical study of local mean age of air. Seventh International Conference. Rio de Janeiro. August 13-15. (2001).

[99] Airpak 3.0 User's guide.(2007).

[100] Liang, C., Li, X., Shao, X., & Li, B. Direct relationship between the system cooling load and indoor heat gain in a non-uniform indoor environment. Energy, 191, 116490.(2020).

[101] Versteeg, H. K., & Malalasekera, W. An introduction to computational fluid dynamics: the finite volume method. Pearson education. (1996).

[102] Chen, Q. Comparison of different k-ε models for indoor air flow computations. Numerical Heat Transfer, Part B Fundamentals, 28(3),PP:353-369. (1995).

[103] Yakhot, V. S. A. S. T. B. C. G., Orszag, S. A., Thangam, S., Gatski, T. B., & Speziale, C. G. Development of turbulence models for shear flows by a double expansion technique. Physics of Fluids A: Fluid Dynamics, 4(7), PP:1510-1520. (1992).

[104] Rodi W. Turbulence models and their application in hydraulics. International association for hydraulic research, delft, 3rd edition. (1993).

[105] Chong, J. L. S., Husain, A., & Tuan, T. B. Simulation of airflow in lecture rooms. In Proceedings of the AEESAP International Conference, pp:7-8. (2005).

[106] Accuweather,https://www.accuweather.com/ar/iq/baghdad/207375/july-weather/207375?year=2020

[107] J. P. Holman. Heat transfer. Tenth Edition. (2010).

[108] Khaled. A. Joode. Air condition and refrigeration engineering. 1st edition, 1984.

[109] Ardehali, M. M., Panah, N. G., & Smith, T. F. (2004). Proof of concept modeling of energy transfer mechanisms for radiant conditioning panels. Energy conversion and Management, 45,PP:13-14, 2017.

[110] Karimipanah T, H.B Awbi, Blomqvist C, Sandberg M. Effectiveness of confluent jets ventilation system for classrooms. Conference Paper. (2005).

[111] TAN, H. W., Murata, T., Aoki, K., & Kurabuchi, T. Cooled ceilings/displacement ventilation hybrid air conditioning system: Design criteria. In Roomvent'98 (Stockholm, 14-17 June). (1998).

APPENDICES

Appendix-A

Appendix-A.1

Calculating supply air temperature (T_s) and flowrate (Q_{DV}) for isolated office room (case-I and II)

The supply air flowrate calculated by using the following equation:

$$Q_{DV} = (0.295q_{oe} + 0.132q_l + 0.185q_{ex}) / (\rho\, C_p\, \Delta T_{hf}) \quad \text{....(A-1)}$$

for isolated office room ($q_{ex} = 0$, $q_l = 100W$, $q_{oe} = 270W$, $\Delta T_{hf} = 2^oC$, $\rho = 1.2m^3/s$ and $C_p = 1.005kj/kg.^oC$)

after that the air supply temperature calculated by using the following equation:

$$T_s = T_{dr} - \Delta T_{hf} - [(A_f.\, CL_{DV}) / (0.584Q_{DV}^2 + 1.208A_f.Q_{DV})] \quad \text{….(A-2)}$$

Where:

$$CL_{DV} = q_{oe} + q_l + q_{ex} \quad \text{….(A-3)}$$

exhausted air temperature calculated by:

$$T_e = T_s - \frac{CL_{DV}}{\rho Q_{DV} C_p} \quad \text{….(A-4)}$$

Total cooling load treated by displacement ventilation varied with portion of cooling load treated by chilled ceiling as (270W, 277.5W, 185W and 74W) for (η) equal (0%, 25%, 50% and 80%) respectively.

Table(A-1) shows the values of supply air temperature, exhausted air temperature and air flow rate calculated by above equations for each (η) for two cases(I and II).

Table(A-1) Calculated results for supply air flowrate and temperature for isolated office cases.

η%	**CL_{DV} (W)**	**Q_{DV} (l/s)**	**T_s (^oC)**	**T_e (^oC)**
0	370	38.5	20.7	28.6
25	277.5	28.87	20.2	28.1
50	185	19.25	19.4	27.4
80	74	7.5	17.6	25.6

In this work the supply air flowrate was fixed at (35l/s), then by applied Eqn.(A-4) and by used the parameters in table(A-1), the new values of air supply temperature becomes as shown in table(A-2).

Table(A-2) new calculated values for supply air temperature

η (%)	**CL_{DV} (W)**	**Q_{DV} (m^3/s)**	**T_s (^oC)**
0	370	0.035	20
25	277.5	0.035	21.5
50	185	0.035	23
80	74	0.035	24

The air supply temperature and air flowrate for another cases (non-isolated office room and classroom) can be calculated as the same method above but with heat external (q_{ex}) which calculated by (Hap) program.

Appendix-A.2

HAP PROGRAM RESULTS

Table (A-3) The results of cooling load from (HAP4.9) program for non-isolated office room

	DESIGN COOLING		
	COOLING DATA AT Jul COOLING OA DB / WB 47 °C / 22 °C		
ZONE LOADS	Details	Sensible (W)	Latent (W)
Window & Skylight Solar Loads	1.25 m²	88	-
Wall Transmission	5 m²	105	-
Roof Transmission	-	-	-
Window Transmission	1.25 m²	69	-
Skylight Transmission	0 m²	0	-
Door Loads	2 m²	67	-
Floor Transmission	-	-	-
Partitions	5.5 m²	101	-
Ceiling	-	-	-
Overhead Lighting	100 W	100	-
Task Lighting	-	-	-
Electric Equipment	120 W	120	-
People	2	150	-
Infiltration	-	-	-
Miscellaneous	-	-	-
>> Total Zone Loads	**-**	**800**	**-**

Table (A-4) The results of cooling load from HAP4.9 program for classroom

	DESIGN COOLING		
	COOLING DATA AT JUL 1700 COOLING OA DB / WB 47.0 °C / 22.8 °C		
ZONE LOADS	**Details**	**Sensible (W)**	**Latent (W)**
Window & Skylight Solar Loads	5 m²	338	-
Wall Transmission	18 m²	338	-
Roof Transmission	0 m²	0	-
Window Transmission	5 m²	410	-
Skylight Transmission	-	-	-
Door Loads	2 m²	67	-
Floor Transmission	28 m²	0	-
Partitions	20 m²	390	-
Ceiling	-	-	-
Overhead Lighting	480 W	480	-
Task Lighting	-	-	-
Electric Equipment	210 W	210	-
People	21	1575	-
Infiltration	-	-	-
Miscellaneous	-	-	-
>> Total Zone Loads	**-**	**3808**	**-**

Appendix B

B-1 Flow Meter Calibration

The flow meter calibrated by used the measuring cylinder and stop watch. This method is depend on the needed time to filled the a specific volume and compared it with the flow meter reading .Fig.(B-3) shows the flow meter calibration .The average error is (±2%)

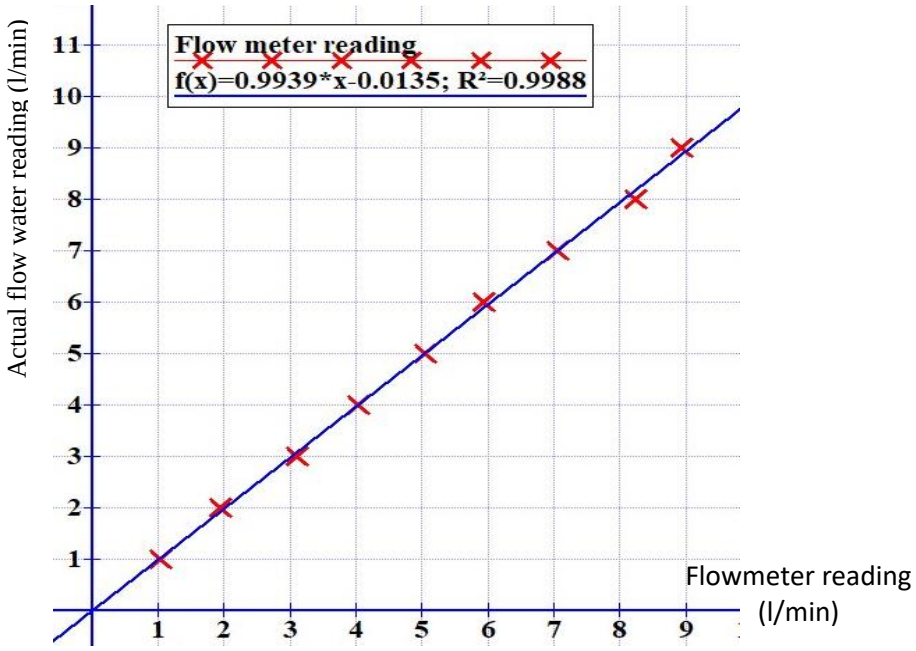

Fig.(B-1) flow meter calibration curve

B-2 Certificate of CO_2, Temperature, RH data logger

Shenzhen BCTC Technology Co.,Ltd.
A.Floor 3, 44 Building, Tanglang Industrial Park B,
Taoyuan Street, Nanshan District, Shenzhen, China

Certificate of Compliance

Certificate Number: BCTC-150403524

Applicant	:	**Dongguan Xintai Instrument Co., Ltd** No 149, Chunfeng Road, Longbeiling, Tangxia Town, Dongguan City, Guangdong, China
Manufacturer	:	**Dongguan Xintai Instrument Co., Ltd** No 149, Chunfeng Road, Longbeiling, Tangxia Town, Dongguan City, Guangdong, China
Product	:	**CO2/Temp./RH Data Logger**
M/N	:	**HT-2000**
Test Standard	:	**EN 55022: 2010** **EN 61000-3-2: 2014, EN 61000-3-3: 2013** **EN 55024: 2010** **EN 61000-4-2: 2009, EN 61000-4-3: 2006+A1:2008+A2:2010** **EN 61000-4-4: 2012, EN 61000-4-5: 2014** **EN 61000-4-6: 2014, EN 61000-4-8: 2010, EN 61000-4-11: 2004**

The EUT described above has been tested by us with the listed standards and found in compliance with the council EMC directive 2014/30/EU. It is possible to use CE marking to demonstrate the compliance with this EMC Directive. It is only valid in connection with the test report number: BCTC-150403524.

CE

SHENZHEN BCTC TECHNOLOGY CO., LTD.
APPROVED
Manager
Apr. 10, 2015

This certificate of conformity is based on a single evaluation of the submitted sample(s) of the above mentioned product. It does not imply an assessment of the whole product and relevant. Directives have to be observed.

Tel: 400-788-9558 0755-33019988 Http://www.bctc-lab.com Http://www.btc-lab.com

خلاصـــــه البحث:

يتسم صيف العراق بارتفاع درجات الحرارة نهارا خاصة في المناطق الوسطى والجنوبية. تسبب ارتفاع درجة الحرارة في ارتفاع استهلاك الطاقة الكهربائية لتغطية حاجة الناس لتكييف الهواء. في هذه الدراسة تم استخدام سقف مبرد مدمج مع نظام التهوية الإزاحية (DV/CC).

اتخذت مدينة الحلة لدراسة هذا النظام. وهي مدينة تقع في وسط العراق عند خط الطول (44.42) وخط العرض (32.46) وتتميز بمناخ حار وجاف في الصيف.

تم استخدام نموذج غرفة المكتب المعزولة في العمل التجريبي ، بينما درست غرفة المكتب غير المعزولة والصف الدراسي كتحليل عددي فقط. تم دراسة تأثير شكل ناشر إمداد الهواء وجزء حمل التبريد المعالج بالسقف المبرد على عمر الهواء ومعايير الراحة الحرارية مثل ((Predicted Mean Vote(PMV و Predicted Percentage Dissatisfied(PPD) ومؤشر أداء انتشار الهواء (ADPI)). بالإضافة إلى ذلك تمت دراسة الزمن المستغرق لإزالة الملوثات (مثل ثاني أكسيد الكربون) من منطقة شاغلي الحيز تجريبيًا وعدديًا.

تتمثل الأهداف العامة لهذا العمل الموصوف في الاطروحة في دراسة أداء نظام (DV/CC) في المناخ الحار والجاف للحصول على مستوى أعلى من راحة الإنسان وجودة الهواء الداخلي من خلال دراسة عمر الهواء وتوزيع درجة الحرارة في ظل ظروف متنوعة. استخدام (ANSYS AIRPAK.3.0.16) كبرنامج (CFD) في التحليلات العددية.

احتوت الدراسة على ستة حالات ، كل حالة بها أربعة اختبارات على أساس حمل التبريد المعالج بالسقف المبرد (0 ، 25 ، 50 و 80٪ بالنسبة لحمل التبريد الكلي). تم عزل الحالتين الأولى والثانية (case-I and case-II) مع موزع هواء مستطيل ونصف دائري على التوالي. درس الحالة الاولى والثانية

تجريبياً وعددياً بحمل تبريد إجمالي يساوي (370 وات). كانت الحالتان الثالثة والرابعة (case-III and case-IV) عبارة عن غرفة مكتب غير معزولة بحمل تبريد اجمالي (800 واط) بينما كانت الحالتان الخامسة والسادسة (case-V and case-VI) عبارة عن صف دراسي بحمل تبريد اجمالي (3808 واط). لدراسة عمر الهواء ومعايير الراحة الحرارية في كل حالة ، تم تثبيت سرعة تزويد الهواء للحالات (I، II، III و IV) عند (0.25م/ثا) بينما بالنسبة للحالات (V و VI) تم تثبيتها عند (0.3م/ثا). درجة حرارة إمداد الهواء لكل حالة اعتمدت على حمل التبريد المعالج عن طريق تهوية الإزاحة. بالإضافة إلى ذلك ، استخدمت الدراسة ولكل حالة أداة (CBE) التي أنتجها مركز الطاقة للتنبؤ بالراحة الحرارية.

أظهرت النتائج الرئيسية أن عمر الهواء الموقعي يزداد بحوالي (35 ثا و 25 ثا) لغرفة المكتب والصف الدراسي على التوالي مع زيادة حمل التبريد المعالج بالسقف المبرد بنسبة (25%). الناشر نصف الدائري اعطى افضلية في تقليل عمر الهواء بحوالي (10%) في الصف الدراسي و(6%) في غرفة المكتب مقارنة بالناشر المستطيل. كما انه حسن قيم (PMV) و (PPD) و (ADPI) بحوالي (0.03, 0.5%, 2%)على التوالي.استخدام الناشر شبه الدائري اعطى افضلية في فعالية توزيع درجة الحرارة بنسبة(8%) في الغرفة الغير معزولة و (2.5%) بالنسبة للصف الدراسي. حقق نظام (DV/CC) ظروف الراحة الحرارية في الغرفة المعزولة ، بينما في الغرفة الغير معزولة ، كانت الراحة الحرارية تعتمد على متوسط درجة الحرارة المشعة كعامل رئيسي.

جمهورية العراق

وزارة التعليم العالي والبحث العلمي

جامعـــة بابـل/ كلية الهندسة

قسم الهندسة الميكانيكية

تقييم عمر الهواء للتنبؤ براحة شاغلي الحيز من خلال اعتماد نظام التهوية الازاحية والسقف المبرد في مناخ العراق

رسالة مقدمة الى قسم الهندسة الميكانيكية في جامعة بابل كجزء من متطلبات نيل درجة الدكتوراه في الهندسة/ الهندسة الميكانيكية/ قدرة

من قبل

علي عيدان شبيب حمد

بإشراف

الأستاذ الدكتور

علاء عباس مهدي

الأستاذ الدكتور

احمد كاظم حسين

1442 هـ

2022 م